UNIVERSITÉ DE STRASBOURG

ÉCOLE DOCTORALE 414 Science de la Vie et de la Santé

Architecture et Réactivité de l'ARN – IBMC Strasbourg

THÈSE présentée par :

Alessandra MARENNA

soutenue le : **29 septembre 2017**

pour obtenir le grade de : **Docteur de l'université de Strasbourg**

Discipline/ Spécialité : Aspects Moléculaires et Cellulaires de la Biologie

Staphylococcus aureus protein S1, an RNA chaperone involved in translation initiation and sRNA regulation

THÈSE dirigée par :

Mr MARZI Stefano	CR1, IBMC, Université de Strasbourg

RAPPORTEURS :

Mme DOCK-BREGEON Anne-Catherine	DR2, LBI2M, Station Biologique de Roscoff
Mr REDDER Peter	Prof., LMGM, Université de Toulouse III

AUTRES MEMBRES DU JURY :

Mme GUILLIER Maude	CR1, IBPC, Paris
Mr GIEGE Philippe	DR2, IBMP, Université de Strasbourg

Acknowledgements

I would like to start by thanking my committee members Anne-Catherine Dock-Bregeon, Maude Guillier, Peter Redder and Philippe Giege for their interest in my work.

I would like to express my special appreciation and thanks to Pascale and Stefano.
Pascale, thank you for giving me the opportunity to join your group and to explore the world of science. Thank you for all the scientific discussions, recommendations, constructive criticism and personal understanding. I greatly benefited from your keen scientific insight and your ability to put complex ideas into simple terms.

Stefano, thanks for always being ready to draw an explanation, for insightful comment and always making me focus on the question. Thanks for maintaining a positive spirit, for teaching me how to be critical in science as in life.
During the writing of this thesis, you gave me the support and the energy I needed to move on. You are for me an extremely reliable source of knowledge. Thanks for broadening my horizons.

Thank you to Isabelle, most of the work performed in this thesis would not have succeeded without your guidance and inspiration. Thank you also for your support in my private life.

Anne-Catherine, thank you for your friendship, your persistent encouragement during stormy times and for your precious help in the bench work. I will keep you in my heart. Thank you.

I would like to direct a warm and broad thank you to all the colleagues in “436 lab” Melodie, she is a true friend. Delphine is an amazing person in too many ways. Arnauld, Emma, Lucas, Laura and Maria Rosaria for informal, friendly and helpful working environment.

I've met many people along the way but I've got just few friends that I will love for all my life. My journey was made millions times more enjoyable by you Terry, Zongfu and Simona. Thank you for sharing so many good moments with me.

To my Daddy.

I am indebted to my mother and to my sister. I am very thankful for their thoughtfulness, support and encouragement in any and everything I do. In the last period of my life, I took decisions probably difficult to understand but I always had the feeling to have both of you on my side. Thank you for existing and making my life so special. Thanks for giving me the best advice coming deeply from your hearts. My apologies to both of you for having declined some of our meetings.

Above all, thanks to my amazing boyfriend. Daniele, you have been more than any, the greatest support, suffering with me at times and celebrating at others. Your high expectations continue to push me and you make me feel like I can do anything.

To Ludovica Mariafrancesca, right now, the joys of my life and to whom this thesis is dedicated.

List of abbreviations

Proteins and complexes

30S-PIC 30S pre-initiation complex

30S-IC 30S initiation complex

70S-IC 70S initiation complex

BSA « bovine serum albumin »

IF Initiation factor

OB Oligonucleotide/oligosaccharide binding

ORF Open reading frame

PNPase Polynucleotide phosphorylase

RNase Ribonuclease

RNA

mRNA messanger RNA

sRNA regulatory RNA

tRNA Transfert RNA

itRNA Initiatot tRNA

RBS Ribosomal binding site

SD Shine and Dalgarno sequence

UTR Untranslated region

Metabolites/Ions

Ca Calcium

Cl Chlorine

Fe Iron

K Potassium

Mg Magnesium

Na Sodium

Ni Nickel

NH4 Ammonium

ROS Reactive oxygen species

Bacteria

B. subtilis *Bacillus subtilis*

E. coli *Escherichia coli*

S. aureus *Staphylococcus aureus*

Media and antibiotics

LB Lysogeny broth

BHI Brain heart infusion

NZM Minimal media

Amp Ampicillin

Cam Chloramphenicol

Kan Kanamycin

Chemical reagents

EtBr Ethidium bromide

DTT Dithiothreitol

EDTA Ethylenediaminetetraacetic acid

IPTG Isopropyl β-D-1-thiogalactopyranoside

P32 Phosphorus-32

SDS Sodium dodecyl sulfate

General

Å Angström

°C Celsius degrees

cpm Count per minute

OD Optical density

g grams

K_D Dissociation constant

L Litre

M Molar

mol Mole

nt nucleotide

pb base pair

pI isoelectric point

UV ultraviolet

V volt

vol volume

W watt

WT wild-type

Table des matières

Acknowledgements i

List of abbreviations iii

Synopsis de la thèse en Français 1

I. Introduction 3

II. Résultats 4

II.1. Fonction de *Sau*S1 dans la traduction 4

II.2. *Sau*S1 est une protéine chaperone de l'ARN 8

III. Discussion et perspectives 10

IV. Bibliographie 13

Introduction 15

I. *Staphylococcus aureus* is a versatile opportunistic human pathogen 17

II. Virulence determinants in *Staphylococcus aureus* play central role in its pathogenesis 19

II.1. Tissue colonization 21

II.2. Immune evasion (non CWA or Eap) 22

II.3. Tissue invasion and dissemination 22

III. Regulation of the expression of virulence factors 29

III.1 Regulation of PSM production and other virulence factors by the *agr* locus 30

III.2. Two component regulatory system SaeRS 33

III.3. The global regulator SarA 33

III.4. *S. aureus* sigma factors 34

IV. Antibiotic resistances in *Staphylococcus aureus* 35

V. Translation and its control in *S. aureus* 37

V.1. Translation initiation, a check point for regulation 37

V.2. A view on the Translation Initiation in Gram-negative bacteria 38

V.3. S. aureus ribosome structure and specific features 42

V.4. A glimpse on Staphylococcus aureus translation machinery and its control 45

Objectives and experimental strategies 59

I. How *S. aureus* ribosome initiates translation of structured mRNAs? 61

I.1. Biological questions and objectives 61

I.2. Main experimental strategies 61

II. Could *Sau*S1 be involved in regulatory mechanisms mediated by small non-coding RNAs? 63

II.1. Biological questions and Objectives 63

II.2. Main experimental strategies 64

III. Summary of the main experimental strategies 65

Results 67
I. Result I: translation functions of *Sau*S1 69
I. Result I: translation functions of *Sau*S1 (manuscript ready for submission) 71
Staphylococcus aureus S1 activates translation initiation of PSMα toxins and stimulates the production of several other secreted virulence factors 71
II. Result II: *Sau*S1 is an RNA chaperone involved in different steps of sRNA-dependent regulation and of RNA metabolism in *S. aureus* 125
II.1. *Sau*S1 helps translation initiation of structured mRNAs 125
II.2. Phenotypic characterization of *rpsA* mutants 126
II.3. *SauS1* and its constellation of RNAs. RIP-seq (co-immunoprecipitation and RNA-seq) analysis 129
II.4. *SauS1* forms stable complexes with various sRNAs but does not interact with all of them 133
II.5. *SauS1* forms a ternary complex with RsaI and RsaG 134
II.6. RsaI binding site for RsaG is hindered into a pseudoknot structure 136
II.7. Probing the interaction between RsaI and RsaG by footprinting experiments 138
II.8. Characterization of RNA annealing and strand displacement activities of S1 by FRET experiments 139
Discussions and Perspectives 141
I. *Staphylococcus aureus* S1 as translational activator. Further considerations 143
I.1. General discussion 143
I.2. Perspectives 145
II. Involvement of *Sau*S1 in sRNAs stabilization 147
II.1. General discussion 147
II.2. Perspectives 148
III. Involvement of *Sau*S1 in sRNA-target recognition 149
III.1. General discussion 149
III.2. Perspectives 152
IV. Involvement of *Sau*S1 in tRNA maturation 153
IV.I. General statement 153
IV.2. Perspectives 157
V. Involvement of *Sau*S1 in *cis-acting* regulatory elements 157
VI. General conclusion 159
Materials and Methods 161
Media and growth of bacteria 163
Purification of SauS1 163
Sonication 163

First Ni-NTa column purification 164
Dialysis 164
Protein concentration 165
Second Ni-Nta column purification 165
FPLC using anion exchange column 165
SDS-PAGE analysis 166
Co-immunoprecipitation assays 167
Deep-sequencing analysis 167
Bandshift on polyacrylamide gel 168
Chemical probing of S. aureus RsaI 168
Enzymatic probing of RsaI 168
Footprinting RsaI*/RsaG 169
FRET 170
Northern Blot 170
In vitro transcription of RNA-DIG probes 170
Migration, transfer, hybridization and detection 171
30S ribosomal subunits purification 172
Toeprinting assay 172
5' end Labeling of oligonucleotides 172
Toeprinting 173
Sequences preparation 173
References 175

Synopsis de la thèse en Français

La protéine S1 chez *Staphylococcus aureus*, une protéine chaperonne de l'ARN impliquée dans l'initiation de la traduction et la régulation médiée par des ARN non codants

I. Introduction

Staphylococcus aureus est une bactérie pathogène opportuniste à Gram-positif, responsable d'un grand nombre d'infections communautaires et nosocomiales qui peuvent être bénignes comme les furoncles, ou beaucoup plus graves telles que des pneumonies, des ostéomyélites, et des endocardites. Cette bactérie est aussi capable de s'adapter rapidement à divers environnements. Cette adaptation rapide requiert un changement de l'expression de gènes qui s'effectue aussi bien au niveau transcriptionnel, traductionnel que post-traductionnel. Contrôler la traduction a l'avantage d'apporter une réponse rapide nécessaire pour les processus adaptatifs. Les régulations de la traduction s'effectuent majoritairement à l'étape de l'initiation qui est l'étape limitante de la synthèse des protéines, et au cours de laquelle l'ARN messager (ARNm) se lie à l'ARN de transfert (ARNt) initiateur sur la petite sous-unité du ribosome (30S). L'ARNm exerce un rôle clé dans ces mécanismes de régulation, en présentant des structures particulières dans leurs régions 5' non codantes qui peuvent soit directement influer sur la reconnaissance du ribosome, soit être reconnues par des protéines régulatrices ou des ARN non codants (ARNnc). Ainsi, les ARNm régulés sont souvent fortement structurés. Néanmoins pour être activement traduit, le site de liaison du ribosome sur l'ARNm doit être accessible. Chez *Escherichia coli*, l'initiation de la traduction des ARNm structurés est facilitée par l'action de la protéine ribosomique S1 qui est une protéine chaperonne de l'ARN capable de déstabiliser les structures des ARNm et de favoriser l'adaptation du codon d'initiation sur le canal de décodage du ribosome (Duval *et al.*, 2013). La protéine S1 d'*E. coli* (*Eco*S1) est constituée de six domaines OB-fold et est ancrée à la sous-unité 30S grâce aux deux premiers domaines, alors que la protéine S1 de *S. aureus* (*Sau*S1) est plus courte (quatre domaines OB-fold) et ne contient pas le premier domaine qui sert à l'ancrage sur le ribosome. La fonction de cette protéine chez ce pathogène majeur de l'homme n'était pas encore connue au début de ma thèse.

Les objectifs de ma thèse ont été (1) d'élucider les mécanismes moléculaires qui permettent au ribosome de *S. aureus* de reconnaître ces ARNm structurés pour initier leur traduction et (2) de caractériser les fonctions de *Sau*S1 dans le métabolisme des ARN.

Nous avons récemment démontré que les sous-unités 30S purifiées de *S. aureus* ne contiennent pas S1, et ne sont pas capables de former efficacement des complexes d'initiation avec des ARNm structurés de *S. aureus* (Introduction, §V.4. Article 1 : Khusainov, Marenna *et al.*, 2016). Pendant ma thèse, j'ai démontré que la protéine *Sau*S1 n'interagit pas directement avec la sous-unité 30S mais est capable de stimuler *in vitro* et *in vivo* l'initiation de la traduction de certains ARNm structurés par une interaction directe. Par l'utilisation de diverses approches incluant des études d'interactome, de mutagenèse, de FRET, de cartographie en solution, de toe-printing (pour analyser la formation des complexes ribosomiques) et de retard sur gel, j'ai également montré que *Sau*S1 agit comme une protéine chaperonne de l'ARN et qu'elle peut former différents complexes cellulaires impliqués dans des régulations dépendantes des ARNnc et dans les processus de maturation/dégradation de l'ARN.

II. Résultats

II.1. Fonction de *Sau*S1 dans la traduction

Le premier objectif de mon projet de thèse a porté sur la caractérisation de l'impact fonctionnel de la protéine *Sau*S1 sur l'initiation de la traduction d'ARNm structurés spécifiques. Du fait que j'ai montré que *Sau*S1 n'est pas strictement une protéine ribosomique, mon objectif a été de caractériser les cibles *in vivo* pour mieux comprendre l'étendue de ses fonctions biologiques. Dans un premier temps, en collaboration avec I. Caldelari, j'ai utilisé l'approche RIP-Seq qui est basé sur l'expression d'une protéine *Sau*S1 portant à son extrémité C-terminale une étiquette Flag. Après immunoprécipitation, les ARN co-purifiés à *Sau*S1 ont été identifiés par séquençage haut débit.

Nous avons ainsi identifié plusieurs classes d'ARN enrichis avec *Sau*S1 dont plusieurs ARNm, ARN régulateurs (ARNnc, « riboswitch ») et ARNt. Les interactions directes entre certains des ARN cibles et *Sau*S1 ont été validées par des expériences de gel retard et par la détermination de la structure des complexes par cartographie en solution. De manière intéressante, parmi les ARNm, nous avons identifié l'opéron

αpsm1-4 qui code pour quatre peptides appelés « Phenol-soluble modulins » ou PSM, qui sont des exo-toxines dont la synthèse est activée par le système de densité cellulaire *agr*. Les PSM (« Phenyl Soluble Modulins ») appartiennent à une famille de peptides amphipathiques composés d'hélices alpha. Cet ARNm est fortement structuré et les quatre sites de reconnaissance du ribosome sont tous engagés dans des structures en tige-boucle. L'analyse du transcriptome comparatif provenant des souches HG001 sauvage et Δ*rps*A montre une régulation négative de l'opéron αpsm1-4. Nous avons émis l'hypothèse que la délétion de *Sau*S1 a entrainé une chute de la traduction de l'ARNm et par conséquent une déstabilisation de l'ARNm. De manière intéressante, d'autres ARNm cibles identifiés codent aussi pour des exo-toxines impliquées dans la virulence et la structure secondaire de leurs ARNm sont prédites pour adopter des structures dans leurs régions 5' non traduites qui pourraient moduler l'accessibilité de la sous-unité 30S.

Dans ce manuscrit, nous avons analysé en détail le mécanisme d'action de *Sau*S1 sur l'opéron αpsm1-4. Nous avons ainsi démontré que *Sau*S1 active la formation du complexe d'initiation impliquant la sous-unité 30S, l'ARNm αpsm1-4, et l'ARNt initiateur. Des expériences *in vivo* ont confirmé le rôle important de *Sau*S1 pour recruter l'ARNm dans les polysomes. Dans ce travail, j'ai bénéficié de l'expertise de plusieurs membres de l'équipe. Isabelle Caldelari a construit plusieurs souches mutées au niveau du gène *rps*A, et a introduit l'étiquette Flag au niveau de l'extrémité C-terminale de la protéine pour effectuer les expériences de co-immunoprécipitation. Celle-ci a également mesuré le temps de demie vie de l'ARNm αpsm1-4 dans les souches sauvage HG001 et la souche mutant Δ*rps*A. Lucas Herrgott a suivi la traduction *in vivo* des ARNm αpsm1-4 et *hu* en analysant les profils des polysomes, suivi de l'analyse des ARNm par des expériences de Northern blot. Iskander Khusainov a préparé les sous-unités 30S de *S. aureus*, qui ont été utilisées pour des études structurales (Khusainov *et al.,* 2017). Dans ce qui va suivre, j'ai résumé les résultats que j'ai obtenu et qui ont été décrits dans le manuscrit présenté dans la partie résultat (§ I.1).

II.1.1. SauS1 ne suit pas le profil d'expression des protéines ribosomiques mais est synthétisée dès le milieu de la phase exponentielle de la croissance.

Au cours de la phase exponentielle de la croissance bactérienne, la synthèse des protéines ribosomiques est liée à la transcription des ARN ribosomiques et est régulée selon les changements environnementaux et aux différentes phases de croissance

(Nomura, 1999; Kaczanowska and Rydén-Aulin, 2007). *Sau*S1, codée par le gène *rpsA*, a un profil d'expression caractéristique puisque sa synthèse n'est pas stimulée dans les conditions où les autres protéines ribosomiques sont activement produites, par exemple en réponse aux stress antibiotiques, comme il a été récemment démontré par une analyse de spectrométrie de masse (Bonn *et al.*, 2016). Afin de comprendre le mécanisme de régulation, j'ai analysé l'expression de l'ARNm *rpsA* en fonction de la phase de croissance (Figure 1) par des expériences de Northern et suivi la synthèse de la protéine par Western. L'ARNm *rpsA* présente deux isoformes à cause de deux sites d'initiation de la transcription (TSS) (Figure 1a). Le transcrit court est constitutivement exprimé alors que le transcrit long commence à être exprimé à 3 h et s'accumule en fin de croissance (Figure 1b). Un profil de transcription similaire est observé dans d'autres souches de *S. aureus* (Figure 1c) indiquant un mécanisme de régulation conservé. Le profil d'expression de la protéine *Sau*S1, analysée par Western, montre que sa synthèse est en phase avec l'expression du transcrit long (Figure 1d).

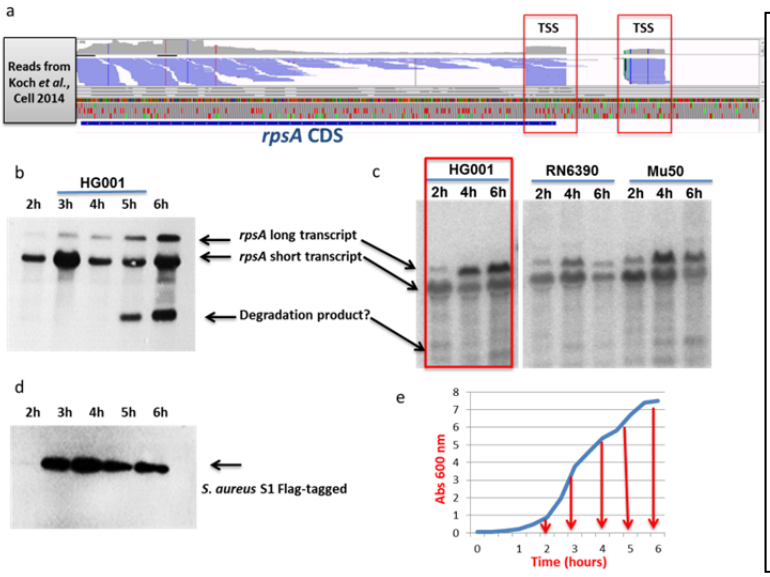

Figure 1 : Profils d'expression de *rpsA*. a) L'ARNm *rpsA* a deux TSS (jeux de données SRR949025 ENA-EBI obtenu par Koch *et al.*, 2014 réaligné sur le génome HG001 et visualisé avec IGV). b) et c) Les expériences de Northern montrent l'expression de l'ARNm *rpsA* dans différentes souches. Les ARN totaux ont été préparés à partir de cultures bactériennes en milieu BHI arrêté à différents moments de la croissance (2h, 3h, 4h, 6h). d) Analyse en Western de *Sau*S1 à partir d'un extrait protéique de cultures en BHI à 2h, 3h, 4h, 5h et 6h. e) Courbe de croissance de *S. aureus* qui montre les phases où les échantillons ont été prélevés.

II.I.2. SauS1 n'est pas une protéine essentielle mais est liée au métabolisme des ARN

Afin de mieux comprendre la fonction de *Sau*S1, j'ai délété le gène *rps*A par remplacement allélique. Chez *E. coli*, le gène *rps*A est essentiel et la protéine ribosomique *Eco*S1 est requise pour la traduction de la majorité des ARNm (Duval *et al.*, 2013). L'absence de phénotype de croissance observée dans la souche de *S. aureus* mutante dans des conditions de culture optimale de laboratoire indique que *Sau*S1, contrairement à *E. coli*, n'est pas essentielle. Toutefois, nous avons effectué une étude comparative des protéomes et des transcriptomes de la souche sauvage (HG001) et de la

souche mutante (HG001 Δ*rpsA*). Dans la souche mutante, le niveau d'expression de nombreux ARNm et ARNnc est altéré alors qu'un défaut de la maturation de certains ARNt a été detecté. Des expériences de rifampicine ont été réalisées pour suivre la stabilité de l'ARNm αpsm1-4. Le temps de demie-vie est clairement diminué dans la souche mutante. Ce résultat pourrait suggérer un rôle de *Sau*S1 dans la traduction (voir manuscrit dans la partie résultat, Figure 13).

II.I.3. SauS1 n'interagit pas avec le ribosome mais active la synthèse des PSM

Pour caractériser l'impact de *Sau*S1 sur la traduction de l'ARNm *psm* αpsm1-4, nous avons analysé les profils des polysomes couplés à des expériences de Northern. De cette façon, nous avons évalué le taux de traduction de l'ARNm dans les souches sauvage (WT) et mutante Δ*rps*A. Une différence importante est observée dans la quantité de l'ARNm *psm* αpsm1-4 trouvée dans les polysomes entre les deux souches: en absence de *Sau*S1, beaucoup moins d'ARNm (2,5 fois moins) est engagé sur les ribosomes pour être traduit. Ce comportement est spécifique de l'ARNm *psm* αpsm1-4, puisque l'ARNm *hu* est légèrement mieux traduit (1,78 fois plus) (Figure 2a et b). Pour confirmer l'implication directe de *Sau*S1 dans la traduction des PSM, j'ai purifié *Sau*S1 et ai testé son activité sur la formation du complexe d'initiation de la traduction par des expériences de Toe-printing. Les résultats ont montré que l'addition de *Sau*S1 augmente fortement la formation d'un complexe d'initiation actif sur l'ARNm *psm* αpsm1-4 (Figure 2c). Cet effet est spécifique puisqu'aucun effet n'a été observé pour un ARNm non structuré tel que l'ARNm *spa* codant pour la protéine A (manuscrit dans partie résultats, Figure S3).

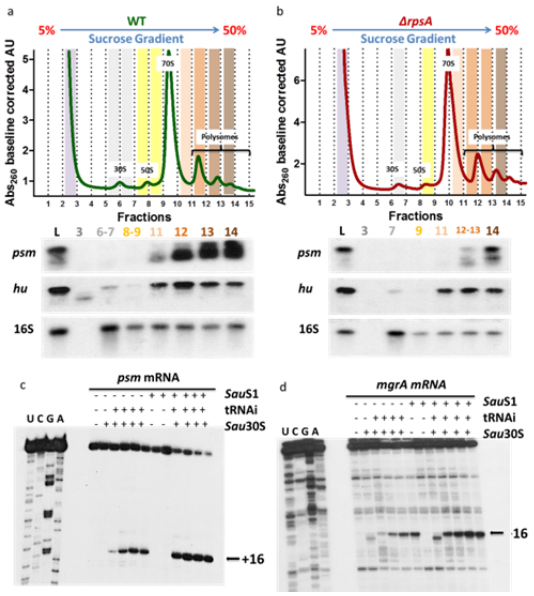

Figure 2 Effet de *Sau*S1 sur la traduction de l'ARNm *psm*, *hu* et *mgrA*. a) et and b), les profils des polysomes sont couplés à une analyse par Northern des ARNm *psm* et *hu* dans les souches WT et *ΔrpsA* (a et b, respectivement). L= lysat cellulaire. l'ARN 16S en ligne L est utilisé pour la normalisation. c) et d), effet de la protéine *Sau*S1 sur la formation des complexes d'initiation impliquant les ARNm de *S. aureus psm* c) et *mgrA* d). Les expériences montrent que l'addition de la protéine S1 induit la formation d'un complexe d'initiation actif surtout à des concentrations très faibles de 30S. L'arrêt de la réverse transcriptase en position +16 indique la présence du ribosome fixé à l'ARNm.

II.2. *Sau*S1 est une protéine chaperone de l'ARN

II.2.1. SauS1 interagit avec d'autres ARN

Afin d'identifier les partenaires protéiques et les ARN de *Sau*S1 *in vivo*, nous avons effectué des expériences d'immunoprécipitation suivies par des analyses protéomiques et de séquençage haut débit des ARN. Cela a permis de caractériser les protéines et les ARN qui ont été enrichis avec la protéine étiquetée. Parmi les ARN, nous avons trouvé plusieurs ARNnc dont RsaI, RsaH, RsaG, RsaE et RsaD, des ARNm hautement structurés comme les *psm*, des éléments régulateurs agissant en *cis* appelés « riboswitch » incluant celui de la flavine mononucléotide (FMN), et de nombreux ARNt.

Pour valider *in vitro* l'interaction directe entre S1 et les ARN, j'ai visualisé la formation des complexes par des expériences de gel retard. Celles-ci montrent que *Sau*S1 forme un complexe stable avec RsaI et RsaH (Figure 3a et b), et une interaction faible avec RsaE (données non montrées), alors qu'aucune interaction n'a été observée avec les autres ARNnc (RsaA et RsaG ; partie résultats, Figure 20). J'ai également vérifié l'interaction directe entre S1 et l'ARNm *psm* (Figure 3c).

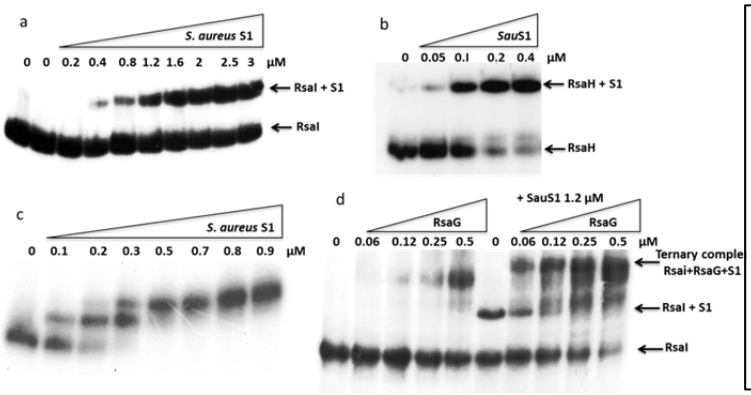

Figure 3. Analyse de la formation des complexex S1-ARN par gel retard. Formation du complexe entre les ARNnc RsaI (a) et RsaH (b), et l'ARNm *psm* (c). les ARN sont marqués radioactivement en 5' et les concentrations croissantes de S1 ont été ajoutées.
(d) A gauche, la formation du complexe entre RsaI et RsaG en absence de S1. A droite, la même expérience en présence de *Sau*S1. Un complexe ternaire entre RsaI, RsaG et S1 est observé.

Parmi les protéines potentiellement partenaires de *Sau*S1, nous avons détecté deux machineries cellulaires majeurs, le dégradosome avec tous ses composants hautement enrichis (dont les ribonucléases J1, J2, Y, la PNPase et l'hélicase CshA) et le ribosome.

II.2.2. Quel est le mécanisme d'action de SauS1?

Des expériences effectuées par Delphine Bronesky dans notre laboratoire ont démontré une interaction directe entre RsaI et RsaG, et comme nous n'avons pas mis en évidence de formation de complexe entre *Sau*S1 et RsaG, nous avons vérifié la possible formation d'un complexe ternaire qui pourrait expliquer les résultats de la co-immunoprécipitation. De manière intéressante, des expériences de formation des complexes par gel retard montrent clairement une bande retardée spécifique qui correspondrait au complexe formé entre RsaI, *Sau*S1 et RsaG (Figure 3d). De plus, la présence de S1 augmente de manière significative l'affinité entre RsaI et RsaG.

J'ai ensuite effectué *in vitro* des expériences d'empreinte en utilisant la cartographie en solution SHAPE qui modifie les riboses, DMS pour modifier les adénines en position N1 et les cytosines en position N3, et diverses ribonucléases qui coupent les régions en simple brin (RNase T1 pour les guanines) et en double brin (RNase V1). De cette façon, j'ai obtenu la structure de RsaI et identifié le site d'interaction avec RsaG. Les résultats sont en faveur de l'existence d'une structure en pseudoknot dans RsaI qui implique deux régions hautement conservées chez tous les staphylocoques: un motif riche en guanines exposé dans une boucle et une séquence interhélicoidale riche en uridines. Le motif riche en guanines se lie à un motif conservé riche en cytosines de RsaG (Geissmann *et al*, 2009). Par des expériences de pontage, j'ai montré une interaction possible entre *Sau*S1 et la séquence riche en uridines de RsaI. Il est possible que S1

pourrait perturber la structure en pseudoknot de RsaI afin de faciliter l'interaction avec RsaG (Partie résultats, Figure 24).

II.2.3. SauS1 est une protéine chaperone de l'ARN

*Sau*S1 interagit directement avec ses ARNm et ARNnc cibles et stimule l'interaction ARN-ARN probablement en modifiant leur structure secondaire. Pour vérifier si *Sau*S1 stimule la cinétique de l'interaction ARN-ARN et fonctionne comme une protéine chaperone de l'ARN, j'ai effectué des expériences préliminaires de « time resolved FRET » avec des oligonucléotides d'ARN modèle couplés à des fluorophores. La présence de *Sau*S1 accélère la formation des appariements ARN-ARN de 5 fois (Partie résultats, Figure 27).

III. Discussion et perspectives

Malgré le fait que la protéine *Sau*S1 n'est pas une protéine essentielle, elle est impliquée dans plusieurs processus cellulaires fondamentaux résumés dans la figure 4.

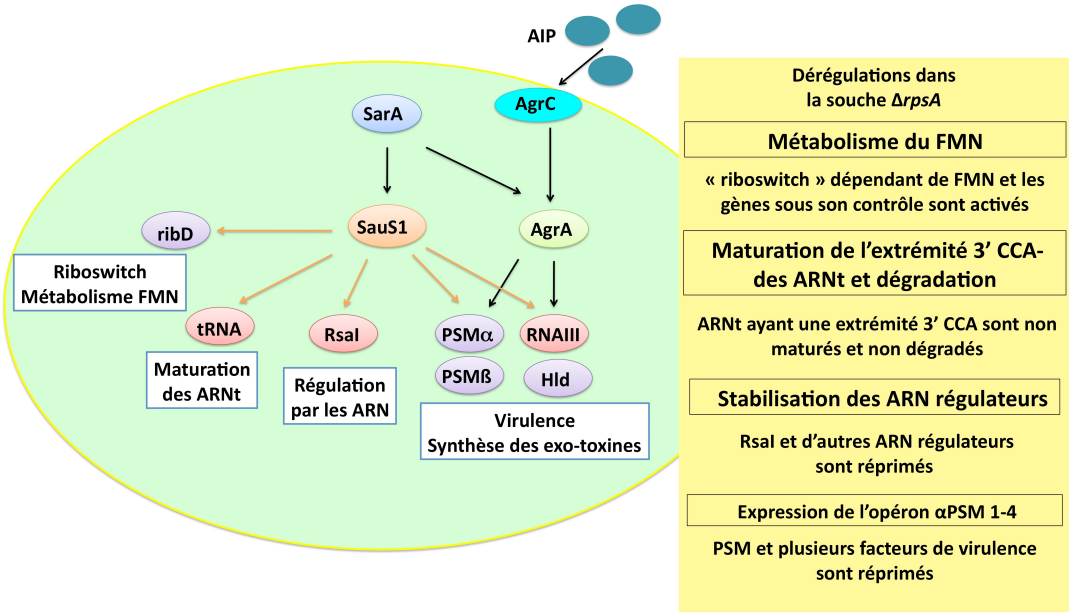

Figure 4. Les différentes fonctions de la protéine *Sau*S1: La protéine kinase membranaire AgrC active le régulateur de réponse AgrA lorsque le peptide signal sécrété AIP a atteint une concentration seuil. Les trois locus *PSM*s sont contrôlés à la fois au niveau transcriptionel par AgrA et au niveau traductionnel par *Sau*S1. SarA est un des facteurs activant la synthèse de *rpsA* et des transcrits *psm*. Des expériences de co-immunoprécipitation utilisant une version modifiée de *Sau*S1 portant une étiquette Flag suivies d'un séquençage des ARN a permis l'identification *in vivo* de différentes cibles ARN incluant divers ARNm, ARN régulateurs, riboswitch et des ARNt dont le CCA est aussi présent dans le gène. Toutes ces ARNs ont un taux affecté dans la souche mutante Δ*rpsA*. Des exemples de dérégulations pour chaque classe d'ARN sont donnés dans l'encadré de couleur jaune.

Même si elle n'est pas associée directement au ribosome, *Sau*S1 favorise l'initiation de la traduction d'ARNm structurés. Le mécanisme de cette stimulation n'est pas encore connu mais il est possible que *Sau*S1, comme *Eco*S1, puisse fragiliser les structures d'ARNm au niveau des sites d'initiation de la traduction, facilitant l'accès au ribosome. Nous avons démontré que l'ARNm *psm* αpsm1-4 nécessite *Sau*S1 pour faciliter l'initiation de sa traduction. A forte concentration (> 1 µM), les PSMα possèdent une activité lytique *in vitro* sur les neutrophiles (Löffler *et al.,* 2010) et sur les érythrocytes (Cheung et Otto, 2012). Ce pouvoir lytique est lié à leur propriété amphipathique. En fait, les PSMα s'agrègent à la surface des membranes pour former des pores transmembranaires. En outre, il a été montré que PSMα1 et PSMα2 présentaient une activité bactéricide contre les bactéries d'un genre différent de *Staphylococcus*. Ainsi ces toxines confèreraient *à S. aureus* la capacité d'entrer en compétition avec d'autres espèces bactériennes pour la colonisation de l'hôte (Joo et Otto, 2011).

*Sau*S1 peut-elle moduler la virulence de *S. aureus* en agissant sur la production des PSM? Pour aborder cette question, en collaboration avec l'équipe de François Vandenesch (Lyon), nous caractériserons l'impact fonctionnel de la protéine S1 sur la pathogénicité de *S. aureus*, en utilisant différentes approches *in vivo* et *in vitro*: dosage par spectrométrie de masse des PSM dans les surnageants de culture, infection des cellules immunitaire (macrophages, neutrophiles), analyse de la formation de biofilms entre les souches sauvage et mutante *ΔrpsA* et la souche mutante complémentée avec un plasmide qui exprime le gène *rps*A sous son propre promoteur, et analyse de l'effet de *Sau*S1 dans divers modèles d'infection chez la souris.

Des résultats plus récents montrent que *Sau*S1 est aussi requise pour faciliter la traduction de l'ARNIII qui code pour l'hémolysine delta, un autre peptide de type PSM induit par le système *agr*. Il a été suggéré que la traduction de *hld* est retardée de 1h par rapport à la transcription de l'ARNIII. Ce décalage entre transcription et traduction a aussi été observé pour les autres PSMα. Du fait que la protéine *Sau*S1 est exprimée principalement à haute densité cellulaire, nous proposons que la protéine serait responsable de cet effet de décalage pour activer de manière coordonnée la traduction des PSM. Nous envisageons d'utiliser un promoteur constitutif pour exprimer *SauS1* et analyser si, dans ce contexte, le délai entre la transcription et la traduction des PSM est aboli.

S1 est-elle impliquée dans des processus de régulation des ARNnc? Dans diverses bactéries à Gram-négatif, les protéines chaperones, dont Hfq et ProQ, participent à la régulation des ARNnc en les stabilisant et en facilitant leurs appariements avec leurs ARNm cibles. Chez *S. aureus*, aucune protéine n'a encore été impliquée dans ces mécanismes. ProQ n'est pas présente, et Hfq a une composition en acides aminés différente au niveau du site de liaison de l'ARN, ce qui ne permet pas de former des complexes ARN-ARN. Nous avons trouvé que *Sau*S1 est directement associée à plusieurs ARNnc et avons montré que cela pourrait, au moins dans un cas, stimuler l'hybridation entre l'ARNnc et sa cible (RsaI-RsaG). Bien que l'activité chaperone à l'ARN de *Sau*S1 a été démontrée, les mécanismes détaillés par lesquels elle favorise l'interaction ARN-ARN doivent encore être élucidés. Des résultats préliminaires suggèrent que celle-ci favorise la cinétique d'appariement entre deux fragments d'ARN dans un système modèle. Pour montrer que la cinétique de liaison de l'ARNnc aux cibles est stimulée par S1, il sera possible d'utiliser l'appareil SwitchSense disponible dans notre unité. Nous pourrons tester différents systèmes ARNnc-cibles en présence ou en absence de *Sau*S1.

Est-ce que S1 est impliquée dans la stabilité et la maturation des ARN? *Sau*S1 a été retrouvée en association avec le dégradosome, la machinerie responsable pour la dégradation/maturation des ARN. Les nombreux ARNt identifiés dans les expériences de co-immunoprécipitation suggèrent un défaut de maturation qui devra être confirmé par des expériences de Northern.

Ainsi, pour la première fois, l'ensemble de mes résultats ont permis de démontrer le rôle clé d'une protéine fixant l'ARN pour la traduction d'ARNm structuré et pour la régulation de l'expression des gènes. Il sera intéressant de vérifier si ces fonctions sont conservées dans les bactéries de type Gram-positif et qui sont éloignés dans l'évolution telles que *Bacillus subtilis*. L'utilisation d'autres approches telles que le Grad-seq devrait aider à mettre en évidence d'autres protéines impliquées dans la régulation post-transcriptionnelle de l'expression des gènes de *S. aureus* (Smirnov *et al.*, 2016).

IV. Bibliographie

Cheung G.Y.C., Duong A.C., Otto M. Direct and synergistic hemolysis caused by Staphylococcus phenol-soluble modulins: implications for diagnosis and pathogenesis. *Microbes Infect.* 2012 Apr;14(4):380-6. doi: 10.1016/j.micinf.2011.11.013. Epub 2011 Dec 7.

Cheung G.Y.C., Otto M. Phenol-soluble modulines-critical determinants os staphylococcal virulence. *FEMS Microbiol Rev.* 2014 Jul;38(4):698-719. doi: 10.1111/1574-6976.12057. Epub 2014 Jan 16

Duval M., Korepanov A.,, Fuchsbauer O., Fechter P., Haller A., Fabbretti A., Marzi S. et al. Ribosomal protein S1 unfolds structured mRNAs onto the ribosome for active translation initiation. *PLoS Biol.* 2013 Dec; 11(12): e1001731

Geissmann T., Chevalier C., Cros M.J., Boisset S., Fechter P., Noirot C., Romby P. et al. A search for small noncoding RNAs in Staphylococcus aureus reveals a conserved sequence motif for regulation. *Nucleic Acids Res.* 2009 Nov;37(21):7239-57. doi: 10.1093/nar/gkp668.

Green C. J., Vold B. S. Staphylococcus aureus has clustered tRNA genes. , *J Bacteriol.* 1993 Aug;175(16):5091

Joo H-S, Cheung G.Y.C., Otto M. Antimicrobial activity of community-associated methicillin- resistant Staphylococcus aureus is caused by phenol-soluble modulin derivatives. *J Biol Chem.* 2011 Mar 18;286(11):8933-40. doi: 10.1074/jbc.M111.221382. Epub 2011 Jan 28

Kaczanowska M. and Rydén-Aulin M.. Ribosome biogenesis and the translation process in Escherichia coli. *Microbiol Mol Biol Rev.* 2007 Sep;71(3):477-94

Khusainov I., Marenna A., Cerciat M., Fechter P., Hashem Y., Marzi S., Romby P., Yusupova G., Yusupov M. A glimpse on Staphylococcus aureus translation machinary and its control. Mol Biol 2016 Jul-Aug;50(4):549-557

Koch G., Yepes A., Forsner K.U., Wermser C., Stengel S.T., Modamio J., Ohlsen K., Foster K.R., Lopez D. Evolution of resistence to a last-resort antibiotiv in Staphylococcus aureus via bacterial competition. *Cell* 2014 Aug28 ; 158(5) :1060-71.doi : 10.1016j

Löffler B., Hussain M., Grundmeier M., Brück M., Holzinger D., Varga G., et al. Staphylococcus aureus panton-valentine leukocidin is a very potent cytotoxic factor for human neutrophils. *PLoS Pathog.* 2010 Jan 8;6(1):e1000715. doi: 10.1371/journal.ppat.1000715

Nomura M. Regulation of Ribosome Biosynthesis in Escherichia coli and Saccharomyces cerevisiae: Diversity and Common Principles *J Bacteriol.* 1999 Nov; 181(22): 6857–6864

Roberts R.J. Staphylococcal transfer ribonucleic acids. *J Biol Chem.* 1974 Aug 10;249(15):4787-96

Smirnov A, Förstner KU, Holmqvist E, Otto A, Günster R, Becher D, Reinhardt R, Vogel J. Grad-seq guides the discovery of ProQ as a major small RNA-binding protein. *Proc Natl Acad Sci U S A.* 2016 Oct 11;113(41):11591-11596.

Introduction

I. *Staphylococcus aureus* is a versatile opportunistic human pathogen

Staphylococcus aureus was discovered in 1880 by Sir Alexander Ogston (Ogston, 1881). He observed grape-like clusters of bacteria when examining a purulent discharge from patients with post-operative wounds and he named them "staphyle", the greek expression for a bunch of grapes. Few years later, in 1884, Friedrich Julius Rosenbach succeeded in isolating yellow bacterial colonies from abscesses and named them *Staphylococcus aureus*, "aureus" from the latin word referred to golden color caused by the presence of carotenoids (Rosenbach, 1884). 121 years later, this golden pigment staphyloxanthin, has been demonstrated to be one of the many virulence factors produced by *S. aureus*. It shields the microbe from oxidation-based clearance promoted by the neutrophil oxidative burst, thus allowing its survival in blood (Liu et al., 2005).

Among staphylococci, *S. aureus* is the most virulent and pathogenic for humans, being responsible of wide range of diseases from a variety of skin, wound and deep tissue infections to more life-threatening conditions such as pneumonia, endocarditis, septic arthritis and septicemia (**Figure 1**). This bacterium is one of the most common species responsible for nosocomial infections and it might also cause food poisoning, scalded-skin syndrome and toxic shock syndrome, through production of several toxins. Intriguingly, despite its invasive opportunism, *S. aureus* replicates and evolves in a large proportion of the human population as a harmless colonizing organism that might never cause diseases. Approximately 30% of the population is asymptomatically colonized by *S. aureus* (Wertheim et al., 2005). The anterior nasal mucosa is the most frequent site for the colonization of healthy human carriers (Kluytmans et al., 1997); other anatomical sites are throat (Mertz et al., 2007), perineum, gastrointestinal tract (Yotis, 1963), axillae, groin (Gordon and Lowy, 2008), and vagina (Bourgeois-Nicolaos et al., 2010). Although humans are the primary natural reservoirs, domestic animals, livestock, and fomites may serve as adjunctive reservoirs.

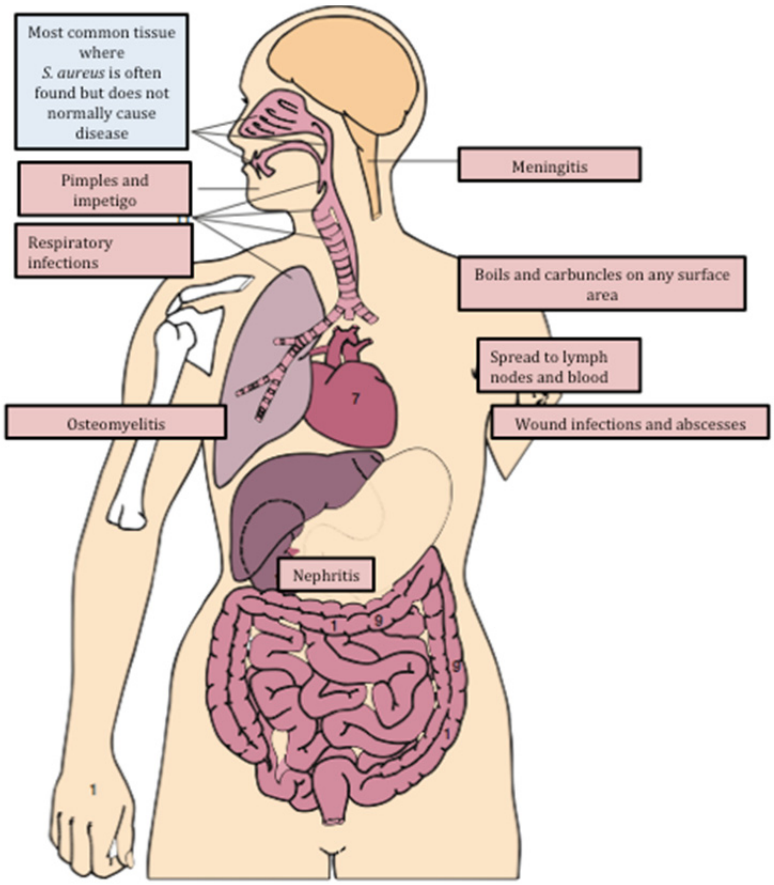

Figure 1. Sites of colonization and diseases caused by *S. aureus*. *Staphylococcus aureus* can be a human commensal or a potentially lethal opportunistic pathogen. Indeed, it is able to survive and multiply within the human body by creating microenvironments that protect it from host immune attack (Rooijakkers et al., 2005). It can cause life-threatening diseases, as well as minor diseases such as soft tissue infections.

S aureus is a Gram-positive bacterium, has a cell diameter of 0.6 µm, is non-motile, non-spore-forming, and is a facultative anaerobe. It belongs to the genus *Staphylococcus* of the *Micrococcaceae* family. This genus is traditionally divided in two groups based on the bacteria ability to produce coagulase, an enzyme that causes blood clotting. The coagulase-positive staphylococci includes *Staphylococcus aureus*, and the coagulase-negative staphylococci (CoNS) are common commensals of the skin. Both coagulase and staphyloxanthin are contributing to the host immune system evasion strategies, part of *S. aureus* impressive armory which relies on antigens (adhesins and capsule) that facilitate adhesion to host cells, enzymes (coagulases, lipases, hyaluronidases, staphylokinases, nucleases) for tissue degradation and nutrient acquisition, and toxins (α–, β– and δ- haemolysins, P-V leukocidins, enterotoxins, exfoliative toxins, Toxic Shock Syndrome toxin) for the evasion of host defenses. Their production requires the need for *S. aureus* to make physiological adjustments for energy conservation. Thus, the virulence

factors are primarily targets of gene regulation, which reprogram the *S. aureus* lifestyle upon infection.

II. Virulence determinants in *Staphylococcus aureus* play central role in its pathogenesis

S. aureus has a circular chromosome of 2.8 M base pairs (bp) with low G+C composition (32.8%). Its genome has about 2700 coding sequences among which approximately 23% have still unknown functions (data from the most recent annotation of the strain HG001 (Caldelari et al., 2017). Several virulence factors are chromosomally encoded while others are parts of pathogenicity islands (PIs), which are the repository of many toxins, adherence and invasion factors, superantigens, and secretion systems (Novick et al., 2010; Novick and Ram, 2016; Novick and Subedi, 2007).

The pathogenicity of *S. aureus* is a complex process based on extremely coordinated expression of virulence factors at appropriate time among the different stages of host infection (**Table 1**): colonization, escape host immuno-defense, growth and cell division, and spreading (**Figure 2**). Their expression also responds to a plethora of environmental cues including bacterial cell density, amino acid limitation, metal depletion, decreased pH, and oxidant production. Through integration of these environmental cues, *S. aureus* can simultaneously coordinate expression of the genes coding for surface proteins involved in adhesion and defense against the host immune-system and only later during the post-exponential phase, *S. aureus* starts to secrete toxins able to disrupt host cells and tissues facilitating the spread of the infection (Thammavongsa et al., 2015).

Studying the expression pattern of virulence factors during the infection in the host could be quite difficult (Burian et al., 2010; Cheung et al., 2004; Montgomery et al., 2008; Que et al., 2005) and many factors, including cellular immune factors and nutrient conditions, might add an extra layer of regulation. In a few studies, the use of serum in *S. aureus* cultures to induce the expression of virulence factors (Ishii et al., 2014; Oogai et al., 2011) has produced promising results, but most commonly, bacterial media, such as Trypticase soy broth (TSB), brain heart infusion (BHI) broth, and Luria-Bertani (LB) broth, have been used for *S. aureus* growing. In the following description of several

major virulence factors, their timed expression is referred to different phases of the growth in these media.

VIRULENCE FACTORS	PUTATIVE FUNCTIONS
Cell surface factors	
Staphylococcal protein A (SpA)	Bind to IgG, interfering with opsinization and phagocytosis
Fibronectin-binding proteins (FnbpA and FnbpB)	Attachment to fibronectin and plasma clot
Clumping factor proteins (ClfA and ClfB)	Mediate clumping and adherence to fibrinogen in the presence of fibronectin
Capsular polysaccharides	Reduce phagocytosis by neutrophils; enhance bacterial colonization and persistence on mucosal surfaces
Staphyloxanthin	Resistance to neutrophil reactive oxidant-based phagocytosis
Secreted factors	
Superantigens	
Staphylococcal enterotoxins (SEA, B, C, D, E, G and Q)	Massive activation of T cells and antibody presenting cells
Toxic shock syndrome toxin-1 (TSST-1)	Massive activation of T cells and antibody presenting cells
Cytolytic toxins	
α-hemolysin	Induce lysis on a wide spectrum of cells, mainly platelets and monocytes
β-hemolysin	Hydrolysis of sphingomyelin of the plasmatic membrane of monocytes, erythrocytes, neutrophils and lymphocytes; make cells susceptible to other lytic agents
γ-hemolysin	Induce lysis on erythrocytes and leukocytes
Leukocidin family	
Leukocidins E/D and M/F-PV	Induce lysis on leukocytes
Panton-Valentine leukocidin (PVL)	Induce lysis on leukocytes
Various exoenzymes	
Lipases	Inactivate fatty acids
Proteases	
Serine (e.g. exfoliative toxins ETA and ETB)	Inactivate neutrophil activity; activate T cells (only ETA and ETB)
Cysteine (e.g. staphopain)	Block neutrophil activation and chemotaxis
Aureolysin	Inactivate antimicrobial peptides
Hyaluronidase	Degrade hyaluronic acid
Staphylokinase (SAK)	Activate plasminogen; inactivate antimicrobial peptides
Coagulase	
CoA	Coagulation promoting virulence factor
Miscellaneous proteins	
Staphylococcal complement inhibitor (SCIN)	Inhibit complement activation
Extracellular fibrinogen binding protein (Efb)	Inhibit complement activation
Chemotaxis inhibitory protein of S. aureus (CHIPS)	Inhibit chemotaxis and activation of neutrophils
Formyl peptide receptor-like 1 inhibitory protein (FLIPr)	Inhibit chemotaxis of neutrophils
Extracellular adherence protein (Eap)	Inhibit neutrophil migration

Table 1 Major virulence factors involved in the pathogenesis of *Staphylococcus aureus* and respective putative functions.

II.1. Tissue colonization

Interaction with endothelial cells is a critical primordial step of infection and several bacterial proteins have been shown to be involved. They include secreted proteins and Cell Wall Associated proteins (CWA). Hereafter, I provide few examples of different mechanisms with which they promote adhesion and prevent clearance by the host immune system.

The extracellular adherence protein (Eap) of *S. aureus* participates in a wide range of protein–protein interactions that facilitate the initiation and dissemination of *Staphylococcal* disease. Eaps are secreted proteins involved in adherence and internalization of bacteria in eukaryotic cells (Haggar et al., 2003; Palma et al., 1999). They have strong anti-inflammatory properties resulting in a decreased recruitment of neutrophils at the sites of infection. These immunomodulating proteins are also able to inhibit T and B cells proliferation (Haggar et al., 2005).

The cell-surface proteins are the frontline of infection, involved in adhesion, internalization, colonization (Malachowa et al., 2011; Sibbald et al., 2006), invasion of non-phagocytic host cells (Foster et al., 2014), and immune evasion. *S. aureus* produces up to 24 CWA, which are covalently anchored to the cell wall peptidoglycan. Among them the most abundant are the protein A (*spa*), Sbi and the fibronectin binding proteins (FnBPs) (Foster et al., 2014). *Sp*a is expressed during the exponential growth phase (Gao and Stewart, 2004). It is involved both in adhesion to host cells and in evading innate immune responses mediated by immunoglobulins binding, bacterial opsonisation and stimulation of TNF-α pro-inflammatory response (Atkins et al., 2008; DeDent et al., 2007; Gonzalez et al., 2015; Thammavongsa et al., 2015; Zecconi and Scali, 2013). Protein A also impacts the normal function of B-cells and induces their apoptosis, thus preventing the host from developing immunological memory (Goodyear and Silverman, 2004). Staphylococcal binder of immunoglobulin (Sbi) is both a secreted and CWA protein that, as protein A, binds to IgG (Smith et al., 2011). Both forms of the proteins participate in immune evasion whereas only the secreted form triggers the activation of the complement (Smith et al., 2012). Indeed, the secreted form of Sbi interacts with the antigen recognition of B-cells, rendering the pathogen undetectable and as a result, opsonins are not released and the immune response is not triggered (Markiewski and Lambris, 2007; Smith et al., 2012; Toapanta and Ross, 2006). Binding to the IgGs

contained in the human serum stimulates its expression, this is why in laboratory growth conditions, Sbi expression is very low. Fibronectin binding proteins (Fnbps) are adhesins, which as other cell wall-associated proteins, are expressed during the exponential phase of bacterial growth (Fitzgerald et al., 2012). They form fibronectin bridges required to stabilize the adhesion of the pathogen to host tissues (Martin et al., 2012; Piroth et al., 2008). Moreover, FnbpA and FnbpB are able to bind platelets whose activation and aggregation promotes thrombus formation (Kerrigan et al., 2002). The formation of platelet-fibrin thrombi protects bacteria from neutrophil recognition (Hartleib et al., 2000).

II.2. Immune evasion (non CWA or Eap)

Normally, the blood coagulation system is a process resulting in the formation of a blood clot, which closes the injured part of the vessel. However, this process can also be activated by the immune system in response to infection. In this case, the bacteria are trapped in a blood coat preventing their dissemination in other sites of the body. Many organisms, including *S. aureus* have developed strategies able to convert the blood coagulation as an advantage to ensure their survival. Indeed, when a clot or eventually an abscess is formed, the bacteria are protected from the host immune attack. Coagulase (Coa) is the main coagulation-promoting factor produced by *S. aureus.* In combination with other proteins, it activates the host prothrombin inducing fibrin formation that protects the pathogen against phagocytosis by immune cells (Friedrich et al., 2003; Kroh et al., 2009) and promotes abscess formation (Cheng et al., 2010; McAdow et al., 2012)).

S. aureus has also other specific proteins that affect the innate and adaptive immune system. The innate immune modulators such as chemotaxis inhibitory protein (CHIPS) and the staphylococcal complement inhibitor (SCIN), are employed in the inactivation of the human complement (van Wamel et al., 2006).

II.3. Tissue invasion and dissemination

S. aureus secreted proteins are involved in host tissue damage, inflammation, invasion and disruption of the host immune system in order to facilitate bacteria dissemination (Foster, 2005; Lin and Peterson, 2010; Malachowa et al., 2011). These secreted factors

can be divided into four groups: superantigens, exoenzymes, miscellaneous proteins and cytolytic (poreforming) toxins.

II.3.1 Superantigens

Superantigens (Sags) are secreted immune-stimulatory low-molecular weight (19,000 to 30,000 Da) enterotoxins involved in many human diseases, including allergy, autoimmune diseases, food poisoning and toxic shock syndrome (TSS) (Chesney et al., 1997; Parrillo, 1993; Reingold et al., 1982). These proteins are exceptionally resistant to heat, to proteolysis and acidic conditions and they are highly resistant to desiccation (Dinges et al., 2000; McCormick et al., 2001). The production of superantigens interferes with antibody production and phagocytic cell chemotaxis. Indeed, irrespective of their antigen specificity and function, Sags induce massive activation of T cells resulting in a cytokine overproduction, aggravation of allergic inflammation and shock (Xu and McCormick, 2012).

II.3.2 Exoenzymes

S. aureus secretes several extracellular enzymes whose principal goal is to disrupt host tissues, to inactivate host antimicrobial mechanisms (e.g. antibodies and complement mediators), and to produce nutrients for bacterial growth and facilitate dissemination. In the large group of exoenzymes are included lipases, proteases and staphylokinase (SAK).

Lipases are deoxyribonuclease (DNase) and fatty acid modifying enzymes that catalyze the hydrolysis of the ester bonds between glycerol and fatty acids to form triglycerides and this is believed to aid the bacteria to breakdown host tissue resulting in nutrients availability (Lu et al., 2012). Among the proteolytic enzymes produced by *S. aureus* there are the metalloproteinase (aureolysin, Aur), the serine glutamyl endopeptidase referred to as the V8 protease (serine protease, SspA) and two related cysteine proteinases, the staphopain (ScpA) and the cysteine protease (SspB) (Arvidson et al., 2000). Their deletion resulted in increased abundance of secreted and surface-associated virulence factors. Indeed, these proteases work to degrade indiscriminately both "self" and "host" proteins.

The metalloprotease, Aureolysin (Aur) is responsible for the proteolytic cleavage and activation of SspA (Drapeau, 1978) as well as for the cleavage of the surface-associated clumping factor ClfB, which protects the bacteria from phagocytosis (McAleese et al., 2001). The SspA protease, produced from a polycistronic operon with *sspB* (Reed et al., 2001), was shown to induce the cleavage of fibrinogen-binding protein (McGavin et al., 1997), of surface protein A (Spa) (Karlsson et al., 2001), and host proteins such as the heavy chain of all human immunoglobulin classes (Prokesova et al., 1992).

The secreted cysteines Staphopain A (ScpA) and Staphopain B (SspB) are known to induce cleavage of different host substrates including fibrinogen, collagen and elastin (Potempa et al., 1988). ScpA degrades fibers composed of elastin in the connective tissues, and both ScpA and SspB contribute to the turnover of collagen, the main component of the connective tissue (Potempa et al., 1988). In the bloodstream, fibrinogen cleavage by ScpA and SspB interferes with plasma clotability, resulting in a tendency to induce bleeding (Ohbayashi et al., 2011). ScpA can also inhibit neutrophil activation and chemotaxis (Laarman et al., 2012). The proteolitic susceptibility of cell-wall associated proteins such as FnBP and Protein A, both involved in adherence to host cells, could suggest that these extracellular proteases are important for the release of *S. aureus* from colonization sites to other sites of the human body. It has also been proposed that the degradation of toxins, such as α-haemolysin, induced by the proteases may downregulate *in vivo*, the virulence of *S. aureus* (Shaw et al., 2004).

Staphylokinases (SAKs) are potent extracellular prothrombin activators (Osamu Matsuo, Masashi Sakai , 2017 - (Dinges et al., 2000) able to convert human plasminogen (plg) to active plasmin (Kwiecinski et al., 2010), a serine protease with a broad-spectrum of substrates such as fibrin, collagen and elastin. Plasmin-mediated proteolysis of different extracellular substrates potentially contributes to bacterial virulence by facilitating staphylococci entry into the deeper host tissues (Bergmann and Hammerschmidt, 2007; Bhattacharya et al., 2012; Sanderson-Smith et al., 2012). The role of this factor in virulence is however controversial. Indeed, Jin *et al.* showed that staphylokinase-deficient *S. aureus* strain is more virulent compared to wild-type strain, whereas Piechowicz *et al.* did not find such a phenotype (Jin et al., 2003; Piechowicz et al., 2010).

II.3.3. Cytolytic (poreforming) toxins

Immune evasion is, to a large extent, due to cytolytic toxins which are secreted to kill immune cells, among which the most important are the bi-component leukotoxin family, α-toxin and the phenolsoluble modulin (PSM) peptides (Otto, 2014).

II 3.3.1 Leukotoxins

S. aureus strains associated with human infections produce four types of leukotoxins: the Panton-Valentine Leukocidin (PVL), gamma (γ)-haemolysin (HlgACB), Leukotoxin ED (LukED), and Leukotoxin AB/GH (LukAB/GH). They are bi-component proteins composed of two subunits secreted separately and then assembled in hexameric or heptameric oligomers having high affinity for leukocytes. They mainly act by forming pore in the membranes of leukocytes leading to their lysis, all four leukotoxins have also been demonstrated to kill human neutrophils (Loffler et al., 2010). Moreover, the γ-haemolysin can cause the lysis of red blood cells thus promoting the survival of *S. aureus* in bloodstream (Kaneko et al., 1997; Malachowa et al., 2011).

II.3.3.2 α-haemolysin

S. aureus α-toxin (α-haemolysin, Hla) is the prototype for the class of small β-barrel pore-forming cytotoxins (PFTs) (Parker and Feil, 2005). For many years, *Staphylococcus aureus* α-toxin has been considered as the major virulence factor. Indeed, this peptide is secreted as a water soluble monomer and then oligomerized into a heptameric structure on the host cell membrane to introduce pores and to cause host cell lysis (Berube and Bubeck Wardenburg, 2013). Following the recent identification of multiple toxin receptors, it is now understood that PFTs exert subtle changes in cell activity and host physiology even at sub-lytic concentrations. Exposure to α-toxin can cause cellular death by necrosis, apoptosis, or pyroptosis, through activation of different cellular pathways (Craven et al., 2009; Essmann et al., 2003).

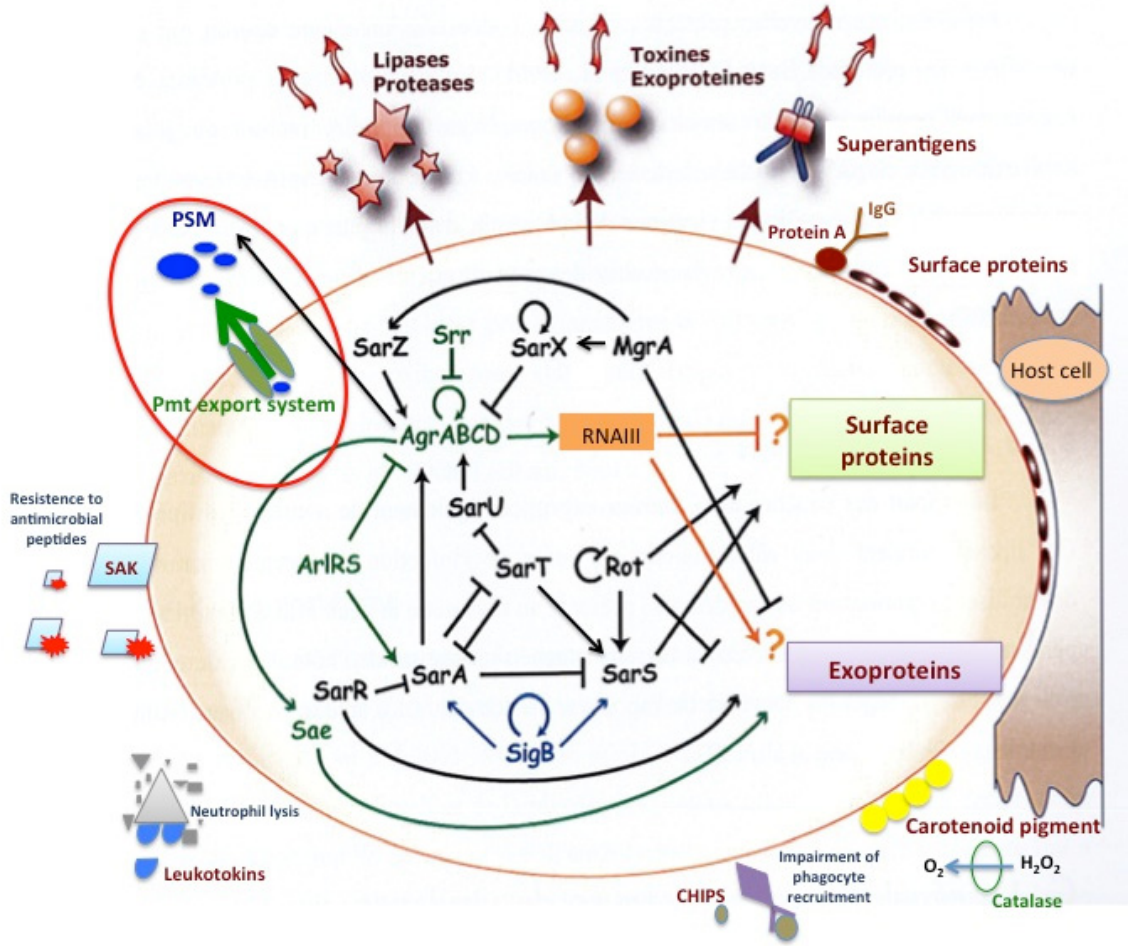

Figure 2 Mechanisms by which *S. aureus* escape host innate immune defense and virulence factors regulation. The synthesis of virulence factors is under the control of sophisticated mechanisms of regulation. Two component system (green), global transcriptional regulator (black) and the Sigma B factor (Blue). Golden carotenoid pigment provides an antioxidant shield whereas catalase detoxifies hydrogen peroxide. Resistance to cationic antimicrobial peptides is afforded by positive charge modifications of the cell wall, aureolysin-mediated proteolysis, and binding/inactivation by staphylokinase. Protein A binds Fc domains of Igs in a nonopsonic manner. The pore-forming toxins g-haemolysin and Panton-Valentine leukocidin preferentially target leukocyte membranes causing their lysis. The plasminogen (PG) binding protein staphylokinase (SAK) activates the zymogen to the active protease plasmin, which can degrade complement opsonin C3b and the immunoglobulin Fc domain. (Adapted from (Nizet, 2007).

II.2.3.3 PSMs

PSMs are virtually produced by all staphylococcal species and given their crucial role in *S. aureus* pathogenicity, they have recently received large interest. In *S. aureus*, PSMs constitute a group of seven different peptides that are encoded by three different loci in the bacterial genome (Cheung et al., 2014; Wang et al., 2007) (**Figure 3**).

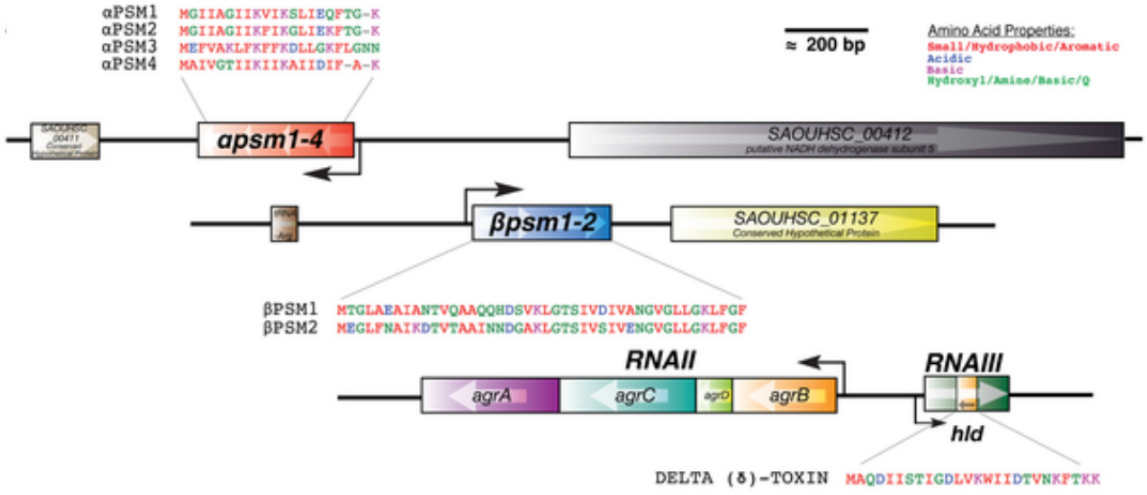

Figure 3 Phenol soluble modulins are small peptides expressed from three loci of the *S. aureus* genome. Phenol soluble modulins (PSMs) are encoded in two operons, the alpha (*αPSM1* to *4*) and beta (*βPSM1* to *2*) operons, and δ-toxin is embedded within the regulatory RNAIII (*hld*). (Figure adapted from (Schwartz et al., 2012).

Their coding sequences are small enough to have eluded detection by conventional gene annotation programs, and they are still poorly annotated in public databases (Wang et al., 2007). We have recently sequenced and annotated the genome of the strain HG001, a derivative of RN1 (NCT8325) strain with restored *rbsU* (a positive activator of SigB). Prokka software (Seemann, 2014), used to predict coding sequences (CDS), has failed to include the *psmα* locus which has been manually added (Caldelari et al., 2017). The α-type peptides are ~20 to 25 amino acids in size and, in *S. aureus*, comprise PSMα 1-4 and the δ-toxin, which are encoded by the *psmα* and *hld* loci, respectively. *S. aureus* PSMβ1 and PSMβ2 are members of the larger (~45-amino-acid) β-type PSMs and are encoded by the *psmβ* locus. The *hld* gene is embedded within RNAIII, the intracellular effector of the accessory gene regulator (agr) system ((Novick et al., 1993), see § III). In *S. aureus*, PSMα peptides and δ-toxin are highly abundant, with δ-toxin usually more strongly expressed than PSMα probably to compensate its only moderate cytolytic capacities. Only small amounts of PSMβ peptides are produced under common laboratory conditions (Cheung et al., 2010).

PSMs are responsible for the development of *S. aureus* infections, particularly in highly virulent strains. The secretion of these peptides does not occur via canonical system, such as Sec-dependent transport, but requires dedicated secretion mechanisms. The Phenol-soluble modulin transporter (Pmt), present in all staphylococcal species, was recently identified as specific PSM exporter. Pmt consists of four genes (*pmtA, pmtB,*

pmtC, pmtD), encoding an ABC transporter with two separate membrane parts (PmtB, PmtD) and two separate ATPases (PmtA, PmtC). It assists PSM transport in a specific and energy-dependent fashion (Chatterjee et al., 2013). Interestingly, the ABC is essential for bacterial survival. Indeed, its deletion leads to an abnormal accumulation of PSM toxins in the cytoplasm, resulting in growth deficiency, cellular defect and autolysis (Chatterjee and Otto, 2013). Pmt is ubiquitously present among all Staphylococcus species and is responsible of exporting all types of PSM peptides. Upstream of the pmtA-D genes is a gene predicted to encode a transcriptional regulator named PmtR. Binding of PmtR to the operator of the *pmt* promoter causes repression of the *pmt* cluster. PSMs bind to PmtR and disrupt the PmtR-pmt promoter complex, which enables pmt transcription. Thus, PSMs positively influence the expression of pmt to facilitate their own export (Joo et al., 2016; Joo and Otto, 2016). Moreover, Pmt act to protect *S. aureus* from the antimicrobial activity of the PSM secreted by other co-colonizing staphyloccocal bacteria (Cogen et al., 2010).

Despite the fact that these toxins have different structures and different target specificity, their mechanism of action is quite similar. At low doses (nanomolar concentration), they form β-barrel pores in the cytoplasmic membranes of target cells and cause leakage of the cell's content while, when present at high doses (micromolar concentration), they have cytolytic activity. In contrast to α-toxins and bi-component leukotoxins that induce membrane pore formation by binding to specific receptors, the PSMs are believed to induce the disruption of cytoplasmic membrane in a less specific manner without receptor recognition. Most probably, the phospholipid composition and membrane charge are important for cell susceptibility to PSMs (Otto, 2015).

PSMα of *S. aureus* and *S. epidermidis*, are able to lyse human white and red blood cells (Otto, 2012). Additionally, as soluble molecules they also contribute to biofilm detachment/dissemination acting as surfactant-like peptides (Kong et al., 2006; Periasamy et al., 2012; Tsompanidou et al., 2011). This process allows the spread of the infection in other parts of the body (Periasamy et al., 2012). In contrast to this activity, it has been also demonstrated that, when polymerized into amyloid fibers, some PSMs promote biofilm stability (Schwartz et al., 2012). These PSM fibers share morphological and biophysical characteristics with functional bacterial amyloids such as curli in *Escherichia coli*, TasA of *Bacillus subtilis*, and the Fap fimbriae in *Pseudomonas*

aeruginosa (Chapman et al., 2002; Dueholm et al., 2013; Romero et al., 2010). In this regard, the recent solved crystal structure of full-length PSMα3 peptide, revealed a distinctive "cross-α" amyloid-like architecture of the molecules, in which amphipathic α helices stacked perpendicular to the fibril axis into tight self-associating sheets. It was shown that the "cross-α " fibrillation of PSMα3 is responsible for cytotoxicity, confirming that this mode of assembly has specific functions in *S. aureus* (Tayeb-Fligelman and Landau, 2017).

In addition to chromosomally encoded PSM peptides, *S. aureus* secretes PSM-mec toxins belonging to the PSM α-type. They are encoded on a mobile antibiotic resistance cassette (SCC Staphylococcal cassette chromosome) (Chatterjee et al., 2011; Kaito et al., 2011) that influences cytolytic ability, methicillin resistance, biofilm formation, cell spreading, and the expression of other virulence factors such as other PSMs, resulting in a significant impact on *S. aureus* pathogenicity (Qin et al., 2016). The amount of secreted Psm-mec is highly variable among different MRSA strains and is strongly correlated to the level of synthesis of PSMα peptides (Chatterjee et al., 2011). The *psm-mec* RNA has been shown to alter the stability of *agrA* mRNA most probably through basepairings (Kaito et al., 2013) although these data have not been reproduced in another strain background (Cheung et al., 2014). These data suggested that *psm-mec* RNA has a dual function, acting as an antisense RNA and coding a PSM peptide. Such a dual activity has been well recognized for RNAIII, the intracellular effector of quorum sensing system, which also encodes a PSM (see § III).

III. Regulation of the expression of virulence factors

To regulate this coordinated expression of virulence factors, multiple trans-acting modulators, including regulatory proteins, secondary metabolites, small peptides, and RNAs, are brought into play (Novick and Geisinger, 2008; Wyatt et al., 2010). I will thereafter describe only several of these regulators to illustrate the complexity of the regulatory networks, which are aimed to fine tune the expression of the virulence factors in a dynamic manner according to various external and internal stimuli.

III.1 Regulation of PSM production and other virulence factors by the *agr* locus

Timing and fine regulation of virulence determinants during infection and development of acute staphylococcal disease might be achieved by putting genes involved in pathogenicity under the control of common regulators such as *agr* quorum sensing system. The *agr locus* is comprised of two adjacent units, RNAII and RNAIII (transcribed in opposite directions) that are under the control of P2 and P3 promoters, respectively. RNAII codes for a cell-density cassette, *agrD* and *agrB*, and for the bacterial two-component signal transduction system (TCS), composed of the sensor histidine kinase AgrC and its response regulator AgrA. The processing of the precursor peptide AgrD by the protease AgrB, produce an autoinducing thiolactone peptide (AIP), which is continuously released in the extracellular environment. AgrA is activated by AgrC through phosphorylation in response to a threshold concentration of the secreted AIP. In turn, the phosphorylated form of AgrA directly enhances the transcription of RNAII and RNAIII by binding to its promoter regions (Queck et al., 2008) (**Figure 4**).

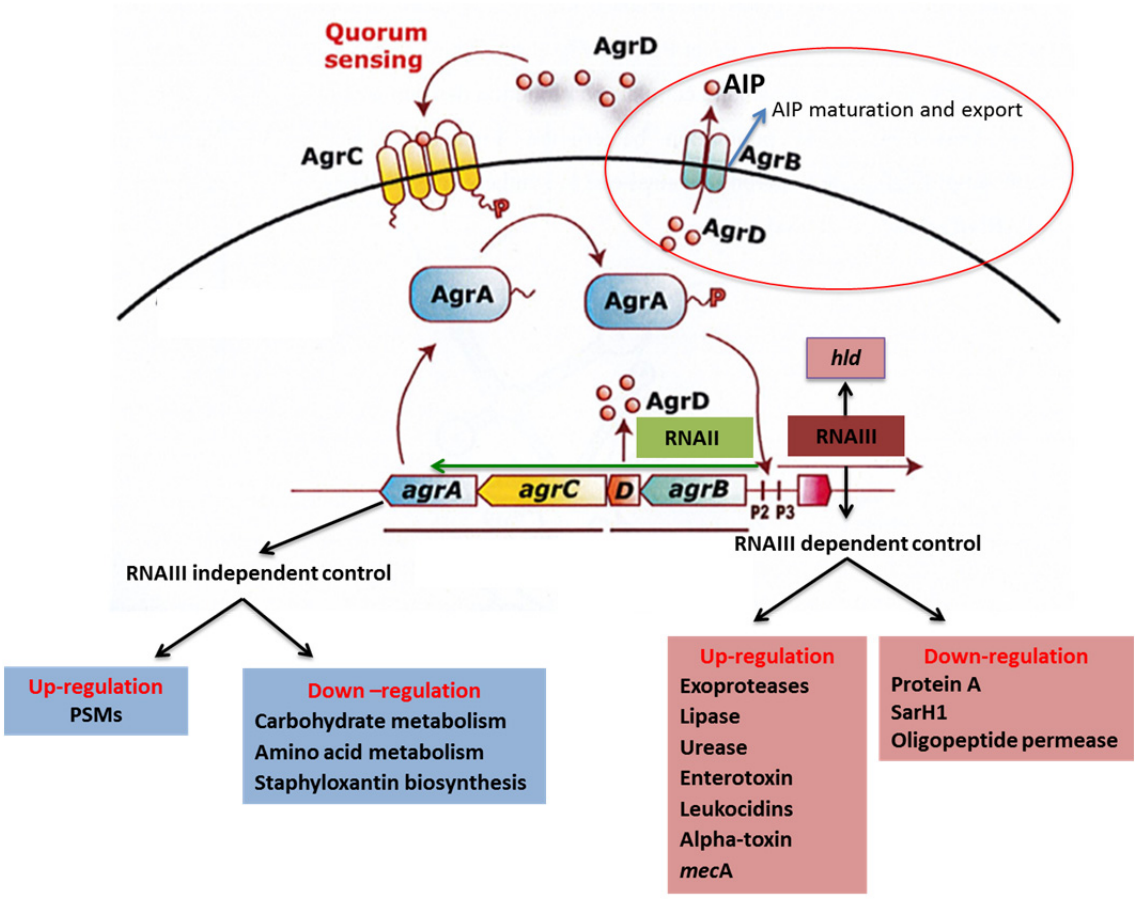

Figure 4. Schematic representation of *S. aureus agr* regulatory system. The *agr* operon consists of two transcriptional units RNAII and RNAIII, driven by the promoters P2 and P3, respectively. RNAII is an operon of four genes, *agr BDCA*, encoding AgrB responsible for processing and exporting AgrD, the AIP precursor. At threshold levels of AIP, AgrC will be autophosphorylated, leading to the phosphorylation of

AgrA. AgrA activates RNAIII expression. Many RNAIII-dependent agr targets contain a series of key virulence factors such as proteases and toxins while the PSMs are regulated *via AgrA* in an RNAIII-independent way (adapted from Queck et al., 2008).

RNAIII and AgrA are the two main intracellular effectors of the *agr* system. RNAIII is composed of 14 hairpin structures, which are organized in different functional modules (Benito et al., 2000). The RNA is responsible for the regulation of the synthesis of many virulence factors. It positively affects the synthesis of several exoproteins including α-toxin, β-haemolysin, TSST-1 and leukotoxins (Morfeldt et al., 1995; Novick and Geisinger, 2008; Novick et al., 1993; Oscarsson et al., 2006), while it negatively controls the expression of several cell wall-associated proteins including protein A, coagulase (*coa*) and fibronectin binding proteins (**Figure 5**). The 5' end of RNAIII, activates the translation of α-haemolysin by disrupting the intramolecular RNA secondary structure sequestering the *hla* ribosomal binding site (Morfeldt et al., 1995; Novick et al., 1993). The RNAIII 3' domain represses the translation of several virulence factors including protein A and of the global regulator of toxins Rot through direct binding to the Shine nd Dalgarno (SD) sequence of the mRNAs. The resulting complexes are composed of an imperfect duplex sequestaring the SD sequence of mRNAs, and in turn prevent the formation of initiation complexes. The mRNAs bound to RNAIII are then rapidly degraded by the double-strand-specific endoribonuclease III (RNase III) (Chevalier et al., 2010). It was also demonstrated that both the 3' and 5' ends of RNAIII interact with the 5' UTR of *mgrA* mRNA preventing its degradation (Bronesky et al., 2016) (**Figure 5**).

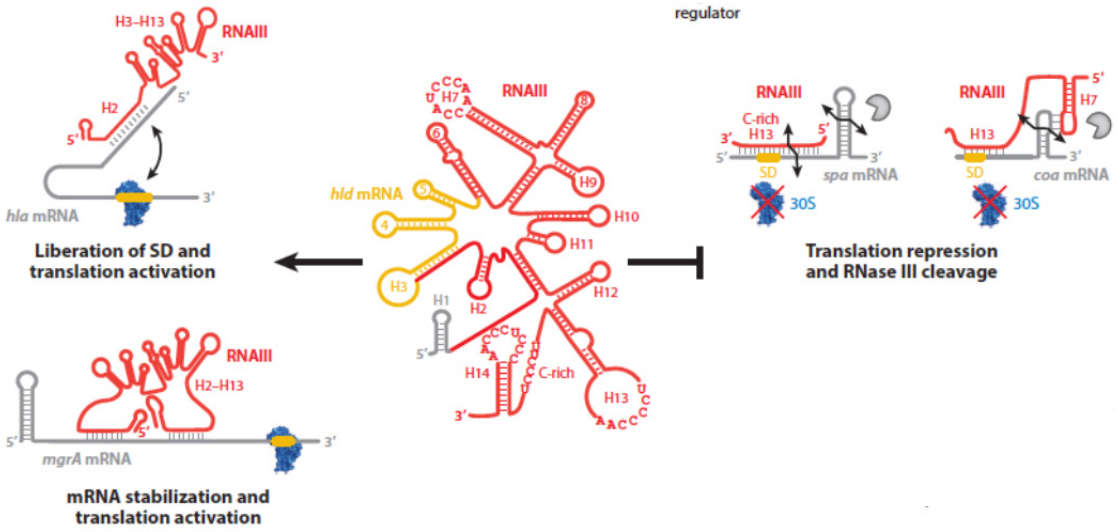

Figure 5: Mechanism of action of RNAIII on its target mRNAs. Genomic organization of the quorum-sensing *agr* system is given at top. The schematic secondary structure of RNAIII (red) is from Benito *et al.* The *hld* gene encoding δ-haemolysin is yellow. The various C-rich sequence motifs of RNAIII are the seed sequences that bind to the Shine and Dalgarno (SD) sequence of mRNA targets (gray). Various topologies

of RNAIII-mRNA are given. Binding of RNAIII to several mRNAs (spa, coa) can prevent binding of the 30S small ribosomal subunit, and in several cases this step is followed by rapid degradation initiated by the double strand–specific endoribonuclease III (gray circle). Binding of RNAIII to target mRNAs can also activate synthesis of exotoxins. For *hla* mRNA, interaction with RNAIII prevents the formation of an inhibitory structure sequestering the SD, whereas for *mgrA* mRNA, binding of RNAIII stabilizes the mRNA against an RNase attack. In these latter cases, the seed sequences initiating basepairings between RNAIII and mRNA targets (*hla*, *mgrA*) have not yet been demonstrated. Abbreviation: AIP, autoinducing thiolactone peptide. Adapted from (Bronesky et al., 2016).

Embedded in RNAIII, there is the *hld* gene coding for the PSM δ-toxin, the haemolysin delta. In 1995, Novick and Balaban have shown that RNAIII is transcribed at the mid-exponential phase of bacterial growth, while the PSM δ-toxin starts to be synthesized during the post-exponential phase. The delay of 1 hour, between the transcription of the RNAIII and the appearance of the PSM δ-toxin, was eliminated by the deletion of the 3' non coding part of RNAIII. These data suggested the existence of unknown *trans*-acting factor that would control the expression of δ-toxin during the bacterial growth. Moreover, the RNAIII secondary structure showed baseparings between the 3' and the 5' ends of the molecule, suggesting that a conformational rearrangement is required for *hld* translation (**Figure 5**).

AgrA not only activates its own operon and RNAIII, but also the transcription of the *PSM*α, *PSM*β, and *psm-mec* (Chatterjee et al., 2011; Chatterjee et al., 2013; Queck et al., 2008). Based on these data, Queck *et al.* (2008) have suggested that the RNAIII-dependent regulatory circuits and the *agrA* quorum-sensing system have been combined during evolution in order to synchronize the cell density changes to virulence gene expression during infection. Although the regulation of PSM transcription is clearly linked to AgrA, other mechanisms for their regulation also existed.

PSMs are produced at extremely high levels in response to specific external stimuli that could be independent of the cell density, reaching ~ 60% of the total secreted protein mass in *S. aureus* (Chatterjee and Otto, 2013). The quorum-sensing system is activated only in response to sufficient concentration of AIP, however, there is faster regulation of PSM expression via intracellular signaling molecules. When internalized by leukocytes or neutrophils, *S. aureus* produces high level of (p)ppGpp which quickly activate PSM production by a non yet characterized mechanism (Geiger et al., 2012). This data suggested that both *agr*-dependent (Surewaard et al., 2012) and *agr*-independent (Geiger et al., 2012) responses co-exist to ensure immediate and continued production of PSMs, allowing *S. aureus* to escape host immune-response and to induce cell lysis. The

production of the PSMα is also positively modulated by SarA. Indeed, by down-regulating the expression of aureolysin (Aur), SarA decreases the rate of PSM degradation (Antignac et al., 2007; Zielinska et al., 2011).

III.2. Two component regulatory system SaeRS

The *sae* locus codified for SaeRS TCS regulates the expression of many virulence factors: it up-regulates α-, β- and γ- haemolysins (Goerke et al., 2005; Liang et al., 2006) and down-regulates Protein A (Giraudo et al., 1997). As other typical TCSs, the signaling cascade in the SaeRS TCS starts when the histidine kinase SaeS detects environmental signals coming from human neutrophils or peptides (Geiger et al., 2008). As the consequence, SaeS autophosphorylates and transfer its phosphoryl group to SaeR that binds to SaeR binding sequence (SBS) and, in most cases, activates the transcription of the target genes (Liu et al., 2016).

III.3. The global regulator SarA

Among the global regulatory systems identified in *S. aureus*, the staphylococcal accessory regulator A (sarA) and its several homologues, are the most well characterized. The *sar* locus is composed of three overlapping transcripts *sarA, sarC,* and *sarB* originating from the P1, P3, and P2 promoters, respectively. The promoters P1 and P2 are SigA dependent, while the P3 promoter is dependent on SigB. SarA is constitutively expressed and it regulates several genes (Manna et al., 1998). By binding to a consensus motif rich in AT in the promoter regions of target genes (Novick and Jiang, 2003), SarA up-regulates the expression of some virulence factors including Fnbps (for adhesion to the host cells), α- and β-haemolysins (for tissue spread) and down-regulates other genes encoding Protein A and proteases (Chan and Foster, 1998; Cheung et al., 1994).

Several SarA homologues have been identified, and all of them contribute to modulate the *agr* system (**Figure 2**; (Cheung et al., 2008)). SarR is involved in the inhibition of SarA and in the regulation of several virulence factors during the exponential and stationary phases of growth (Manna and Cheung, 2001; Manna and Cheung, 2006). SarS

is a DNA binding protein involved in the activation of transcription of *spa* during the exponential phase of bacterial growth (Cheung et al., 2004). SarT activates the expression of SarS while it inhibits the α-haemolysin. The transcription of this factor is also repressed by SarA and AgrA (Cheung et al., 2001). SarU is repressed by SarT, it activates the *agr* operon. In contrast, SarX represses the *agr* operon when activated by MgrA (Manna and Cheung, 2006). MgrA, which activates the *agr* operon, is repressed by SarS. MgrA works as a multiple gene regulator, which inhibits the synthesis of several secreted proteases (Ingavale et al., 2005; Luong et al., 2003). SarZ activates the *agr* operon and the expression of SspA, while it represses SarS. Upon its MgrA-dependent activation, it regulates important genes involved in biofilm formation (Tamber and Cheung, 2009). Finally, the global regulator Rot negatively affects the transcription of numerous factors including lipase, haemolysins, proteases, while positively regulates many other genes including cell surface adhesins. It acts as an antagonist of *agr* which represses its synthesis during the stationary phase of bacterial growth (McNamara et al., 2000; Said-Salim et al., 2003).

III.4. *S. aureus* sigma factors

The regulation of virulence factors is also mediated by sigma factors (σ), which bind to the core RNA polymerase to form the holoenzyme able to recognize specific promoters (Palma and Cheung, 2001). *S. aureus* have four sigma factors (σ^A, σ^B, σ^S, σ^H). σ^A is responsible for the expression of housekeeping genes essential for growth (Deora et al., 1997). σ^B regulates the expression of genes involved in several cellular functions such as stress responses (Deora and Misra, 1996) and in virulence (Bischoff et al., 2001; Horsburgh et al., 2002). It up-regulates FnbpA and the coagulase (CoA), and downregulates haemolysins and serine protease A (Bischoff et al., 2004; Entenza et al., 2005). However, the effect of σ^B on virulence might result via the regulation of transcriptional factors such as *sarA*, *sarS*, and *rot*. It has also been shown to be involved in antibiotic resistance, biofilm formation and in bacterial internalization into host cells (Nair et al., 2003; Rachid et al., 2000). σ^H has been demonstrated as a key actor for competence development (Morikawa et al., 2012). The factor also modulates prophage integration and excision through the regulation of the integrase expression (Tao et al.,

2010). For the last Sigma factor σ^S, its regulon is still not yet defined but high levels of the factor were observed in cells grown in the presence of serum. Its inactivation decreased the fitness of *S. aureus* at high temperature, and the infectivity of the mutant strain was altered in a murine model of septic arthritis (Miller et al., 2012; Peton et al., 2016).

IV. Antibiotic resistances in *Staphylococcus aureus*

S. aureus is able to invade and survive within neutrophils and macrophages, leading to its incomplete clearance even in the presence of high levels of antibiotics. The introduction of penicillin in the early 1940s positively influenced the prognosis of patients with staphylococcal infections. However, few years later, penicillin-resistant staphylococci were recognized, first in the hospitals and then in the community. The resistance to penicillin is mediated by *blaZ*, the gene that encodes β-lactamase. This predominantly extracellular enzyme, synthesized when staphylococci are exposed to β-lactam antibiotics, hydrolyzes the β-lactam ring of penicillin deactivating the antibacterial properties of the molecule (Chambers and Deleo, 2009; Lowy, 2003). With the emergence of resistance to the penicillins, a semi-synthetic antibiotic methicillin, which is derived from penicillin but resistant to β-lactamase inactivation, became the molecule of choice for the treatment *S. aureus* infections. However, immediately after its introduction, methicillin-resistant (MRSA) bacteria were isolated (Jevons, 1961). The gene responsible for methicillin resistance is named *mecA,* it is located on a mobile genetic element known as *mec* element (SSCmec) (Chambers, H. F. 1997) that serves as a vehicle for gene exchange among staphylococcal species (Hacker et al., 2004). *MecA* is responsible for synthesis of the penicillin-binding protein 2a (PBP2a), a membrane-bound enzyme located at the membrane-cell wall interface and involved in the peptidoglycan synthesis (Ghuysen, 1994). PBP2a substitutes for other PBSPs and, given its low affinity for all β-lactam antibiotics, allows staphylococci to survive even in the presence of high concentrations of this drug. Under the pressure of intensive emerging antibiotic resistant strains, the last remaining antibiotic to which MRSA strains were susceptible was the vancomycin, able to inhibit *S. aureus* cell wall. The reduced susceptibility to vancomycin was due to the synthesis of an unusually cell wall containing dipeptides (D-Ala-D-Ala) capable of binding the antibiotic, sequestering it

and thereby reducing availability of the drug for intracellular target molecules. Fortunately, these resistant strains did not spread substantially, possibly due to increased fitness cost. The ability of *S. aureus* to develop resistance to antibiotic treatments is dynamic and has changed significantly over the years. It could virtually acquire resistance against all antimicrobial agents available in hospitals and communities (DeLeo et al., 2010). Hence, the reengineering of existing antibiotics and the synthesis of new therapeutic alternatives are urgently needed.

V. Translation and its control in *S. aureus*

V.1. Translation initiation, a check point for regulation

The above described orchestration of *S. aureus* virulence demonstrates the ability that bacteria have to rapidly sense their environment and constantly adapt their physiology in response to its variations. Several extracellular and intracellular signals (e.g. the quorum sensing peptide described for the *agr* system) are detected and associated to multi-step regulations at the transcriptional and post-transcriptional levels, which contribute to reprogramming the bacterial proteome. Among the different regulatory mechanisms, translational control can ensure a rapid and transient. The RNAIII-directed translational silencing or activation mechanisms represent a typical example of how protein synthesis could be regulated. In the vast majority of the cases, changes in translational efficiency are the result of a modulation of its initiation process (Romby, 2007) during which the ribosome assembles on the mRNA in the order of seconds (Gold, 1988; Kennell and Riezman, 1977). This slow, rate-limiting step of protein synthesis provides the time window necessary for regulation between mRNA transcription and active translation or mRNA degradation. Even if in bacteria, transcription, translation and mRNA degradation are interconnected processes and often coupled (Burmann et al., 2010; Campos and Jacobs-Wagner, 2013; Das et al., 1967; Mehdi and Yudkin, 1967; Proshkin et al., 2010; Shin and Moldave, 1966; Stent, 1964), large 5' and 3' Untranslated Regions (5'UTR, 3'UTR) which are often structured, strongly impact translation initiation and are therefore target of several regulatory mechanisms (Geissmann et al., 2009b; Marzi et al., 2008a; Ruiz de los Mozos et al., 2013). Bacterial translation initiation is a highly conserved process, but some differences and specific features among distant bacteria have been observed. This is the case of the Gram-negative bacterium *Escherichia coli* and the Gram-positive low G+C content *S. aureus* which have diverged more than 10 million years ago,.

I will thereafter describe the details of the bacterial initiation process mainly derived from studies on Gram-negative bacteria and will illustrate some structural differences between *E. coli* and *S. aureus* ribosomes. The description of the main functional differences between the initiation processes is included in the joined review "A glimpse on *Staphylococcus aureus* translation machinery and its control" (Khusainov et al., 2016) where I am second author.

V.2. A view on the Translation Initiation in Gram-negative bacteria

In contrast to eukaryotes and archaea (for reviews see (Londei, 2005; Pestova et al., 2007)), the initiation process in bacteria involves a rather low number of *trans*-acting factors. Three initiation factors (IF1, IF2, IF3) kinetically assist the formation of the translation initiation complex, with the 30S small ribosomal subunit, the aminoacylated and formylated initiator tRNA (fMet-tRNA^{fMet}) and the mRNA (**Figure 6**; (Simonetti et al., 2008). The three factors have no direct influence on the recruitment of the mRNA (Milon et al., 2012) but exert specific functions. IF3 acts as "fidelity factor". It helps in the selection of initiator tRNA (fMet-tRNA^{fMet}) by destabilizing the binding of other tRNAs in the P site of the ribosome (Hartz et al., 1990; Milon et al., 2012). It is also known to strongly anchor the 30S subunit preventing the association with the large ribosomal subunit so to maintain a cellular pool of 30S for translation initiation (Grigoriadou et al., 2007). IF2 is a GTPase factor that binds specifically to fMet-tRNA^{fMet} and correctly positions it on the 30S to favour the 50S joining (Simonetti et al., 2013; Simonetti et al., 2008). IF1, the smallest of the three initiation factors, binds to the A site of the 30S ribosomal subunit (Carter et al., 2001) where physically it prevents tRNA binding and prepares the P site for fMet-tRNA^{fMet} binding. The formation of the "30S initiation complex" (30SIC) takes place at the Ribosome Binding Site (RBS) of the mRNA. The mRNA stably binds the 30S *via* its Shine-Dalgarno sequence (SD) complementary to the anti SD (aSD) sequence at the 3' end of the 16S rRNA (Hui and de Boer, 1987; Jacob et al., 1987; Shine and Dalgarno, 1974). For many bacterial mRNAs, the selection of the correct start codon (usually AUG) depends largely on the formation of this short SD-aSD helix. Once the 30SIC complex is formed, the translational reading frame is set and protein synthesis can start. During the following steps of translation initiation, the joining of the large ribosomal subunit (50S) to the 30SIC leads to the formation of the "70S initiation complex" (70SIC; made by the small and the large ribosomal subunits, the fMet-tRNA^{fMet} and the mRNA), ready for the first peptide bond formation. During this transition, the adjustment of fMet-tRNA^{fMet} in the ribosomal P-site and the release of all factors are coupled with the hydrolysis of the GTP molecule bound to IF2 (Allen et al., 2005; Myasnikov et al., 2005; Simonetti et al., 2008). The formation of the correct 70SIC marks the irreversible transition to the elongation phase.

The binding of the mRNA to the 30S subunit is one of the most critical steps of translation initiation and the target of the majority of known translation regulations. It takes place into two sequential steps, first the localization on the platform of the 30S to form the 30S pre-initiation complex, and then the accommodation into the mRNA channel (**Figure 6**).

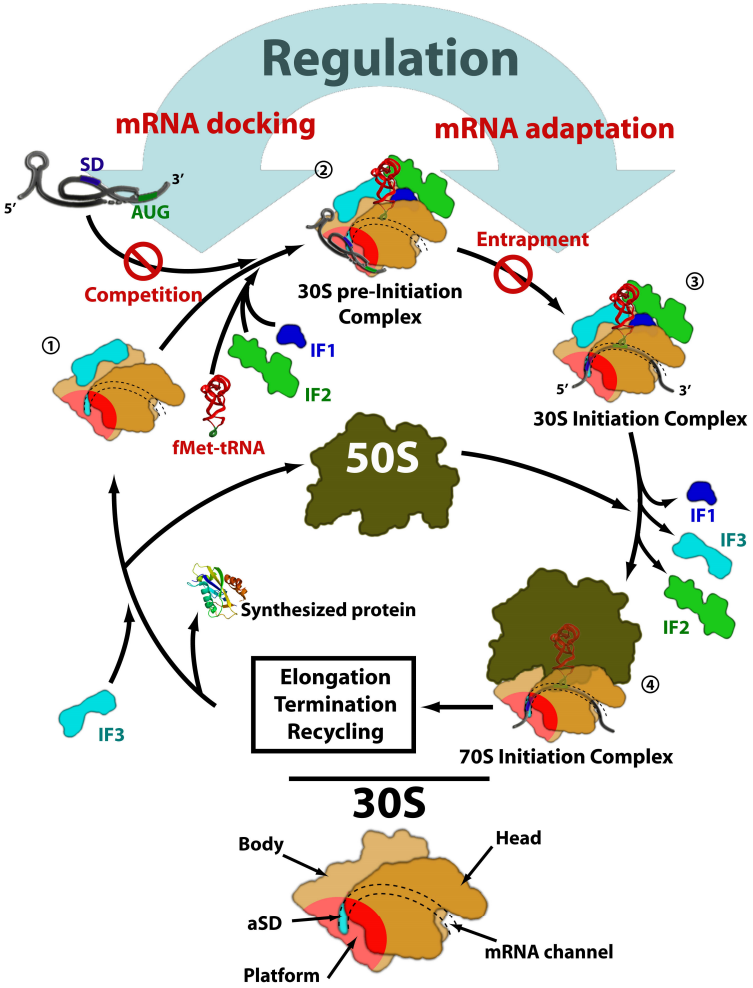

Figure 6. A schematic view of the initiation process of translation and its regulation in *Escherichia coli*. Three initiations factors (IF3 in light blue, IF1 in blue and IF2 in green) bind to the 30S subunit (in orange). The platform binding center is in red with the anti-SD (aSD) sequence in cyan. Structured mRNA binds to 30S in two distinct steps: the docking of the mRNA on the platform of the 30S subunit is followed by the accommodation of the mRNA into the normal path to promote the codon-anticodon interaction in the P site. These two steps are submitted to tight control, through the alternative competition and entrapment mechanisms. Numbers refer to: 1) the cellular pool of initiating 30S subunits bound to IF3; 2) 30S pre-Initiation Complex refers to the docking step of the structured mRNA; 3) 30S Initiation Complex refers to the active complex in which the mRNA is accommodated into the normal path forming the codon-anticodon interaction; 4) 70S Initiation Complex, the 50S subunit (in brown) joins the 30S Initiation Complex to proceed protein synthesis. The scheme is derived from (Marzi et al., 2008b). At the bottom, the different domains of the 30S subunit, the mRNA channel and the aSD sequence are given.

V.2.1. E. coli r-protein S1, an RNA chaperone associated with the ribosome for structured mRNA translation

E. coli S1 is an atypical ribosomal protein: S1 is the largest (61KDa) protein of the 30S subunit, is among the ribosomal proteins with documented high affinity for numerous mRNAs (Draper et al., 1977), is the most acidic (pI= 4.7) r-protein (Kaltschmidt and Wittmann, 1970), it is the last protein to associate on the 30S and its interaction with the 30S is weak and reversible. *Eco*S1 is essential for growth and its functional relevance is related to its ability to simultaneously bind mRNAs and the ribosome. Indeed, S1 mediates initiation of translation by binding the 5' UTR of mRNAs, thus increasing their affinity for the ribosome up to 5000 fold (Draper and von Hippel, 1979; Katunin et al., 1980). This is especially evident for weak SD-containing mRNAs, which necessitate S1 to be stabilized on the 30S (Komarova et al., 2005). In *E. coli*, S1 is also responsible of the accommodation of the mRNA in the 30S decoding channel, a slow process essential for the translation of structured mRNAs (Duval et al., 2013b).

*Eco*S1 is composed of 6 OB fold domains (**Figure 7**): the first two domains, d1 and d2, are essential for 30S subunit binding, while the domains d3 and d4 together with d1 and d2 form the minimal protein that recognize mRNAs and allow their accommodation into the decoding channel (Duval et al., 2013b; Duval et al., 2017). The last two C-terminal domains are dispensable and have regulatory functions related to RNA maturation/degradation (unpublished data from the laboratory).

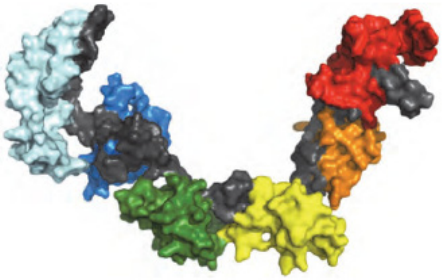

Figure 7. Modelled structure of *E. coli* S1. Domain 1 in light blue, domain 2 in dark blue, domain 3 in green, domain 4 in yellow, domain 5 in orange and domain 6 in red. Model realized by Stefano Marzi.

To date, X-ray and/or Cryo-EM ribosomal structures of Gram-negative bacteria such as *E. coli* and *Thermus Thermophilus,* have failed to visualize S1. In this regard, it has to be considered that the purification of ribosomes for X-ray studies involves a step of deliberate removal of S1 in order to increase the homogeneity of the ribosomes and to obtain better diffracting crystals (Schuwirth et al., 2005; Yusupov et al., 2001), while Cryo-EM investigations might be not suitable for a highly dynamic protein due to the averaging of different conformations. Recently, the S1 N-terminal domain (d1) was

nevertheless observed by Cryo-EM interacting *via* a zinc binding pocket to the ribosomal protein S2 on the 30S platform (Byrgazov et al., 2015). Crosslinking experiments in combination with high resolution mass spectrometry analysis have also placed S1 in the same region on the ribosome (Lauber et al., 2012). The platform between the head and the body of the 30S (**Figure 8**) is thus formed by S1 and several other r-proteins (S2, S7, S11, S18 and S21) together with two rRNA helices (h26 and h40) that are surrounding the aSD close to one extremity of the decoding channel. Since both r-protein S1 and the aSD are on the platform, we can imagine that several mRNAs would transit on this site before getting into the mRNA decoding channel. A systematic structure and sequence analysis revealed that conserved residues of the r-proteins of the platform form patches of positive charges on its surface that could localize folded mRNA regardless of their specific structure or sequence (Marzi et al., 2007). Interestingly, it has been observed that even sequences that have low propensity to form structures, like poly(A) or poly(U), get folded into compact structures similar to hairpins close to r-protein S2 (Yusupova et al., 2006) (**Figure 8**).

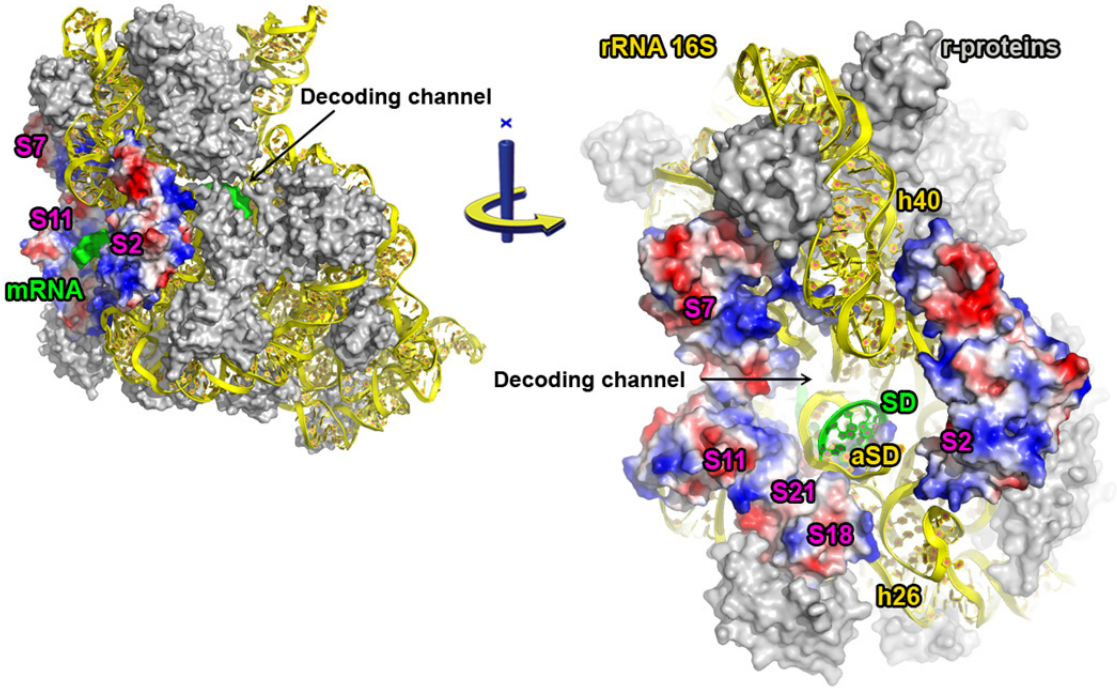

Figure 8. The platform of the 30S. On the left, view of the 30S subunit showing the localization of the platform. On the right, enlarged and rotated view of the platform showing the charge distribution of the r-proteins composing it. S2, S7, S11, S18 and S21 are forming a nest of positive charges (blue surfaces) around the aSD. Negatively charged amino acids are represented in red. The mRNA (green) is shown accommodated into the decoding channel. The model in the figure has been obtained using the coordinates of *E. coli* ribosome (pdb file 4TP8) which contains all the r-proteins of the platform but S1 and the mRNA pathway described in the *T. thermophilus* translation initiation complex (pdb file 4HGR).

V.3. S. aureus ribosome structure and specific features

The structures of the bacterial 70S ribosomes have been extensively studied in Gram-negative bacteria such as *E. coli* (e.g. (Schuwirth et al., 2005; Noeske et al., 2015)) and *T. thermophilus* (e.g. (Yusupov et al., 2001; Yusupova et al., 2001)), but have received little attention in Gram-positive bacteria (Beckert et al., 2015; Eyal et al., 2015; Sohmen et al., 2015). Recently, structures of *S. aureus* large ribosomal 50S subunit bound to specific antibiotics (Eyal et al., 2015) and of the whole 70S (Khusainov et al., 2017) have shed light on some features specific to *S. aureus*.

Concerning the 30S platform, two main differences could be spotted. The most evident is the absence of ribosomal protein S1 (**Figure 9**), which slightly changes the charge distribution of the two platforms, making more positive the one from *S. aureus* in the region which is close to the 3' end of the 16S rRNA (aSD) and the h26. The second difference is in the length of h26, which is incremental when going from *T. thermophilus* (19 nt) through *E. coli* (25 nt), *B. subtilis* (26 nt) to *S. aureus* (27 nt). Such variations at a strategic ribosomal region could reflect species-specific involvement of h26 in translation initiation and regulation.

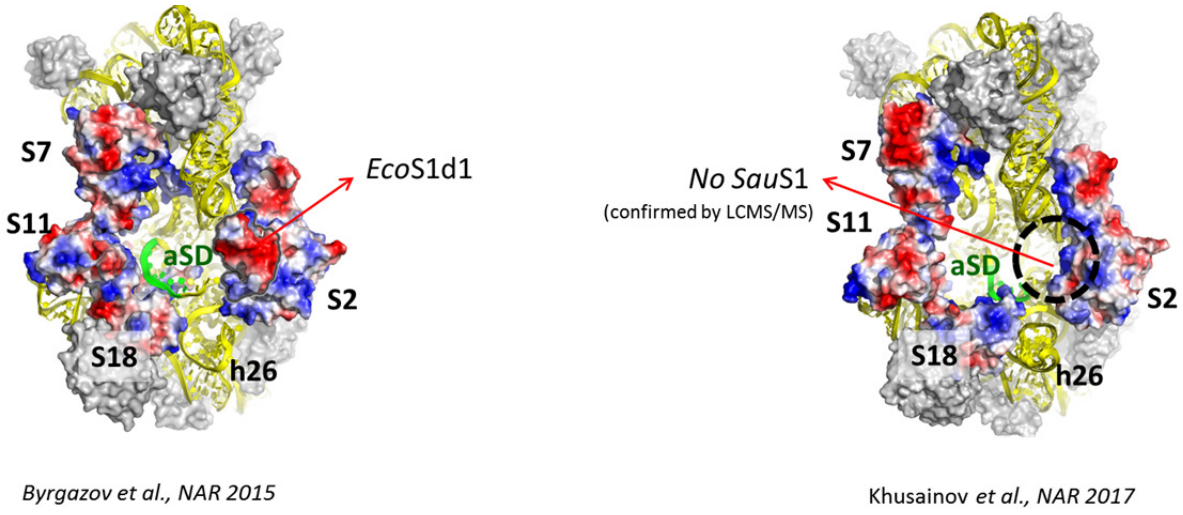

Figure 9. *E. coli* and *S. aureus* 30S platform. On the left, *E. coli* platform as in figure 10, with the exception that the structure used here contains also d1 (Byrgazov et al., 2015). On the right, charge distribution of the r-proteins from *S. aureus* 70S structure (Khusainov et al., 2017). The charge distribution is similar in the two structures, but the absence of S1 increases even more the positively rich environment surrounding the aSD, which also appears shifted toward h26 in *S. aureus* structure.

V.3.1. S. aureus protein S1, a shorter protein not associated with the ribosome

S1 is found in almost all Gram-negative and in several Gram-positive bacteria. A shorter form (45 kDa) exists in chloroplasts, but is absent in eukaryotic cells. Phylogenetic studies have indicated that S1 from low G+C Gram-positive bacteria (Firmicutes), such as *B. subtilis* and *S. aureus*, would not contain the ribosome binding domain d1 (Salah et al., 2009) (**Figure 10**).

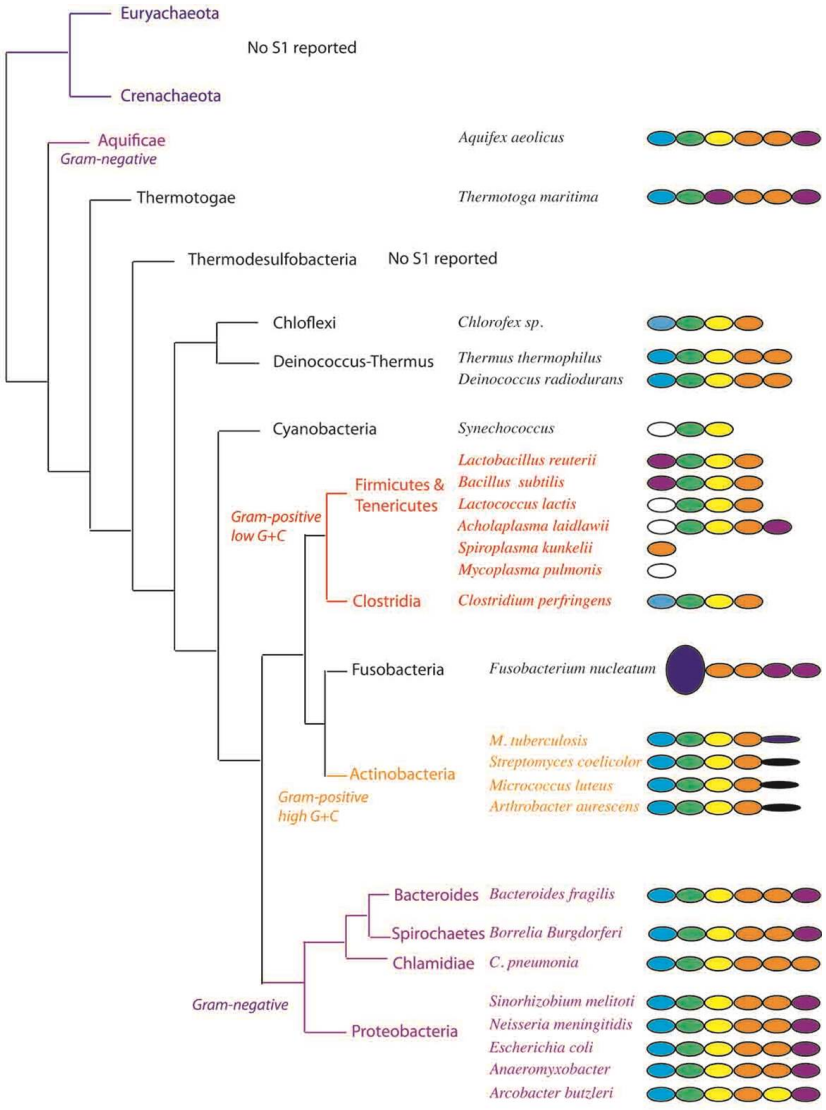

Figure 10. Schematic representation of the organization of protein S1 in different bacteria. Colors have been attributed for conserved domains: domain 1 in blue, domain 2 in green, domain 3 in yellow, as domains 4/5 in orange and domain 6 in magenta. The OB fold domains, which could not be assigned to any *E. coli* domain are in white. The domains not identified as OB fold domains are in deep blue. The figure is adapted from (Salah et al., 2009).

Indeed, after purification of *S. aureus* 30S and 70S ribosomes (Fechter et al., 2009), only traces of r-protein S1 were observed by mass spectrometry analysis, suggesting that the protein is not tightly associated with the ribosome (Khusainov et al., 2016). It was

previously demonstrated that *B. subtilis* S1 plays no major role in translation and is not an essential protein (Farwell et al., 1992; Juhas et al., 2014; Vellanoweth and Rabinowitz, 1992). It was thus proposed that Firmicutes obviate the need of S1 acting on the 30S because the majority of mRNAs carry short 5' UTRs with strong SD sequences (Omotajo et al., 2015). However in *S. aureus*, numerous mRNAs carrying long 5' or 3' UTRs have been reported (Anderson et al., 2006; Lasa et al., 2011; Ruiz de los Mozos et al., 2013). They include mRNAs encoding virulence determinants, various transcriptional regulators, and metabolic enzymes. How does *S. aureus* ribosome translate them is one of the key question that I have addressed during my PhD project.

In the following review paper, using toe-printing assays, we have monitored the behavior of isolated *S. aureus* 30S and 70S ribosomes and compared them with *E. coli* ribosomes containing or not S1. Different mRNAs have been used in which the SDs were exposed in loops or shaded into hairpins, demonstrating that *S. aureus* 30S, as the *E. coli* S1-depleted 30S, could not efficiently bind to structured mRNAs.

V.4. A glimpse on Staphylococcus aureus translation machinery and its control

Khusainov Iskander, Marenna Alessandra, Cerciat Marie, Fechter Pierre, Hashem Yaser, Marzi Stefano, Romby Pascale, Yusupova Gulnara & Yusupov Marat

My contribution to the work presented in this review was related to the characterization of *S. aureus* ribosome. Mass-spectrometry analysis of purified 70S has shown the absence of *Sau*S1. By gel filtration assay I have demonstrated the inability of the protein to assemble on the 30S ribosomal subunit.

I also contributed to the discussion of the results with all the authors and I have participated to the final writing of the manuscript.

ISSN 0026-8933, Molecular Biology, 2016, Vol. 50, No. 4, pp. 477–488. © Pleiades Publishing, Inc., 2016.

REVIEWS

UDC 577.217.34

A Glimpse on *Staphylococcus aureus* Translation Machinery and Its Control[1]

I. Khusainov[a, b], A. Marenna[c], M. Cerciat[a], P. Fechter[c, 2], Y. Hashem[c], S. Marzi[c], P. Romby[c, *], G. Yusupova[a], and M. Yusupov[a, b, **]

[a] *IGBMC (Institute of Genetics and of Molecular and Cellular Biology), Department of Structural Biology and Genomics, Illkirch, F-67404 France; Inserm, U596, Illkirch, F-67400 France; CNRS, UMR7104, Illkirch, F-67400 France; Université Louis Pasteur, Strasbourg, F-67000 France*

[b] *Institute of Fundamental Medicine and Biology, Kazan Federal University, Kremlyovskaya St. 18, Kazan, 420008 Russia*

[c] *Architecture et Réactivité de l'ARN, Université de Strasbourg, CNRS, IBMC, 15 Rue René Descartes, 67084 Strasbourg, France*

*e-mail: *p.romby@ibmc-cnrs.unistra.fr; **marat@igbmc.fr*

Received February 23, 2016; in final form, February 23, 2016

Abstract—*Staphylococcus aureus* is a major opportunistic and versatile pathogen. Because the bacteria rapidly evolve multi-resistances towards antibiotics, there is an urgent need to find novel targets and alternative strategies to cure bacterial infections. Here, we provide a brief overview on the knowledge acquired on *S. aureus* ribosomes, which is one of the major antibiotic targets. We will show that subtle differences exist between the translation at the initiation step of Gram-negative and Gram-positive bacteria although their ribosomes display a remarkable degree of resemblance. In addition, we will illustrate using specific examples the diversity of mechanisms controlling translation initiation in *S. aureus* that contribute to shape the expression of the virulence factors in a temporal and dynamic manner.

Keywords: *Staphylococcus aureus*, quorum sensing, regulatory RNAs, post-transcriptional regulation

DOI: 10.1134/S002689331604004X

INTRODUCTION

Protein synthesis is an essential process across all domains of life, which is carried out by the ribosome. Although the ribosome is universally conserved machinery, significant differences were found in the composition of the ribosomal proteins, in extension/reduction of rRNA regions, and in the associated factors between eubacteria, archaea, eukaryotes and their organelles [1–6]. Due to its essential function, the ribosome represents one of the main antibiotic targets [7, 8]. Extensive biochemical and structural studies have now revealed the molecular mechanisms of numerous antibacterial drugs acting directly on the ribosome functioning [8]. Intriguingly, the vast majority of antibiotics act to interfere with the elongation step of protein synthesis while only a few of them interfere with the initiation step [8]. Because initiation of translation and primarily the mRNA recruitment diverge significantly in the three kingdoms of life (reviewed in [9, 10]), these differences could be potentially exploited for drug design against major human pathogens.

The structures of the bacterial 70S ribosomes have been extensively studied in Gram-negative bacteria such as *Escherichia coli* [11, 12] and *Thermus thermophilus* [13, 14], but have received little attention in Gram-positive bacteria [15–17]. *Staphylococcus aureus* is a Gram-positive bacterium that is recognized as a major human opportunistic and versatile pathogen, which causes a large spectrum of infections [18]. Importantly, methicillin-resistant strains (MRSA) are now widespread and are responsible for severe infections in the community as well as in the hospital [19], and strains resistant to vancomycin have also emerged [20, 21]. A recent study shows that MRSA isolates spontaneously diversify into distinct strains that evolve new antibiotic resistance via competition between bacterial cells within a monoclonal population [22]. A monoclonal population of cells is thus heterogeneous due to the fact that the bacteria should constantly compete for space and acquisition of nutrients [23]. Hence, there is an urgent need to develop alternative anti-bacterial strategies [24–26] but also to better understand the mechanisms leading to the bacterial genetic variation [27].

The recent structure of *S. aureus* large ribosomal 50S subunit bound to specific antibiotics shed light on their mechanism of action and highlight peripheral

[1] The article is published in the original.

[2] Present address: UMR 7242, 300 boulevard Sébastien Brant, 67412 Illkirch cedex, France.

motifs specific to *S. aureus* [16]. Furthermore, significant differences in ribosome functioning have been described between low GC content Gram-positive and Gram-negative bacteria [28–32]. The present review will be focus on specific characteristics of the translation initiation in *S. aureus*. In addition, we will illustrate the diversity of mechanisms regulating the recruitment of the ribosomes on the mRNAs that have a direct functional impact on bacterial pathogenesis.

REGULATION OF *S. aureus* TRANSLATION INITIATION

S. aureus has developed numerous mechanisms to respond to changing environments and to colonize nearly all niches within a host. Such amazing adaptation is accompanied by a significant remodeling of gene expression and particularly of the virulence determinants mainly driven by transcriptional regulatory proteins [33]. Besides, it is now well admitted that protein-mediated transcriptional control and RNA/protein-mediated translational control are intertwined. Genome-wide studies have discovered a high number of large and small RNAs, which selectively bind to mRNA targets to regulate primarily translation initiation (for reviews [34, 35]). In addition, the discovery of overlapping operons led to the hypothesis that widespread antisense transcription would significantly impact gene regulation at the translational and post-transcriptional levels [36]. Other mRNAs are characterized by large 5' and 3' untranslated regions (UTR) which contain specific structures or sequence signatures that modify the genetic response at the translational level. Hence, a high diversity of mechanisms at the translational level has been evidenced as illustrated by several examples below.

***Trans*-acting regulatory RNAs.** The first *S. aureus* regulatory RNA has been discovered by Novick et al. [37] as the main intracellular effectors of the quorum sensing *agr* system. *S. aureus* produces a battery of virulence factors that are responsible for defense against the host immune response, adhesion, invasion, acquisition of novel nutrients, and dissemination in host tissues [38, 39]. The *agr* system is pivotal for the temporal regulation of two sets of virulence factors, adhesins and exotoxines. It is composed of two divergent transcripts, RNAII encodes a quorum sensing cassette (AgrBD) and a two-component system (AgrAC) while RNAIII is the multifunctional RNA, which encodes a PSM δ-hemolysin (*hld*). Besides its coding capacity, RNAIII promotes the switch between the expression of surface proteins and the synthesis of excreted toxins [35]. These regulatory properties are endowed within the non-coding parts of RNAIII, which primarily act as antisense RNA to activate or repress the translation of target mRNAs. On one hand, its 5'UTR binds to the leader region of *hla* mRNA encoding α-hemolysin to prevent the formation of an inhibitory structure in order to facilitate ribosome recruitment [40] (Fig. 1a). In addition, the 5' and 3' ends of RNAIII both interact with the leader of *mgrA* mRNA to enhance the mRNA stability [41]. On the other hand, its large 3'UTR is primarily acting as a repressor domain (Fig. 1a). This domain is the most highly conserved domain of RNAIII, which contains four C-rich sequence repeats located in unpaired regions [42]. This sequence motif acts as a seed sequence, which initiates basepairing interactions with the Shine and Dalgarno (SD) sequence of target mRNAs (Fig. 1a). The initial GC-rich pairings confer a fast association rate constant for the formation of the complex, and in general are subsequently propagated either to form long duplexes or are stabilized by additional distant pairings according to the mRNA signals (Fig. 1a) [43]. However, in all cases binding of RNAIII prevents the loading of the ribosome and the formation of the initiation complex. These mRNAs encode virulence factors expressed at the surface of the cell (protein A, coagulase, SA1000, Sbi), and the transcriptional repressor of toxins, Rot [43–47]. Through the inhibition of Rot translation, RNAIII indirectly activates the transcription of exotoxins. Such regulatory circuits create a temporal delay between the repression of adhesin synthesis and the induction of exotoxin production enabling an effective transition of the pathogen for spreading and dissemination [48].

Later on, the search for small non-coding RNAs (sRNAs) has revealed the existence of a class of sRNAs carrying unpaired C-rich sequence motif similar to RNAIII [50, 52, 53]. Determination of the functions of several sRNAs demonstrated that this sequence motif is indeed a characteristic signature for translational repressors. For instance, the SigB-dependent RsaA sRNA represses translation initiation of the global transcriptional regulator MgrA through a sequestration of the SD sequence in a manner similar to RNAIII [49] (Fig. 1a). Through MgrA regulation, RsaA attenuates the severity of systemic infections and enhances chronic infection [49]. Another example is *S. aureus* RsaE which represses at the translational level mRNAs involved in the TCA cycle under specific conditions of stresses, NO induction, and when carbon sources are decreasing [50, 53, 54]. In both cases, an unpaired C-rich motif binds to the SD sequence of the mRNAs. Because many mRNAs in Gram-positive bacteria have a strong SD sequence (AGGAGG) and a rather short 5'UTR, targeting the SD is a rapid way to prevent the recruitment of the ribosome and to arrest translation even during the transcription process. However, these examples also demonstrate that additional basepairing interactions outside the SD region are required to ensure a specific response.

***Cis*-acting regulatory RNAs.** In *S. aureus*, UTRs of mRNAs are generally of small size, but exceptions of mRNAs carrying large 5' or 3'UTRs have been reported [51, 55, 56]. They include mRNAs encoding virulence determinants, various transcriptional regulators, and metabolic enzymes. Large 5'UTRs are

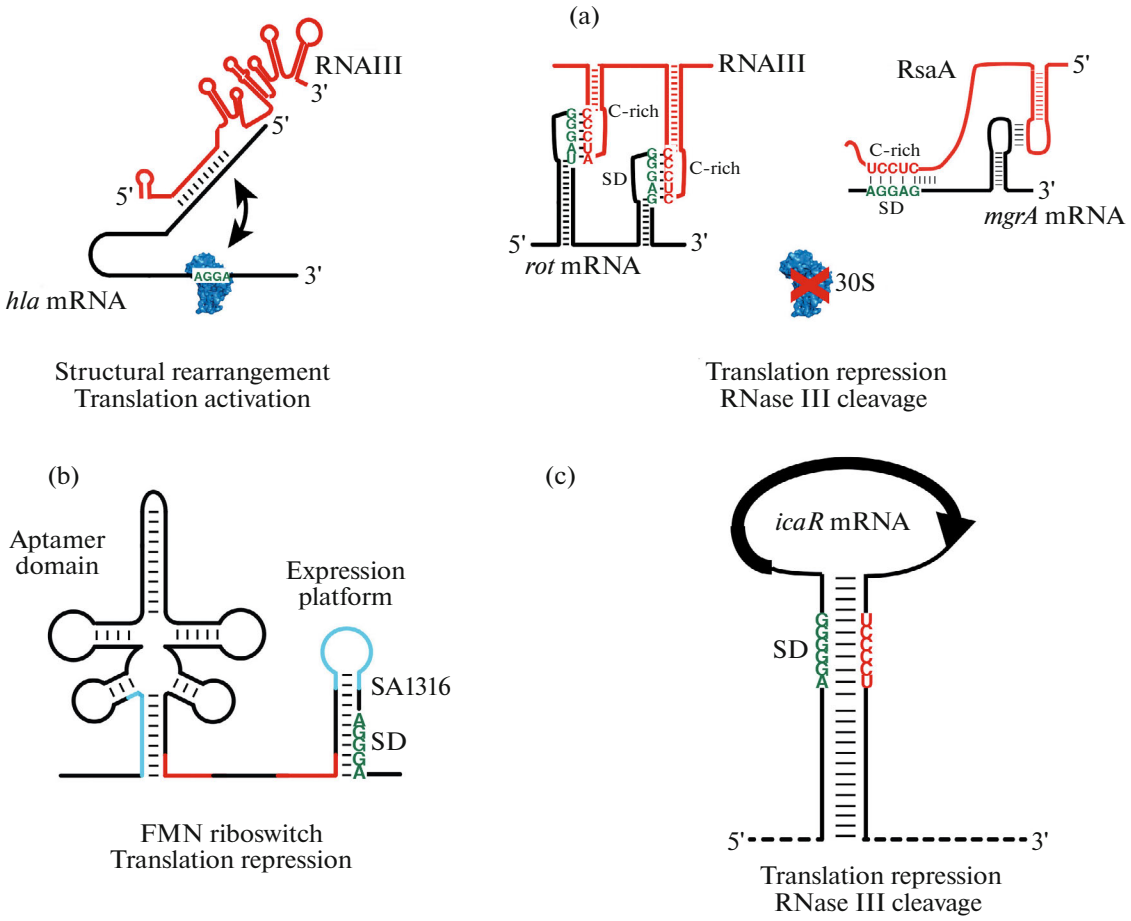

Fig. 1. Mechanisms regulating translation initiation. (a) Examples of *trans*-acting RNAs acting as antisense RNAs. *S. aureus* RNAIII binds to the 5'UTR of *hla* mRNA to prevent the formation of basepairings sequestering the Shine and Dalgarno (SD) sequence, and to favor the ribosome recruitment [40]. Two C-rich motifs of RNAIII bind to two hairpin loops of *rot* mRNA; one of them includes the SD sequence, to form two loop-loop interactions that prevent ribosome binding [43, 45]. The small non coding RNA, RsaA, binds to the SD sequence via its C-rich motif to repress the translation of *mgrA* mRNA. In both cases, the repression of translation is subsequently followed by RNase III degradation [49]. (b) Example of a *cis*-acting regulatory riboswitch responding to flavin mononucleotide (FMN) intracellular concentration. Binding of FMN in the cleft formed by the compact structure of the aptamer domain led to the stabilization of a hairpin structure sequestering the SD sequence to repress translation initiation of the downstream gene SA1316 [50]. (c) Example of a long-distance interaction affecting in *cis* the translation of *icaR* mRNA. A C-rich motif in the 3'UTR of *icaR* mRNA binds to the SD sequence to prevent translation, and creates a structure suitable for RNase III cleavages [51].

often the reservoirs of regulatory signals such as the riboswitches, which are direct sensors for intracellular metabolite concentrations [57]. Riboswitch consists of a sensor/aptamer domain containing a binding pocket specific for a dedicated metabolite and of an expression platform controlling the downstream transcripts. At least seven *S. aureus* operons are under the control of riboswitches that respond to the intracellular concentrations of S-adenosylmethionine (SAM), thiamine pyrophosphate (TPP), flavin mononucleotide (FMN), lysine, glycine, guanine, 7-aminomethyl-7-deazaguanine (preQ1), and glucosamine-6-phosphate (Glc-6P) [50, 58]. Most of them are regulated through a premature transcription arrest [52], while only one FMN-sensing riboswitch is expected to control the translation of a hypothetical protein. Binding of FMN to the aptamer domain is predicted to stabilize the formation of a hairpin structure sequestering the SD sequence (Fig. 1b). Because many of these riboswitches regulate the synthesis of essential proteins involved in amino acid biosynthesis, as well as co-factors and nucleotide biosynthesis, they were used as targets for the design of drugs that could constitutively repress the synthesis of essential enzymes [59, 60]. For instance, a pyrimidine derivative compound PC1 binds to the *S. aureus* guanine riboswitch to constitutively repress the expression of *guaA*. This compound showed bactericidal activity against *S. aureus* and significantly reduced mammary gland infection in mice [61]. This compound was more recently assayed to treat bovine intra-mammary infections [62]. Although a significant reduction in bacterial concen-

trations was observed in the milk after PC1 treatment, the clearance of the bacterial was not completely achieved. However, these studies show that riboswitches are still promising drug targets for the search of novel classes of antibiotics.

In contrast to the 5'UTRs, large 3'UTRs have been underestimated [51, 56, 63]. Recent findings have revealed the importance of a long 3'UTR in *icaR* mRNA, which encodes a transcriptional repressor of biofilm formation. IcaR controls the transcription of the operon *icaADBC* required for the synthesis of the main exopolysaccharidic polymer PIA-PNAG, a major component of the biofilm matrix. Surprisingly, the 390 nt-long 3'UTR of *icaR* appears to be a negative determinant for the translation initiation of it own mRNA (Fig. 1c). The 3'UTR contains a C-rich sequence motif that binds to the SD sequence to prevent ribosome binding, and subsequently recruits RNase III for cleavage [51]. Disrupting this interaction resulted in the accumulation of IcaR and inhibited biofilm formation. This study shows that the 3'UTR can act in *cis* to block the ribosome binding site in the 5'UTR by a mechanism that is reminiscent of RNAIII and other *trans*-acting sRNAs from *S. aureus* (Fig. 1c). A significant number of mRNAs carrying large 3'UTRs have been recently mapped suggesting that the circularization of mRNA is not so uncommon in bacteria. In addition, these regions might also contain specific binding sites for *trans*-acting factors modifying the mRNA stability or translability, or can also be the reservoir of small regulatory RNAs as recently demonstrated in *Salmonella typhimurium* [64].

These examples demonstrate the importance of the translation regulation for the physiology of *S. aureus*. Analyzing the translational control on a global scale in *S. aureus* in response to the host and *vice versa* [65] will certainly open new horizons and insights into the pathogenesis, persistence of the bacteria within the host, and evolution of the strains.

SPECIFIC FEATURES OF *S. aureus* TRANSLATION INITIATION

Translation initiation is the rate-limiting step of protein synthesis [66]. This is probably why many regulatory events modulate the mRNA binding to the 30S ribosomal subunit [67–69] (Fig. 1). The initiation process of bacteria requires three initiation factors, IF1, IF2 and IF3, which in addition of the mRNA, and the initiator fMet-tRNA^{fMet}, assembled in a multi-step process on 30S to form an active initiation complex [66]. The efficiency of mRNA binding to 30S is independent of the initiation factors and relies solely on specific signatures present on the mRNAs such as the presence of SD sequence (GGAGG), the nature of the initiation codon, the distance between the initiation codon and the SD, the presence or not of structured motif within the mRNA track [70, 71]. Although this process is conserved among bacteria, significant differences have been observed between Gram-negative bacteria (*E. coli*) and low GC content Gram-positive bacteria such as *Bacillus subtilis* and *S. aureus*. Some of these features are described below.

Different mRNA binding properties of the 30S from low GC content Gram-positive and Gram-negative bacteria. In bacteria, the mRNA is recruited at a strategic position at the exit site of the 30S subunit surrounded by several key ribosomal proteins (r-proteins): S1, S2, S7, S11, S18 and S21 [66, 69]. Among these r-proteins, the largest r-protein S1 in *E. coli* with its six OB-fold (oligonucleotide/oligosaccharide-binding fold) domains confers to the 30S the ability to recognize any type of mRNAs [72–75]. Particularly, S1 has been shown to compensate the lack of a strong SD in many mRNAs, and to confer an RNA chaperone activity to the 30S that is essential for the unfolding of structured mRNAs in order to accommodate the initiation codon into the P-site. In *E. coli*, the essential activity of S1 is linked to its association with the 30S via its N-terminal OB-fold domain [75–77]. A phylogenetic study revealed that S1 from Gram-negative bacteria and high GC content Gram-positive bacteria (*Micrococcus*) contained at least the first four OB-fold domains that retained full 30S and RNA binding capacity, and the RNA chaperone activity [29, 75]. Interestingly, it has been shown that *Micrococcus luteus* S1 was able to substitute *E. coli* S1 on the 30S [28]. In contrast, S1 from low GC content Gram-positive bacteria, which contained only four OB-fold domains, has lost the N-terminal domain that was shown to promote specific binding with S2 on *E. coli* 30S [78]. This probably explained why *B. subtilis* S1 plays no major role in translation [28, 79]. Indeed, *B. subtilis* ribosomes have similar properties than S1-depleted *E. coli* ribosomes which have lost their abilities to translate mRNAs with no or weak SD sequence. Addition of S1 from *E. coli* or from *M. luteus* to the S1-depleted *E. coli* ribosomes restored the 30S properties to translate mRNAs bearing weak SD but these proteins had no effect on *B. subtilis* ribosomes [28, 79]. Another characteristic of *B. subtilis* ribosomes is the greater tolerance for the non-AUG initiation codons than *E. coli* ribosome but the presence of a strong SD significantly enhanced the capacity of *E. coli* ribosomes to utilize non-AUG codons [79]. It was thus proposed that firmicutes obviate the need of S1 acting on the 30S because the majority of mRNAs carry a strong SD sequence [80].

Because S1 is very similar in *B. subtilis* and *S. aureus* [29], we have analyzed the ability of *S. aureus* 30S subunits to form initiation complexes using various *S. aureus* mRNA substrates (Figs. 2, 3).

After purification of the 30S and 70S ribosomes [81], only traces of r-protein S1 were observed by mass spectrometry analysis suggesting that the protein is not tightly associated with the ribosome (results not shown). We then monitored the formation of initiation complexes formed by mRNA, 30S subunit and the ini-

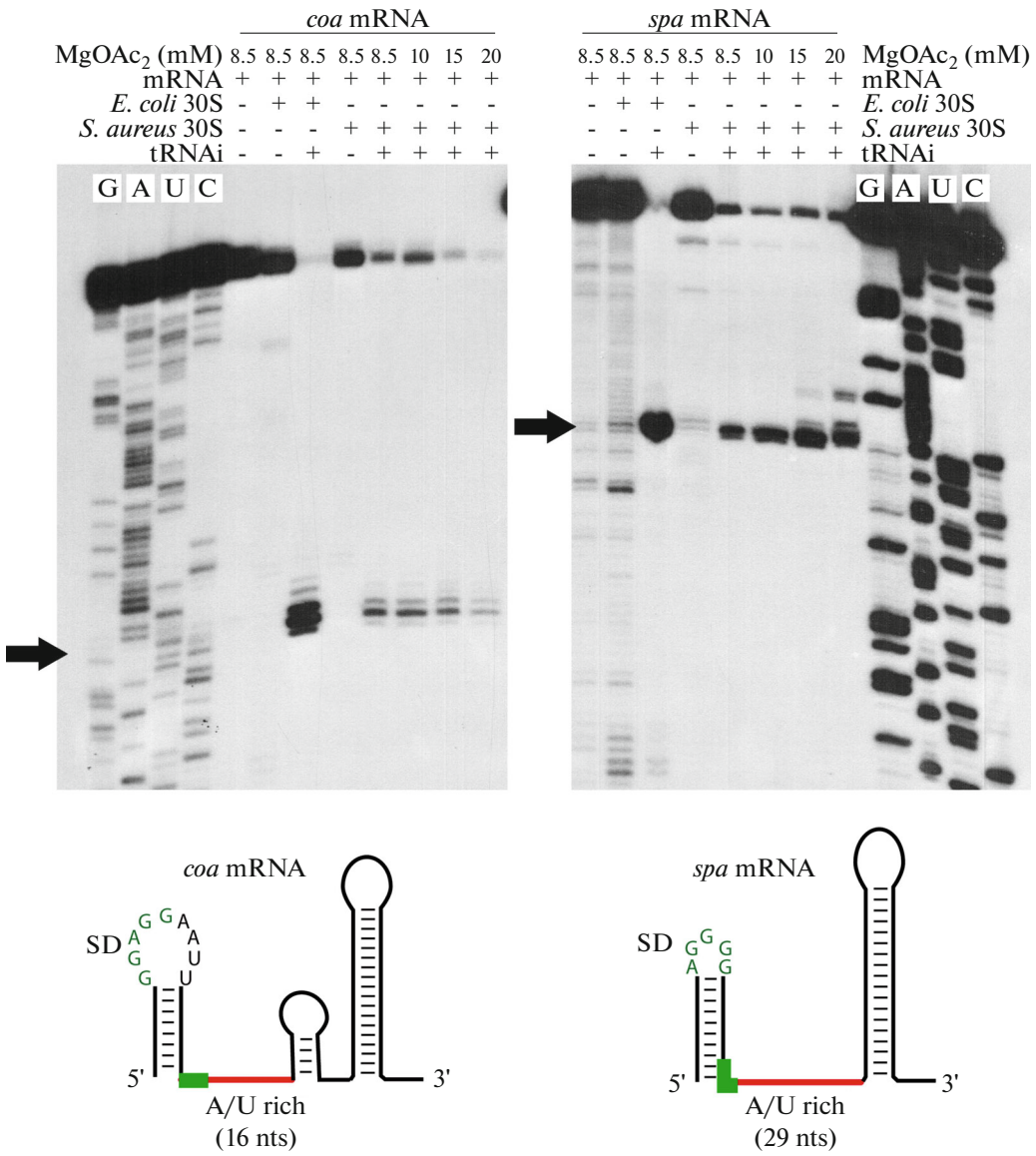

Fig. 2. Formation of simplified initiation ribosomal complex by toeprinting assays involving *coa* mRNA and *spa* mRNA encoding two virulence factors. The mRNAs (12 nM) were incubated with either *E. coli* 30S or *S. aureus* 30S (300 nM), and the initiator $tRNA^{fMet}$ (1 μM). The effect of increasing concentrations of magnesium (8.5 mM to 20 mM) was monitored on the formation of the initiation complex. Lanes G, A, U, C are sequencing ladders. Secondary structure models of *coa* and *spa* mRNAs are shown. SD is for the Shine and Dalgarno sequence (nucleotides in green). The initiation triplet is schematized by a green rectangle. The toeprint at position +16 is shown by an arrow. Experimental conditions were described in Fechter et al. [81]. nts is for nucleotides.

tiator tRNA using toeprinting assays [81, 82]. This approach is based on a premature reverse transcription arrest (called toeprint) caused by the formation of the simplified initiation complex, giving the exact position of the 3' edge of the 30S location on the mRNA. The signature of an active initiation complex is given by the position of the toeprint at position +16 from the AUG codon [82]. We first show that *S. aureus* 30S binds efficiently to *spa* and *coa* mRNAs, which encode two major virulence factors, protein A and coagulase, respectively. These two mRNAs harbor the same structure and sequence signatures, i.e. short 5'UTR, strong SD sequence present in a hairpin loop, and a rather long unpaired AU rich motif just downstream the initiation codon [44, 46] (Fig. 2). Conversely, two other mRNAs *mgrA* and *icaR*, which encode major transcriptional regulatory proteins, were poorly recognized by *S. aureus* 30S (Fig. 3). These two mRNAs contain a large and structured 5'UTR, in which the SD is embedded into a secondary structure [41, 49, 51]. It remains to be addressed whether these two mRNAs are less well translated in vivo than the virulence factors (protein A and coagulase). However, a comparative analysis performed with the *E. coli* ribo-

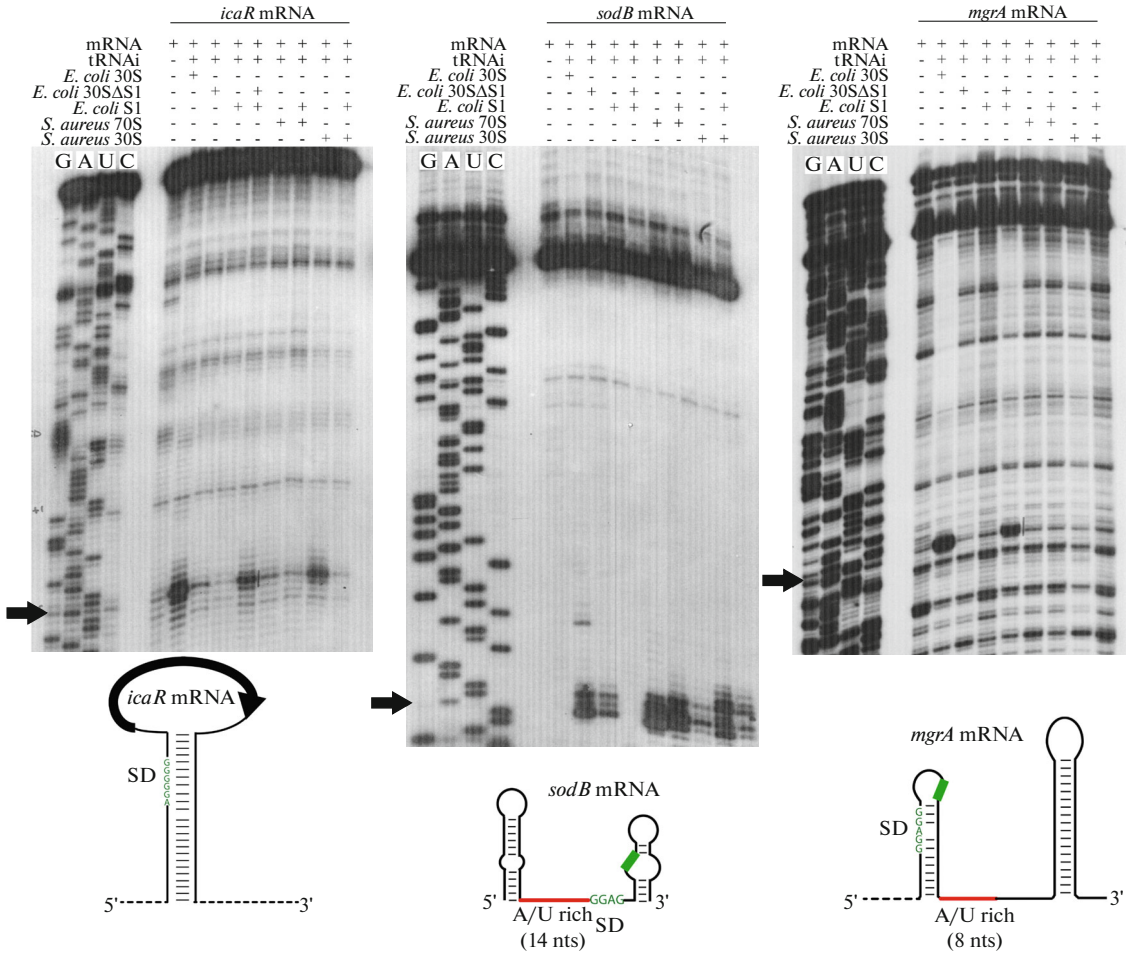

Fig. 3. Effect of *E. coli* ribosomal protein S1 on the formation of various initiation complexes involving *S. aureus icaR* and *mgrA* mRNAs and *E. coli sodB* mRNA. The mRNAs (12 nM) were incubated with *E. coli* 30S (300 nM), or *E. coli* S1-depleted 30S (as prepared in Duval *et al.* [75]), or with *E. coli* S1-depleted 30S pre-incubated with purified r-protein S1 (350 nM) in the presence of the initiator $tRNA^{fMet}$ (1 μM) (tRNAi). The same experiments were carried out with either *S. aureus* 70S or 30S (300 nM) either in the absence or in the presence of *E. coli* r-protein S1 (350 nM), and in the presence of the initiator $tRNA^{fMet}$ (1 μM). The toeprint at position +16 is shown by an arrow. The experiments show that the addition of *E. coli* S1 to the *E. coli* S1-depleted ribosome restored the formation of the initiation complex as evidenced by the toeprint at +16 while addition of *E. coli* S1 to the *S. aureus* ribosome inhibits the formation of the ternary initiation complex. Secondary structure models of *S. aureus icaR* and *mgrA* mRNAs, and of *E. coli sodB* mRNA are shown below the autoradiographies. SD is for the Shine and Dalgarno sequence (nucleotides in green). The initiation triplet is schematized by a green rectangle. The toeprint at position +16 is shown by an arrow. Experimental conditions were described in Fechter et al. [81].

somes containing S1, showed that the 30S are able to form initiation complexes with both *mgrA* and *icaR* mRNAs (Fig. 3). This efficient recognition was linked to the presence of S1 because S1-depleted *E. coli* 30S were not able to recognize the two structured mRNAs while mRNA binding was restored using S1-depleted 30S saturated with purified *E. coli* S1 added in *trans* (Fig. 3). Hence, these experiments indicate that the *S. aureus* 30S behaves as the *E. coli* S1-depleted 30S for the recognition of structured mRNAs. We finally compared the formation of the initiation complex formed with *E. coli sodB* mRNA encoding a superoxide dismutase and the ribosomes of either *E. coli* or of *S. aureus*. This mRNA is recognized by *E. coli* ribosomes in a manner independent of S1 [75]. Indeed, the toeprinting assays revealed that both *E. coli* and *S. aureus* ribosomes are able to form initiation complexes with *sodB* mRNA in a similar manner (Fig. 3). Surprisingly, the toeprint was strongly decreased if *E. coli* S1 was added to *S. aureus* ribosomes. The same result was also obtained with *icaR* mRNA (Fig. 3). We propose that *E. coli* S1 does not efficiently bind to *S. aureus* ribosome although most of the key residues in *E. coli* S2 that recognize the N-terminal domain of *E. coli* S1 are also conserved in *S. aureus* S2 [78]. This probably suggests that the S1 binding site in *E. coli* is more complex than expected [75]. The observed inhibition of the toeprint might result from a direct interaction of S1 with mRNAs outside of the ribosome. For instance *sodB* mRNA presents a large unpaired AU-rich

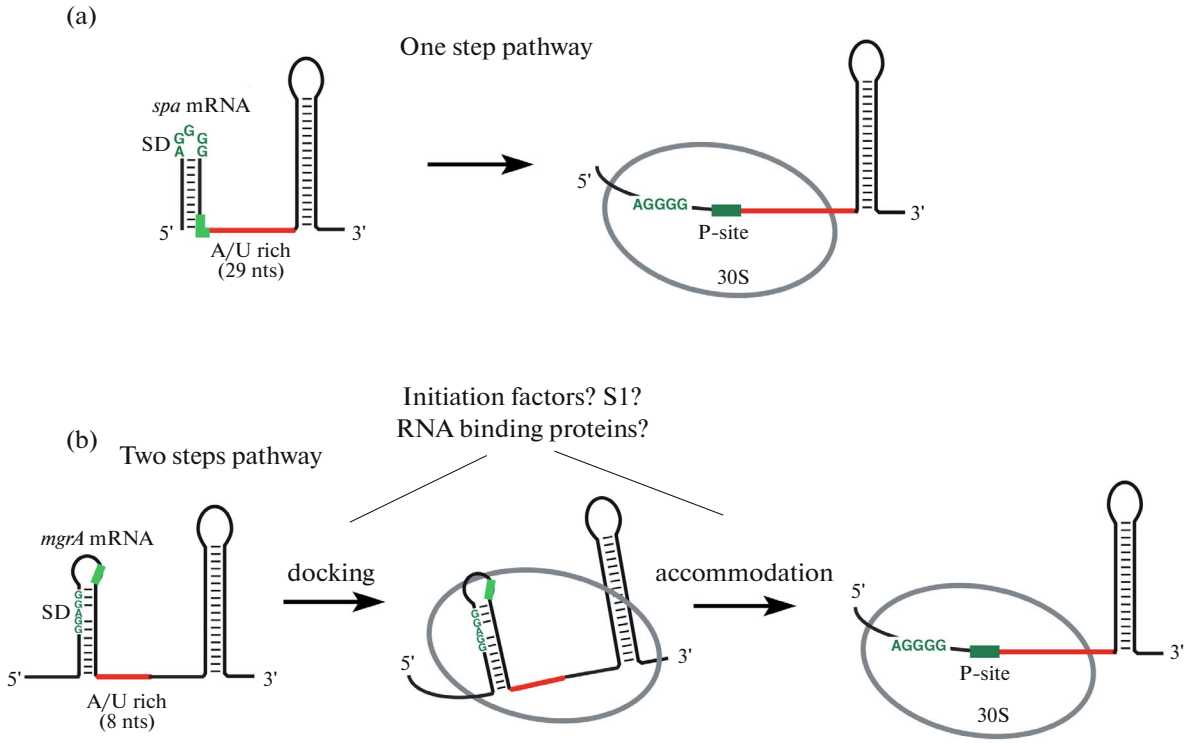

Fig. 4. Possible mechanisms for the formation of initiation complexes in *S. aureus*. (a) In the one-step pathway, the weakly structured mRNA (such as *spa* mRNA) is directly recruited on the 30S ribosomal subunit through its unpaired Shine and Dalgarno (SD) sequence. Due to the strong SD-antiSD interaction, the unpaired initiation codon will be located directly in the P-site. (b) For mRNAs carrying structures sequestering the SD (such as *mgrA* mRNA), it is expected that the recognition will involve at least two steps pathway where docking will be followed by the accommodation process to promote the correct positioning of the initiation codon. It is not yet known in vivo whether the unfolding process of the mRNA structure in *S. aureus* occurs on the ribosome through the action of the initiation factors or of an unknown RNA-binding protein or outside the ribosome possibly through the binding of protein S1. In these particular examples, the ribosome might also recognize the SD during the transcription process of the mRNA, i.e. before the formation of the inhibitory structure.

sequence just upstream the SD, known to be a typical binding site for S1 [75] (Fig. 3).

Taken together, these data show that the presence of a strong and unpaired SD in mRNA is necessary to be recognized by *S. aureus* 30S (Fig. 4a). How do *S. aureus* ribosomes initiate the translation of structured mRNAs is still an open question (Fig. 4b). Do structured mRNAs bind first to the platform of the 30S? Clearly, the melting and chaperone properties of *E. coli* S1 were not able to help *S. aureus* ribosome to unfold mRNA structure and liberate the SD sequence. Many questions remain to be explored. Does the shorter protein S1 in *S. aureus* contribute to the translation of structured mRNAs through direct mRNA binding outside of the ribosome? Do other *trans*-acting factors (RNA chaperone proteins, RNA helicases) act on the ribosome to promote translation of specific structured mRNAs? Does the coupling between transcription and translation provide a window allowing the ribosome to load on mRNA before the formation of structures within the ribosome binding site?

Ribosome hibernation, another mechanism to regulate translation initiation during growth. The formation of inactive ribosomal dimers, also referred to as 100S ribosomes or as hibernating ribosomes, repress protein synthesis in bacteria [83]. Inactive ribosome dimers are usually formed as a response of bacterial cells to unfavorable conditions and can be rapidly rescued after normalization of environment [84]. Formation of dimers is supposed to increase the survival rate under stress conditions [85]. In *B. subtilis*, a recent study showed that the dimers are formed during the early stationary phase and these dimers are required to facilitate rapid regrowth of cells if they are facing better nutrient conditions [86]. However, unlike in *E. coli* the 100S ribosomes in *S. aureus* were found in all growth phases [30] questioning on their exact roles under rich medium conditions during cell growth.

The mechanism of 100S ribosomes formation also varies between bacterial species. Many γ-proteobacteria (including *E. coli*) express three proteins: hibernation promoting factor (HPF, former name YhbH) [87], ribosome modulation factor (RMF) [85, 88] and protein YfiA (former names RaiA or protein Y) [89]. The formation of 100S ribosomes is driven by the concomitant binding of RMF and HPF proteins [90] while YfiA prevents the recycling of ribosomes and favors the formation of translationally inactive 70S

[89]. Despite of high similarity with HPF (~40%), YfiA occupies partially the RMF binding site [90, 91]. Instead in firmicutes (such as *S. aureus*), only one protein called long HPF has been identified [92]. Its N-terminal domain shares high similarity with short HPF and YfiA, but not with RMF protein (reviewed in [93]). This unique HPF protein can both promote the formation of 100S dimers and of non-functional 70S [30, 92].

Phenotypic analysis revealed that the depletion of RMF in *E. coli* leads to reduced long-term viability and stress tolerance during stationary phase while depletion of short HPF or YfiA do not cause strong cellular defects [93]. In contrast, depletion of the long HPF protein leads to decreased survival of *Lactococcus lactis* under stress conditions [94], decreased pathogenesis in *Listeria monocytogenes* [95], and enhanced sensitivity to prolonged antibiotic exposure [96]. Crystal structure of *E. coli* ribosome bound to YfiA showed that the protein is located close to the region where mRNA, tRNAs and initiation factors bind during protein synthesis [97]. Heterologous crystal structures of *T. thermophilus* 70S ribosome with *E. coli* hibernation factors showed that HPF shares the binding site with YfiA, whereas RMF binds next to the anti-SD region and prevents interaction of 16S rRNA and mRNA during the initiation process [91]. Single particle cryo-electron microscopy and cryo-electron tomography confirmed the presence of *E. coli* ribosome dimers in situ [98]. Ribosomal proteins S2, S9, S10 and helix 39 of 16S rRNA make contacts between two 70S particles but the hibernation factors were not directly involved in the contacts [91, 98]. The authors suggested that the dimerization occurs as a result of structural rearrangement of the head of 30S upon binding of RMF. However, it is still unclear whether the same mechanism and contacts are involved in ribosome dimerization in the long HPF in *S. aureus*. Due to high similarity between the short HPF of *E. coli* and the N-terminal domain of long HPF in *S. aureus*, we propose that these two proteins would share the same binding site on the ribosome, and that the C-terminal domain of long HPF might be directly involved in contacts between the two ribosomes in *S. aureus*. Hence, solving the high-resolution structure of the ribosome dimers from *S. aureus* will shed light on one biological mechanism that might promote successful persistence of this severe pathogen in response to stress conditions or antibiotic treatments.

TOWARDS THE HIGH RESOLUTION OF THE TRANSLATION MACHINERY IN *S. aureus*

Although the core of the bacterial ribosome is very conserved, certain peculiarities existed between the ribosomes of different bacterial species. These differences may determine some specifications for mRNA recognition, regulation of translation, and susceptibility to antibiotics. Two structures of low GC content Gram-positive ribosomes have been recently solved. The MifM-stalled 70S ribosome from *B. subtilis* was solved at a resolution of 3.5–3.9 Å by cryoelectron microscopy [15, 17] and the crystal structure of *S. aureus* 50S subunit was elucidated at a resolution of 3.5 Å [16]. The majority of the rRNAs of the core of *S. aureus* 50S subunit is structurally highly conserved. However, several helices, primarily located on the periphery of the ribosome, show sequence and length variability among different bacteria [16]. In contrast to the rRNA, more differences were observed for ribosomal proteins. Although the globular domains as well as the structural elements interacting with rRNAs are rather conserved, many of the r-proteins contained specific extensions. This is the case of universal r-protein uL3 and bacteria-specific r-protein bL17, which both carry a loop motif unique to staphylococci extending toward the solvent side at the periphery of the ribosome. Also the extension at the C-terminus of uL16 is located on the solvent side, while the protein is at the interface close to the tRNA binding sites. Interestingly, bL27 also carries an extended N-terminus that should be cleaved by a specific protease before the assembly of the 70S ribosome [32]. Although the N-terminal part of bL27 was only traced from residue 19 due to its high flexibility in the crystal structure [16], this domain is expected to be located in the proximity to the peptidyl-transferase center (PTC) and of the 5'-end of the P-site tRNA [16]. Nevertheless, these structural features alone could neither explain the different activities in protein synthesis and translation initiation as compared to *E. coli* ribosomes, nor the requirement of higher concentration of magnesium to avoid subunit dissociation as reported in earlier studies [99]. The crystal structure of *S. aureus* 50S was also solved in the presence of several antibiotics such as linezolid, telithromycin, and pleuromutilin revealing unexpected features in the orientation of some of the antibiotics specific for *S. aureus* [16].

Clearly, one of the important challenges for the future will be to determine the structure of the full ribosome under physiological conditions and/or trapped by antibiotics. It should better highlight the peculiarities located at strategic positions of the ribosome, such as the PTC, the decoding center, the tRNA binding sites, and the mRNA channel. Furthermore, more knowledge is required for the *trans*-acting factors (initiation factors, S1, RNA-binding proteins, RNA helicases, etc.) that could modulate the functioning of *S. aureus* ribosome at the initiation step. Time is certainly arrived to better understand at the molecular level, the differences observed in protein synthesis and control between Gram-negative bacteria and the low GC content Gram-positive bacteria, which comprise many human pathogens, such as *S. aureus*. These studies should pave the way to identify specific strategies to selectively inhibit *S. aureus* pathogenesis and/or growth with less effect on the

human microbiome and less selective pressure on resistant population.

ACKNOWLEDGMENTS

We thank all the members of our respective teams for helpful discussions. This work was supported by the 'Centre National de la Recherche Scientifique' (CNRS), 'Institut National de la Santé et de la Recherche Médicale' (INSERM), and the University of Strasbourg. This work benefits from funding from the state managed by the French National Research Agency as part of the Investments for the future program under the framework of the LabEx: ANR-10-LABX-0036_NETRNA (to P.R., Y.H.), from ANR-15-CE11-0021-01 (to G.Y.), from European Research Council advanced grant 294312 (to M.Y.), and from the Russian Government Program of Competitive Growth of Kazan Federal University (to M.Y., I.K. and G.Y.).

REFERENCES

1. Klinge S., Voigts-Hoffmann F., Leibundgut M., Ban N. 2012. Atomic structures of the eukaryotic ribosome. *Trends Biochem. Sci.* **37**, 189–198.
2. Melnikov S., Ben-Shem A., Garreau de Loubresse N., Jenner L., Yusupova G.Z., Yusupov M.M. 2012. One core, two shells: Bacterial and eukaryotic ribosomes. *Nat. Struct. Mol. Biol.* **19**, 560–567.
3. Petrov A.S., Bernier C.R., Hsiao C., Norris A.M., Kovacs N.A., Waterbury C.C., Stepanov V.G., Harvey S.C., Fox G.E., Wartell R.M., Hud N.V., Williams L.D. 2014. Evolution of the ribosome at atomic resolution. *Proc. Natl. Acad. Sci. U. S. A.* **111**, 10251–10256.
4. Sharma M.R., Wilson D.N., Datta P.P., Barat C., Schluenzen F., Fucini P., Agrawal R.K. 2007. Cryo-EM study of the spinach chloroplast ribosome reveals the structural and functional roles of plastid-specific ribosomal proteins. *Proc. Natl. Acad. Sci. U. S. A.* **104**, 19315–19320.
5. Amunts A., Brown A., Toots J., Scheres S.H., Ramakrishnan V. 2015. Ribosome. The structure of the human mitochondrial ribosome. *Science.* **348**, 95–98.
6. Greber B.J., Bieri P., Leibundgut M., Leitner A., Aebersold R., Boehringer D., Ban N. 2015. Ribosome. The complete structure of the 55S mammalian mitochondrial ribosome. *Science.* **348**, 303–308.
7. Poehlsgaard J., Douthwaite S. 2005. The bacterial ribosome as a target for antibiotics. *Nat. Rev. Microbiol.* **3**, 870–881.
8. Wilson D.N. 2014. Ribosome-targeting antibiotics and mechanisms of bacterial resistance. *Nat. Rev. Microbiol.* **12**, 35–48.
9. Allen G.S., Frank J. 2007. Structural insights on the translation initiation complex: Ghosts of a universal initiation complex. *Mol. Microbiol.* **63**, 941–950.
10. Myasnikov A.G., Simonetti A., Marzi S., Kloholz B.P. 2009. Structure–function insights into prokaryotic and eukaryotic translation initiation. *Curr. Opin. Struct. Biol.* **19**, 300–309.
11. Schuwirth B.S., Borovinskaya M.A., Hau C.W., Zhang W., Vila-Sanjurjo A., Holton J.M., Cate J.H. 2005. Structures of the bacterial ribosome at 3.5 Å resolution. *Science*. **310**, 827–834.
12. Noeske J., Wasserman M.R., Terry D.S., Altman R.B., Blanchard S.C., Cate J.H. 2015. High-resolution structure of the *Escherichia coli* ribosome. *Nat. Struct. Mol. Biol*. **22**, 336–341.
13. Yusupov M.M., Yusupova G.Z., Baucom A., Lieberman K., Earnest T.N., Cate J.H., Noller H.F. 2001. Crystal structure of the ribosome at 5.5 Å resolution. *Science*. **292**, 883–896.
14. Yusupova G.Z., Yusupov M.M., Cate J.H., Noller H.F. 2001. The path of messenger RNA through the ribosome. *Cell*. **106**, 233–241.
15. Beckert B., Kedrov A., Sohmen D., Kempf G., Wild K., Sinning I., Stahlberg H., Wilson D.N., Beckmann R. 2015. Translational arrest by a prokaryotic signal recognition particle is mediated by RNA interactions. *Nat. Struct. Mol. Biol*. **22**, 767–773.
16. Eyal Z., Matzov D., Krupkin M., Wekselman I., Paukner S., Zimmerman E., Rozenberg H., Bashan A., Yonath A. 2015. Structural insights into species-specific features of the ribosome from the pathogen *Staphylococcus aureus. Proc. Natl. Acad. Sci. U. S. A.* **112**, E5805–5814.
17. Sohmen D., Chiba S., Shimokawa-Chiba N., Innis C.A., Berninghausen O., Beckmann R., Ito K., Wilson D.N. 2015. Structure of the *Bacillus subtilis* 70S ribosome reveals the basis for species-specific stalling. *Nat. Commun*. **6**, 6941.
18. Lowy F.D. 1998. *Staphylococcus aureus* infections. *New Engl. J. Med*. **339**, 520–532.
19. Kreiswirth B., Kornblum J., Arbeit R.D., Eisner W., Maslow J.N., McGeer A., Low D.E., Novick R.P. 1993. Evidence for a clonal origin of methicillin resistance in *Staphylococcus aureus. Science*. **259**, 227–230.
20. Pofelski J., Pavese P., Brion J.P., Marrakchi C., Gay E., Recule C., Stahl J.P. 2003. *Staphylococcus aureus* meningitis with intermediate sensitivity to glycopeptides. Therapeutic indications. *Presse Med*. **32**, 217–220.
21. Howden B.P., Davies J.K., Johnson P.D., Stinear T.P., Grayson M.L. 2010. Reduced vancomycin susceptibility in *Staphylococcus aureus*, including vancomycin-intermediate and heterogeneous vancomycin-intermediate strains: Resistance mechanisms, laboratory detection, and clinical implications. *Clin. Microbiol. Rev*. **23**, 99–139.
22. Koch G., Yepes A., Forstner K.U., Wermser C., Stengel S.T., Modamio J., Ohlsen K., Foster K.R., Lopez D. 2014. Evolution of resistance to a last-resort antibiotic in *Staphylococcus aureus* via bacterial competition. *Cell*. **158**, 1060–1071.
23. Nadell C.D., Xavier J.B., Foster K.R. 2009. The sociobiology of biofilms. *FEMS Microbiol. Rev*. **33**, 206–224.
24. Cegelski L., Marshall G.R., Eldridge G.R., Hultgren S.J. 2008. The biology and future prospects of antivirulence therapies. *Nat. Rev. Microbiol*. **6**, 17–27.
25. Gordon C.P., Williams P., Chan W.C. 2013. Attenuating *Staphylococcus aureus* virulence gene regulation: A

medicinal chemistry perspective. *J. Med. Chem.* **56**, 1389–1404.

26. Gray B., Hall P., Gresham H. 2013. Targeting *agr*- and *agr*-like quorum sensing systems for development of common therapeutics to treat multiple gram-positive bacterial infections. *Sensors.* **13**, 5130–5166.
27. Messina J.A., Thaden J.T., Sharma-Kuinkel B.K., Fowler V.G.J. 2016. Impact of bacterial and human genetic variation on *Staphylococcus aureus* infections. *PLoS Pathog.* **12**, e1005330.
28. Farwell M.A., Roberts M.W., Rabinowitz J.C. 1992. The effect of ribosomal protein S1 from *Escherichia coli* and *Micrococcus luteus* on protein synthesis in vitro by *E. coli* and *Bacillus subtilis. Mol. Microbiol.* **6**, 3375–3383.
29. Salah P., Bisaglia M., Aliprandi P., Uzan M., Sizun C., Bontems F. 2009. Probing the relationship between Gram-negative and Gram-positive S1 proteins by sequence analysis. *Nucleic Acids Res.* **37**, 5578–5588.
30. Ueta M., Wada C., Wada A. 2010. Formation of 100S ribosomes in *Staphylococcus aureus* by the hibernation promoting factor homolog SaHPF. *Genes Cells.* **15**, 43–58.
31. Chirgadze Y.N., Clarke T.E., Romanov V., Kisselman G., Wu-Brown J., Soloveychik M., Chan T.S., Gordon R.D., Battaile K.P., Pai E.F., Chirgadze N.Y. 2015. The structure of SAV1646 from *Staphylococcus aureus* belonging to a new "ribosome-associated" subfamily of bacterial proteins. *Acta Crystallogr. D: Biol. Crystallogr.* **71**, 332–337.
32. Wall E.A, Caufield J.H., Lyons C.E., Manning K.A., Dokland T., Christie G.E. 2015. Specific N-terminal cleavage of ribosomal protein L27 in *Staphylococcus aureus* and related bacteria. *Mol. Microbiol.* **95**, 258–269.
33. Ibarra J.A., Perez-Rueda E., Carroll R.K., Shaw L.N. 2013. Global analysis of transcriptional regulators in *Staphylococcus aureus. BMC Genomics.* **14**, 126.
34. Felden B., Vandenesch F., Bouloc P., Romby P. 2011. The *Staphylococcus aureus* RNome and its commitment to virulence. *PLoS Pathog.* **7**, e1002006.
35. Tomasini A., Francois P., Howden B.P., Fechter P., Romby P., Caldelari I. 2014. The importance of regulatory RNAs in *Staphylococcus aureus. Infect. Genet. Evol.* **21**, 616–626
36. Lasa I., Toledo-Arana A., Gingeras T.R. 2012. An effort to make sense of antisense transcription in bacteria. *RNA Biol.* **9**, 1039–1044.
37. Novick R.P., Ross H.F., Projan S.J., Kornblum J., Kreiswirth B., Moghazeh S. 1993. Synthesis of staphylococcal virulence factors is controlled by a regulatory RNA molecule. *EMBO J.* **12**, 3967–3975.
38. Novick R.P., Geisinger E. 2008. Quorum sensing in staphylococci. *Annu. Rev. Genet.* **42**, 541–564.
39. Geisinger E., Muir T.W., Novick R.P. 2009. *agr* receptor mutants reveal distinct modes of inhibition by staphylococcal autoinducing peptides. *Proc. Natl. Acad. Sci. U. S. A.* **106**, 1216–1221
40. Morfeldt E., Taylor D., von Gabain A., Arvidson S. 1995. Activation of alpha-toxin translation in *Staphylococcus aureus* by the trans-encoded antisense RNA, RNAIII. *EMBO J.* **14**, 4569–4577.
41. Gupta R.K., Luong T.T., Lee C.Y. 2015. RNAIII of the *Staphylococcus aureus* agr system activates global regulator MgrA by stabilizing mRNA. *Proc. Natl. Acad. Sci. U. S. A.* **112**, 14036–14041.
42. Benito Y., Kolb F.A., Romby P., Lina G., Etienne J., Vandenesch F. 2000. Probing the structure of RNAIII, the *Staphylococcus aureus agr* regulatory RNA, and identification of the RNA domain involved in repression of protein A expression. *RNA.* **6**, 668–679.
43. Boisset S., Geissmann T., Huntzinger E., Fechter P., Bendridi N., Possedko M., Chevalier C., Helfer A.C., Benito Y., Jacquier A., Gaspin C., Vandenesch F., Romby P. 2007. *Staphylococcus aureus* RNAIII coordinately represses the synthesis of virulence factors and the transcription regulator Rot by an antisense mechanism. *Genes Dev*, **21**, 1353–1366.
44. Huntzinger E., Boisset S., Saveanu C., Benito Y., Geissmann T., Namane A., Lina G., Etienne J., Ehresmann B., Ehresmann C., Jacquier A., Vandenesch F., Romby P. 2005. *Staphylococcus aureus* RNAIII and the endoribonuclease III coordinately regulate *spa* gene expression. *EMBO J.* **24**, 824–835.
45. Geisinger E., Adhikari R.P., Jin R., Ross H.F., Novick R.P. 2006. Inhibition of rot translation by RNAIII, a key feature of *agr* function. *Mol. Microbiol.* **61**, 1038–1048.
46. Chevalier C., Boisset S., Romilly C., Masquida B., Fechter P., Geissmann T., Vandenesch F., Romby P. 2010. *Staphylococcus aureus* RNAIII binds to two distant regions of *coa* mRNA to arrest translation and promote mRNA degradation. *PLoS Pathog.* **6**, e1000809
47. Chabelskaya S., Bordeau V., Felden B. 2014. Dual RNA regulatory control of a *Staphylococcus aureus* virulence factor. *Nucleic Acids Res.* **42**, 4847–4858.
48. Nitzan M., Fechter P., Peer A., Altuvia Y., Bronesky D., Vandenesch F., Romby P., Biham O., Margalit H. 2015. A defense-offense multi-layered regulatory switch in a pathogenic bacterium. *Nucleic Acids Res.* **43**, 1357–1369.
49. Romilly C., Lays C., Tomasini A., Caldelari I., Benito Y., Hammann P., Geissmann T., Boisset S., Romby P., Vandenesch F. 2014. A non-coding RNA promotes bacterial persistence and decreases virulence by regulating a regulator in *Staphylococcus aureus. PLoS Pathog.* **10**, e1003979.
50. Geissmann T., Marzi S., Romby P. 2009. A search for small noncoding RNAs in *Staphylococcus aureus* reveals a conserved sequence motif for regulation. *Nucleic Acids Res.* **37**, 7239–7259.
51. Ruiz de los Mozos I., Vergara-Irigaray M., Segura V., Villanueva M., Bitarte N., Saramago M., Domingues S., Arraiano C.M., Fechter P., Romby P., Valle J., Solano C., Lasa I., Toledo-Arana A. 2013. Base pairing interaction between 5'- and 3'-UTRs controls icaR mRNA translation in *Staphylococcus aureus. PLoS Genet.* **9**, e1004001.
52. Beaume M., Hernandez D., Farinelli L., Deluen C., Linder P., Gaspin C., Romby P., Schrenzel J., Francois P. 2010. Cartography of methicillin-resistant *S. aureus* transcripts: Detection, orientation and temporal expression during growth phase and stress conditions. *PLoS ONE.* **5**, e10725.

53. Bohn C., Rigoulay C., Chabelskaya S., Sharma C.M., Marchais A., Skorski P., Borezee-Durant E., Barbet R., Jacquet E., Jacq A., Gautheret D., Felden B., Vogel J., Bouloc P. 2010. Experimental discovery of small RNAs in *Staphylococcus aureus* reveals a riboregulator of central metabolism. *Nucleic Acids Res.* **38**, 6620–6636.

54. Durand S., Braun F., Lioliou E., Romilly C., Helfer A.C., Kuhn L., Quittot N., Nicolas P., Romby P., Condon C. 2015. A nitric oxide regulated small RNA controls expression of genes involved in redox homeostasis in *Bacillus subtilis. PLoS Genet*. **11**, e1004957.

55. Anderson K.L., Roberts C., Disz T., Vonstein V., Hwang K., Overbeek R., Olson P.D., Projan S.J., Dunman P.M. 2006. Characterization of the *Staphylococcus aureus* heat shock, cold shock, stringent, and SOS responses and their effects on log-phase mRNA turnover. *J. Bacteriol.* **188**, 6739–6756.

56. Lasa I., Toledo-Arana A., Dobin A., Villanueva M., de Los Mozos I.R., Vergara-Irigaray M., Segura V., Fagegaltier D., Penades J.R., Valle J., Solano C., Gingeras T.R. 2011. Genome-wide antisense transcription drives mRNA processing in bacteria. *Proc. Natl. Acad. Sci. U. S. A.* **108**, 20172–20177.

57. Barrick J.E., Breaker R.R. 2007. The distributions, mechanisms, and structures of metabolite-binding riboswitches. *Genome Biol.* **8**, R239.

58. Caldelari I., Fechter P., Lioliou E., Romilly C., Chevalier C., Gaspin C., Romby P. 2011. A current overview of regulatory RNAs in *Staphylococcus aureus*. In: *Regulatory RNAs in Prokaryotes.* Eds. Marchfelder A., Hess W. Wien: Wiley.

59. Mulhbacher J., St-Pierre P., Lafontaine D.A. 2010. Therapeutic applications of ribozymes and riboswitches. *Curr. Opin. Pharmacol.* **10**, 551–556.

60. Breaker R.R. 2011. Prospects for riboswitch discovery and analysis. *Mol. Cell.* **43**, 867–879.

61. Mulhbacher J., Brouillette E., Allard M., Fortier L.C., Malouin F., Lafontaine D.A. 2010. Novel riboswitch ligand analogs as selective inhibitors of guanine-related metabolic pathways. *PLoS Pathog.* **6**, e1000865.

62. Ster C., Allard M., Boulanger S., Lamontagne Boulet M., Mulhbacher J., Lafontaine D.A., Marsault E., Lacasse P., Malouin F. 2013. Experimental treatment of *Staphylococcus aureus* bovine intramammary infection using a guanine riboswitch ligand analog. *J. Dairy Sci.* **96**, 1000–1008.

63. Linder P., Lemeille S., Redder P. 2014. Transcriptome-wide analyses of 5'-ends in RNase J mutants of a gram-positive pathogen reveal a role in RNA maturation, regulation and degradation. *PLoS Genet.* **10**, e1004207.

64. Chao Y., Vogel J. 2016. A 3'UTR-derived small RNA provides the regulatory noncoding arm of the inner membrane stress response. *Mol. Cell.* **61**, 352–363.

65. Westermann A.J., Forstner K.U., Amman F., Barquist L., Chao Y., Schulte L.N., Muller L., Reinhardt R., Stadler P.F., Vogel J. 2016. Dual RNA-seq unveils noncoding RNA functions in host-pathogen interactions. *Nature*. **529**, 496–501.

66. Simonetti A., Marzi S., Jenner L., Myasnikov A., Romby P., Yusupova G., Klaholz B.P., Yusupov M. 2009. A structural view of translation initiation in bacteria. *Cell. Mol. Life Sci.* **66**, 423–436.

67. Romby P., Springer M. 2007. Translational control in prokaryotes. In: *Translational Control in Biology and Medicine.* Eds. Matthews M.B.S.N., Hershey J.W.B. Cold Spring Harbor: Cold Spring Harbor Lab. Press, pp. 803–827.

68. Wagner E.G., Romby P. 2015. Small RNAs in bacteria and archaea: Who they are, what they do, and how they do it. *Adv. Genet.* **90**, 133–208.

69. Duval M., Simonetti A., Caldelari I., Marzi S. 2015. Multiple ways to regulate translation initiation in bacteria: Mechanisms, regulatory circuits, dynamics. *Biochimie.* **114**, 18–29.

70. Studer S.M., Joseph S. 2006. Unfolding of mRNA secondary structure by the bacterial translation initiation complex. *Mol. Cell.* **22**, 105–115.

71. Milon P., Maracci C., Filonava L., Gualerzi C.O., Rodnina M.V. 2012. Real-time assembly landscape of bacterial 30S translation initiation complex. *Nat. Struct. Mol. Biol.* **19**, 609–615.

72. Boni I.V., Isaeva D.M., Musychenko M.L., Tzareva N.V. 1991. Ribosome-messenger recognition: mRNA target sites for ribosomal protein S1. *Nucleic Acids Res.* **19**, 155–162.

73. Tzareva N.V., Makhno V.I., Boni I.V. 1994. Ribosome-messenger recognition in the absence of the Shine-Dalgarno interactions. *FEBS Lett.* **337**, 189–194.

74. Sorensen M.A., Fricke J., Pedersen S. 1998. Ribosomal protein S1 is required for translation of most, if not all, natural mRNAs in *Escherichia coli* in vivo. *J. Mol. Biol.* **280**, 561–569.

75. Duval M., Korepanov A., Fuchsbauer O., Fechter P., Haller A., Fabbretti A., Choulier L., Micura R., Klaholz B.P., Romby P., Springer M., Marzi S. 2013. *Escherichia coli* ribosomal protein S1 unfolds structured mRNAs onto the ribosome for active translation initiation. *PLoS Biol.* **11**, e1001731.

76. Byrgazov K., Manoharadas S., Kaberdina A.C., Vesper O., Moll I. 2012. Direct interaction of the N-terminal domain of ribosomal protein S1 with protein S2 in *Escherichia coli. PLoS ONE.* **7**, e32702.

77. Byrgazov K., Vesper O., Moll I .2013. Ribosome heterogeneity: Another level of complexity in bacterial translation regulation. *Curr. Opin. Microbiol.* **16**, 133–139.

78. Byrgazov K., Grishkovskaya I., Arenz S., Coudevylle N., Temmel H., Wilson D.N., Djinovic-Carugo K., Moll I. 2015. Structural basis for the interaction of protein S1 with the *Escherichia coli* ribosome. *Nucleic Acids Res.* **43**, 661–673.

79. Vellanoweth R.L., Rabinowitz J.C. 1992. The influence of ribosome-binding-site elements on translational efficiency in *Bacillus subtilis* and *Escherichia coli* in vivo. *Mol. Microbiol.* **6**, 1105–1114.

80. Omotajo D., Tate T., Cho H., Choudhary M. 2015. Distribution and diversity of ribosome binding sites in prokaryotic genomes. *BMC Genomics.* **16**, 604-612.

81. Fechter P., Chevalier C., Yusupova G., Yusupov M., Romby P., Marzi S. 2009. Ribosomal initiation complexes probed by toeprinting and effect of trans-acting translational regulators in bacteria. *Methods Mol. Biol.* **540**, 247–263.

82. Hartz D., McPheeters D.S., Traut R., Gold L. 1988. Extension inhibition analysis of translation initiation complexes. *Methods Enzymol.* **164**, 419–425.

83. Yoshida H., Maki Y., Kato H., Fujisawa H., Izutsu K., Wada C., Wada A. 2002. The ribosome modulation factor (RMF) binding site on the 100S ribosome of *Escherichia coli*. *J. Biochem*. **132**, 983–989.

84. Wada A., Yamazaki Y., Fujita N., Ishihama A. 1990. Structure and probable genetic location of a "ribosome modulation factor" associated with 100S ribosomes in stationary-phase *Escherichia coli* cells. *Proc. Natl. Acad. Sci. U. S. A*. **87**, 2657–2661.

85. Yamagishi M., Matsushima H., Wada A., Sakagami M., Fujita N., Ishihama A. 1993. Regulation of the *Escherichia coli rmf* gene encoding the ribosome modulation factor: Growth phase- and growth rate-dependent control. *EMBO J.* **12**, 625–630.

86. Akanuma G., Kazo Y., Tagami K., Hiraoka H., Yano K., Suzuki S., Hanai R., Nanamiya H., Kato-Yamada Y., Kawamura F. 2016. Ribosome dimerization is essential for the efficient regrowth of *Bacillus subtilis*. *Microbiology*. **162** (3), 448–458. doi 10.1099/mic.0.000234

87. Maki Y., Yoshida H., Wada A. 2000. Two proteins, YfiA and YhbH, associated with resting ribosomes in stationary phase *Escherichia coli*. *Genes Cells*. **5**, 965–974.

88. Izutsu K., Wada A., Wada C. 2001. Expression of ribosome modulation factor (RMF) in *Escherichia coli* requires ppGpp. *Genes Cells*. **6**, 665–676.

89. Agafonov D.E., Kolb V.A., Nazimov I.V., Spirin A.S. 1999. A protein residing at the subunit interface of the bacterial ribosome. *Proc. Natl. Acad. Sci. U. S. A*. **96**, 12345–12349.

90. Ueta M., Yoshida H., Wada C., Baba T., Mori H., Wada A. 2005. Ribosome binding proteins YhbH and YfiA have opposite functions during 100S formation in the stationary phase of *Escherichia coli*. *Genes Cells*. **10**, 1103–1112.

91. Polikanov Y.S., Blaha G.M., Steitz T.A. 2012. How hibernation factors RMF, HPF, and YfiA turn off protein synthesis. *Science*. **336**, 915–918.

92. Ueta M., Wada C., Daifuku T., Sako Y., Bessho Y., Kitamura A., Ohniwa R.L., Morikawa K., Yoshida H., Kato T., Miyata T., Namba K., Wada A. 2013. Conservation of two distinct types of 100S ribosome in bacteria. *Genes Cells*. **18**, 554–574.

93. Yoshida H., Wada A. 2014. The 100S ribosome: Ribosomal hibernation induced by stress. *Wiley Interdisc. Rev. RNA*. **5**, 723–732.

94. Puri P., Eckhardt T.H., Franken L.E., Fusetti F., Stuart M.C., Boekema E.J., Kuipers O.P., Kok J., Poolman B. 2014. *Lactococcus lactis* YfiA is necessary and sufficient for ribosome dimerization. *Mol. Microbiol*. **91**, 394–407.

95. Kline B.C., McKay S.L., Tang W.W., Portnoy D.A. 2015. The *Listeria monocytogenes* hibernation-promoting factor is required for the formation of 100S ribosomes, optimal fitness, and pathogenesis. *J. Bacteriol*. **197**, 581–591.

96. McKay S.L., Portnoy D.A. 2015. Ribosome hibernation facilitates tolerance of stationary-phase bacteria to aminoglycosides. *Antimicrob. Agents Chemother*. **59**, 6992–6999.

97. Vila-Sanjurjo A., Schuwirth B.S., Hau C.W., Cate J.H. 2004. Structural basis for the control of translation initiation during stress. *Nat. Struct. Mol. Biol*. **11**, 1054–1059.

98. Ortiz J.O., Brandt F., Matias V.R., Sennels L., Rappsilber J., Scheres S.H., Eibauer M., Hartl F.U., Baumeister W. 2010. Structure of hibernating ribosomes studied by cryoelectron tomography in vitro and in situ. *J. Cell Biol*. **190**, 613–621.

99. Mao J.C.H. 1967. Protein synthesis in a cell-free extract from *Staphylococcus aureus*. *J. Bacteriol*. **94**, 80–86.

Objectives and experimental strategies

I. How *S. aureus* ribosome initiates translation of structured mRNAs?

I.1. Biological questions and objectives

As I have mentioned in the introduction, *S. aureus* has evolved sophisticated means to tune the efficiency of translation of different genes in response to the host, stress and various environmental changes. Gene expression regulation is often exerted at the earliest step of protein biosynthesis, the initiation process, when the mRNA is recruited on the 30S ribosomal subunit and accommodated in the decoding channel for the interaction with the initiator tRNA at the P site. Specific features of mRNAs such as the length and the position of the SD sequence (Chen et al., 1994; Vimberg et al., 2007), the «stand-by » site acting as an enhancer sequence preceding the SD (Salis et al., 2009), the type of initiation codon and the secondary structures at the 5' UTR, are all key determinants for translation efficiency. Transcriptomic analysis of *S. aureus* has revealed that numerous mRNAs encoding for virulence factors, stress responses and metabolism, carry large structured 5' and 3' UTR where regulatory domains are potentially embedded (Ruiz de los Mozos et al., 2013). If Gram-negative ribosomes have the ability to deal with a wealth of different structures and different SD strengths thanks to their protein S1 (Duval et al., 2013a), *S. aureus* ribosomes do not carry S1 and did not show the same plasticity in recognizing structured mRNAs (Khusainov et al., 2016). Nevertheless, those structured mRNAs have to be translated, at least in some specific conditions, and translational regulators are expected to compensate for the loss of the associated S1. Alternatively, *Sau*S1 would still induce the translation of specific mRNAs outside of the 30S, acting as a translational activator. The first aim of my thesis was to understand the impact of *Sau*S1 on translation initiation of structured mRNAs and on cell physiology.

I.2. Main experimental strategies

In order to decipher the impact that *Sau*S1 could have on the initiation of translation of specific mRNAs, I have used different experimental approaches. I also have benefit from the expertise of the team members: Isabelle Caldelari designed and performed some experiments, Anne-Catherine Helfer and Lucas Herrgott gave their technical support and

conceptual advice, Melodie Duval, Delphine Bronesky and Emma Desgranges gave me intellectual contribution and have also stimulated scientific discussions.

- First I have followed the expression profiles of the *rpsA* gene (*Sau*S1) by Northern blot and Western blot analysis, to understand in which conditions the protein accumulated. Its expression profile has been compared with other r-proteins giving some insights on its regulatory functions.
- Mutagenesis of the *rpsA* gene (complete deletion or intron insertion) has been carried out to better understand its functions. Indeed, I have used the *rpsA* mutant strains to look for phenotypic alteration using different stress conditions. Moreover, comparative transcriptomic and quantitative proteomic analyses of the wild type and mutant Δ*rpsA* strains have revealed the genes for which the expression is regulated by *Sau*S1, providing some hints on the mRNA targets which would require S1 for their translation.
- Using comparative (Δ*rpsA*/WT) polysome profiles coupled with Northern blot analysis, we have monitored the effect of *Sau*S1 *in vivo* on the level of translation of selected target mRNAs.
- The mRNAs issued from the OMICS analysis and confirmed by the polysome profiles, have been then validated *in vitro* by toe-printing assays to monitor the effect of purified *Sau*S1 on the formation of initiation complexes using isolated 30S ribosomal subunit. In parallel, I have analyzed the ability of *Sau*S1 to directly bind the mRNAs and to present them to the ribosomes using gel retardation assays (EMSA) and gel filtration chromatographies, respectively.

In collaboration with F. Vandenesch (Centre International de Recherche en Infectiologie, CIRI, Lyon), the Δ*rpsA* mutant strain will be used to monitor the effect of *SauS1* on virulence. Cellular and animal models to check host interaction and infectivity are indeed available in Lyon and can be used to specifically analyze tissue colonization, immune system evasion and dissemination.

II. Could *Sau*S1 be involved in regulatory mechanisms mediated by small non-coding RNAs?

II.1. Biological questions and Objectives

In Gram-negative bacteria, most if not all of the identified sRNAs, requires the Sm-like protein Hfq for their stability and functional activation (Wagner and Romby, 2015). Hfq forms a ring-shaped homohexamer that binds the U-rich terminator at the 3′ end of most sRNAs (Otaka et al., 2011) protecting the Hfq-associated sRNAs from cellular ribonucleases (Brennan and Link, 2007; Valentin-Hansen et al., 2004) and helping them to recognize their target mRNAs (Storz et al., 2011; Updegrove et al., 2016). Several mechanisms of regulation mediated by Hfq have also been described in *E. coli.* In association with sRNAs, Hfq can directly repress or activate the translation of target mRNAs by sequestering/liberating their RBS. Deletion of *E. coli hfq* leads to pleiotropic effects such as growth defect, sensitivity to UV light and increased cell length (Tsui et al., 1994). Mutations in *hfq* also decreased virulence in several pathogens (for review, see Vogel and Papenfort 2006). In contrast to this, the function of Hfq in low G+C Gram-positive bacteria is still unclear and controversial. In *S. aureus*, Hfq has been shown to interact with RNAIII, but it neither enhance its recognition with target mRNAs (Zheng et al., 2016) and nor affects their stability (Boisset et al., 2007; Preis et al., 2009). Furthermore, it is not involved in antibiotic resistance and stress responses, it is dispensable for metabolic pathway regulations and no phenotypes were linked to its deletion (Bohn et al., 2007; Geisinger et al., 2006; Huntzinger et al., 2005). Even if Hfq seems to be dispensable for riboregulation by sRNAs in low G+C Gram-positive bacteria (e.g. Firmicutes) (Jousselin et al., 2009), other aspects have to be taken into account. First, it has been shown that in methicillin-resistant staphylococcal strain (MRSA), Hfq largely contributes to stress resistance and pathogenicity (Liu *et al*., 2010), suggesting a strain-dependent function of this protein. Second, Hfq homologues are found in several species belonging to Firmicutes division (Sun et al., 2002; Valentin-Hansen et al., 2004) with high conservation of the amino acids of the proximal and distal faces, which bind to sRNA and mRNA, respectively (Sun et al., 2002). Interestingly, another region of Hfq has been shown to be essential for the annealing activity, *i.e.* the Arginine-rich rim region (Panja et al., 2013). The ability of increasing the rate of RNA base-pairings and of

stabilizing the sRNA–mRNA complex, depend on the number of Arginine residues in this region (Zheng et al., 2016). In *E. coli*, Hfq rim contains three arginines, in *B. subtilis* only one and in *S. aureus* none, explaining why the protein does not mediates the annealing.

*Eco*S1 is an RNA chaperone protein which is able to promote strand displacement (Rajkowitsch and Schroeder, 2007). It binds numerous mRNAs to induce structural rearrangements and to facilitate the binding of the ribosome (Duval et al., 2013b). This activity is primarily carried out by its first four domains (d1 to d4) (Duval et al., 2017). Except d1, all the other domains are present in *Sau*S1. Is SauS1 able to bind RNAs outside the ribosome context? Which are the RNA partners of *Sau*S1? Does *SauS1* interact with other protein partners? Could *Sau*S1 also participate to the sRNA-dependent regulation? Does *Sau*S1 protect sRNA from degradation or help them to promote annealing to the target RNAs? The second aim of my thesis was to address the SauS1 regulatory functions expanding our investigation beyond its possible translation roles. Its impact on sRNA-dependent regulations has been particularly studied.

II.2. Main experimental strategies

The transcriptomic analysis obtained from the first part of my thesis has provided some indications on different roles of *Sau*S1 in *S. aureus* RNA metabolism. In order to understand which complexes involve *Sau*S1 and which RNAs are direct targets, different *in vivo* and *in vitro* approaches have been used.

- A strain carrying a flag-tagged version of the *rpsA* gene constructed by Isabelle Caldelari has been used to perform co-immunoprecipitation (Co-IP) assays. RNA-seq and LC/MSMS analyses of the purified complexes identified the *in vivo* targets of *Sau*S1.
- Several RNAs specifically co-immunoprecipitated with *Sau*S1 have been validated *in vitro* using gel retardation assays.
- The possible effect of *Sau*S1 on sRNA-target RNAs interaction has been monitored using gel-retardation assays, and the annealing activity of *Sau*S1 has been followed by FRET analysis.
- The localization of *SauS1* on several sRNA targets has been checked by footprinting experiments. However, taken into account the transient and dynamic interaction occurring between the chaperone protein and its target

RNAs, we have introduced a crosslinking step to stabilize the ribonucleoprotein particule (RNP).

III. Summary of the main experimental strategies

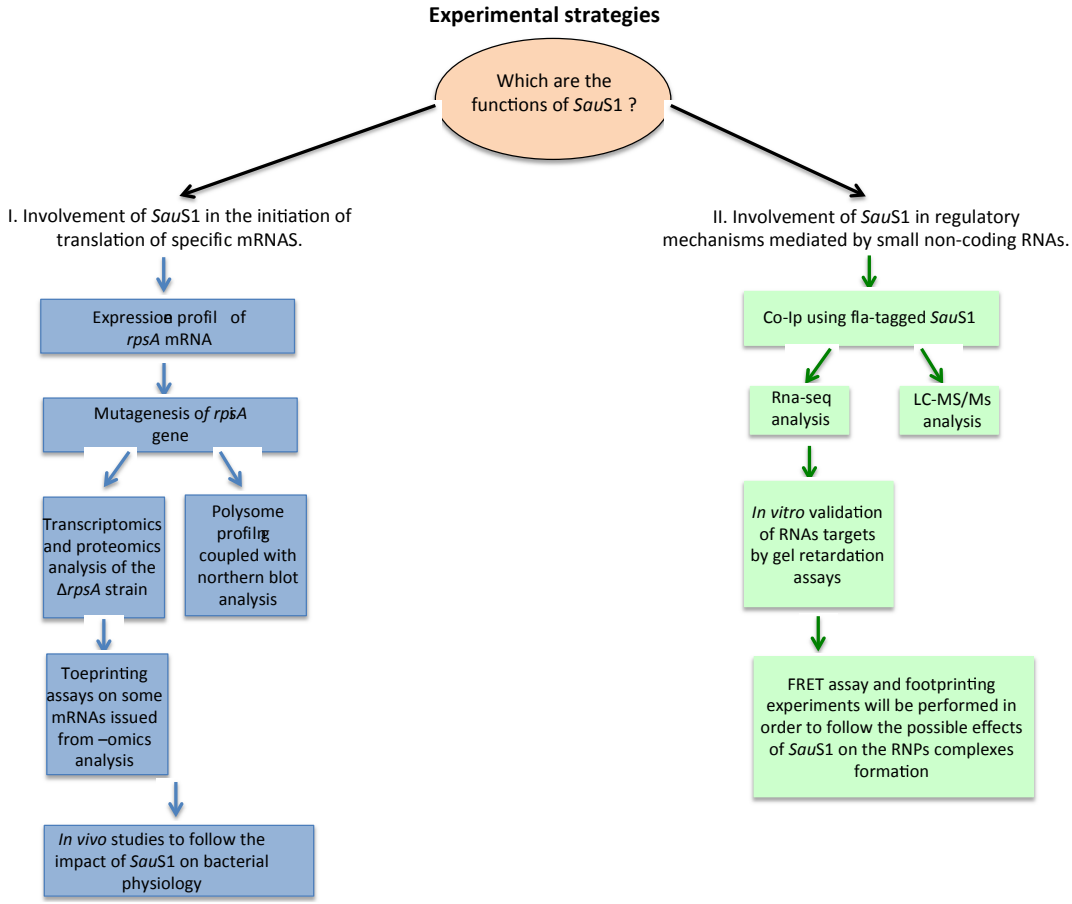

Figure 11 Schematic representation of the experimental approaches that have been used to address the roles of *Sau*S1 in *S. aureus*.

Results

I. Result I: translation functions of *Sau*S1

The first aim of my PhD project deals with the characterization of the functional impact of *Sau*S1 on the initiation of translation of specific structured mRNAs.

Because I showed that *SauS1* is not strictly a ribosomal protein (review in (Khusainov et al., 2016), see introduction), our approach for understanding its biological functions was first based on the characterization of its *in vivo* partners. Rip-Seq assays using chromosomally flag tagged *Sau*S1 were carried out to co-purify the RNA targets that were further identified by sequencing analysis. Interestingly, among the enriched RNAs, we found several RNA classes including mRNAs, regulatory RNAs (sRNAs, riboswitches) and some tRNAs. Using gel retardation assays, I have validated the specificity of the complex formation. To gain information about the molecular mechanism of action of *Sau*S1 on its target RNAs, I have also performed footprinting assays, and FRET experiments to monitor its chaperone activity on a model system.

Among the mRNAs that were co-IP with *Sau*S1, we identified the operon *αpsm1-4* encoding four PSM, which is particularly well structured. Comparative transcriptomic analysis of the wild-type and Δ*rpsA* strains shows down-regulation of several mRNAs, and of the operon *αpsm1-4*. We made the hypothesis that the deletion of *SauS1* caused defects in the translation of the mRNA followed by degradation. Interestingly, many of the identified target mRNAs are involved in virulence and they adopt structures in their 5' untranslated regions that could modulate the accessibility of the 30S ribosomal subunit. In this manuscript, we have analyzed in details the mechanism of action of S1 on the operon *αpsm1-4*. We first demonstrate that *Sau*S1 has a major positive impact on the formation of the simplified 30SIC (toeprintings assays) involving the *psm* mRNA, the initiator tRNA and the 30S subunits. Moreover, *in vivo* experiments using polysome profiles coupled with Northern blot experiment have demonstrated the central role of *Sau*S1 in the initial step of translation of these peptides.

In this work, I have also benefited from the expertise and the collaboration of several team members. I. Caldelari made the two introns insertion mutants of *rpsA* gene and a strain in which *Sau*S1 carries a flag-tag at its C-terminal domain and performed the purification of the RNAs for the CoIP experiment. Moreover, she has performed the Northern blot to monitor the expression profile of *rpsA* mRNA in various staphylococcal

strains, and to measure the half-life of the *psm* mRNA in the wild-type and mutant *ΔrpsA* strains. Lucas Herrgott has monitored the *in vivo* translation of the *psm* and *hu* mRNAs using polysome profiles followed by Northern blot analysis. Iskander Khusainov has prepared the *S. aureus* 30S ribosomal subunit, which was used for structural studies.

I. Result I: translation functions of *Sau*S1 (manuscript ready for submission)

Staphylococcus aureus S1 activates translation initiation of PSMα toxins and stimulates the production of several other secreted virulence factors

Marenna A.[1], Herrgott L.[1], Khusainov I.[1], Kuhn L.[2], Romby P.[1], Caldelari I.[1]* and Marzi S.[1]*

[1]Université de Strasbourg, CNRS, Architecture et Réactivité de l'ARN, UPR9002, F-67000 Strasbourg, France

[2]Plateforme Protéomique Strasbourg-Esplanade FRC 1589, Université de Strasbourg, Centre National de la Recherche Scientifique, F-67000, France.

*To whom correspondence should be addressed. Tel: 33 (0) 388417051 (S.M.); 33(0) 388417068 (P.R.); Fax: 33(0) 3886022188; Email: s.marzi@ibmc-cnrs.unistra.fr i.caldelari@ibmc-cnrs.unistra.fr

ABSTRACT (155 words)

Staphylococcus aureus is a formidable human pathogen that uses secreted cytolytic factors to injure immune cells and promote infection of its host. Of these proteins, the PSM family of pore-forming toxins play critical roles in *S. aureus* pathogenesis. The regulatory mechanisms governing the expression of these toxins are incompletely defined. Whole-genome transcriptomics, *S. aureus* exoprotein proteomics, and translation analyses revealed that ribosomal protein S1 (*Sau*S1), which in not associated with the ribosome, influences the expression and production of exotoxins (PSMs, α-haemolysin, δ-haemolysin and γ-haemolysins) and exoenzymes (proteases and lipases). We could demonstrate that *Sau*S1 specifically promotes translation initiation of the *αpsm* 1-4 operon by binding its highly structured mRNA. We propose that the presence of structures at the RBS of different toxins requires additional translation activators, which could be either sRNA or S1 protein. *Sau*S1 belongs to a new class of RNA chaperones that play key roles in the regulation of translation in *S. aureus*.

INTRODUCTION

Staphylococcus aureus is a low G+C content Gram-positive bacterium, which is a major human opportunistic pathogen, causing a large spectrum of infections (e.g.(Lowy, 1998). Persistent colonization of human nasals with *S. aureus* has been observed for approximately 30% of the population, which are also more susceptible to develop an infection (Wertheim et al., 2005). During the colonization and infection processes, *S. aureus* often reprograms its lifestyle in response to many environmental variations including amino acid and carbon source limitation, iron depletion, decreased pH, and oxidative stress. Many studies have shown that the bacteria sequentially synchronize the expression of genes encoding surface proteins involved in adhesion and defense against the host immune system and, later, numerous toxins (α–, β– and δ- hemolysins, P-V leukocidins, enterotoxins, exfoliative toxins, Toxic Shock Syndrome toxin and PSM peptides) and enzymes (coagulases, lipases, hyaluronidases, staphylokinases, nucleases) are secreted to disrupt host cells and tissues, facilitating the spread of the infection (Thammavongsa et al., 2015). The production of these virulence factors requires physiological adjustments for energy conservation and a fine coordination with its metabolism (Somerville and Proctor, 2009). Responsible for these adaptive responses are multiple interconnected regulatory networks, built on Two Component Systems, sigma factors, transcriptional regulatory proteins (Ibarra et al., 2013) and small non-coding RNAs (sRNAs) (e.g., for reviews (Felden et al., 2011; Tomasini et al., 2014)).

A recognized master regulator of *S. aureus* virulence is the regulatory RNAIII encoded by the *agr* system (Janzon and Arvidson, 1990; Novick et al., 1993). The *agr* system senses the cellular density and triggers the transition from production of surface-bound proteins (adhesion mode) to the secretion of soluble exotoxins and degradative enzymes (dissemination mode) (Geisinger et al., 2009; Novick and Geisinger, 2008; Tomasini et al., 2014). The switch is mainly promoted by the ability of RNAIII to enhance or repress the translation of target mRNAs through the formation of basepairing interactions. Both activation and repression influence the structural context of the Ribosome Binding Sites (RBS) of the target mRNAs and their ability to be efficiently recognized by *S. aureus* 30S ribosomal subunits. For instance, the 5’ region of RNAIII binds to the leader region of *hla* mRNA encoding α-haemolysin, to prevent the formation of an inhibitory structure involving the Shine and Dalgarno (SD) sequence (Morfeldt et al., 1995). On the other hand, the 3’ domain of RNAIII contains four C-rich sequence motifs located in unpaired regions (Benito et al., 2000), which directly base-pairs with the SD sequences of target mRNAs preventing ribosome binding and the formation of the initiation complexes. These mRNAs encode for virulence factors expressed at the cell surface (protein A, coagulase, SA1000, Sbi), and the

transcriptional repressor of toxins, Rot (Boisset et al., 2007; Chabelskaya et al., 2014; Chevalier et al., 2010; Geisinger et al., 2006; Huntzinger et al., 2005). Through the inhibition of Rot translation, RNAIII indirectly activates the transcription of exotoxins.

Besides RNAIII, the response regulatory protein AgrA also contributes to the *agr* regulon by affecting the expression of numerous metabolic enzymes and by activating the membrane-injuring toxins Phenol Soluble Modulines, PSMα and PSMβ, as well as *hld* a third PSM encoded by RNAIII (Queck et al., 2008). The translation of PSMα and δ-haemolysin (Hld) is nevertheless delayed. Even if the onset of PSMα production is anticipated by 2 h compared to δ-haemolysin (Vuong et al., 2004), only a small amount of peptide is produced and a real activation takes place later, at the same time as δ-haemolysin, α-haemolysin and several exoprotein production (Balaban and Novick, 1995; Li et al., 2010; Vandenesch et al., 1991; Vuong et al., 2004). Thus, an exceptional temporal control correlates the expression of *hla*, *psm-α* and *hld*, which could not be simply explained by the intervention of RNAIII and AgrA, the two effectors of the quorum sensing system. It has been proposed that an unknown translational factor should be responsible for the delay in δ-haemolysin and PSMα production (Balaban and Novick, 1995; Li et al., 2010; Vandenesch et al., 1991; Vuong et al., 2004).

In bacteria, changes in translation efficiency are correlated with specific mRNA features, including structures responding to the intracellular concentration of metabolites (riboswitches), to pH changes (fermentation…), temperature, or to the binding of regulatory proteins or sRNAs (Duval et al., 2015; Romby, 2007; Wagner and Romby, 2015). Opening of mRNA structures on the 30S ribosomal subunit is a slow process operated in Gram-negative and in high G+C content Gram-positive bacteria, by ribosomal protein S1 (Duval et al., 2013). S1 is an RNA chaperone composed by six OB-fold domains bearing distinct functions. Domain 1 was shown to be responsible for ribosome anchoring through specific binding with r-protein S2 (Byrgazov et al., 2015; Byrgazov et al., 2012; Duval et al., 2013). Phylogenetic studies have indicated that S1 from low G+C Gram-positive bacteria, such as *B. subtilis* and *S. aureus*, would not contain the ribosome binding domain (Salah et al., 2009). Indeed, after purification of *S. aureus* 30S and 70S ribosomes, only traces of r-protein S1 were observed by mass spectrometry analysis, suggesting that the protein is not tightly associated with the ribosome (Khusainov et al., 2016; Khusainov et al., 2017). It was previously demonstrated that *B. subtilis* S1 plays no major role in translation and is not an essential protein (Farwell et al., 1992; Juhas et al., 2014; Vellanoweth and Rabinowitz, 1992). It was thus proposed that firmicutes obviate the need of S1 acting on the 30S because the majority of mRNAs carry short 5' UTRs with strong SD sequences (Omotajo et al., 2015). However, in *S. aureus*,

mRNAs carrying long 5' or 3' UTRs have been reported (Anderson et al., 2006; Lasa et al., 2011; Ruiz de los Mozos et al., 2013). They include mRNAs encoding virulence factors, various transcriptional regulators, and metabolic enzymes. We have recently analyzed *in vitro* the ability of *S. aureus* 30S subunits to form initiation complexes using various *S. aureus* mRNA substrates, in which the SD was either located in unpaired and flexible regions, or sequestered into hairpins. *S. aureus* 30S, as the *E. coli* S1-depleted 30S, could not recognize structured mRNAs (Khusainov et al., 2016) suggesting that a translation activator would be necessary to translate structured mRNAs.

Here, we show that *S. aureus* S1 (*Sau*S1) which is expressed in late-exponential phase, is not a ribosomal protein. *Sau*S1 is not essential for the growth in rich medium *in vitro* but is required for the correct coordination of virulence factors, by affecting the production of exotoxins (PSMs, α-haemolysin, δ-haemolysin and γ-haemolysins) and exoenzymes (proteases and lipases). Moreover, we demonstrate that *Sau*S1 can directly bind the highly structured α*psm1-4* mRNA operon, promoting translation initiation of its four peptides. We propose that the presence of structures at the RBS of different toxins requires additional translation activators, which could be either sRNA or S1 protein. The translational functions of *Sau*S1 are not broad, but rather specific to structured mRNAs in order to facilitate their recruitment on the ribosome.

MATERIAL AND METHODS

Strains, plasmids and growth conditions

S. aureus strains, plasmids and PCR primers used in this study are listed in **Table S1**. *E. coli strain* DC10B (Monk et al., 2012) was used as a host strain for plasmid construction. Plasmids extracted from *E. coli* DC10B can be used directly for *S. aureus* electroporation. *E. coli* strain was cultivated in Luria-Bertani (LB) medium (1% peptone, 0.5% yeast extract, 1% NaCl) supplemented with ampicillin (100 µg/ml) when necessary. LB-agar plates (with or without ampicillin) were also used for growth on solid medium. *S. aureus* strains were grown in Brain-Heart Infusion (BHI) medium (Sigma-Aldrich) supplemented with erythromycin (10 µg/ml) when necessary. Blood-agar (VWR Chemicals) and BHI plates (with or without erythromycin) were used for growth on solid medium.

Plasmids were prepared from transformed *E. coli* pellets using the Nucleospin Plasmid kit (Macherey-Nagel). Transformation of both *E. coli* and *S. aureus* strains was performed by electroporation (Bio-Rad Gene Pulser). The plasmid for *rpsA* complementation was prepared using pCN51 as template vector (Charpentier et al., 2004). Synthesis of PCR products was performed using Phusion Polymerase (Thermoscientific). To remove the cadmium inducible

promoter, pCN51 was digested by *Sph*I/*Pst*I. The P1-*rpsA* promoter region was amplified by PCR and cloned into pCN51 following *Sph*I/*Pst*I digestion, forming pCN51::*rpsA*.

Northern blot

Total RNAs were prepared from different volumes of *S. aureus* HG001, HG001, RN6390 and Mu50 cultures taken at 2, 4 and 6 h of growth. After centrifugation, bacterial pellets were resuspended in RNA Pro Solution (MP Biomedicals). Lysis was performed with FastPrep and the RNA purification followed strictly the procedure described for the FastRNA Pro Blue Kit (MP Biomedicals). Electrophoresis of total RNAs (10 µg) was performed on 1% agarose gel containing 20 mM guanidium thiocyanate. After migration, RNAs were vacuum transferred on nitrocellulose membrane. Hybridization with specific digoxygenin (DIG)-labelled probes complementary to *rpsA* sequence followed by luminescent detection was carried out as described previously (Boisset et al., 2007). Hybridization with DNA radioactively labelled probes complementary to *psm* and 5S sequences have been detected by autoradiography film exposition.

Western blot

S. aureus BCJ100-*Sau*S1-flag culture (100 ml) have been growth in BHI at 37°C and samples were taken at 2, 3, 4, 5 and 6 h. A total of 1 OD for each of them was pelleted by centrifugation and suspended in Laemmli SDS PAGE loading buffer. Total proteins have been separated on 12% SDS-PAGE polyacrylamide gel and transferred on western blot PVDF membranes (Biorad) using trans-blot turbo transfer system (Biorad) setted on low molecular weight proteins for 5 min. The membrane was incubated for 1 h (or overnight) in blocking solution (4,8% of milk in TBS-Tween20 (Sigma Aldrich)). The membrane was washed and incubated with anti-flag antibody (Sigma) at a 1:2500 dilution in TBS-Tween20 for 1 h at 20°C under continuous agitation. The membrane was then washed 3 times for 10 min with TBS-Tween20 and further incubated with goat anti-mouse IgG (H+C) HRP antibody (Biorad) diluted 1:2500 in TBS-Tween20 for 1 h at 20°C under continuous agitation. The membrane was then washed and the result detected using detection reagent GE Healthcare (Amersham, western blotting detection reagents).

Mutagenesis of the *rspA* gene

Three different mutants have been constructed to abolish *Sau*S1 production in the HG001 strain. A complete deletion mutant (Δ*rpsA*) has been obtained by allelic replacement according to Boisset et al. (2007). Alternatively, transposon introns containing several stop codons were inserted at position 111 after the AUG start codon (*rpsA*111::LtrB) or at position 1029 close to the last domain of S1 (*rpsA*1029::LtrB) according to (Kiedrowski et al., 2011) using the primers described in **Table S1**. The deletion of *rpsA* gene and the insertion of the intron were followed by Northern blot analysis (data do not shown). Mass-spectrometry analysis has confirmed the absence of *Sau*S1 in all the three strains.

RNA preparation and transcriptomics analysis

S. aureus HG001 wild-type (WT) and Δ*rpsA* mutant strains were grown in 50 ml BHI medium to an OD_{600nm} of 5 (6h of culture at 37°C), immediately chilled on ice, and then pelleted by centrifugation (3750 rpm, 15 min, 4°C). Lysis was performed with FastPrep and the RNA purification followed strictly the procedure described for the FastRNA Pro Blue Kit (MP Biomedicals). DNase I (0.1 U/µl) treatment was performed 1h at 37°C. The reactions mixtures were then purified by phenol/chloroform/isoamylalcohol and subsequent ethanol precipitation. RNA pellets were re-suspended in sterile milliQ water. RNA quality and quantity assessments were performed on Agilent Nano Chip on the Bioanalyzer 2100. The RNAs for total transcriptomics were then treated to deplete abundant rRNAs, and the cDNA libraries were performed using the Random Hexamer approach and sequenced with Illumina Mi-seq using a V4 chemistry sequencing kit (Illumina). Each RNA-seq was performed in duplicates. The standard protocol used is the "TruSeq Stranded mRNA" which is based on the TruSeq Illumina kit. It preserves the information about the orientation of the transcripts and produces reads of 150 nts, which map on the complementary strand. The reads were then processed to remove adapter sequences and poor quality reads by Trimmomatic (Bolger et al., 2014), then they were converted to the FASTQ format with FASTQ Groomer (Blankenberg et al., 2010), and were aligned on the HG001 genome (Caldelari et al., 2017) using BOWTIE2 (Langmead et al., 2009). Finally, the number of reads mapping to each annotated feature has been counted with HTSeq (Anders et al., 2015) using the interception non-empty protocol. All processing steps were performed using the Galaxy platform (Afgan et al., 2016). To estimate the enrichment values for the differential expression analysis for the transcriptomic experiment, we used DEseq2 (Varet et al., 2016). The statistical analysis process includes data normalization, graphical exploration of raw and normalized data, test for differential expression for each feature between the conditions, raw p-value adjustment, and export of lists of features having a significant differential expression (threshold p-value=0.05; fold change threshold=2) between the conditions.

Preparation of RNAs for *in vitro* experiments

Transcription of full *psm* operon, *spa*, *mgrA* and RNAIII was performed using linearized pUC18 vectors (Romilly et al., 2014) or PCR fragments containing the T7 promoter (See **Table S1**). The RNAs were *in vitro* transcribed using T7 RNA polymerase, and purified using a 6% polyacrylamide-8 M urea gel electrophoresis. After elution with 0.5 M ammonium acetate pH 6.5 containing 1 mM EDTA, the RNAs were precipitated in cold absolute ethanol, washed with 85% ethanol and vacuum-dried. The labelling of the 5' end of dephosphorylated RNAs (*psm*, RNAIII) and DNA oligonucleotides were performed with T4 polynucleotide kinase (Fermentas) and [γ^{32}P] ATP as previously described (Boisset et al., 2007). Before use, cold or labelled RNAs were renaturated by incubation at 90°C for 1 min in 20 mM Tris-

HCl pH 7.5, cooled 1 min on ice, and incubated 10 min at 20°C in ToeP+ buffer (20 mM Tris-HCl pH 7.5, 10 mM $MgCl_2$, 60 mM KCl, 1 mM DTT).

_Sau_S1 cloning and purification

*Sau*S1 coding sequence with an His(6)-tag and a TEV cleavage site at the N-terminus (Table S1) was cloned into the pQE30 vector (Quiagen), then transformed into *E. coli* M15. Expression and purification of *Sau*S1 was done as described in (Duval et al., 2013) with the following modifications. After the first Ni-NTA chromatography, the fractions containing *Sau*S1, were dyalized in Buffer Q (20 mM Tris-HCl pH 7.5, 2 mM $MgCl_2$, 40 mM NH_4Cl, 1 mM EDTA, 6 mM β-mercaptoethanol), concentrated to 25 mg/ml and the N-terminal His-tag enzymatically removed using Tev protease (Protean) digestion following the manufacture protocol. The cleaved tag and the His-tagged Tev have been then removed by a second Ni-NTA chromatography to isolate not retained *Sau*S1. Finally, *Sau*S1 was purified on a mono Q column. The protein was dialyzed and stored at -20°C in the storage buffer (20 mM Tris HCl pH 7.5, 2 mM $MgCl_2$, 100 mM NH_4Cl, 1 mM EDTA, 1 mM DTT, 10% glycerol).

Differential proteomics for cytoplasmic and secreted proteins

Triplicate protein extracts from supernatant or cytoplasm of HG001 (WT) and Δ*rpsA* mutant strain both transformed with the empty pCN51 plasmid, and the Δ*rpsA* mutant strain complemented with a plasmid expressing *Sau*S1 (pCN51::*rpsA*), were analyzed in separate LC/MS experiments. MS/MS spectra numbers were compared for each protein. Total protein extracts were prepared as follows: 1.5 ml of a *S. aureus* culture (OD_{600nm} = 5) was centrifuged and the pellet resuspended in 150 µl of Lysis buffer P (10 mM Tris pH 7.5, 20 mM NaCl, 1 mM EDTA, 5 mM $MgCl_2$) in the presence of 50 µg/ml lysostaphin, 15 µl of protease inhibitor cocktail (Thermo Fischer Scientific), 2 µl DNase 10 U/ µl (Roche), 2 µl RNase 500 µg/ml (Roche) and incubated for 30 min at 37°C. Then, 1 ml Trizol Reagent (Life Technologies) was used according to the manufacturer's protocol. The final protein phases were then precipitated in ice-cold acetone at least for 2h at -20°C. Secreted proteins were prepared as follows: supernatants of cultures were filtered through a 0.22 µM membrane and precipitated with 5 volumes of 0.1 M ammonium acetate in methanol. To quantify protein extracts by Bradford assay, air-dried protein pellets were resuspended in 2D buffer (7 M urea, 2 M thiourea, 4% Chaps, 25 mM Tris-HCl pH 8) for total extracts or Triton buffer (1% triton x100, 50 mM NaCl, 50 mM Tris-HCl pH 8) for secreted proteins. Proteins (5 µg) were precipitated with methanol/0.1 M ammonium acetate, reduced and alkylated (5 mM DTT, 10 mM iodoacetamide), and digested overnight with 1/25 (W/W) of trypsin. The peptide mixtures (1 µg /sample) were analyzed using a NanoLC-2DPlus system coupled to a TripleTOF 5600 mass spectrometer (ABSciex), as previously described (Tomasini et al., 2017). Protein identifications were assigned using Mascot algorithm (version 2.5, Matrix

Science, London, UK) through ProlineStudio 1.2 package (http://proline.profiproteomic.fr/). Data were searched against the *S. aureus* HG001 genome (Caldelari et al., 2017). Peptide modifications allowed during the search were: N-acetyl (protein), carbamidomethylation (C) and oxidation (M). Mass tolerances in MS and MS/MS were set to 20 ppm and 0.5 Da, respectively. Two trypsin missed cleavages sites were allowed. After the import of the Mascot data files, proteins were validated on Mascot pretty rank equal to 1.1% FDR (False Discovery Rate), on peptide spectrum matches (PSM) based on PSM score, and 1% FDR on protein sets on protein set score. A Spectral Counting quantitative strategy was applied on the Mascot identification summaries. To evaluate the reproducibility, a statistical Student t-test was applied to this experiment.

***psm* operon half-life determination**

Bacterial cultures were grown to an OD_{600} of 3. They were then treated with rifampicin (final concentration of 500 µg/ml) to abrogate transcription. RNA samples were collected at indicated time points and quantified by northern blot analysis with ImageQuant TL software (GE Healthcare Life Sciences).

Polysome profiling coupled to Northern blot analysis

WT and Δ*rpsA* mutant strains (transformed with the empty pCN51 plasmid for control) and the same mutant strain complemented with the pCN51::*rpsA* plasmid expressing S1 (**Table S1**) were cultured in BHI mediumat 37°C for 4h (OD_{600} of 4). Chloranphenicol was added to the cultures to have 5 mM of final concentration. After two minutes, the cells have been pelleted by centrifugation (15 minutes at 4°C), resuspended in 500 µl of Lysis buffer R (20 mM Tris pH 7.5, 100 mM NH_4Cl, 10 mM $MgCl_2$, 0.1 % Nonidet p-40, 0.4 % Triton X-100, 1 mM Chloranphenicol, 100 U/ml DNaseI) and disrupted with the FastPrep apparatus (MP Biomedicals). 40 K OD_{260} of cell lysates were loaded on sucrose gradient (5% - 50%) and separed on Biocomp instrument. The RNA was extracted from the fractions using acid phenol at 65°C and then precipitated. Northern blot analysis was performed using 1 µg of RNA.

Toe-printing assays

The preparation of *S. aureus* 30S subunits, the formation of a simplified translational initiation complex with mRNA, and the extension inhibition conditions were performed as previously described (Fechter et al., 2009) with slight modifications in the buffer used to dissociate *Sau*70S into subunits (10 mM Hepes-KOH pH 7.5, 100 mM NH_4Cl, 1 mM $Mg(OAc)_2$, 1 mM DTT). Increasing concentrations of either *Sau*S1 were used to monitor its effects on the formation of the initiation complex with *psm* operon, *spa, mgrA* and RNAIII. Prior to toeprinting assay, *Sau*30S subunits were chilled on ice for 10 min then incubated at 37°C for 15 min in ToeP+ buffer. In parallel, mRNA (0,5 pmol) was annealed to a 5' end-

labeled oligonucleotide (50000 cps), heated at 90°C for 1 min, cooled on ice for 1 min and incubated at RT°C for 10 min in ToeP+ buffer. *Sau*S1 was pre-incubated in ToeP+ buffer for 15 min at 37°C prior to use. 30SIC were constituted at 37°C for 15 min in the presence of the mRNA annealed to the labelled primer and *Sau*30S (0,25; 0,5; 0,75; 1 pmole) pre-incubated or not with 1.5 excess of *Sau*S1. The tRNAi (20 pmoles) was then added and the complexes were formed for 5 min at 37°C. Primer extension reactions were subsequently performed by adding 2 units of AMV-RT at 37°C for 30 min. Reactions were stopped by phenol extraction followed with ethanol precipitation, and samples were loaded on 10% urea-PAGE. Quantification of the toe-printing signals present on the autoradiography was done with ImageQuant TL software (GE Healthcare Life Sciences).

Gel filtration

*Sau*30S were reactivated at 37°C for 10 min and incubated in Buffer G (50 mM KCl, 10 mM NH_4Cl, 10 mM $MgCl_2$, 10 mM Tris HCl pH 7.5, 1 mM DTT) with *Sau*S1 with or without *psm* mRNA. Previously, *Sau*S1 was centrifuged for 1h at 4°C at 13000 rpm in order to remove aggregates, new concentration was measured and the protein re-activated in Buffer G at 37°C for 10 min. 250 pmoles of *Sau*S1 were incubated with 25 pmoles of *Sau*30S ribosomal subunit, for 10 min at 37°C in Buffer G, in a total volume of 50 µl. The mix was then centrifuged at 4°C for 10 min at 4200 rpm and the supernatant was loaded on size exclusion column (GE Healthcare Superose TM 6 Increase 3.2 /300). The eluted peaks for *Sau*30S and the free protein have been then analysed by quantitative LC/MSMS to determine stoichiometric ratios between *Sau*S1 and other ribosomal proteins.

Gel retardation assays

Radiolabelled purified *psm* operon and RNAIII (50000 cps/sample, concentration < 1 pM) were renaturated as described above. For each experiment, increasing concentrations of purified *Sau*S1 (100-900 nM) were added to the 5' end labelled *psm* or RNAIII in a total volume of 10 µl containing the ToeP+ buffer. Complex formation was performed at 37°C during 15 min. After incubation, 10 µl of glycerol blue was added and the samples were loaded on a 10% PAGE under non denaturing conditions (1h, 300 V, 4°C).

RESULTS

*Sau*S1 has an atypical expression profile if compared to other r-proteins

In bacteria, the synthesis of the r-proteins is coordinated to the transcription of the ribosomal RNA, which is regulated according to environmental changes and to the different phases of bacterial growth (Kaczanowska and Ryden-Aulin, 2007; Kjeldgaard et al., 1958; Nomura, 1999; Nomura et al., 1984; Wagner, 1994). Ribosomes need to be quickly assembled, thus r-RNA and r-proteins accumulate already in the lag and early exponential growth phases

(Condon et al., 1995; Rolfe et al., 2012). New ribosomes are also rapidly synthetized to react to ribosome-directed antibiotics challenges (Wenzel and Bandow, 2011). *Sau*S1, encoded by *rpsA* gene, has nevertheless a peculiar expression profile. For instance, in response to linezolid stress, *Sau*S1 is not produced when the other r-proteins are rapidly upregulated (Bonn et al., 2016). We have first monitored the levels of *rpsA* transcript at different stages of bacterial growth in BHI medium by Northern blot (**Figure 12**). The experiment was carried out with *S. aureus* HG001 strain, a derivative of RN1 (NCT8325) strain with restored *rbsU* (Herbert et al., 2010). The data showed that the *rpsA* mRNA has two distinct isoforms with a different pattern of expression. The shorter transcript appears to be constitutively expressed, while the long transcript starts to be expressed at the late exponential phase of growth after 3 h (OD_{600} ~2) and accumulates at the stationary phase (**Figure 12B**). A similar transcription pattern could be observed in other *S. aureus* strains, indicating a conserved mechanism of transcription regulation (**Figure 12D**). The transcripts possibly originate from two different Transcription Start Sites (TSS), as evidenced by aligning raw data from (Koch et al., 2014) on our genome (**Figure 12E**).

We have also monitored in parallel the levels of the protein *Sau*S1 using Western blot analysis (**Figure 12C**). In this experiment, we have introduced into the chromosome of *S. aureus* HG001 a 3xflag tag peptide sequence at the C-terminus of *Sau*S1. After purification of the total protein extracts, the *Sau*S1 protein was detected using an anti-flag antibody. Surprisingly, the data showed that the protein levels do not correspond to the pattern of the mRNA since the protein can only be detected after 3h of growth.

Taken together these data showed that the expression of *Sau*S1 is regulated during the growth phase of the bacteria.

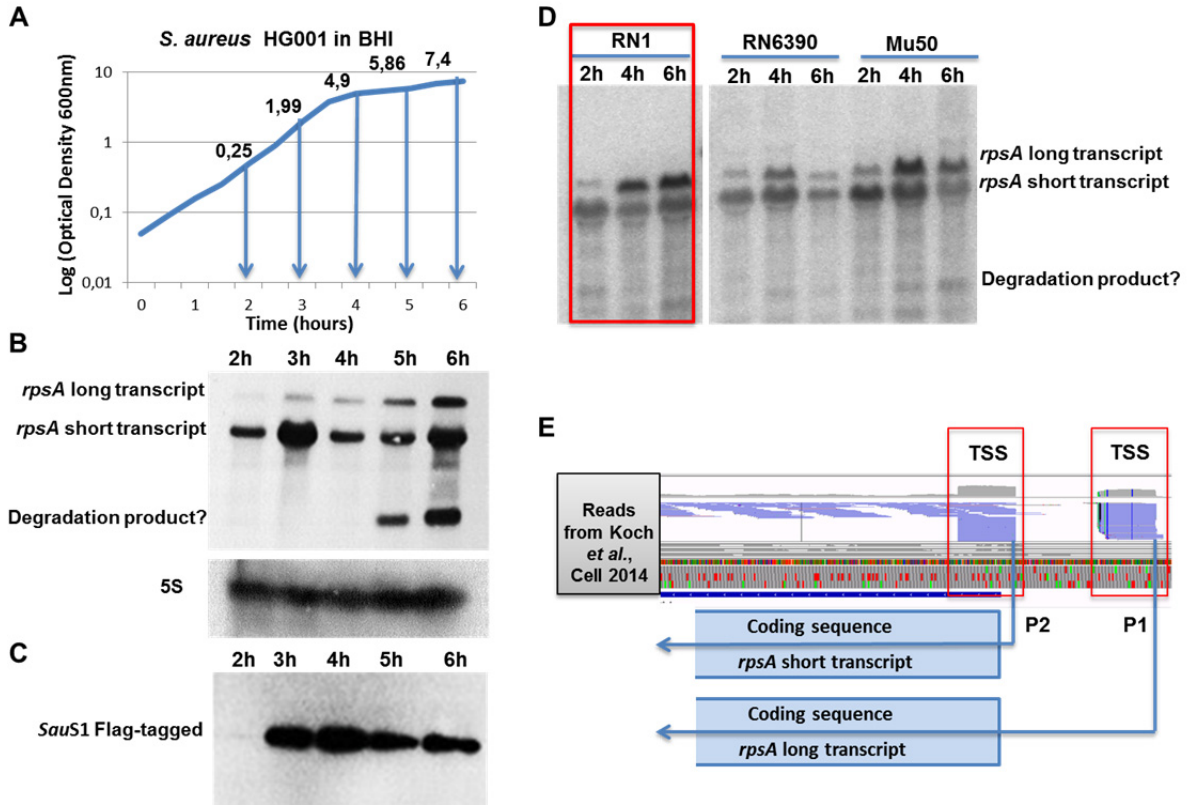

Figure 12: *S. aureus rpsA* expression profile. A. Growth curve of HG001 strain in BHI medium and time points at which cells were harvested for Northern blot and Western blot analyses. B. Northern blot analysis of *rpsA* mRNA detected at different time points of the growth (2h, 3h, 4h, 5h, and 6h). The two transcripts (short and long) are noted on the side of the gel. A short product has been visualized after 5h of growth, which most likely corresponded to a degradation product. C. Western blot analysis on *Sau*S1 detected at different time points of the growth (2h, 3h, 4h, 5h, and 6h). D. Northern blot analysis of *rpsA* mRNA in different *S. aureus* strains (RN1, RN6390 and Mu50). E. Organization of *rpsA* locus and possible transcription units (dataset SRR949025 obtained by (Koch et al., 2014) realigned on the HG001 genome and visualized by IGV (Thorvaldsdottir et al., 2013)). P1 and P2 indicated putative Transcription Start Sites (TSS) from different promoters.

*Sau*S1 has significant effect on the virulon of *S. aureus* as revealed by comparative transcriptomics and proteomics

We have then investigated the impact of *Sau*S1 on *S. aureus* total transcriptome (**Table S1**) by comparing the RNAs expressed from HG001 (WT) and the isogenic Δ*rpsA* mutant strains. Total RNAs were extracted from WT and Δ*rpsA* strains grown to OD_{600} ~5 (6h) in BHI at 37°C. Under these conditions, *Sau*S1 is abundant in the WT (**Figure 12C**). The extracted RNAs were then used for library preparation and sequencing. The data were analyzed and visualized using Galaxy (Afgan et al., 2016) and the Integrative Genomics Viewer (IGV) browser, respectively (Thorvaldsdottir et al., 2013). A detailed protocol for the bioinformatics analysis is provided in Material and Methods. Briefly, we aligned the sequencing reads onto

HG001 genome (Caldelari et al., 2017), counted per feature and normalized. The data were reproduced in two independent experiments.

Rather unexpectedly, the differential expression analysis revealed changes in a small number of mRNAs. Among the 2565 annotated mRNAs, only 47 genes are up- and 55 are down-regulated by at least a factor of 2 (**Tables S2 and S3**). Interestingly, more than 35% of down-regulated mRNAs encoded virulence factors, with the *sspABC* and *αpsm1-4* operons being the less abundant mRNAs in Δ*rsaA* strain. The non-coding transcriptome showed more extensive variations (**Supplementary excel file S1**). Indeed, the majority of tRNAs and half of the annotated sRNAs showed significant decreased levels in the Δ*rpsA* strain such as the quorum-sensing induced RNAIII and 6S RNA (**Table S4**). In addition, the yields of cis-acting regulatory elements such as riboswitches, and T-boxes were also diminished in Δ*rsaA* strain (**Table S4**).

Quantitative differential proteomic and transcriptomic analyses were carried out on total RNA and cytosolic and secreted proteins, prepared from the WT and ΔrpsA mutant strains and the same mutant strain complemented with a plasmid expressing S1. The WT and ΔrpsA mutant strains were also transformed with the pCN51 plasmid for control (**Table S1**). Bacterial growth was performed in BHI medium for 6h. Triplicates experiments have been analyzed by LC/MSMS (**Tables S5, S6**). The differential spectral count analysis nicely correlates with the observed effects on the mRNAs encoding virulence factors (**Table 2**). Of the 79 classified virulence factors, 23 of them are less abundant in the Δ*rpsA* strain. A classification analysis of these factors further evidenced a clear perturbation in the proteins and/or mRNA levels for exoenzymes (serine and cysteine proteases and lipases) and of membrane pore forming toxins, including the four αPMS peptides and the α- δ- and γ-hemolysins (**Table 2**).

These data strongly suggested that S1 altered significantly the virulon. Because the levels of several sRNAs and of RNAIII were enhanced in strain expressing S1, some of the effects primarily on proteases might be indirect. However, this is not the case of *α-psm* and *β-psm* operons, which are transcribed by AgrA (Queck et al., 2008), whose level is not affected by SauS1 (**Supplementary excel file S1**). Therefore, we proposed that S1 might regulate the translation of the *psm* operon, and belongs to the class of post-transcriptional regulatory protein.

Virulence Factors				Transcriptomics ΔrpsA/WT		Proteomics ΔrpsA/WT		Secretomics ΔrpsA/WT		Secretomics ΔrpsA/compl	
id	gene	product	classification	FoldChange	pvalue	FoldChange	pvalue	FoldChange	pvalue	FoldChange	pvalue
HG001_00899	sspA	Glutamyl endopeptidase	Exoenzyme, Serine protease	0,10	2,48E-55	too few peptides		0,17	0,16390	0,03	1,44E-06
HG001_03280	psm-α4	4 αpsm peptide	Toxin, Pore-forming	0,17	2,20E-32	n.d.		n.d.		n.d.	
HG001_03282	psm-α2	2 αpsm peptide	Toxin, Pore-forming	0,29	1,68E-16	n.d.		n.d.		n.d.	
HG001_01009	hly	Alpha-hemolysin	Toxin, Pore-forming	0,31	2,80E-07	0,23	0,02739	0,39	0,02508	0,12	1,90E-19
HG001_00898	sspB	Staphopain B	Exoenzyme, Cysteine protease	0,32	1,26E-11	0,36	0,03388	S1 only	3,32E-03	COMPL only	3,19E-14
HG001_02245	-	65 kDa membrane protein Eap	Ant-toxin_C (CL0386)	0,33	8,93E-13	S1 only	0,00009	0,29	0,02929	2,00	0,05542
HG001_00897	sspC	Staphostatin B	Exoenzyme, Cysteine protease	0,33	3,16E-07	n.d.		n.d.		n.d.	
HG001_02058	hld	Delta-hemolysin	Toxin, Pore-forming	0,35	9,33E-10	n.d.		n.d.		n.d.	
HG001_01006	scn_2	Staphylococcal complement inhibitor	Immune evasion	0,39	1,47E-04	n.d.		n.d.		n.d.	
HG001_02456	sbi	Immunoglobulin-binding protein	Immune evasion	0,39	3,02E-06	n.d.		0,77	0,61590	1,00	0,39920
HG001_01023	psm-β2	2 βpsm peptide	Adherence	0,39	2,92E-10	S1 only	0,23790	n.d.		n.d.	
HG001_03283	psm-α1	1 αpsm peptide	Toxin, Pore-forming	0,41	4,78E-06	n.d.		n.d.		n.d.	
HG001_00264	lip2	Lipase 2	Exoenzyme, Lipase	0,43	2,00E-09	0,25	1,74E-09	0,47	0,05042	0,18	3,06E-19
HG001_02459	hlgB	Gamma-hemolysin component B	Toxin, Pore-forming	0,46	8,94E-05	n.d.		0,11	0,04432	0,02	5,34E-09
HG001_01971	-	65 kDa membrane protein Eap	Adherence	0,46	5,37E-04	n.d.		n.d.		n.d.	
HG001_01943	sspP	Staphopain A	Exoenzyme, Cysteine protease	0,47	1,95E-04	0,43	0,19580	0,42	0,44860	0,04	2,35E-20
HG001_01005	fib_2	Fibrinogen-binding protein	Immune evasion, Adherence	0,47	1,23E-03	n.d.		1,37	0,01020	2,17	7,70E-04
HG001_02458	hlgC	Gamma-hemolysin component C	Toxin, Pore-forming	0,48	3,27E-04	n.d.		1,10	0,19490	0,37	0,07431
HG001_02709	lipA_2	Lipase 1	Exoenzyme, Lipase	0,56	3,18E-03	0,38	0,59470	0,75	0,33890	0,52	0,04707
HG001_03281	psm-α3	3 α psm peptide	Toxin, Pore-forming	0,57	8,89E-05	n.d.		n.d.		n.d.	
HG001_00978	isdA	Iron-regulated surface determinant protein A	Iron uptake,Heme uptake	0,57	0,00757	n.d.		0,76	0,34240	0,71	0,76880
HG001_02044	-	putative leukocidin-like protein 2	Toxin, Pore-forming	0,60	0,01068	n.d.		n.d.		n.d.	
HG001_01340	ebpS	Elastin-binding protein EbpS	Adherence	0,63	0,00097	0,79	0,34790	1,00	0,21290	1,27	0,12920
HG001_02538	fnbA_1	Fibronectin-binding protein A	Adherence	0,63	0,43161	n.d.		1,00	0,63420	2,00	0,36280
HG001_01974	scn_3	Staphylococcal complement inhibitor	Immune evasion	0,68	0,03382	S1 only	0,04092	0,63	0,98870	0,63	0,88640
HG001_02043	-	putative leukocidin-like protein 1	Toxin, Pore-forming	0,69	0,05932	0,70	0,64810	0,43	0,58700	0,21	0,04609
HG001_01978	sak	Staphylokinase	Plasminogen activator	0,69	0,05998	n.d.		n.d.		n.d.	
HG001_01976	chp	Chemotaxis inhibitory protein	Immune evasion	0,71	0,22727	n.d.		1,00	0,41380	0,86	0,68490
HG001_02707	icaB	Poly-beta-1,2C6-N-acetyl-D-glucosamine N-deacetylase	Adherence	0,71	0,23161	n.d.		n.d.		n.d.	
HG001_02539	fnbA_2	Fibronectin-binding protein A	Adherence	0,71	0,06276	n.d.		n.d.		n.d.	
HG001_02669	clfB	Clumping factor B	Immune evasion	0,71	0,03303	n.d.		1,83	0,03239	0,65	0,87440
HG001_00172	scn_1	Staphylococcal complement inhibitor	Immune evasion	0,72	0,22543	n.d.		n.d.		n.d.	
HG001_01972	eap	65 kDa membrane protein Eap	Adherence	0,72	0,06984	n.d.		n.d.		n.d.	
HG001_00728	clfA	Clumping factor A	Immune evasion	0,73	0,02679	0,83	0,65790	0,79	0,56450	1,57	0,09078
HG001_00977	isdB	Iron-regulated surface determinant protein B	Iron uptake, Heme uptake	0,74	0,27830	n.d.		n.d.		n.d.	
HG001_01752	lukDv	Leucotoxin LukDv	Toxin, Pore-forming	0,74	0,26637	n.d.		n.d.		n.d.	
HG001_02708	icaC	poly-beta-1,2C6-N-acetyl-D-glucosamine export protein	Adherence	0,74	0,30381	n.d.		n.d.		n.d.	
HG001_01002	fib_1	Fibrinogen-binding protein	Immune evasion, Adherence	0,74	0,27907	ΔrpsA only	0,24020	0,38	0,35330	1,25	0,37010
HG001_00981	isdE	High-affinity heme uptake system protein	Iron uptake, Heme uptake	0,75	0,29359	n.d.		n.d.		n.d.	
HG001_02706	icaD	Poly-beta-1,2C6-N-acetyl-D-glucosamine synthesis protein	Adherence	0,78	0,39029	n.d.		n.d.		n.d.	
HG001_00767	tlyC	Hemolysin C	Allows resistance to high Mg++	0,79	0,17686	n.d.		n.d.		n.d.	
HG001_00234	esxB	Virulence factor EsxB	Type VII secretion system	0,79	0,34392	n.d.		n.d.		n.d.	
HG001_01753	lukEv	Leucotoxin LukEv	Toxin, Pore-forming	0,79	0,41746	n.d.		n.d.		n.d.	
HG001_00979	isdC	Iron-regulated surface determinant protein C	Iron uptake, Heme uptake	0,80	0,43470	n.d.		n.d.		n.d.	
HG001_01973	hlb_1	Phospholipase C	Toxin, Hydrolase	0,82	0,47461	n.d.		n.d.		n.d.	
HG001_00233	esaC	hypothetical protein	Type VII secretion system	0,83	0,40675	n.d.		n.d.		n.d.	
HG001_00980	isdD	hypothetical protein	Iron uptake, Heme uptake	0,84	0,51617	n.d.		n.d.		n.d.	
HG001_00231	essB	putative membrane protein essB	Type VII secretion system	0,84	0,43664	n.d.		n.d.		n.d.	
HG001_00984	isdG	Heme oxygenase (staphylobilin-producing) 1	Iron uptake, Heme uptake	0,85	0,57256	n.d.		n.d.		n.d.	
HG001_02705	icaA	Poly-beta-1%2C6-N-acetyl-D-glucosamine synthase	Adherence	0,85	0,58631	n.d.		n.d.		n.d.	
HG001_02676	aur	Zinc metalloproteinase aureolysin	Exoenzyme, Zinc metalloproteinase	0,87	0,43983	n.d.		n.d.		n.d.	
HG001_00227	esxA	Virulence factor EsxA	Type VII secretion system	0,89	0,50433	1,37	0,49980	n.d.		n.d.	
HG001_00102	ywqE_1	Tyrosine-protein phosphatase YwqE	Antiphagocytosis	0,90	0,50249	S1 only	0,09507	n.d.		n.d.	
HG001_01022	psm-β1	1 βpsm peptide	Adherence	0,905	0,50906	1,00	0,99450	n.d.		n.d.	
HG001_00729	VWbp	Staphylocoagulase	Exoenzyme	0,92	0,76399	n.d.		n.d.		n.d.	
HG001_00230	yukD	YukD	Type VII secretion system	0,92	0,77518	n.d.		n.d.		n.d.	
HG001_02242	hysA	Hyaluronate lyase	Exoenzyme, Spreading factor	0,92	0,73210	n.d.		n.d.		n.d.	
HG001_00101	ywqD_1	Tyrosine-protein kinase YwqD	Antiphagocytosis	0,95	0,72346	0,54	0,40500	n.d.		n.d.	
HG001_00112	epsL	putative sugar transferase EpsL	Antiphagocytosis	0,95	0,72866	n.d.		n.d.		n.d.	
HG001_00983	srtB	Sortase family protein	Iron uptake, Heme uptake	0,95	0,85382	n.d.		n.d.		n.d.	
HG001_00229	essA	Firmicute eSAT-6 protein secretion system EssA	Type VII secretion system	0,97	0,90057	n.d.		n.d.		n.d.	
HG001_00982	isdF	heme-iron transport system permease	Iron uptake, Heme uptake	0,98	0,93560	n.d.		n.d.		n.d.	
HG001_00113	galE	UDP-glucose 4-epimerase	Antiphagocytosis	0,99	0,94326	n.d.		n.d.		n.d.	
HG001_00232	eccCa1	ESX-1 secretion system protein EccCa1	Type VII secretion system	0,99	0,95368	too few peptides		n.d.		n.d.	
HG001_02042	hlb_2	Phospholipase C	Toxin, Hydrolase	0,99	0,97570	n.d.		n.d.		n.d.	
HG001_02457	hlgA	Gamma-hemolysin component A	Toxin, Pore-forming	1,01	0,98451	n.d.		n.d.		n.d.	
HG001_00493	sdrD	Serine-aspartate repeat-containing protein D	Adherence, MSCRAMMs	1,03	0,89302	too few peptides		0,73	0,45960	3,27	1,70E-04
HG001_00115	mnaA_1	UDP-N-acetylglucosamine 2-epimerase	Antiphagocytosis	1,07	0,68686	1,76	0,28740	n.d.		n.d.	
HG001_00104	capD	UDP-glucose 4-epimerase	Antiphagocytosis	1,08	0,60071	Del-S1 only	0,09671	n.d.		n.d.	
HG001_00105	fcl	GDP-L-fucose synthase	Antiphagocytosis	1,11	0,48166	Del-S1 only	0,00667	n.d.		n.d.	
HG001_02704	icaR	Biofilm operon icaADBC HTH-type negative transcriptional regulator	Adherence	1,17	0,39326	0,76	0,73090	n.d.		n.d.	
HG001_00228	esaA	Secretion accessory protein EsaA/YueB @ Bacteriophage SPP1 receptor	Type VII secretion system	1,18	0,36029	n.d.		n.d.		n.d.	
HG001_00100	cap8A_1	Capsular polysaccharide type 8 biosynthesis	Antiphagocytosis	1,19	0,25569	0,43	0,55600	n.d.		n.d.	
HG001_00106	wbpI	UDP-2,2C3-diacetamido-2,2C3-dideoxy-D-glucuronate 2-epimerase	Antiphagocytosis	1,19	0,27180	1,00	0,98980	n.d.		n.d.	
HG001_00027	yfkN_1	Trifunctional nucleotide phosphoesterase	Immune evasion	1,25	0,15295	S1 only	0,10630	1,25	0,29720	1,67	0,21470
HG001_00114	wbpA	UDP-N-acetyl-D-glucosamine 6-dehydrogenase	Antiphagocytosis	1,27	0,14709	0,65	0,51870	n.d.		n.d.	
HG001_00111	cap5L	putative glycosyl transferase	Antiphagocytosis	1,29	0,10239	n.d.		n.d.		n.d.	
HG001_00103	pglF	UDP-N-acetyl-alpha-D-glucosamine C6 dehydratase	Antiphagocytosis	1,33	0,16077	n.d.		n.d.		n.d.	
HG001_00060	spa	Immunoglobulin G-binding protein A	Immune evasion, Adherence	1,35	0,07927	n.d.		0,86	0,05719	5,00	2,02E-11

Table 2: Differential transcriptomics and proteomics analysis of virulence factors expression in Δ*rpsA*. Fold change (Δ*rpsA*/WT) and p-values were calculated for the transcriptomics analysis by DESeq2 using shrinkage estimation for dispersions and fold changes (Varet et al., 2016), for the proteomics by the R-Studio software. Fold change estimations and p-values have p-values<0.005 (high significance), when highlighted by dark-grey boxes they have p-values>0.001; light-grey boxes indicate 0.005>p-values>0.001.

_Sau_S1 protects *psm* mRNA operon against *in vivo* degradation.

Due to the structural resemblance of *Sau*S1 to the ribosomal protein *Eco*S1, we make the hypothesis that the protein would regulate the translation initiation process of the *psm* operon. Indeed, in Gram-positive bacteria, stabilization of mRNAs can be due to the binding

of the ribosome or of key factors close to their 5' ends (Condon, 2003). To test whether the decreased level of *psm* mRNA (0.17; **Table 2**) in the Δ*rpsA* strain could be due to a more rapid turnover, we have analysed its stability by measuring the kinetics of its degradation after rifampicin treatment, an antibiotic which prevents initiation of new transcripts by binding to the β subunit of RNA polymerase (Campbell et al., 2001). Rifampicin was added to WT and the mutant *rpsA*111::LtrB strains grown in BHI to OD_{600}=3 (4h), when *psm* started to accumulate (**Figure S1**). The *psm* mRNA was detected by Northern blot using total RNAs extracted after 2, 4, 8, 15, 30, 45 and 60 min (**Figure 13A**). Quantification, normalization and interpolation of the data by linear regression in logarithmic scale, showed that the *psm* transcript is highly stable, with a half-life of 77.02 min in the WT strain. In contrast to the majority of the transcripts (90%), which have half-lives shorter than 5 min (Roberts et al., 2006), this operon is one of the most stable transcript. In the mutant strain, the *psm* half-life appears to be significantly shorter and was decreased to 46.52 min (**Figure 13B).**

Therefore, these data showed that SauS1 has a significant effect on the stabilization of the *psm* operon, in agreement with the transcriptomics and proteomics analysis.

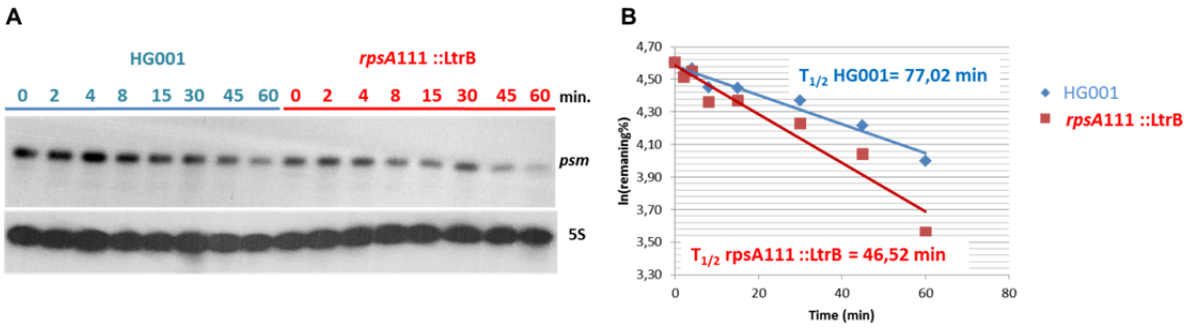

Figure 13. *psm* mRNA stability. A. Northern blot analysis of the *psm* transcript in WT and *rpsA*111::LtrB. Cells were growth at 37°C in BHI and treated with rifampicin at 4h. Total RNA was extracted after 2, 4, 8, 15, 30, 45 and 60 min. *psm* mRNA and 5S rRNA were probed with specific oligonucleotides (**Table S1**). B. After quantification of the Northern blot signals and normalization of each point to the corresponding 5S signals, the % of remaining *psm* mRNA has been plotted to calculate *psm* half-lifes in the two strains. $T_{1/2}$HG001 (WT) is 77.02 min, while in absence of *Sau*S1, $T_{1/2}$*rpsA*111::LtrB decreases to 46.52 min.

Polysome occupancy of *psm* mRNA is higher in presence of *Sau*S1

Because the effect of S1 on the mRNA stability can be the result of an enhanced translation, we have analyzed the mRNA distribution using polysome profile analysis coupled with Northern blot experiments. The experiments were done on WT and mutant Δ*rpsA* strains grown in BHI at 37°C until mid-exponential phase (OD_{600}=4). Translation was then stopped by adding chloramphenicol to the cultures and the cells were rapidly harvested by centrifugation. After cell lysis, polysomes have been separated *via* ultracentrifugation on a 5-50% sucrose gradient. The RNA was extracted from each fraction and Northern blot was done using specific oligonucleotides to detect *psm*, *hu* mRNAs and 16S rRNA. Quantification

and normalization on the 16S rRNA level have revealed huge differences on the amount of *psm* mRNA recruited in the polysomes in the two strains (**Figure 14AB**). In the absence of *Sau*S1, much less mRNA (0.23 fold change Δ*rpsA*/WT) is engaged on the ribosomes to be translated compared to WT strain. Moreover, we could show that translation activation by *Sau*S1 is specific for *psm* mRNA. Indeed, the translation of *hu* mRNA does not depend on *Sau*S1 and its polysome occupancy does not significantly vary (1.27 fold). Because in both WT and mutant Δ*rpsA* strain, we did not detect the free mRNA in the fractions of low density (**Figure 14AB**), we could not exclude that the observed differences in the polysome fractions reflect the variation in *psm* mRNA levels. However, one cannot exclude that the free *psm* transcript, which is not protected by the ribosomes, is also rapidly degraded.

These data showed that the S1-dependent stabilization of the *psm* mRNA might result from an enhanced translatability.

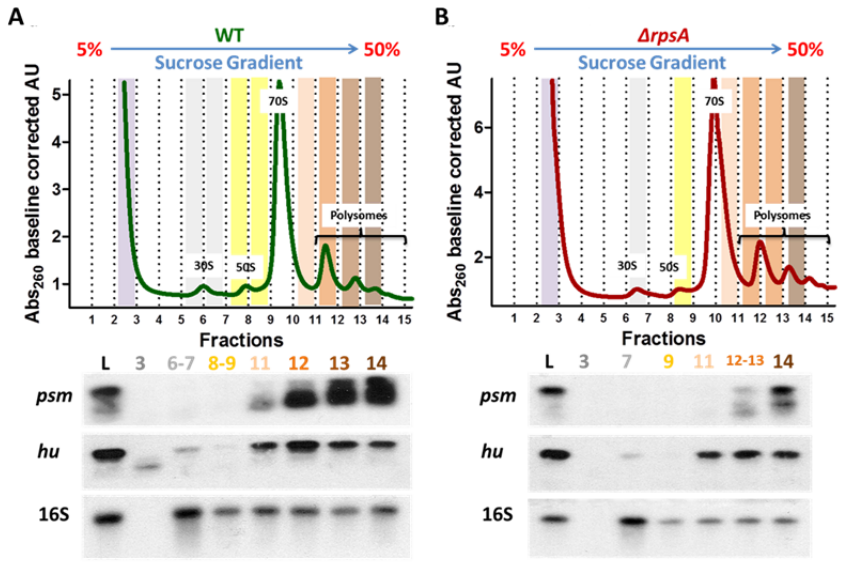

Figure 14. Effects of *Sau*S1 on the translation of *psm* and *hu* mRNAs by polysome profile coupled with Northern blot analysis. WT and Δ*rpsA* strains (A and B, respectively) were cultured in BHI at 37°C until OD_{600}=4, translation was stopped with chloramphenicol and polysomes fractionated on a 5-50% sucrose gradient. The RNA was extracted from each fraction and Northern blot was done using specific oligonucleotides to detect *psm*, and *hu* mRNAs, and 16S rRNA. L= cellular lysate. The 16S rRNA in the L line was used for the normalization.

***SauS1* specifically promotes ribosome binding on *psm* mRNA**

Toe-printing assays (Hartz et al., 1988) were used to decipher the effect of *Sau*S1 on the formation of the ternary initiation complex formed in the presence of *psm* mRNA, the initiator tRNA and the *Sau*30S subunit (**Figure 15**). We have verified that *Sau*S1 was not bound to the 30S. A toe-print is observed at position +16 (+1 is the adenine of the start codon) if the

mRNA occupies the decoding channel stabilized by the codon-anticodon interaction with the initiator tRNA. The *psm* operon contains four coding regions (CDS) and is predicted to be highly structured (**Figure S2**). In this structure, the four RBS are hindered into stable hairpin structures. **Figure 15A** shows that, without *Sau*S1 the toe-prints at the four RBSs are very weak. Even at the highest *Sau*30S concentration, they are barely detectable or above the noise with the exception of the first toe-print suggestion that the ribosome better recognized the first RBS. However, much stronger toe-print signals could be observed in the presence of the purified *Sau*S1 at the four translation initiation sites. *Sau*S1 stimulatory effect seems to be more pronounced for the 4th RBS, followed by the 2nd, while it is less marked for the 1st and the 3rd. Because the toeprint at the 1st RBS was too close to the full extended product to be quantified, we have repeated the experiment and used a different RT primer (**Table S1**) to uniquely detect this signal (**Figure 15B**). Quantification has been obtained from three independent experiments to establish the Kd using non-linear fitting of a single exponential between the plotted values. The calculated Kd for 30S binding are 0.13 and 0.03 µM for the *Sau*30S and *Sau*30S+S1, respectively. Thus *Sau*S1 helps the 30S to recruit *psm* mRNA increasing its affinity by a factor of ~4.

The observed *in vitro* stimulatory effect of *Sau*S1 on the formation of the initiation complexes with the *psm* operon is also compatible with the better recruitment of the *psm* transcript on polysomes (**Figure 14**) in the WT strain rather than in the mutant Δ*rpsA* strain.

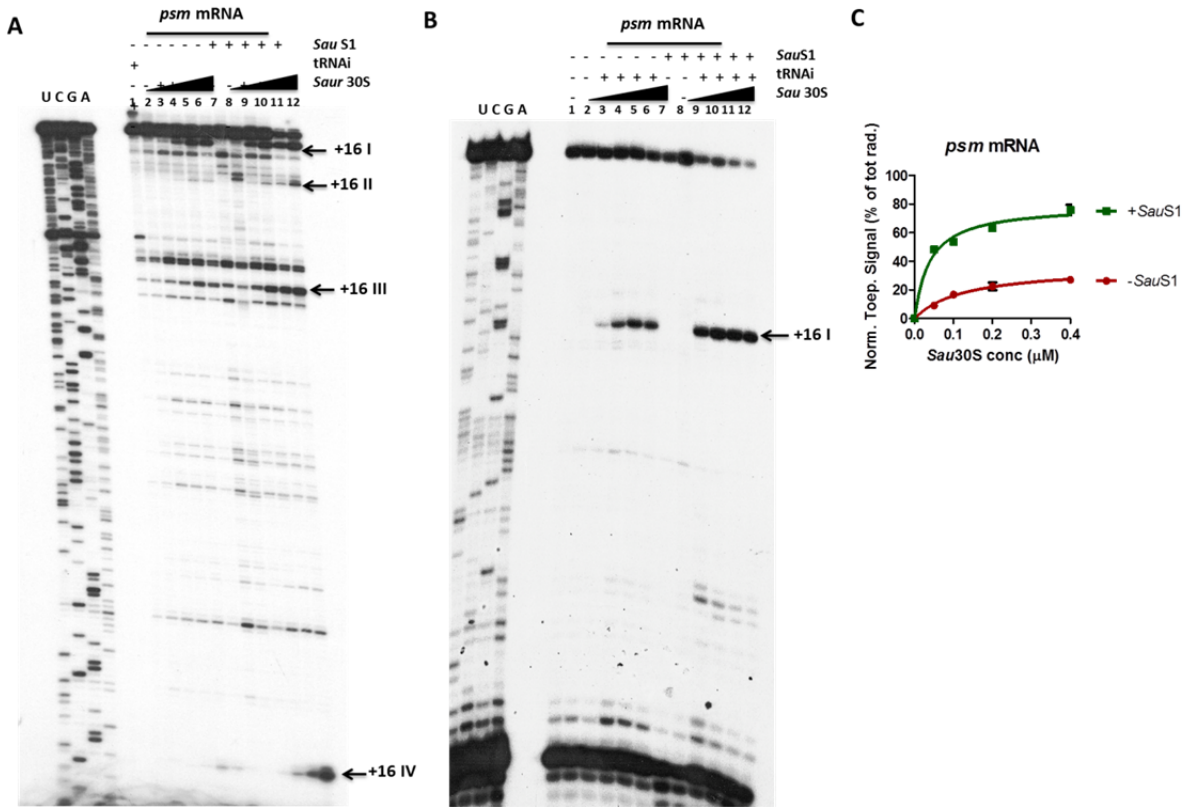

Figure 15. Toeprinting assays to monitor the effect of *Sau*S1 on the translation initiation complex formation with *psm* mRNA. (A) Effect of *Sau*S1 on the formation of initiation complex using *psm* mRNA and an oligonucleotide that anneals at the 3' end of the mRNA. When present, *Sau*S1 was pre-incubated with the ribosome at a constant 1.6 molar ratio. Lane 1: incubation control of mRNA ; Lane 2: incubation control of mRNA with 30S subunits ; Lanes 3, 4, 5 and 6: formation of the initiation complex containing mRNA, increasing concentration of 30S (25, 50, 100, 200 nM) and fMet-tRNA. Lane7: incubation control of mRNA with purified *Sau*S1. Lane 8: incubation control of mRNA, 30S and *Sau*S1. Lanes 9, 10, 11 and 12: formation of initiation complex in presence of *Sau*S1 and increasing concentrations of 30S (25, 50, 100, 200 nM). Lanes U, A, G, C: sequencing ladders. The toe-printing signals at position +16 are indicated by arrows. (B) Toe-printing done with an oligonucleotide annealing close to the 5' end to better visualize the 1st RBS of the *psm* mRNA. Same legend as in the panel A. (C) Quantification of the toe-printing using ImageQuanTL software (GE Healthcare). Signals were normalized according to the total amount of radioactivity (full-lenght extension and +16 product bands).

In order to assess if the activity of *Sau*S1 is specifically linked to the alleviation of translation repression mediated by cis-acting mRNA structures, we tested by toe-printing one more natural *S. aureus*. *spa* mRNA, which harbours distinct structural features. A short 5' UTR containing a strong SD sequence exposed in a hairpin loop, and an unpaired AU rich sequence downstream the start codon which has low propensity of forming stable structures (predicted ΔG= -2.7 kcal/mol) (**Figure S3 and S4**). We have previously shown that *E. coli* ribosomes, containing or not S1, are able to form initiation complexes with *spa* mRNA (Khusainov et al., 2016). As shown in **Figure S3**, *Sau*S1 enhances only very weakly the formation of the translation initiation complex on *spa* mRNA.

*Sau*S1 stimulates *psm* translation initiation by binding directly to the mRNA

To further investigate the mechanism by which *Sau*S1 stimulates translation of the *psm* mRNA, we checked its ability to interact with the 30S ribosome. Mass spectrometry analyses of purified *S. aureus* 70S and 30S have shown only traces of *Sau*S1 (Khusainov et al., 2016; Khusainov et al., 2017). This could have been resulted from dissociation occurring during ribosome purification or could be due to its inability to bind the ribosome. To address this question we forced a possible interaction by incubating large excess of *Sau*S1 with *Sau*30S. Gel filtration chromatography (GFC) was used to purify the complex, which has been analyzed by LC/MSMS to determine the protein content (**Figure 16A**). The chromatogram, following the absorbance of the 30S at 280 nm, shows a single peak where all 30S r-proteins have been found except *Sau*S1 (**Table S7**), which was eluted at a later time. This data indicates that *Sau*S1 does not interact with the 30S. The same experiment was then performed in the presence of *psm* mRNA (**Figure 16B**). The obtained absorbance profile resembles strictly the previous one, while the spectral count analysis of the fractions

indicates the presence of *Sau*S1 on the 30S at a level compatible with the other r-proteins (**Table S7**).

We then analyzed whether *Sau*S1 binds directly to *psm* mRNA using gel retardation assays (**Figure 16C**). *In vitro* 5' end-labelled *psm* was incubated with increasing concentrations of *Sau*S1. The data showed that *Sau*S1 is able to form two distinct complexes with *psm* mRNA possibly indicating that two *Sau*S1 molecules are able to bind to the mRNA with different affinity (between 100-200 nM and around 300 nM). To finally prove that the activation mechanism relies on the formation of *Sau*S1-*psm* complex, a new toe-printing assay was done on *psm* mRNA pre-incubated with *Sau*S1 before the addition of the 30S and the initiator tRNA (**Figure S5)**. A strong enhancement of the initiation complex formation on the 1st CDS could be observed even at a low concentration of *Sau*S1 (100 nM).

Taken together, these data revealed that *Sau*S1 is not a ribosomal protein but activates *psm* translation through a direct binding with *psm* mRNA, possibly at multiple sites. The presence of inhibitory structures on *psm* RBSs would suggest a possible remodeling of the RNA structure upon *Sau*S1 interaction, which would liberate their SD sequences to facilitate the 30S recruitment.

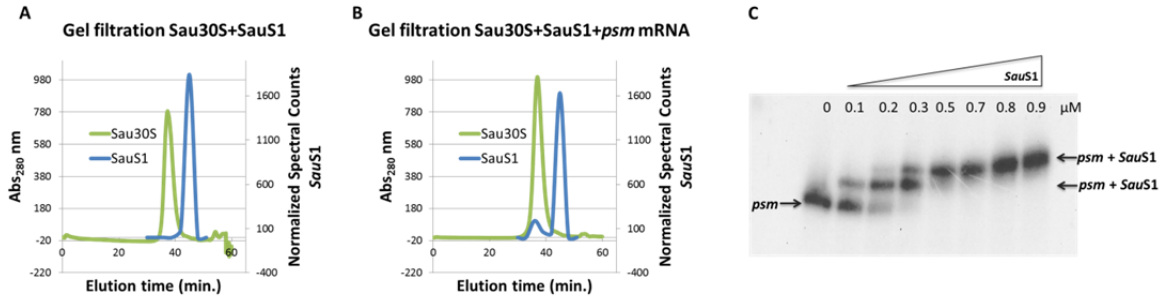

Figure 16. *Sau*S1 activates translation of *psm* by direct binding to the mRNA. A. Chromatogram of the gel filtration (Superose TM 6 Increase 3.2/300) for the *Sau*30S+*Sau*S1 complex (green profile) indicating the peak for the *Sau*30S and the peak for *Sau*S1 (blue profile) observed by spectral counts analysis of the fractions. B. As for panel A. with the sole exception that *psm* mRNA has been added to the complex. *Sau*S1 spectral counts in the different fractions have been normalized to the total *Sau*S1 counts obtained in each of the two experiments. Peaks in panel A and B could be directly compared. C. Gel retardation assays to monitor *Sau*S1 binding to *psm* mRNA. The 5' end-labelled *psm* mRNA was incubated with increasing concentrations (nM) of *Sau*S1. Two complexes could be detected. The positions of the complexes and of the free *psm* are indicated by arrows.

DISCUSSION

In bacteria, the main determinant for mRNA recruitment on the 30S is the SD sequence which base-pairs with the 3' end of the 16S rRNA in the center of the 30S platform, a positively charged ring shape environment made by several key r-proteins (S1, S2, S7, S11,

S18 and S21)(Duval et al., 2015; Simonetti et al., 2009). Among these r-proteins, the largest r-protein S1 confers to the *E. coli* 30S the ability to recognize any type of mRNAs (e.g.,(Boni et al., 1991; Duval et al., 2013; Sorensen et al., 1998; Tzareva et al., 1994)). Particularly, S1 has been shown to increase the affinity of weak SD containing mRNAs, and to confer an RNA chaperone activity to the 30S that is essential to unfold different structures promoting mRNA accommodation into the decoding channel. In *E. coli*, the essential activity of S1 is linked to its N-terminal OB-fold domain, which directly interacts with the 30S (Byrgazov et al., 2015; Byrgazov et al., 2012; Duval et al., 2013). A phylogenetic study revealed that S1 from Gram-negative bacteria and high G+C content Gram-positive bacteria (i.e., actinobacteria) share similar domain organization containing at least the first four OB-fold domains that retained full 30S and RNA binding capacity, and the RNA chaperone activity (Duval et al., 2013; Duval et al., 2017; Salah et al., 2009). In contrast, S1 from low G+C content Gram-positive bacteria (firmicutes), contained only four OB-fold domains (Salah et al., 2009). A specific domain alignment analysis, strongly suggested that *Sau*S1 organization is most likely d3-d2-d3-d4, and does not carry the domain required for ribosome binding (**Supplementary Figure S6**).

Here, we show that *Sau*S1 is not an essential protein as it was demonstrated for other Gram-positive bacteria (e.g. in *B. subtilis* (Kobayashi et al., 2003), and in *S. pneumoiae* (Song et al., 2005)), and is not a ribosomal protein since we did not observe any detectable interaction with the 30S and the 70S ribosomes. Despite its non-ribosomal localization, we provide the first example of translation activation involving S1 in the major bacterial pathogen *S. aureus*. Specifically, we show that *Sau*S1 strongly and specifically activates the translation of the structured *psm* operon mRNA. Our data suggest that *SauS1* plays multiple functions in gene regulation: (i) the protein facilitates the ribosome binding to *psm* mRNA operon at the initiation step of protein synthesis; (ii) *Sau*S1 is present on polysomes only through its interaction with *psm* mRNA; (ii) transcriptomics and proteomics analysis revealed that *Sau*S1 is also an important regulator of exotoxin production, and might be a partner of sRNA-mediated regulation.

Although previous experiments suggested that S1 homologues had different properties and functions in Enterobacteriaceae and in low G-C Gram-positive bacteria, we show here that *Sau*S1 still exerts an important function in translation disconnected from the ribosome. The lack of the N-terminal domain most likely coincides with the fact that many mRNAs in low G-C Gram-positive bacteria contains strong SD sequences. Although additional experiments will be required to assess the molecular mechanism of S1-dependent activation of *psm* translation, we propose that *Sau*S1 has evolved as a translational regulator and RNA chaperone protein, in a way reminiscent to the cold shock protein CspA in *E. coli* (Giuliodori et al., 2010). Indeed, the *psm* operon is predicted to be a highly structured RNA in

which the four SD and the coding sequences are sequestered into hairpin motifs. These hairpins are connected through unpaired A/U rich regions (**Figure S2**), which are known to be ideal binding sites for *E. coli* S1 (Boni et al., 1991; Duval et al., 2013). Band shift experiments revealed that several proteins bind to *psm* transcript with low or medium affinities (from 100 to 300 nM). . These data suggested that *Sau*S1 forms dynamic complexes with RNA and most probably acts as an RNA chaperone to remodel the RNA structure, which becomes competent for translation. Another example of a structured RNA encoded *psm* is RNAIII, which contained several long-range interactions bringing in close proximity its 5' and 3' non coding regions (Benito et al., 2000). Noteworthy, it has been shown that the translation of the PSM delta-hemolysin and the activation of many exotoxins are delayed after the transcription of RNAIII, and this delay was abolished if the 3' non coding region of RNAIII is deleted (Balaban and Novick, 1995). It is tempting to propose that *Sau*S1 might help to promote the RNAIII conformational switch allowing the recruitment of the ribosome on *hld* RBS.

What could be the rationale of the *Sau*S1 regulation? The transcription of *rpsA* is regulated upon cell growth and its synthesis enhances strongly at the late exponential level. The functional significance for the existence of the two transcripts awaits for more experimental data. Nevertheless, the accumulation of S1 at the late exponential level corresponded to the expression pattern of the longest of the two transcripts (**Figure 12**). Intriguingly, this expression pattern follows the synthesis of the quorum sensing system RNAIII and of many exotoxins, for which the expression was found downregulated in the mutant *rpsA* (**Table 2**). These exotoxins include the PSMs (α-PSM, ß-PSM, Hld), the endopeptidases SspAB, the fibronectin binding proteins (FnbA and FnbB), and hemolysins (Hla, Hld, HlgB and HlgC). The PSMs are short, amphipathic α-helical peptides, which play key roles in virulence by promoting lysis of neutrophils, and contributing to the dissemination of biofilm-associated infection (reviewed in Otto, 2013). In contrast to many exotoxins, the transcription of PSM is strictly dependent on the *agr* quorum sensing system. A recent study revealed that SarA is required for the PSM synthesis as well as other exotoxins contributing to the acute phase of *S. aureus* osteomyelitis (Loughran et al., 2016) but this regulatory event could be the result of the SarA-dependent activation of AgrA transcription (Loughran et al., 2016; Queck et al., 2008). Interestingly, the expression of *rpsA* is also drastically reduced in different *sarA* mutant strains (Loughran et al., 2016; Roberts et al., 2006). Because SarA is strongly induced during the transition from late exponential phase to stationary phase (Manna et al., 1998), it might be responsible for the coordination of *rpsA* transcription with that of *psm*. The strict regulation of PSMs expression under both the quorum sensing control and *SauS1* might be necessary for the concerted action during acute infection, when they

are produced to promote dissemination and tissue lysis. Since they contribute to biofilm detachment/dissemination (Kong et al., 2006; Periasamy et al., 2012; Tsompanidou et al., 2011), an early induction could expose *S. aureus* to the host immune system before a critical mass could have been attained. In that regard, it is worth to notice that *Sau*S1 could also regulate the translation of the *sspABC* operon, coding endopeptidases important for immune suppression and infection dissemination (Imamura et al., 2005; Jusko et al., 2014; Ohbayashi et al., 2011). Their expression is *agr*-dependent, probably mediated by Rot, as inactivation of *rot* in an *agr* mutant resulted in upregulation of *sspABC* mRNA levels (Said-Salim et al., 2003). Rot levels are not changed in our Δ*rpsA* mutant (**Supplementary excel file S1**), leaving open the possibility that *Sau*S1 would also enhance their translation. Nevertheless, many other regulators have been described, like σ^B, SarA, MgrA, SaeRS, SarV, SarR, SarS, SrrAB and ArlRS (Bischoff et al., 2004; Cheung et al., 2001; Fournier et al., 2001; Luong et al., 2003; Manna et al., 2004; Novick and Jiang, 2003). Given the complexity of *sspABC* regulation, assessing the impact of *Sau*S1 would require individual analysis on the different pathways. Noteworthy, the RBSs of *sspA* and *sspB* are predicted to be embedded into inhibitory structures that would require the chaperone activity of *Sau*S1 for active translation (**Figure S4**). A similar situation could be shared by other virulence genes, such as the immune evasion protein *sbi,* which shows structured RBS (**Figure S4**) and a decreased level despite the strong *Sau*S1-dependent reduction of the levels of the two translational repressor RNAs, SprD and RNAIII (Chabelskaya et al., 2014). Taken together, S1 adds another layer of regulation to modulate the expression of virulence factors (**Figure 17**).

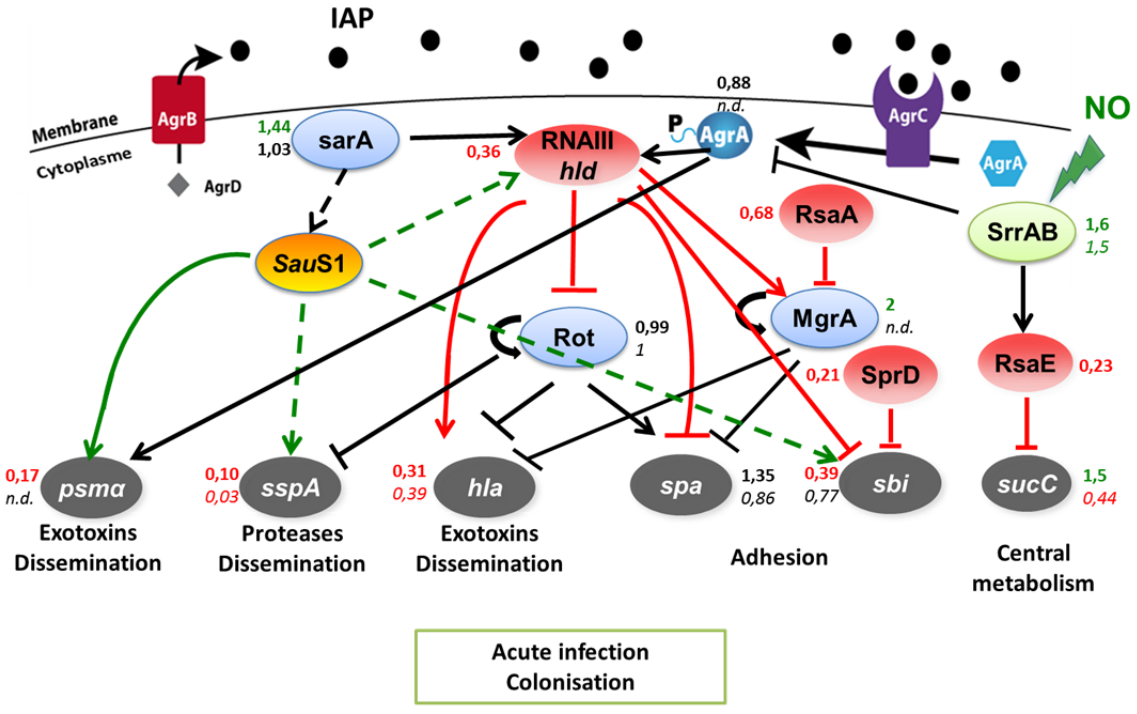

Figure 17. Impact of *Sau*S1 on the regulatory circuits involved in virulence gene expression. Only parts of the regulatory circuits taken from the literature have been represented. SarA might induce *rpsA* transcription coordinating *Sau*S1 expression with the transcription of RNAIII which is also under the control of the quorum sensing system (*agr*) *via* the activation of the transcription factor AgrA. *Sau*S1 activates the translation of PSMα peptides and possibly also Ssp proteins, Sbi and δ-hemolysin (*hld*). The feedforward loop motif involving RNAIII, the transcriptional regulator Rot and the circuits controlled by RsaA, SprD and RsaE are also represented. The transcriptional regulatory proteins are in blue, the regulatory RNAs are in red and the target proteins are in purple, SauS1 is green. Values reported on the sides of each gene represent their fold changes in the Δ*rpsA* mutant, as transcripts (upper values) or proteins (lower values). The transcriptional regulation is shown by black line, sRNA regulation is shown by red line while *Sau*S1 translation regulation is shown with green lines. Arrows correspond to activation while bars correspond to repression. Regulations shown by dotted lines await experimental validation.

Interestingly, the production of toxins and exoenzymes was reported to be specifically perturbed by sub-inhibitory concentration of linezolid antibiotic (Coyle et al., 2003; Diep et al., 2012; Dumitrescu et al., 2007; Gemmell and Ford, 2002; Otto et al., 2013). Linezolid targets the A site of the ribosome and blocks peptide bond formation (Wilson et al., 2008). At sub-inhibitory concentration, it promotes the synthesis of new ribosomal proteins to make more ribosomes (Bonn et al., 2016). However, under these conditions, *Sau*S1 is no more synthesized, thus producing a situation similar to the mutant Δ*rpsA* strain. It is possible that the specific effect of linezolid on the synthesis of virulence factors is linked to the incapacity of the newly synthesized ribosome to recognize the structured mRNAs encoded these toxins and exoenzymes.

Finally, the yields of several sRNAs appear to be significantly reduced in Δ*rpsA* strain. Such a phenotype has been largely demonstrated in Enterobacteriaceae for the RNA chaperone Hfq (Cui et al., 2013; Sonnleitner et al., 2006; Updegrove et al., 2016; Vogel and Luisi, 2011) and for ProQ (Smirnov et al., 2016; Smirnov et al., 2017). These two proteins are key co-factors helping the sRNAs to regulate the expression of mRNAs at the post-transcriptional level. Mutations in *hfq* also decrease virulence in several pathogens (for review, see (Vogel and Papenfort, 2006)). In contrast to this, the function of Hfq in low G+C Gram-positive bacteria is still unclear and controversial (Bouloc and Repoila, 2016), and there is no ProQ equivalent in *S. aureus* (Attaiech et al., 2017; Olejniczak and Storz, 2017). In *S. aureus,* Hfq binds to RNAs, but it neither enhances the recognition between antisense RNAs and their target mRNAs (Zheng et al., 2016) nor the stability of sRNAs (Boisset et al., 2007; Preis et al., 2009). Furthermore, no major phenotypes were linked to its deletion in *S.*

699 *aureus* (Bohn et al., 2007). By acting on the stability of several sRNAs, such as RNAIII,
700 RsaE, RsaA, and SprD, known to bind mRNAs and to affect their translation (reviewed in
701 (Felden et al., 2011; Mandin and Guillier, 2013; Tomasini et al., 2014), *Sau*S1 might be a
702 key partner of sRNA regulation. Some of the observed deregulations in the mutant Δ*rpsA*
703 strain might be indirect. For instance, the *hla* reduced expression could be explained by less
704 amount of the translational activator RNAIII (Morfeldt et al., 1995), and the enhanced levels
705 of the pleiotropic regulatory protein MgrA might be due to a decreased level of its main
706 repressor RsaA (Romilly et al., 2014).
707 This work shows that SauS1 belongs to a new class of RNA chaperones that play
708 key roles in the regulation of translation in *S. aureus* and most probably in Gram-positive
709 bacteria. Our current study provides some hints for further investigation of the molecular
710 functions and mechanisms of *Sau*S1 in gene regulation.
711

712 **ACKNOWLEDGEMENT**
713 We are grateful to Anne-Catherine Helfer for her help in the toe-printing assay on the RNAIII,
714 to Javier Rol for the RNAIII band-shift experiment and to Philippe Hammann for his
715 assistance with mass spectrometry analysis (IBMC proteomic platform).
716

717 **FUNDING**
718 This work was supported by the Centre National de la Recherche Scientifique (CNRS) to
719 [P.R.], by the ANR agency (ANR RIBOSTAPH) [P.R.] and has been published under the
720 framework of the LABEX: ANR-10-LABX-0036 NETRNA to [P.R.], a funding from the state
721 managed by the French National Research Agency as part of the investments for the future
722 program. In addition, the LABEX NetRNA granted the mass spectrometry instrumentation.

723

REFERENCES

Afgan, E., Baker, D., van den Beek, M., Blankenberg, D., Bouvier, D., Cech, M., Chilton, J., Clements, D., Coraor, N., Eberhard, C.*, et al.* (2016). The Galaxy platform for accessible, reproducible and collaborative biomedical analyses: 2016 update. Nucleic Acids Res *44*, W3-W10.

Anders, S., Pyl, P.T., and Huber, W. (2015). HTSeq--a Python framework to work with high-throughput sequencing data. Bioinformatics (Oxford, England) *31*, 166-169.

Anderson, K.L., Roberts, C., Disz, T., Vonstein, V., Hwang, K., Overbeek, R., Olson, P.D., Projan, S.J., and Dunman, P.M. (2006). Characterization of the Staphylococcus aureus heat shock, cold shock, stringent, and SOS responses and their effects on log-phase mRNA turnover. Journal of bacteriology *188*, 6739-6756.

Attaiech, L., Glover, J.N., and Charpentier, X. (2017). RNA Chaperones Step Out of Hfq's Shadow. Trends in microbiology *25*, 247-249.

Balaban, N., and Novick, R.P. (1995). Translation of RNAIII, the Staphylococcus aureus agr regulatory RNA molecule, can be activated by a 3'-end deletion. FEMS microbiology letters *133*, 155-161.

Benito, Y., Kolb, F.A., Romby, P., Lina, G., Etienne, J., and Vandenesch, F. (2000). Probing the structure of RNAIII, the Staphylococcus aureus agr regulatory RNA, and identification of the RNA domain involved in repression of protein A expression. RNA (New York, NY) *6*, 668-679.

Bischoff, M., Dunman, P., Kormanec, J., Macapagal, D., Murphy, E., Mounts, W., Berger-Bachi, B., and Projan, S. (2004). Microarray-based analysis of the Staphylococcus aureus sigmaB regulon. Journal of bacteriology *186*, 4085-4099.

Blankenberg, D., Gordon, A., Von Kuster, G., Coraor, N., Taylor, J., and Nekrutenko, A. (2010). Manipulation of FASTQ data with Galaxy. Bioinformatics (Oxford, England) *26*, 1783-1785.

Bohn, C., Rigoulay, C., and Bouloc, P. (2007). No detectable effect of RNA-binding protein Hfq absence in Staphylococcus aureus. BMC Microbiol *7*, 10.

Boisset, S., Geissmann, T., Huntzinger, E., Fechter, P., Bendridi, N., Possedko, M., Chevalier, C., Helfer, A.C., Benito, Y., Jacquier, A.*, et al.* (2007). Staphylococcus aureus RNAIII coordinately represses the synthesis of virulence factors and the transcription regulator Rot by an antisense mechanism. Genes & development *21*, 1353-1366.

Bolger, A.M., Lohse, M., and Usadel, B. (2014). Trimmomatic: a flexible trimmer for Illumina sequence data. Bioinformatics (Oxford, England) *30*, 2114-2120.

Boni, I.V., Isaeva, D.M., Musychenko, M.L., and Tzareva, N.V. (1991). Ribosome-messenger recognition: mRNA target sites for ribosomal protein S1. Nucleic Acids Res *19*, 155-162.

Bonn, F., Pane-Farre, J., Schluter, R., Schaffer, M., Fuchs, S., Bernhardt, J., Riedel, K., Otto, A., Volker, U., van Dijl, J.M.*, et al.* (2016). Global analysis of the impact of linezolid onto virulence factor production in S. aureus USA300. International journal of medical microbiology : IJMM *306*, 131-140.

Bouloc, P., and Repoila, F. (2016). Fresh layers of RNA-mediated regulation in Gram-positive bacteria. Current opinion in microbiology *30*, 30-35.

Byrgazov, K., Grishkovskaya, I., Arenz, S., Coudevylle, N., Temmel, H., Wilson, D.N., Djinovic-Carugo, K., and Moll, I. (2015). Structural basis for the interaction of protein S1 with the Escherichia coli ribosome. Nucleic Acids Res *43*, 661-673.

Byrgazov, K., Manoharadas, S., Kaberdina, A.C., Vesper, O., and Moll, I. (2012). Direct interaction of the N-terminal domain of ribosomal protein S1 with protein S2 in Escherichia coli. PloS one *7*, e32702.

Caldelari, I., Chane-Woon-Ming, B., Noirot, C., Moreau, K., Romby, P., Gaspin, C., and Marzi, S. (2017). Complete Genome Sequence and Annotation of the Staphylococcus aureus Strain HG001. Genome announcements *5*.

Campbell, E.A., Korzheva, N., Mustaev, A., Murakami, K., Nair, S., Goldfarb, A., and Darst, S.A. (2001). Structural mechanism for rifampicin inhibition of bacterial rna polymerase. Cell *104*, 901-912.
Chabelskaya, S., Bordeau, V., and Felden, B. (2014). Dual RNA regulatory control of a Staphylococcus aureus virulence factor. Nucleic Acids Res *42*, 4847-4858.
Charpentier, E., Anton, A.I., Barry, P., Alfonso, B., Fang, Y., and Novick, R.P. (2004). Novel cassette-based shuttle vector system for gram-positive bacteria. Applied and environmental microbiology *70*, 6076-6085.
Cheung, A.L., Schmidt, K., Bateman, B., and Manna, A.C. (2001). SarS, a SarA homolog repressible by agr, is an activator of protein A synthesis in Staphylococcus aureus. Infection and immunity *69*, 2448-2455.
Chevalier, C., Boisset, S., Romilly, C., Masquida, B., Fechter, P., Geissmann, T., Vandenesch, F., and Romby, P. (2010). Staphylococcus aureus RNAIII binds to two distant regions of coa mRNA to arrest translation and promote mRNA degradation. PLoS pathogens *6*, e1000809.
Condon, C. (2003). RNA processing and degradation in Bacillus subtilis. Microbiology and molecular biology reviews : MMBR *67*, 157-174, table of contents.
Condon, C., Squires, C., and Squires, C.L. (1995). Control of rRNA transcription in Escherichia coli. Microbiological reviews *59*, 623-645.
Coyle, E.A., Cha, R., and Rybak, M.J. (2003). Influences of linezolid, penicillin, and clindamycin, alone and in combination, on streptococcal pyrogenic exotoxin a release. Antimicrobial agents and chemotherapy *47*, 1752-1755.
Cui, M., Wang, T., Xu, J., Ke, Y., Du, X., Yuan, X., Wang, Z., Gong, C., Zhuang, Y., Lei, S.*, et al.* (2013). Impact of Hfq on global gene expression and intracellular survival in Brucella melitensis. PloS one *8*, e71933.
Diep, B.A., Equils, O., Huang, D.B., and Gladue, R. (2012). Linezolid effects on bacterial toxin production and host immune response: review of the evidence. Current therapeutic research, clinical and experimental *73*, 86-102.
Dumitrescu, O., Boisset, S., Badiou, C., Bes, M., Benito, Y., Reverdy, M.E., Vandenesch, F., Etienne, J., and Lina, G. (2007). Effect of antibiotics on Staphylococcus aureus producing Panton-Valentine leukocidin. Antimicrobial agents and chemotherapy *51*, 1515-1519.
Duval, M., Korepanov, A., Fuchsbauer, O., Fechter, P., Haller, A., Fabbretti, A., Choulier, L., Micura, R., Klaholz, B.P., Romby, P.*, et al.* (2013). Escherichia coli ribosomal protein S1 unfolds structured mRNAs onto the ribosome for active translation initiation. PLoS biology *11*, e1001731.
Duval, M., Marenna, A., Chevalier, C., and Marzi, S. (2017). Site-Directed Chemical Probing to map transient RNA/protein interactions. Methods (San Diego, Calif) *117*, 48-58.
Duval, M., Simonetti, A., Caldelari, I., and Marzi, S. (2015). Multiple ways to regulate translation initiation in bacteria: Mechanisms, regulatory circuits, dynamics. Biochimie *114*, 18-29.
Farwell, M.A., Roberts, M.W., and Rabinowitz, J.C. (1992). The effect of ribosomal protein S1 from Escherichia coli and Micrococcus luteus on protein synthesis in vitro by E. coli and Bacillus subtilis. Molecular microbiology *6*, 3375-3383.
Fechter, P., Chevalier, C., Yusupova, G., Yusupov, M., Romby, P., and Marzi, S. (2009). Ribosomal initiation complexes probed by toeprinting and effect of trans-acting translational regulators in bacteria. Methods in molecular biology (Clifton, NJ) *540*, 247-263.
Felden, B., Vandenesch, F., Bouloc, P., and Romby, P. (2011). The Staphylococcus aureus RNome and its commitment to virulence. PLoS pathogens *7*, e1002006.
Fournier, B., Klier, A., and Rapoport, G. (2001). The two-component system ArlS-ArlR is a regulator of virulence gene expression in Staphylococcus aureus. Molecular microbiology *41*, 247-261.
Geisinger, E., Adhikari, R.P., Jin, R., Ross, H.F., and Novick, R.P. (2006). Inhibition of rot translation by RNAIII, a key feature of agr function. Molecular microbiology *61*, 1038-1048.

Geisinger, E., Muir, T.W., and Novick, R.P. (2009). agr receptor mutants reveal distinct modes of inhibition by staphylococcal autoinducing peptides. Proceedings of the National Academy of Sciences of the United States of America *106*, 1216-1221.
Gemmell, C.G., and Ford, C.W. (2002). Virulence factor expression by Gram-positive cocci exposed to subinhibitory concentrations of linezolid. The Journal of antimicrobial chemotherapy *50*, 665-672.
Giuliodori, A.M., Di Pietro, F., Marzi, S., Masquida, B., Wagner, R., Romby, P., Gualerzi, C.O., and Pon, C.L. (2010). The cspA mRNA is a thermosensor that modulates translation of the cold-shock protein CspA. Molecular cell *37*, 21-33.
Hartz, D., McPheeters, D.S., Traut, R., and Gold, L. (1988). Extension inhibition analysis of translation initiation complexes. Methods Enzymol *164*, 419-425.
Herbert, S., Ziebandt, A.K., Ohlsen, K., Schafer, T., Hecker, M., Albrecht, D., Novick, R., and Gotz, F. (2010). Repair of global regulators in Staphylococcus aureus 8325 and comparative analysis with other clinical isolates. Infection and immunity *78*, 2877-2889.
Huntzinger, E., Boisset, S., Saveanu, C., Benito, Y., Geissmann, T., Namane, A., Lina, G., Etienne, J., Ehresmann, B., Ehresmann, C*., et al.* (2005). Staphylococcus aureus RNAIII and the endoribonuclease III coordinately regulate spa gene expression. The EMBO journal *24*, 824-835.
Ibarra, J.A., Perez-Rueda, E., Carroll, R.K., and Shaw, L.N. (2013). Global analysis of transcriptional regulators in Staphylococcus aureus. BMC genomics *14*, 126.
Imamura, T., Tanase, S., Szmyd, G., Kozik, A., Travis, J., and Potempa, J. (2005). Induction of vascular leakage through release of bradykinin and a novel kinin by cysteine proteinases from Staphylococcus aureus. The Journal of experimental medicine *201*, 1669-1676.
Janzon, L., and Arvidson, S. (1990). The role of the delta-lysin gene (hld) in the regulation of virulence genes by the accessory gene regulator (agr) in Staphylococcus aureus. The EMBO journal *9*, 1391-1399.
Juhas, M., Reuss, D.R., Zhu, B., and Commichau, F.M. (2014). Bacillus subtilis and Escherichia coli essential genes and minimal cell factories after one decade of genome engineering. Microbiology (Reading, England) *160*, 2341-2351.
Jusko, M., Potempa, J., Kantyka, T., Bielecka, E., Miller, H.K., Kalinska, M., Dubin, G., Garred, P., Shaw, L.N., and Blom, A.M. (2014). Staphylococcal proteases aid in evasion of the human complement system. Journal of innate immunity *6*, 31-46.
Kaczanowska, M., and Ryden-Aulin, M. (2007). Ribosome biogenesis and the translation process in Escherichia coli. Microbiology and molecular biology reviews : MMBR *71*, 477-494.
Khusainov, I., Marenna, A., Cerciat, M., Fechter, P., Hashem, Y., Marzi, S., Romby, P., Yusupova, G., and Yusupov, M. (2016). [A glimpse on Staphylococcus aureus translation machinery and its control]. Molekuliarnaia biologiia *50*, 549-557.
Khusainov, I., Vicens, Q., Bochler, A., Grosse, F., Myasnikov, A., Menetret, J.F., Chicher, J., Marzi, S., Romby, P., Yusupova, G*., et al.* (2017). Structure of the 70S ribosome from human pathogen Staphylococcus aureus. Nucleic Acids Res *45*, 1026.
Kiedrowski, M.R., Kavanaugh, J.S., Malone, C.L., Mootz, J.M., Voyich, J.M., Smeltzer, M.S., Bayles, K.W., and Horswill, A.R. (2011). Nuclease modulates biofilm formation in community-associated methicillin-resistant Staphylococcus aureus. PloS one *6*, e26714.
Kjeldgaard, N.O., Maaloe, O., and Schaechter, M. (1958). The transition between different physiological states during balanced growth of Salmonella typhimurium. Journal of general microbiology *19*, 607-616.
Kobayashi, K., Ehrlich, S.D., Albertini, A., Amati, G., Andersen, K.K., Arnaud, M., Asai, K., Ashikaga, S., Aymerich, S., Bessieres, P*., et al.* (2003). Essential Bacillus subtilis genes. Proceedings of the National Academy of Sciences of the United States of America *100*, 4678-4683.
Koch, G., Yepes, A., Forstner, K.U., Wermser, C., Stengel, S.T., Modamio, J., Ohlsen, K., Foster, K.R., and Lopez, D. (2014). Evolution of resistance to a last-resort antibiotic in Staphylococcus aureus via bacterial competition. Cell *158*, 1060-1071.

884 Kong, K.F., Vuong, C., and Otto, M. (2006). Staphylococcus quorum sensing in biofilm
885 formation and infection. International journal of medical microbiology : IJMM *296*, 133-139.
886 Langmead, B., Trapnell, C., Pop, M., and Salzberg, S.L. (2009). Ultrafast and memory-
887 efficient alignment of short DNA sequences to the human genome. Genome biology *10*, R25.
888 Lasa, I., Toledo-Arana, A., Dobin, A., Villanueva, M., de los Mozos, I.R., Vergara-Irigaray, M.,
889 Segura, V., Fagegaltier, D., Penades, J.R., Valle, J*., et al.* (2011). Genome-wide antisense
890 transcription drives mRNA processing in bacteria. Proceedings of the National Academy of
891 Sciences of the United States of America *108*, 20172-20177.
892 Li, M., Cheung, G.Y., Hu, J., Wang, D., Joo, H.S., Deleo, F.R., and Otto, M. (2010).
893 Comparative analysis of virulence and toxin expression of global community-associated
894 methicillin-resistant Staphylococcus aureus strains. The Journal of infectious diseases *202*,
895 1866-1876.
896 Loughran, A.J., Gaddy, D., Beenken, K.E., Meeker, D.G., Morello, R., Zhao, H., Byrum, S.D.,
897 Tackett, A.J., Cassat, J.E., and Smeltzer, M.S. (2016). Impact of sarA and Phenol-Soluble
898 Modulins on the Pathogenesis of Osteomyelitis in Diverse Clinical Isolates of
899 Staphylococcus aureus. Infection and immunity *84*, 2586-2594.
900 Lowy, F.D. (1998). Staphylococcus aureus infections. The New England journal of medicine
901 *339*, 520-532.
902 Luong, T.T., Newell, S.W., and Lee, C.Y. (2003). Mgr, a novel global regulator in
903 Staphylococcus aureus. Journal of bacteriology *185*, 3703-3710.
904 Mandin, P., and Guillier, M. (2013). Expanding control in bacteria: interplay between small
905 RNAs and transcriptional regulators to control gene expression. Current opinion in
906 microbiology *16*, 125-132.
907 Manna, A.C., Bayer, M.G., and Cheung, A.L. (1998). Transcriptional analysis of different
908 promoters in the sar locus in Staphylococcus aureus. Journal of bacteriology *180*, 3828-
909 3836.
910 Manna, A.C., Ingavale, S.S., Maloney, M., van Wamel, W., and Cheung, A.L. (2004).
911 Identification of sarV (SA2062), a new transcriptional regulator, is repressed by SarA and
912 MgrA (SA0641) and involved in the regulation of autolysis in Staphylococcus aureus. Journal
913 of bacteriology *186*, 5267-5280.
914 Monk, I.R., Shah, I.M., Xu, M., Tan, M.W., and Foster, T.J. (2012). Transforming the
915 untransformable: application of direct transformation to manipulate genetically
916 Staphylococcus aureus and Staphylococcus epidermidis. mBio *3*.
917 Morfeldt, E., Taylor, D., von Gabain, A., and Arvidson, S. (1995). Activation of alpha-toxin
918 translation in Staphylococcus aureus by the trans-encoded antisense RNA, RNAIII. The
919 EMBO journal *14*, 4569-4577.
920 Nomura, M. (1999). Regulation of ribosome biosynthesis in Escherichia coli and
921 Saccharomyces cerevisiae: diversity and common principles. Journal of bacteriology *181*,
922 6857-6864.
923 Nomura, M., Gourse, R., and Baughman, G. (1984). Regulation of the synthesis of
924 ribosomes and ribosomal components. Annual review of biochemistry *53*, 75-117.
925 Novick, R.P., and Geisinger, E. (2008). Quorum sensing in staphylococci. Annual review of
926 genetics *42*, 541-564.
927 Novick, R.P., and Jiang, D. (2003). The staphylococcal saeRS system coordinates
928 environmental signals with agr quorum sensing. Microbiology (Reading, England) *149*, 2709-
929 2717.
930 Novick, R.P., Ross, H.F., Projan, S.J., Kornblum, J., Kreiswirth, B., and Moghazeh, S. (1993).
931 Synthesis of staphylococcal virulence factors is controlled by a regulatory RNA molecule.
932 The EMBO journal *12*, 3967-3975.
933 Ohbayashi, T., Irie, A., Murakami, Y., Nowak, M., Potempa, J., Nishimura, Y., Shinohara, M.,
934 and Imamura, T. (2011). Degradation of fibrinogen and collagen by staphopains, cysteine
935 proteases released from Staphylococcus aureus. Microbiology (Reading, England) *157*, 786-
936 792.
937 Olejniczak, M., and Storz, G. (2017). ProQ/FinO-domain proteins: another ubiquitous family
938 of RNA matchmakers? Molecular microbiology *104*, 905-915.

939 Omotajo, D., Tate, T., Cho, H., and Choudhary, M. (2015). Distribution and diversity of
940 ribosome binding sites in prokaryotic genomes. BMC genomics *16*, 604.
941 Otto, M.P., Martin, E., Badiou, C., Lebrun, S., Bes, M., Vandenesch, F., Etienne, J., Lina, G.,
942 and Dumitrescu, O. (2013). Effects of subinhibitory concentrations of antibiotics on virulence
943 factor expression by community-acquired methicillin-resistant Staphylococcus aureus. The
944 Journal of antimicrobial chemotherapy *68*, 1524-1532.
945 Periasamy, S., Joo, H.S., Duong, A.C., Bach, T.H., Tan, V.Y., Chatterjee, S.S., Cheung,
946 G.Y., and Otto, M. (2012). How Staphylococcus aureus biofilms develop their characteristic
947 structure. Proceedings of the National Academy of Sciences of the United States of America
948 *109*, 1281-1286.
949 Preis, H., Eckart, R.A., Gudipati, R.K., Heidrich, N., and Brantl, S. (2009). CodY activates
950 transcription of a small RNA in Bacillus subtilis. Journal of bacteriology *191*, 5446-5457.
951 Queck, S.Y., Jameson-Lee, M., Villaruz, A.E., Bach, T.H., Khan, B.A., Sturdevant, D.E.,
952 Ricklefs, S.M., Li, M., and Otto, M. (2008). RNAIII-independent target gene control by the
953 agr quorum-sensing system: insight into the evolution of virulence regulation in
954 Staphylococcus aureus. Molecular cell *32*, 150-158.
955 Roberts, C., Anderson, K.L., Murphy, E., Projan, S.J., Mounts, W., Hurlburt, B., Smeltzer, M.,
956 Overbeek, R., Disz, T., and Dunman, P.M. (2006). Characterizing the effect of the
957 Staphylococcus aureus virulence factor regulator, SarA, on log-phase mRNA half-lives.
958 Journal of bacteriology *188*, 2593-2603.
959 Rolfe, M.D., Rice, C.J., Lucchini, S., Pin, C., Thompson, A., Cameron, A.D., Alston, M.,
960 Stringer, M.F., Betts, R.P., Baranyi, J.*, et al.* (2012). Lag phase is a distinct growth phase
961 that prepares bacteria for exponential growth and involves transient metal accumulation.
962 Journal of bacteriology *194*, 686-701.
963 Romby, P., and Springer, M. (2007). Translational control in prokaryotes. In Translational
964 control in biology and medicine, M.B. Mathews, Sonenberg, N., and Hershey, J. W. B., ed.
965 (Cold Spring Harbour: Cold Spring Harbour Laboratory Press), pp. 803-827.
966 Romilly, C., Lays, C., Tomasini, A., Caldelari, I., Benito, Y., Hammann, P., Geissmann, T.,
967 Boisset, S., Romby, P., and Vandenesch, F. (2014). A non-coding RNA promotes bacterial
968 persistence and decreases virulence by regulating a regulator in Staphylococcus aureus.
969 PLoS pathogens *10*, e1003979.
970 Ruiz de los Mozos, I., Vergara-Irigaray, M., Segura, V., Villanueva, M., Bitarte, N.,
971 Saramago, M., Domingues, S., Arraiano, C.M., Fechter, P., Romby, P.*, et al.* (2013). Base
972 pairing interaction between 5'- and 3'-UTRs controls icaR mRNA translation in
973 Staphylococcus aureus. PLoS genetics *9*, e1004001.
974 Said-Salim, B., Dunman, P.M., McAleese, F.M., Macapagal, D., Murphy, E., McNamara, P.J.,
975 Arvidson, S., Foster, T.J., Projan, S.J., and Kreiswirth, B.N. (2003). Global regulation of
976 Staphylococcus aureus genes by Rot. Journal of bacteriology *185*, 610-619.
977 Salah, P., Bisaglia, M., Aliprandi, P., Uzan, M., Sizun, C., and Bontems, F. (2009). Probing
978 the relationship between Gram-negative and Gram-positive S1 proteins by sequence
979 analysis. Nucleic Acids Res *37*, 5578-5588.
980 Simonetti, A., Marzi, S., Jenner, L., Myasnikov, A., Romby, P., Yusupova, G., Klaholz, B.P.,
981 and Yusupov, M. (2009). A structural view of translation initiation in bacteria. Cellular and
982 molecular life sciences : CMLS *66*, 423-436.
983 Smirnov, A., Forstner, K.U., Holmqvist, E., Otto, A., Gunster, R., Becher, D., Reinhardt, R.,
984 and Vogel, J. (2016). Grad-seq guides the discovery of ProQ as a major small RNA-binding
985 protein. Proceedings of the National Academy of Sciences of the United States of America
986 *113*, 11591-11596.
987 Smirnov, A., Wang, C., Drewry, L.L., and Vogel, J. (2017). Molecular mechanism of mRNA
988 repression in trans by a ProQ-dependent small RNA. The EMBO journal *36*, 1029-1045.
989 Somerville, G.A., and Proctor, R.A. (2009). At the crossroads of bacterial metabolism and
990 virulence factor synthesis in Staphylococci. Microbiology and molecular biology reviews :
991 MMBR *73*, 233-248.

Song, J.H., Ko, K.S., Lee, J.Y., Baek, J.Y., Oh, W.S., Yoon, H.S., Jeong, J.Y., and Chun, J. (2005). Identification of essential genes in Streptococcus pneumoniae by allelic replacement mutagenesis. Molecules and cells *19*, 365-374.
Sonnleitner, E., Schuster, M., Sorger-Domenigg, T., Greenberg, E.P., and Blasi, U. (2006). Hfq-dependent alterations of the transcriptome profile and effects on quorum sensing in Pseudomonas aeruginosa. Molecular microbiology *59*, 1542-1558.
Sorensen, M.A., Fricke, J., and Pedersen, S. (1998). Ribosomal protein S1 is required for translation of most, if not all, natural mRNAs in Escherichia coli in vivo. J Mol Biol *280*, 561-569.
Thammavongsa, V., Kim, H.K., Missiakas, D., and Schneewind, O. (2015). Staphylococcal manipulation of host immune responses. Nature reviews Microbiology *13*, 529-543.
Thorvaldsdottir, H., Robinson, J.T., and Mesirov, J.P. (2013). Integrative Genomics Viewer (IGV): high-performance genomics data visualization and exploration. Briefings in bioinformatics *14*, 178-192.
Tomasini, A., Francois, P., Howden, B.P., Fechter, P., Romby, P., and Caldelari, I. (2014). The importance of regulatory RNAs in Staphylococcus aureus. Infection, genetics and evolution : journal of molecular epidemiology and evolutionary genetics in infectious diseases *21*, 616-626.
Tomasini, A., Moreau, K., Chicher, J., Geissmann, T., Vandenesch, F., Romby, P., Marzi, S., and Caldelari, I. (2017). The RNA targetome of Staphylococcus aureus non-coding RNA RsaA: impact on cell surface properties and defense mechanisms. Nucleic Acids Res.
Tsompanidou, E., Sibbald, M.J., Chlebowicz, M.A., Dreisbach, A., Back, J.W., van Dijl, J.M., Buist, G., and Denham, E.L. (2011). Requirement of the agr locus for colony spreading of Staphylococcus aureus. Journal of bacteriology *193*, 1267-1272.
Tzareva, N.V., Makhno, V.I., and Boni, I.V. (1994). Ribosome-messenger recognition in the absence of the Shine-Dalgarno interactions. FEBS letters *337*, 189-194.
Updegrove, T.B., Zhang, A., and Storz, G. (2016). Hfq: the flexible RNA matchmaker. Current opinion in microbiology *30*, 133-138.
Vandenesch, F., Kornblum, J., and Novick, R.P. (1991). A temporal signal, independent of agr, is required for hla but not spa transcription in Staphylococcus aureus. Journal of bacteriology *173*, 6313-6320.
Varet, H., Brillet-Gueguen, L., Coppee, J.Y., and Dillies, M.A. (2016). SARTools: A DESeq2- and EdgeR-Based R Pipeline for Comprehensive Differential Analysis of RNA-Seq Data. PloS one *11*, e0157022.
Vellanoweth, R.L., and Rabinowitz, J.C. (1992). The influence of ribosome-binding-site elements on translational efficiency in Bacillus subtilis and Escherichia coli in vivo. Molecular microbiology *6*, 1105-1114.
Vogel, J., and Luisi, B.F. (2011). Hfq and its constellation of RNA. Nature reviews Microbiology *9*, 578-589.
Vogel, J., and Papenfort, K. (2006). Small non-coding RNAs and the bacterial outer membrane. Current opinion in microbiology *9*, 605-611.
Vuong, C., Durr, M., Carmody, A.B., Peschel, A., Klebanoff, S.J., and Otto, M. (2004). Regulated expression of pathogen-associated molecular pattern molecules in Staphylococcus epidermidis: quorum-sensing determines pro-inflammatory capacity and production of phenol-soluble modulins. Cellular microbiology *6*, 753-759.
Wagner, E.G., and Romby, P. (2015). Small RNAs in bacteria and archaea: who they are, what they do, and how they do it. Advances in genetics *90*, 133-208.
Wagner, R. (1994). The regulation of ribosomal RNA synthesis and bacterial cell growth. Archives of microbiology *161*, 100-109.
Wenzel, M., and Bandow, J.E. (2011). Proteomic signatures in antibiotic research. Proteomics *11*, 3256-3268.
Wertheim, H.F., Melles, D.C., Vos, M.C., van Leeuwen, W., van Belkum, A., Verbrugh, H.A., and Nouwen, J.L. (2005). The role of nasal carriage in Staphylococcus aureus infections. The Lancet Infectious diseases *5*, 751-762.

1046 Wilson, D.N., Schluenzen, F., Harms, J.M., Starosta, A.L., Connell, S.R., and Fucini, P.
1047 (2008). The oxazolidinone antibiotics perturb the ribosomal peptidyl-transferase center and
1048 effect tRNA positioning. Proceedings of the National Academy of Sciences of the United
1049 States of America *105*, 13339-13344.
1050 Zheng, A., Panja, S., and Woodson, S.A. (2016). Arginine Patch Predicts the RNA
1051 Annealing Activity of Hfq from Gram-Negative and Gram-Positive Bacteria. J Mol Biol *428*,
1052 2259-2264.

1053

1054

SUPPLEMENTARY MATERIALS AND METHODS

SUPPLEMENTARY FIGURES

Figure S1: Northern blot analysis of *psm* expression. (A) HG001 and *rpsA*111::LtrB strains were growth in BHI medium at 37°C, cells were harvested and RNA extracted at pre- (2h), mid- (4h) and post- exponential (6h) phases. The Northern blot was performed with specific oligonucleotide complementary to *psm* mRNA. In the *Sau*S1 mutant strain, much less *psm* signal could be detected. (B) The membrane was colored using ethidium bromide to visualize the rRNAs. Quantification and normalization against total RNAs revelaed that the *psm* operon is 4.6 fold less abundant in the mutant than in the WT strain.

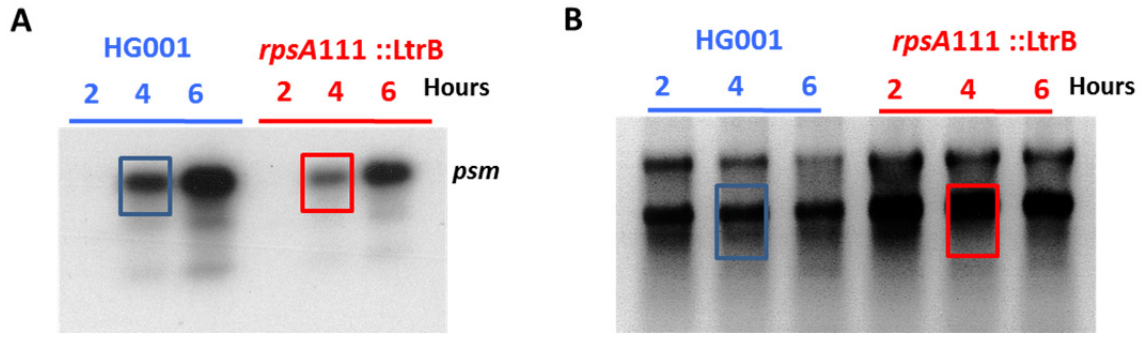

Figure S2: Secondary structure of *psm* mRNA. The secondary structure has been predicted with the Mfold server (Zuker, 2003). The *psm* operon contained four open reading frames encoding PSM1-4. The Ribosome Binding Site are shaded in light-blue. The four toe-printing signals are marked at +16 position by arrows.

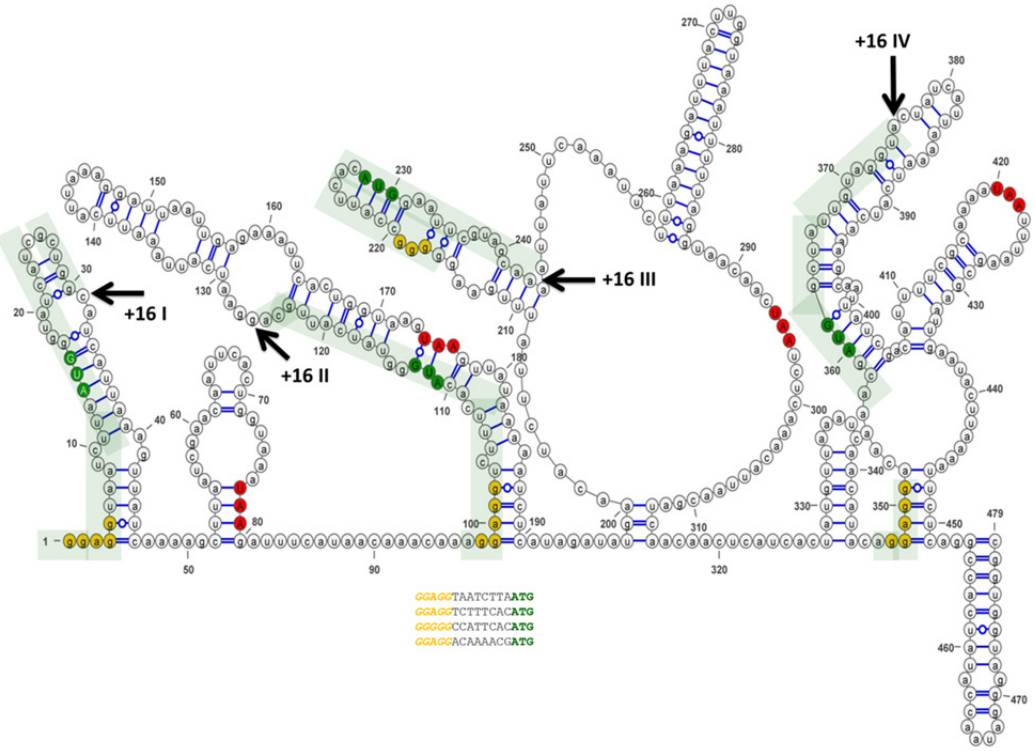

Figure S3. Toeprinting assays to monitor the effect of *Sau*S1 on the translation initiation complex formation with *spa* mRNA. (A) Effect of *Sau*S1 on the formation of initiation complex using *spa* mRNA. When present, *Sau*S1 was pre-incubated with the ribosome at a constant 1.6 molar ratio. Lane 1: incubation control of mRNA ; Lane 2: incubation control of mRNA with 30S subunits ; Lanes 3, 4, 5 and 6: formation of the initiation complex containing mRNA, increasing concentration of 30S (25, 50, 100, 200 nM) and fMet-tRNA. Lane7: incubation control of mRNA with purified *Sau*S1. Lane 8: incubation control of mRNA, 30S and *Sau*S1. Lanes 9, 10, 11 and 12: formation of initiation complex in presence of *Sau*S1 and increasing concentrations of 30S (25, 50, 100, 200 nM). Lanes U, A, G, C: sequencing ladders. The toe-printing signals at position +16 are indicated by arrows. (B) Scheme for the secondary structure of the RBS and beginning of coding region of *spa* mRNA..

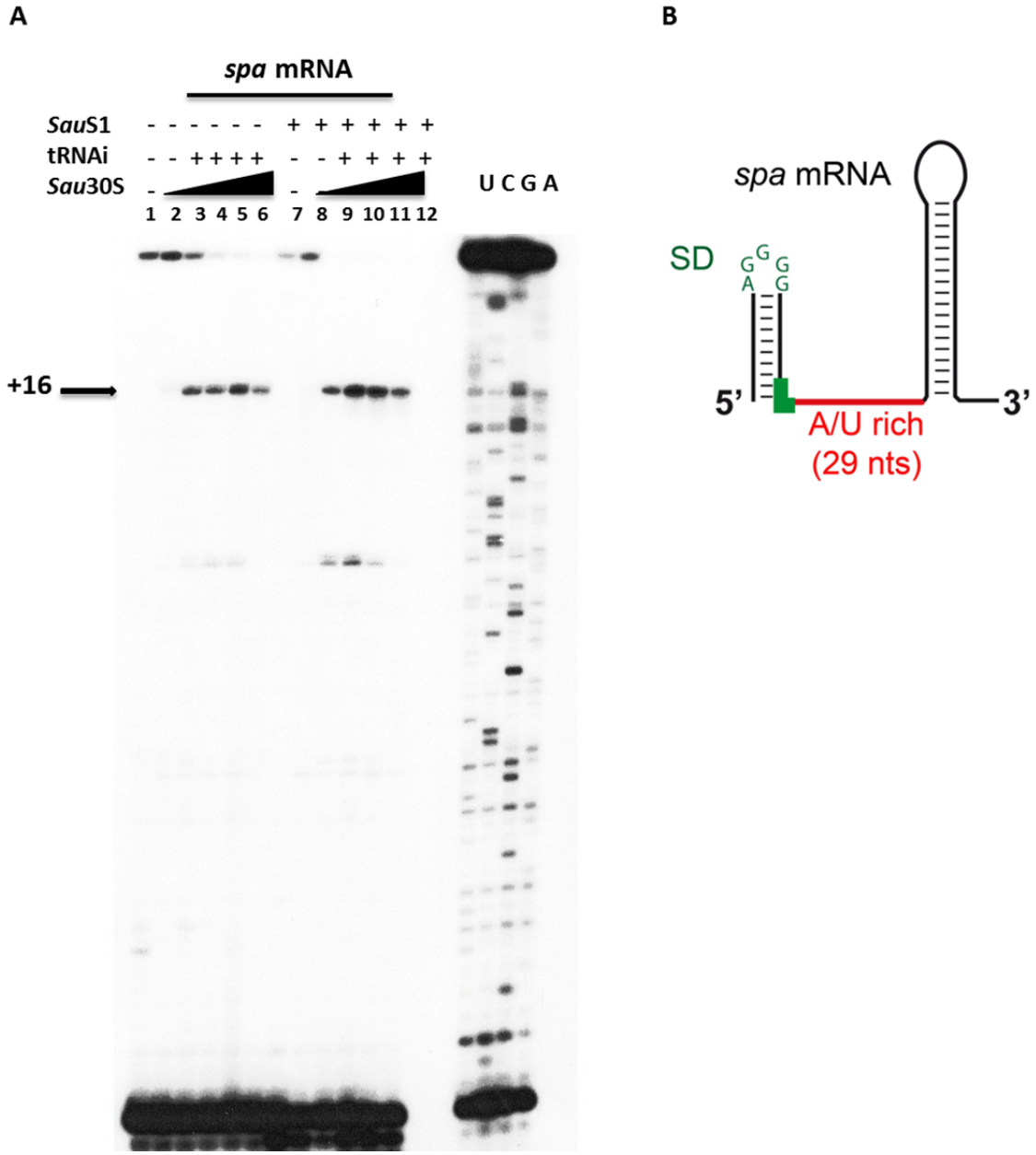

Figure S4: Predicted secondary structures for different Ribosome Binding Sites (RBS) of mRNAs encoding virulence factors. Secondary structures have been predicted with the Mfold server (Zuker, 2003). For *sspA, sspB, sbi, hld* mRNAs, RBSs show structures sequestering their SDs.

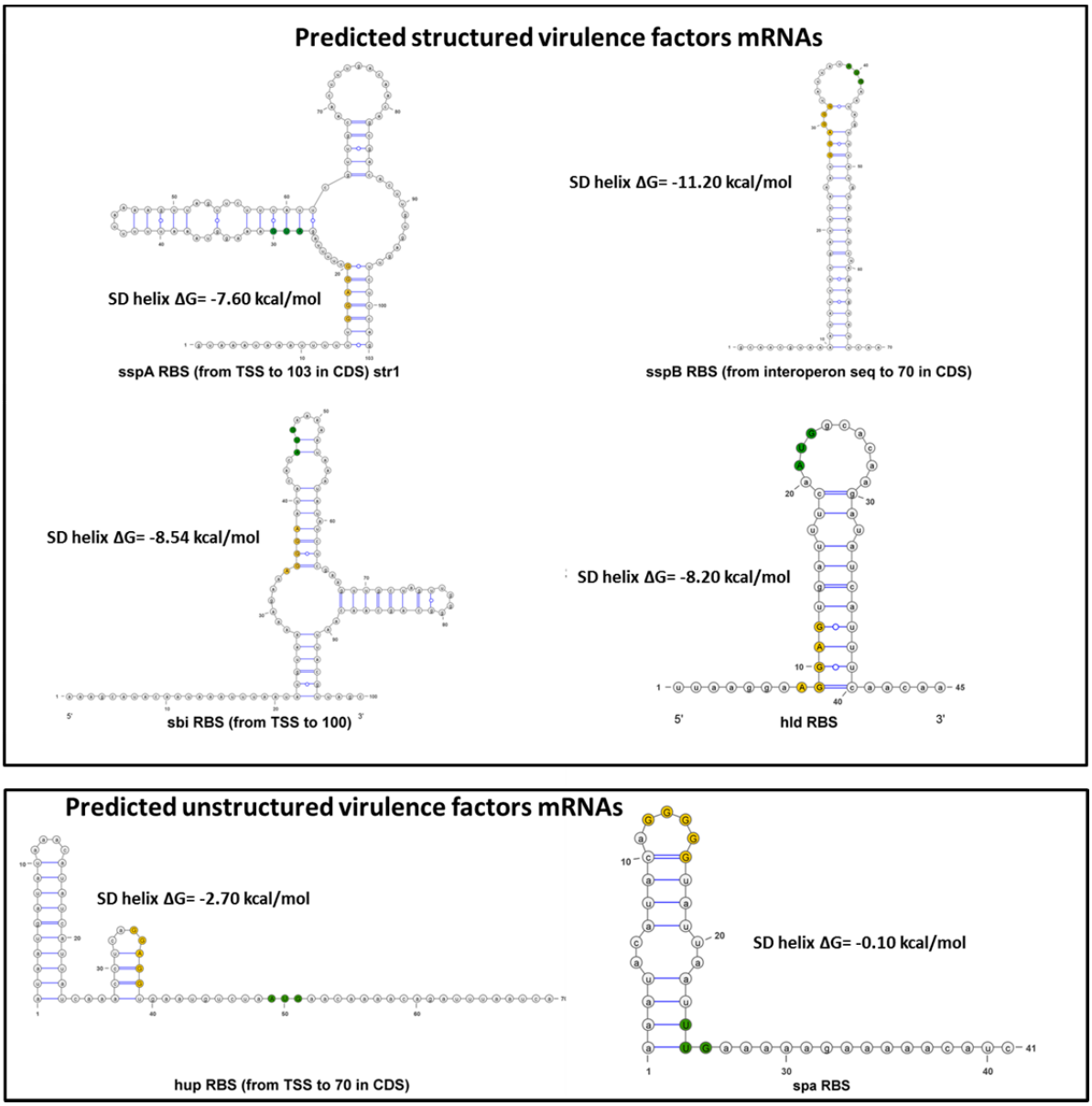

Figure S5: Toe-print with *psm* mRNA pre-incubated with *Sau*S1. Effect of *Sau*S1 on the formation of initiation ribosomal complex on *psm* mRNA. *Sau*S1-*psm* complex has been formed with increasing concentrations of *Sau*S1. Lane 1 : control incubation of mRNA ; lane 2 : mRNA in the presence of 30S ribosomal subunits; lane 3 : formation of the ribosomal initiation complex containing mRNA, the 30S subunits, and tRNAi ; lane 4: mRNA incubated with 30S and SauS1 (400 nM); lanes 5 to 8 : formation of the ribosomal initiation complex in the presence of increasing concentrations of SauS1 : 100, 200, 400 nM. Lanes U, A, G, C : sequencing ladders. The toe-printing signal at the position +16 is indicated by an arrow.

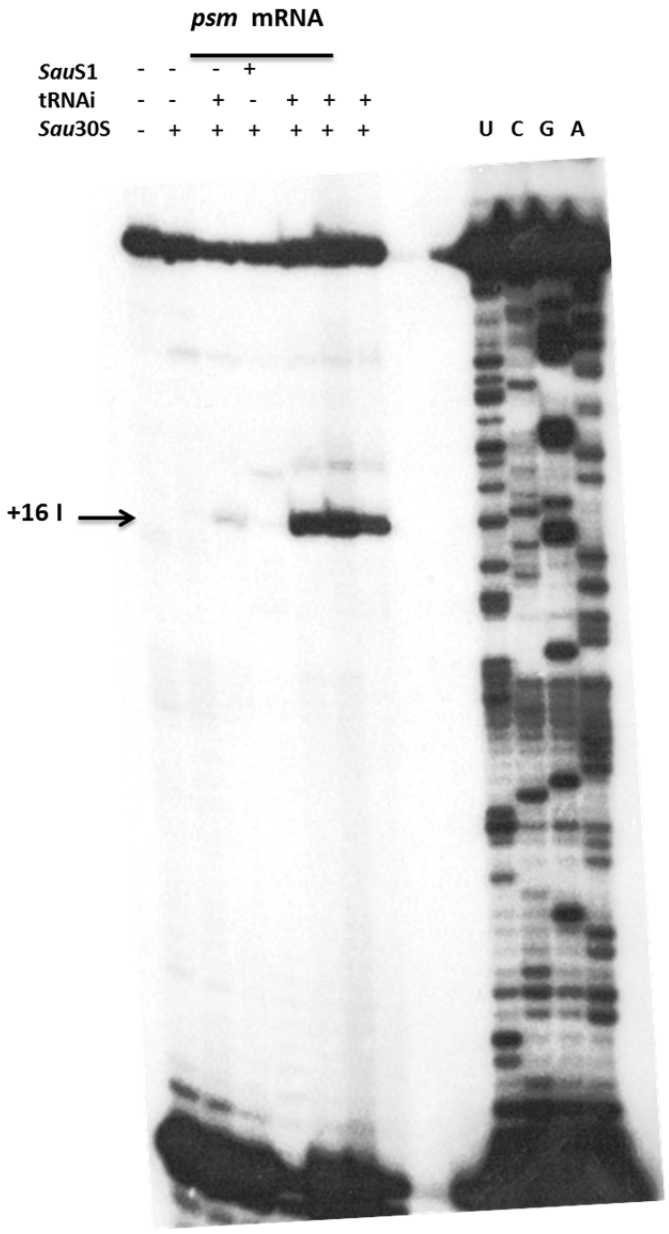

Figure S6: Domains alignment score matrix on *Eco*S1 domains to determine *Sau*S1 domain organization.

Alignment scores matrix for domain similarity

Alignments	EcoS1_d1	EcoS1_d2	EcoS1_d3	EcoS1_d4	EcoS1_d5	EcoS1_d6
SauS1_d1	Score: 58.5	Score: 47.5	Score: 94.5	Score: 72.5	Score: 79.0	Score: 80.0
SauS1_d2	Score: 37.0	Score: 129.0	Score: 49.5	Score: 40.0	Score: 51.5	Score: 73.0
SauS1_d3	Score: 32.0	Score: 32.0	Score: 193.0	Score: 142.5	Score: 139.5	Score: 108.5
SauS1_d4	Score: 32.0	Score: 57.0	Score: 147.5	Score: 153.5	Score: 116.0	Score: 110.0

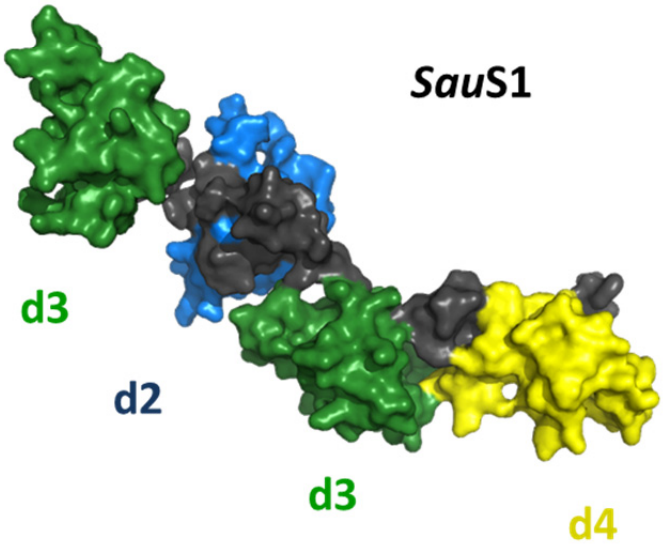

SUPPLEMENTARY TABLES

Table S1: Plasmids, strains and oligos

List of oligos		
NAME	**USAGE**	**Sequences are 5' end to 3' end**
Oligo spa	Toeprinting spa	TTT GCA GGT GTT ACG CC
Oligo PSM 3' 4 CDS	Toeprinting PSM	CTG AGA ATT TTA AGT ATT CAA TTC GC
Ologo PSM 5' only 1' CDS	Toeprinting PSM	CTT TGT TTG TTA TGA AAT CTT ATT TACC
Oligo T7 FW *psm*	PCR and in vitro transcription	ATT ACG AAT TCA ATA CGA CTC ACT ATA GGG ACT CAT AAG CAA AGG AGG TAA TCT TAA
Oligo RW *psm*	PCR and in vitro transcription	TAG AGG ATC CAG TAC TGC CAC CAT CCC TAT TGG TAT AGT GGC C
hu	Northern blot	Tomasini et al., 2017
psm	Northern Blot	CCC ATG TGA AAG ACC TCC TTT GTT TGT TAT GAA ATC TTA TTT AC
5S	Northern Blot	Tomasini A. et al., 2017
16S	Northern Blot	CTTGTGCGGGTCCCCGTC
rpsA PCR T7 FW	Northern Blot DIG	TAA TAC GAC TCA CTA TAG GGG TCT ATC AAT AGA TTT AAT
rpsA PCR RW	Northern Blot DIG	AAA GCA GTT GAA CAA GAA GAA
RNAIII	Northern Blot	Benito et al., 2000
Upstream rpsA FW	ΔrpsA	CTG ATC GGA TCC AGC AGA TGA TGC AGT GAC AT
Upstream rpsA RW	ΔrpsA	CAT CTT GTT TGC CTC CTT ATA CA
Downstream rpsA FW	ΔrpsA	TGT ATA AGG AGG CAA ACA AGA TGT TTA ATA TTT AAT AGT CAA CT
Downstream rpsA RW	ΔrpsA	GAG TCA GGA TCC GAA TAG AAA TCA TAC ACG TCT
Deletion rpsA FW	Verification ΔrpsA	CTG ATC GGA TCC AGC AGA TGA TGC AGT GAC AT
Deletion rpsA RW	Verification ΔrpsA	GAG TCA TTA TAG TTT AAG A TTTTT AAG
Complementation of ΔrpsA FW	ΔrpsA	TTT GCA TGC ATT CCA AAA ATA ATT CAT
Complementation of ΔrpsA RW	ΔrpsA	AAC TGC AGT TAT AGT TTA AGA TTT TT
SauS1 cloning His(6x) TEV FW	Cloning	AAA AAA GCA TGC GAA AAC CTG TAT TTT TCA GAT GAC TGA AGA ATT CAA TGA ATC A
SauS1 cloning RW	Cloning	GCT AAT TAA GCT TTT ATT ATA GTT TAA G
SauS1 intron mutant at position 1089 RW	Mutation rpsA	AAA AAA GCT TAT AAT TAT CCT TAA ATG ACA GAG TAG TGC GCC CAG ATA GGG TG
SauS1 intron mutant at position 1089 FW	Mutation rpsA	CAG ATT GTA CAA ATG TGG TGA TAA CAG ATA AGT CAG AGT ATC TAA CTT ACC TTT CTT TGT
SauS1 intron mutant at position 404 FW	Mutation rpsA	TGA ACG CAA GTT TCT AAT TTC GAT TTC ATT TCG ATA GAG GAA AGT GTC T
SauS1 intron mutant at position 404 RW	Mutation rpsA	AAA AAAA GCT TAT AAT TAT CCT TAA CAA TCG GCG ATG TGC GCC CAG ATA GGG TG

Strains	Description
***E. coli* strains**	
E. coli DC1OB	Used for cloning of plasmids which can be directly transformed in S. aureus cells
***S. aureus* strains**	
HG001	Derivative of 8325-4, rsbU-restored RN1, agr positive
RN6390	Mutated in rsbU that results in a phenotype resembling that of sigB mutant
Mu50	Strain with vancomycin-intermediate resistance
BCJ100	Flag-tag at the C-terminus of rpsA gene
HG001 Δ*rpsA*	Deletion of rpsA gene for allelic replacement using pMAD vector
HG001 pCN51::rpsA	ΔrpsA complemented strain
HG001 rpsA111::LtrB	rpsA insertion mutant 1
RN1 rpsA1029::LtrB	rpsA insertion mutant 2
Plasmids	
pUCN51	Shuttle vector
pUC18	Shuttle vector
pMAD	Thermosensitive origine of replication, constitutively expressed bgaB gene

Table S2: mRNAs UP regulated in Δ*rpsA*

mRNAs UP regulated in Δ*rpsA*					
id	gene	uniprotKB	product	FoldChange	pvalue
HG001_02434	narG	P09152	Respiratory nitrate reductase 1 alpha chain	7,907	6,47E-17
HG001_02438	sirB	O34632	Sirohydrochlorin ferrochelatase	5,676	3,13E-13
HG001_02437	nasD	P42435	Nitrite reductase %5BNAD%28P%29H%5D	4,982	5,93E-11
HG001_00607	sarX	Q2G0D1	HTH-type transcriptional regulator SarX	4,959	2,55E-10
HG001_01334	gpsA	P64191	Glycerol-3-phosphate dehydrogenase %5BNAD%28P%29%2B%5D	4,438	4,83E-23
HG001_01691	ribE	P16440	Riboflavin synthase	4,379	7,96E-23
HG001_01335	der_2	P64060	GTPase Der	3,102	3,97E-13
HG001_02295	-	-	hypothetical protein	3,084	5,73E-06
HG001_01152	glpD	Q7A5V7	Aerobic glycerol-3-phosphate dehydrogenase	2,994	2,33E-13
HG001_01690	ribBA	Q99TA0	Riboflavin biosynthesis protein RibBA	2,927	5,99E-11
HG001_02649	betA	P60337	Oxygen-dependent choline dehydrogenase	2,758	9,79E-09
HG001_01689	ribH	P99141	6%2C7-dimethyl-8-ribityllumazine synthase	2,573	4,93E-10
HG001_02424	narT	O33854	putative nitrate transporter NarT	2,51	0,001146
HG001_00927	ykoE	O34738	Putative HMP/thiamine permease protein YkoE	2,509	4,75E-07
HG001_01571	-	-	hypothetical protein	2,468	1,24E-05
HG001_02436	nasE	P42436	Assimilatory nitrite reductase %5BNAD%28P%29H%5D small subunit	2,462	0,001334
HG001_00780	patA_1	O25526	Peptidoglycan O-acetyltransferase	2,423	1,92E-08
HG001_01692	ribD	P17618	Riboflavin biosynthesis protein RibD	2,352	9,84E-07
HG001_01142	korB	O53181	2-oxoglutarate oxidoreductase subunit KorB	2,347	8,19E-06
HG001_02290	pbuG	O34987	Guanine/hypoxanthine permease PbuG	2,316	9,80E-07
HG001_00527	-	-	hypothetical protein	2,295	1,20E-05
HG001_01306	-	-	hypothetical protein	2,274	1,71E-08
HG001_02433	narH	P11349	Respiratory nitrate reductase 1 beta chain	2,258	0,000768
HG001_01670	-	-	Phosphotransferase enzyme family protein	2,243	1,38E-05
HG001_02112	-	-	hypothetical protein	2,235	1,42E-05
HG001_01705	-	-	hypothetical protein	2,227	0,00216
HG001_02268	rplO	P0A0F6	50S ribosomal protein L15	2,217	2,11E-05
HG001_01501	mtaB_2	P54462	Threonylcarbamoyladenosine tRNA methylthiotransferase MtaB	2,182	0,000671
HG001_02097	mazE	P0C7B4	Antitoxin MazE	2,178	1,78E-05
HG001_02520	-	-	hypothetical protein	2,176	1,07E-05
HG001_01018	-	-	hypothetical protein	2,15	0,000593
HG001_01654	acsA_1	P39062	Acetyl-coenzyme A synthetase	2,145	7,02E-08
HG001_00739	-	-	hypothetical protein	2,145	0,000662
HG001_01212	plsY	Q45064	Glycerol-3-phosphate acyltransferase	2,14	0,001328
HG001_01633	tpx	P99146	putative thiol peroxidase	2,135	2,06E-06
HG001_01082	fabG	P99093	3-oxoacyl-%5Bacyl-carrier-protein%5D reductase FabG	2,097	4,03E-06
HG001_01218	mprF	Q2G2M2	Phosphatidylglycerol lysyltransferase	2,095	3,33E-07
HG001_00741	-	-	hypothetical protein	2,095	5,84E-05
HG001_01141	korA	O53182	2-oxoglutarate oxidoreductase subunit KorA	2,084	4,87E-05
HG001_00604	sle1_2	Q7A7E0	N-acetylmuramoyl-L-alanine amidase sle1	2,066	2,63E-06
HG001_00946	pdhD	P99084	Dihydrolipoyl dehydrogenase	2,049	7,24E-06
HG001_01150	glpF	P18156	Glycerol uptake facilitator protein	2,039	9,83E-05
HG001_02048	ktrB_2	O32081	Ktr system potassium uptake protein B	2,037	0,000973
HG001_02435	nasF	P42437	Uroporphyrinogen-III C-methyltransferase	2,037	0,003747
HG001_00625	mgrA	P0C1S0	HTH-type transcriptional regulator MgrA	2,035	6,72E-06
HG001_00411	-	-	hypothetical protein	2,024	0,0012
HG001_02325	ureC	P67404	Urease subunit alpha	2,014	6,68E-06

Table S3: mRNAs DOWN regulated in Δ*rpsA*

mRNAs DOWN regulated in Δ*rpsA*					
id	gene	uniprotKB	product	FoldChange	pvalue
HG001_01336	rpsA_1	Q7A5J0	30S ribosomal protein S1	0,042	5,20E-82
HG001_00899	sspA	P0C1U8	Glutamyl endopeptidase	0,099	2,48E-55
HG001_03280	psm-4	-	4 psm peptide	0,166	2,20E-32
HG001_01548	-	-	hypothetical protein	0,224	1,24E-25
HG001_03282	psm-2	-	2 psm peptide	0,286	1,68E-16
HG001_01009	hly	Q2G1X0	Alpha-hemolysin	0,312	2,80E-07
HG001_00711	-	-	hypothetical protein	0,317	6,43E-15
HG001_02124	ssb_2	P37455	Single-stranded DNA-binding protein ssb	0,319	2,05E-10
HG001_00898	sspB	Q2FZL3	Staphopain B	0,324	1,26E-11
HG001_02245	-	A6QIG2	65 kDa membrane protein Eap	0,326	8,93E-13
HG001_00897	sspC	Q7A189	Staphostatin B	0,333	3,16E-07
HG001_01874	-	-	hypothetical protein	0,341	9,05E-05
HG001_01463	aroK_2	O67925	Shikimate kinase	0,35	2,01E-10
HG001_02058	hld	P0C1V1	Delta-hemolysin	0,35	9,33E-10
HG001_00735	-	-	hypothetical protein	0,367	5,38E-07
HG001_01006	scn_2	Q6GFB4	Staphylococcal complement inhibitor	0,386	0,000147
HG001_02456	sbi	Q2FVK5	Immunoglobulin-binding protein sbi	0,389	3,02E-06
HG001_01023	-	P11699	Antibacterial protein 3	0,39	2,92E-10
HG001_02683	-	Q2G222	N-acetylmuramoyl-L-alanine amidase domain-containing protein	0,396	2,54E-10
HG001_01877	-	-	hypothetical protein	0,409	0,001013
HG001_03283	psm-1	-	1 psm peptide	0,412	4,78E-06
HG001_00326	tcyP	P54596	L-cystine uptake protein TcyP	0,415	2,63E-08
HG001_00958	-	-	hypothetical protein	0,415	2,94E-06
HG001_02584	-	-	hypothetical protein	0,416	0,000209
HG001_02745	cspLA	P0A355	Cold shock-like protein CspLA	0,417	1,08E-06
HG001_00647	-	-	Electron transfer DM13	0,424	1,91E-06
HG001_00866	-	-	hypothetical protein	0,425	0,00016
HG001_02279	rpmC	P66173	50S ribosomal protein L29	0,426	5,55E-05
HG001_01065	-	-	TM2 domain protein	0,428	3,04E-05
HG001_00264	lip2	P10335	Lipase 2	0,431	2,00E-09
HG001_02492	pnbA	P37967	Para-nitrobenzyl esterase	0,431	5,31E-09
HG001_02454	gpmA_2	P99153	2%2C3-bisphosphoglycerate-dependent phosphoglycerate mutase	0,435	5,35E-08
HG001_01595	rplT	P66108	50S ribosomal protein L20	0,45	6,19E-06
HG001_01890	-	-	hypothetical protein	0,452	0,000418
HG001_01261	cspA_2	Q7A2R8	Cold shock protein CspA	0,453	1,57E-07
HG001_00258	sglT	P96169	Sodium/glucose cotransporter	0,453	1,03E-05
HG001_01456	-	-	hypothetical protein	0,453	0,004245
HG001_02459	hlgB	P0A077	Gamma-hemolysin component B	0,455	8,94E-05
HG001_00609	-	-	hypothetical protein	0,458	3,35E-05
HG001_01899	-	-	hypothetical protein	0,459	0,000744
HG001_02626	-	-	hypothetical protein	0,46	0,000162
HG001_01057	-	-	hypothetical protein	0,46	0,000181
HG001_01971	-	A6QIG2	65 kDa membrane protein Eap	0,462	0,000537
HG001_02001	-	-	HNH endonuclease	0,465	0,004861
HG001_02664	-	-	hypothetical protein	0,466	2,45E-05
HG001_01943	sspP	Q2G2R8	Staphopain A	0,468	0,000195
HG001_01005	fib_2	A6QG59	Fibrinogen-binding protein	0,469	0,001234
HG001_00976	rpmF	P66210	50S ribosomal protein L32	0,473	6,83E-06
HG001_02635	panD	Q2FV23	Aspartate 1-decarboxylase	0,476	0,001569
HG001_02458	hlgC	Q2FVK2	Gamma-hemolysin component C	0,478	0,000327
HG001_00415	spoVG	Q7A7B5	Putative septation protein SpoVG	0,483	2,51E-07
HG001_02678	-	-	hypothetical protein	0,491	0,000331
HG001_01897	-	-	hypothetical protein	0,491	0,003621
HG001_01884	-	-	Helix-turn-helix domain protein	0,493	0,004261

Table S4: non coding RNAs variations in Δ*rpsA*

non coding RNAs variations in ΔrpsA

tRNAs variations in Δ*rpsA*

id	product	F.C.	pvalue
HG001_00441	tRNA-Arg(acg)	0,024	1,08E-39
HG001_01760	tRNA-His(gtg)	0,025	1,74E-61
HG001_01802	tRNA-Tyr(gta)	0,037	3,23E-94
HG001_01814	tRNA-Arg(acg)	0,038	2,54E-29
HG001_01815	tRNA-Leu(taa)	0,04	1,30E-35
HG001_00440	tRNA-Leu(taa)	0,041	2,53E-29
HG001_02195	tRNA-Tyr(gta)	0,041	3,71E-88
HG001_01817	tRNA-Leu(tag)	0,042	2,60E-53
HG001_01800	tRNA-His(gtg)	0,043	4,49E-30
HG001_01809	tRNA-Ser(tga)	0,043	6,97E-31
HG001_02089	tRNA-Leu(gag)	0,044	3,99E-32
HG001_01021	tRNA-Arg(tct)	0,048	4,63E-39
HG001_02197	tRNA-Glu(ttc)	0,048	9,96E-23
HG001_01757	tRNA-Glu(ttc)	0,049	1,10E-21
HG001_02201	tRNA-Ile(gat)	0,05	1,35E-31
HG001_01813	tRNA-Pro(tgg)	0,062	4,62E-18
HG001_01818	tRNA-Lys(ttt)	0,071	3,49E-18
HG001_00442	tRNA-Pro(tgg)	0,071	5,38E-16
HG001_02193	tRNA-Lys(ttt)	0,076	1,82E-15
HG001_00020	tRNA-Glu(ttc)	0,08	2,43E-14
HG001_00438	tRNA-Lys(ttt)	0,08	3,46E-14
HG001_00385	tRNA-Ser(tga)	0,084	1,85E-18
HG001_01807	tRNA-Ser(tga)	0,09	1,28E-16
HG001_01823	tRNA-Ala(tgc)	0,093	4,79E-17
HG001_01763	tRNA-Met(cat)	0,098	6,82E-15
HG001_01806	tRNA-Met(cat)	0,104	1,44E-13
HG001_01798	tRNA-Cys(gca)	0,11	3,47E-12
HG001_02088	tRNA-Gly(tcc)	0,12	3,00E-10
HG001_01797	tRNA-Gly(tcc)	0,158	9,56E-08
HG001_01756	tRNA-Ser(gga)	0,171	3,25E-07
HG001_00437	tRNA-Thr(tgt)	0,187	2,79E-06
HG001_02194	tRNA-Gln(ttg)	0,197	5,57E-06
HG001_01810	tRNA-Met(cat)	0,197	4,53E-06
HG001_01803	tRNA-Thr(tgt)	0,232	4,02E-05
HG001_02196	tRNA-Val(tac)	0,247	9,06E-05
HG001_01799	tRNA-Gln(ttg)	0,265	0,000182
HG001_01819	tRNA-Thr(tgt)	0,285	0,000359
HG001_01804	tRNA-Phe(gaa)	0,291	0,000442
HG001_01796	tRNA-Gly(tcc)	0,298	0,000695
HG001_00436	tRNA-Val(tac)	0,304	0,000723
HG001_01808	tRNA-Asp(gtc)	0,325	0,0013
HG001_00443	tRNA-Ala(tgc)	0,341	0,002103
HG001_01805	tRNA-Asp(gtc)	0,344	0,002053
HG001_01820	tRNA-Val(tac)	0,356	0,002877
HG001_01812	tRNA-Ala(tgc)	0,364	0,003576
HG001_01762	tRNA-Asp(gtc)	0,411	0,008131
HG001_00021	tRNA-Asp(gtc)	0,416	0,008908
HG001_01761	tRNA-Phe(gaa)	0,438	0,012357
HG001_01811	tRNA-Met(cat)	0,441	0,013319
HG001_01758	tRNA-Asn(gtt)	0,445	0,016241
HG001_00874	tRNA-Asn(gtt)	0,458	0,019652
HG001_02198	tRNA-Asn(gtt)	0,469	0,022848
HG001_00873	tRNA-Ser(gct)	0,478	0,020962
HG001_01824	tRNA-Ile(gat)	0,485	0,023908
HG001_01816	tRNA-Gly(gcc)	0,523	0,042309
HG001_01795	tRNA-Gly(tcc)	0,568	0,071387
HG001_00439	tRNA-Gly(gcc)	0,576	0,070428
HG001_01801	tRNA-Trp(cca)	0,62	0,102456
HG001_00707	tRNA-Arg(ccg)	0,652	0,127072
HG001_01794	tRNA-Leu(caa)	0,655	0,131339
HG001_01759	tRNA-Gly(tcc)	0,747	0,236529
HG001_02310	tRNA-Gln(ttg)	3,493	4,00E-06

sRNAs variations in Δ*rpsA*

id	product	F.C.	pvalue
HG001_00584	RsaD	0,115	1,61E-13
HG001_01553	6S	0,143	1,77E-12
HG001_02756	RsaG	0,16	2,20E-11
HG001_02347	RsaOG	0,204	1,30E-31
HG001_01975	SprD	0,215	7,11E-09
HG001_00847	RsaE	0,234	4,80E-05
HG001_02057	RNAIII	0,363	5,71E-09
HG001_01981	rli28	0,418	0,00018
HG001_00880	rli28	0,458	0,00244
HG001_02466	RsaJ	0,558	0,10163
HG001_02470	RsaJ	0,623	0,13983
HG001_02554	fstAT	0,658	0,24125
HG001_00516	RsaA	0,676	0,09411
HG001_01652	RsaB	0,703	0,30954
HG001_01125	rliD	0,732	0,38281
HG001_02471	fstAT	0,768	0,41632
HG001_00710	RsaH	0,832	0,59711
HG001_02469	RsaJ	0,931	0,77697
HG001_01716	STnc490k	0,977	0,90181
HG001_00848	RsaF	0,989	0,96155
HG001_00569	RsaC	1,037	0,89814
HG001_02176	rli28	1,092	0,59565
HG001_01732	fstAT	1,265	0,51022

riboswitches variations in Δ*rpsA*

id	product	F.C.	pvalue
HG001_00755	SAM *metN2*	0,238	8,98E-18
HG001_01043	T-box *ileS*	0,333	3,54E-06
HG001_01345	FMN *ribU*	0,338	1,09E-13
HG001_01598	L20_leader	0,343	7,03E-05
HG001_01680	T-box *leuS*	0,414	1,81E-07
HG001_01225	T-box *trpE*	0,436	0,0012
HG001_01581	T-box *vslS*	0,555	0,01325
HG001_01462	Glycine *gcvT*	0,62	0,10996
HG001_01600	Lysine *lysP_2*	0,645	0,14845
HG001_00303	T-box *metI*	0,669	0,02351
HG001_02363	SAM *mleN_2*	0,71	0,03617
HG001_00458	T-box *cysE*	0,714	0,05277
HG001_01542	T-box *alaS*	0,728	0,28617
HG001_00986	T-box *pheS*	0,78	0,20049
HG001_01713	SAM *metK*	0,815	0,31446
HG001_01251	Lysine *lysC*	0,831	0,29448
HG001_01226	T-box *trpE*	0,874	0,68588
HG001_00013	SAM *metX*	0,894	0,64935
HG001_02122	TPP *tenA*	1,019	0,90794
HG001_00009	T-box *serS*	1,163	0,59618
HG001_01649	T-box *tyrS*	1,219	0,45625
HG001_02182	glmS	1,575	0,09555
HG001_01602	T-box *thrS*	1,813	0,03484
HG001_00469	L10_leader	1,904	0,01479
HG001_02255	L13_leader	2,137	0,00139
HG001_01556	T-box *hisS*	2,192	0,00063
HG001_01693	FMN *ribDEBAH*	2,476	4,48E-09
HG001_00330	Purine	4,508	9,44E-09
HG001_00928	TPP *ykoE*	4,66	2,94E-07

other ncRNAs variations in Δ*rpsA*

HG001_00723	tmRNA SsrA	0,971	0,81765
HG001_00389	SRP	1,538	0,00063
HG001_01304	RNaseP	5,95	5,06E-14

124 **Table S5: Differential Proteomics analysis of Δ*rpsA* and WT HG001**

Proteomics Analysis: UP in Δ*rpsA*

DelS1-enriched proteins (2 MS instruments):

				TT5600+		Q-Exactive+	
accession	gene	uniprotKB	product	p.value	Δ*rpsA* /S1	p.value	ΔrpsA/S1
HG001_01335	der_2	P64060	GTPase Der	0,00000	2,65	0,00000	2,37
HG001_02129	atpC	P63665	ATP synthase epsilon chain	0,00060	Del-S1 only	0,03239	2,08
HG001_01334	gpsA	P64191	Glycerol-3-phosphate dehydrogenase [NAD(P)+]	0,00000	9,70	0,00049	2,06
HG001_00637	glcR	P94591	HTH-type transcriptional repressor GlcR	0,08621	Del-S1 only	0,09671	Del-S1 only
HG001_00607	sarX	Q2G0D1	HTH-type transcriptional regulator SarX	0,08621	Del-S1 only	0,15060	2,86
HG001_01147	mutS_1	Q931S8	DNA mismatch repair protein MutS	0,08621	Del-S1 only	0,15750	2,00
HG001_00120	-	-	hypothetical protein	0,25670	2,00	0,15060	2,86

DelS1-enriched proteins (1 MS instrument):

				TT5600+		Q-Exactive+	
accession	gene	uniprotKB	product	p.value	Δ*rpsA* /S1	p.value	ΔrpsA/S1
HG001_00105	fcl	-	GDP-L-fucose synthase	0,00667	Del-S1 only		
HG001_00232	eccCa1	O69735	ESX-1 secretion system protein EccCa1	0,08621	Del-S1 only		
HG001_01132	phbB	P14697	Acetoacetyl-CoA reductase	0,22510	Del-S1 only		
HG001_00655	kipI_1	P60495	Kinase A inhibitor			0,00863	Del-S1 only
HG001_01415	-	-	hypothetical protein			0,01882	Del-S1 only
HG001_02379	yhaI	P64592	Inner membrane protein YhaI			0,02601	3,31
HG001_01416	srrB	Q5HFT1	Sensor protein SrrB			0,02895	4,29
HG001_00108	-	-	hypothetical protein			0,02895	4,29
HG001_01547	limB_2	Q9EUT9	Limonene 1%2C2-monooxygenase			0,04192	Del-S1 only
HG001_00576	tagH_1	Q7A713	Teichoic acids export ATP-binding protein TagH			0,04192	Del-S1 only
HG001_01351	-	-	hypothetical protein			0,04192	Del-S1 only
HG001_02421	-	-	hypothetical protein			0,04192	Del-S1 only
HG001_02447	-	-	hypothetical protein			0,04192	Del-S1 only
HG001_02474	-	-	hypothetical protein			0,04192	Del-S1 only
HG001_02114	csoR_2	O32222	Copper-sensing transcriptional repressor CsoR			0,04192	Del-S1 only
HG001_00294	ytrB_1	O34641	ABC transporter ATP-binding protein YtrB			0,04192	Del-S1 only
HG001_02106	kdpD	P21865	Sensor protein KdpD			0,04748	6,67
HG001_00170	pflA	Q7A7X5	Pyruvate formate-lyase-activating enzyme			0,07836	3,00
HG001_02387	-	-	hypothetical protein			0,07836	3,00
HG001_01063	priA	P17888	Primosomal protein N'			0,08815	3,29
HG001_01064	-	-	hypothetical protein			0,08948	5,67
HG001_02143	ywlC_2	P39153	Threonylcarbamoyl-AMP synthase			0,08948	5,67
HG001_00392	-	-	Acetyltransferase (GNAT) family protein			0,09671	Del-S1 only
HG001_00104	capD	Q9ZDJ5	UDP-glucose 4-epimerase			0,09671	Del-S1 only
HG001_02446	bdbD	O32218	Disulfide bond formation protein D precursor			0,09671	Del-S1 only
HG001_00066	ala	-	Alanine dehydrogenase			0,09671	Del-S1 only
HG001_01030	ftsL	-	Cell division protein FtsL			0,09671	Del-S1 only
HG001_00055	-	B9E972	Oleate hydratase			0,09671	Del-S1 only
HG001_02187	ebh_3	Q2FYJ6	Extracellular matrix-binding protein ebh precursor			0,09671	Del-S1 only
HG001_02392	tcaA	A6QJJ7	Membrane-associated protein TcaA			0,09671	Del-S1 only
HG001_01734	-	-	hypothetical protein			0,09671	Del-S1 only
HG001_02252	-	-	hypothetical protein			0,09671	Del-S1 only
HG001_01908	-	-	hypothetical protein			0,09671	Del-S1 only
HG001_01962	-	-	hypothetical protein			0,09671	Del-S1 only
HG001_00493	sdrD	Q2G0L4	Serine-aspartate repeat-containing protein D precursor			0,09671	Del-S1 only
HG001_01198	-	-	Cysteine-rich secretory protein family protein			0,09671	Del-S1 only
HG001_02241	adhR	O06008	HTH-type transcriptional regulator AdhR			0,09671	Del-S1 only
HG001_01150	glpF	P18156	Glycerol uptake facilitator protein			0,09671	Del-S1 only
HG001_00791	ydiI	P77781	Esterase YdiI			0,09671	Del-S1 only
HG001_00219	lytM_2	O33599	Glycyl-glycine endopeptidase LytM precursor			0,12740	2,70
HG001_01216	glcT	O33618	GlcA/glcB genes antiterminator			0,12740	2,70
HG001_01197	guaC	P60563	GMP reductase			0,12740	2,70
HG001_00954	-	-	hypothetical protein			0,15060	2,86
HG001_00451	ctsR	Q7A799	Transcriptional regulator CtsR			0,15060	2,86
HG001_02123	sceD	Q2FWF8	putative transglycosylase SceD precursor			0,16370	2,31
HG001_01669	trmB	P67500	tRNA (guanine-N(7)-)-methyltransferase			0,16730	4,33
HG001_00488	dgk	P37530	Deoxyguanosine kinase			0,16730	4,33
HG001_01316	-	Q7A5K4	hypothetical protein			0,16730	4,33
HG001_02380	-	-	Putative 3-methyladenine DNA glycosylase			0,24020	Del-S1 only

125

HG001_01769	-	-	Bacterial ABC transporter protein EcsB	0,24020	Del-S1 only
HG001_00513	yhdG_1	O07576	putative amino acid permease YhdG	0,24020	Del-S1 only
HG001_02600	dapL	A0LEA5	LL-diaminopimelate aminotransferase	0,24020	Del-S1 only
HG001_02362	mleN_2	P54571	Malate-2H(+)/Na(+)-lactate antiporter	0,24020	Del-S1 only
HG001_00684	dosC	P0AA89	Diguanylate cyclase DosC	0,24020	Del-S1 only
HG001_01066	def1	Q819U0	Peptide deformylase 1	0,24020	Del-S1 only
HG001_00424	divIC	P37471	Cell division protein DivIC	0,24020	Del-S1 only
HG001_02634	cocE	Q9L9D7	Cocaine esterase	0,24020	Del-S1 only
HG001_00256	psuG	P33025	Pseudouridine-5'-phosphate glycosidase	0,24020	Del-S1 only
HG001_00052	yxeP_1	P54955	putative hydrolase YxeP	0,24020	Del-S1 only
HG001_02116	-	-	putative hydrolase	0,24020	Del-S1 only
HG001_02157	coaW	Q6G7I0	Type II pantothenate kinase	0,24020	Del-S1 only
HG001_01625	-	Q8XIQ9	Cobalt-dependent inorganic pyrophosphatase	0,24020	Del-S1 only
HG001_01721	menE	P63526	2-succinylbenzoate--CoA ligase	0,24020	Del-S1 only
HG001_00047	-	Q2G1Q1	putative lipoprotein precursor	0,24020	Del-S1 only
HG001_01218	mprF	Q2G2M2	Phosphatidylglycerol lysyltransferase	0,24020	Del-S1 only
HG001_00305	ykuT	O34897	putative MscS family protein YkuT	0,24020	Del-S1 only
HG001_00575	tagA	Q7A714	Putative N-acetylmannosaminyltransferase	0,24020	Del-S1 only
HG001_01220	msrR	Q99Q02	Regulatory protein MsrR	0,24020	Del-S1 only
HG001_00361	-	-	hypothetical protein	0,24020	Del-S1 only
HG001_01593	-	-	hypothetical protein	0,24020	Del-S1 only
HG001_00592	-	-	hypothetical protein	0,24020	Del-S1 only
HG001_01668	ytnP	O34760	putative quorum-quenching lactonase YtnP	0,24020	Del-S1 only
HG001_01149	-	-	Glycerol-3-phosphate responsive antiterminator	0,24020	Del-S1 only
HG001_00406	rsmI	P67087	Ribosomal RNA small subunit methyltransferase I	0,24020	Del-S1 only
HG001_00706	whiA	A0QWV9	Putative sporulation transcription regulator WhiA	0,24020	Del-S1 only
HG001_02090	-	-	Protein SprT-like protein	0,24020	Del-S1 only
HG001_02560	catE_2	P54721	Catechol-2%2C3-dioxygenase	0,24020	Del-S1 only
HG001_00802	yugI_2	P80870	General stress protein 13	0,24020	Del-S1 only
HG001_01227	trpE	P20580	Anthranilate synthase component 1	0,24020	Del-S1 only
HG001_02216	iucA_2	Q47316	N(2)-citryl-N(6)-acetyl-N(6)-hydroxylysine synthase	0,24020	Del-S1 only
HG001_02075	tsaE	O05515	tRNA threonylcarbamoyladenosine biosynthesis protein TsaE	0,24020	Del-S1 only
HG001_01433	malR	P0A4T2	HTH-type transcriptional regulator MalR	0,24020	Del-S1 only
HG001_00204	lytR_1	P60611	Sensory transduction protein LytR	0,24020	Del-S1 only
HG001_01770	ecsA	P55339	ABC-type transporter ATP-binding protein EcsA	0,24020	Del-S1 only
HG001_02440	nirC	P0AC26	Nitrite transporter NirC	0,24020	Del-S1 only
HG001_01002	fib_1	A6QG59	Fibrinogen-binding protein precursor	0,24020	Del-S1 only
HG001_01289	-	Q931R7	hypothetical protein	0,24020	Del-S1 only
HG001_00827	-	A6QIG2	65 kDa membrane protein precursor	0,24020	Del-S1 only
HG001_02498	relJ	P65067	Antitoxin RelJ	0,25280	2,43
HG001_01912	-	P44886	putative acyl-CoA thioester hydrolase	0,30950	3,33
HG001_01078	recG	P64325	ATP-dependent DNA helicase RecG	0,30950	3,33
HG001_00630	phrB	P00914	Deoxyribodipyrimidine photo-lyase	0,30950	3,33
HG001_01011	-	-	hypothetical protein	0,30950	3,33
HG001_02428	nreC	Q7WZY4	Oxygen regulatory protein NreC	0,30950	3,33
HG001_02323	ureA	Q4A0J3	Urease subunit gamma	0,30950	3,33
HG001_01697	arsC2	P0DKS7	Arsenate-mycothiol transferase ArsC2	0,30950	3,33
HG001_01640	ugpQ_2	P10908	Glycerophosphoryl diester phosphodiesterase	0,56390	2,33
HG001_01341	recQ_2	P15043	ATP-dependent DNA helicase RecQ	0,56390	2,33
HG001_00806	glpQ1_1	P96236	putative glycerophosphoryl diester phosphodiesterase 1	0,56390	2,33
HG001_01190	thrB_2	Q8Y4A6	Homoserine kinase	0,56390	2,33
HG001_02521	-	Q99RE8	putative lipoprotein precursor	0,56390	2,33
HG001_00026	yycJ	C0SP91	Putative metallo-hydrolase YycJ	0,56390	2,33
HG001_01831	-	Q99T13	Putative multidrug export ATP-binding/permease protein	0,56390	2,33
HG001_01599	lysP_2	P25737	Lysine-specific permease	0,56390	2,33
HG001_02404	lctP_2	P55910	L-lactate permease	0,56390	2,33
HG001_00769	-	-	hypothetical protein	0,56390	2,33
HG001_01145	-	-	hypothetical protein	0,56390	2,33
HG001_00724	-	-	hypothetical protein	0,56390	2,33
HG001_00402	-	-	hypothetical protein	0,56390	2,33
HG001_02597	copA	Q2FV64	Copper-exporting P-type ATPase A	0,56390	2,33
HG001_01275	arlR	P0C000	Response regulator ArlR	0,56390	2,33

HG001_02338	ssaA2_3	Q7A423	Staphylococcal secretory antigen ssaA2 precursor	0,56390	2,33
HG001_02429	nreB	Q7WZY5	Oxygen sensor histidine kinase NreB	0,56390	2,33
HG001_02423	-	P80485	Acid shock protein	0,56390	2,33
HG001_00036	dus_2	P67717	putative tRNA-dihydrouridine synthase	0,56390	2,33
HG001_00041	-	-	hypothetical protein	0,56390	2,33
HG001_00555	pip	P46541	Proline iminopeptidase	0,56390	2,33
HG001_00319	gpmA_1	Q1MMY4	2%2C3-bisphosphoglycerate-dependent phosphoglycerate mutase	0,24850	2,08
HG001_02125	-	-	hypothetical protein	0,24850	2,08
HG001_02732	yflS	O34726	Putative malate transporter YflS	0,31760	2,00

DelS1-enriched proteins (same global trend):

				TT5600+		Q-Exactive+	
accession	gene	uniprotKB	product	p.value	Δ*rpsA* /S1	p.value	ΔrpsA/S1
HG001_00783	nfuA	P63020	Fe/S biogenesis protein NfuA	0,00060	Del-S1 only	0,41020	1,59
HG001_01439	-	-	hypothetical protein	0,00296	Del-S1 only	0,51770	1,26
HG001_00865	murE_1	Q2FZP6	UDP-N-acetylmuramoyl-L-alanyl-D-glutamate--L-lysine ligase	0,00003	Del-S1 only	0,45480	1,20
HG001_01237	-	-	hypothetical protein	0,00060	Del-S1 only	0,98660	1,00
HG001_01199	lexA_1	P31080	LexA repressor	0,00296	Del-S1 only	0,84250	0,94
HG001_01140	-	-	Calcineurin-like phosphoesterase	0,00012	Del-S1 only	0,72340	0,90
HG001_02210	-	-	hypothetical protein	0,00000	2,08	0,00000	1,68
HG001_01075	rpmB	P23374	50S ribosomal protein L28	0,00195	2,73	0,51230	1,14
HG001_02658	cysJ	O32214	Sulfite reductase [NADPH] flavoprotein alpha-component	0,00031	5,15	0,91510	1,04
HG001_02179	ywpJ_2	P94592	Putative phosphatase YwpJ	0,00323	4,70	0,60280	0,88
HG001_02537	gtaB	Q7A3J9	UTP--glucose-1-phosphate uridylyltransferase	0,00323	4,70	0,63810	0,88
HG001_01457	lipM	P54511	Octanoyltransferase LipM	0,00667	Del-S1 only	0,23040	1,27
HG001_02519	-	-	hypothetical protein	0,00667	Del-S1 only	0,80640	1,17
HG001_01946	-	-	hypothetical protein	0,00667	Del-S1 only	0,98610	1,00
HG001_01552	tcdA	Q46927	tRNA threonylcarbamoyladenosine dehydratase	0,00667	Del-S1 only	0,98910	1,00
HG001_01444	recN	P05824	DNA repair protein RecN	0,00667	Del-S1 only	0,53960	0,84
HG001_00975	-	-	hypothetical protein	0,01525	Del-S1 only	0,36860	1,77
HG001_01284	msrA2	P0A086	Peptide methionine sulfoxide reductase MsrA 2	0,01525	Del-S1 only	0,48320	1,70
HG001_02325	ureC	P67404	Urease subunit alpha	0,01525	Del-S1 only	0,25690	1,39
HG001_01213	parE	P66939	DNA topoisomerase 4 subunit B	0,01525	Del-S1 only	0,69860	1,12
HG001_00543	-	-	YwhD family protein	0,01525	Del-S1 only	0,83010	1,10
HG001_00453	-	P65205	Putative ATP:guanido phosphotransferase	0,01525	Del-S1 only	0,48110	0,73
HG001_01071	prkC	A6QGC0	Serine/threonine-protein kinase PrkC	0,03561	Del-S1 only	0,50490	1,26
HG001_00640	nagA	O34450	N-acetylglucosamine-6-phosphate deacetylase	0,03561	Del-S1 only	0,70910	0,88
HG001_01565	queA	P65951	S-adenosylmethionine:tRNA ribosyltransferase-isomerase	0,03561	Del-S1 only	0,77190	0,87
HG001_00375	metQ_1	P31728	putative D-methionine-binding lipoprotein MetQ precursor	0,08621	Del-S1 only	0,41020	1,59
HG001_01561	recJ	P21893	Single-stranded-DNA-specific exonuclease RecJ	0,08621	Del-S1 only	0,74640	1,31
HG001_01094	rbgA	O31743	Ribosome biogenesis GTPase A	0,08621	Del-S1 only	0,76830	1,11
HG001_00317	-	-	hypothetical protein	0,08621	Del-S1 only	0,86720	1,06
HG001_01632	-	-	N-6 DNA Methylase	0,08621	Del-S1 only	0,88170	1,05
HG001_02372	lyrA	Q7A3Z2	Lysostaphin resistance protein A	0,08621	Del-S1 only	0,99450	1,00
HG001_01280	-	Q7A5M9	putative CtpA-like serine protease	0,08621	Del-S1 only	0,82810	0,93
HG001_00926	ykoD_1	O34362	Putative HMP/thiamine import ATP-binding protein YkoD	0,08621	Del-S1 only	0,62670	0,82
HG001_00211	rbsK	P0A9J6	Ribokinase	0,08621	Del-S1 only	0,29300	0,70
HG001_02736	nhoA	Q00267	N-hydroxyarylamine O-acetyltransferase	0,22510	Del-S1 only	0,41450	1,86
HG001_01788	trmL	P0AGJ7	tRNA (cytidine(34)-2'-O)-methyltransferase	0,22510	Del-S1 only	0,25470	1,74
HG001_00472	rsmC	P39406	Ribosomal RNA small subunit methyltransferase C	0,22510	Del-S1 only	0,41020	1,59
HG001_00520	galK_1	-	Galactokinase	0,22510	Del-S1 only	0,69530	1,16
HG001_01827	ghrB_2	P37666	Glyoxylate/hydroxypyruvate reductase B	0,22510	Del-S1 only	0,98720	1,00
HG001_01104	hslV	P65797	ATP-dependent protease subunit HslV	0,22510	Del-S1 only	0,99610	1,00
HG001_02449	tcyC_2	P39456	L-cystine import ATP-binding protein TcyC	0,22510	Del-S1 only	0,82810	0,93
HG001_01300	der_1	-	GTPase Der	0,22510	Del-S1 only	0,84640	0,93
HG001_01641	-	-	OsmC-like protein	0,22510	Del-S1 only	0,82200	0,93
HG001_02629	pyrD	P0A7E1	Dihydroorotate dehydrogenase (quinone)	0,22510	Del-S1 only	0,70910	0,88

HG001_01144	miaB	Q7A5W3	(Dimethylallyl)adenosine tRNA methylthiotransferase MiaB	0,22510	Del-S1 only	0,57660	0,82
HG001_02226	-	P99173	Zinc-type alcohol dehydrogenase-like protein	0,22510	Del-S1 only	0,33100	0,74
HG001_02649	betA	P60337	Oxygen-dependent choline dehydrogenase	0,22510	Del-S1 only	0,64810	0,70
HG001_02499	yehR	P33354	putative lipoprotein YehR precursor	0,22510	Del-S1 only	0,27880	0,68
HG001_01343	-	P10245	Ferredoxin	0,22510	Del-S1 only	0,51870	0,65
HG001_00433	folK	P43777	2-amino-4-hydroxy-6-hydroxymethyldihydropteridine pyrophosphokinase	0,22510	Del-S1 only	0,47120	0,59
HG001_01606	gapA2	P99067	Glyceraldehyde-3-phosphate dehydrogenase 2	0,00663	2,13	0,16050	1,32
HG001_00539	yhdN_1	P80874	General stress protein 69	0,01041	4,00	0,58980	1,23
HG001_01915	ptpA	P0C5D2	Low molecular weight protein-tyrosine-phosphatase PtpA	0,01584	2,08	0,42150	0,78
HG001_01123	ribF	P0AG40	Riboflavin biosynthesis protein RibF	0,03224	3,30	0,98070	1,00
HG001_01050	pyrP	P39766	Uracil permease	0,03607	6,67	0,69830	0,77
HG001_01129	phnF	P16684	putative transcriptional regulator PhnF	0,03647	3,86	0,83010	1,10
HG001_01666	pepA_2	Q48677	Glutamyl aminopeptidase	0,04946	2,00	0,66670	0,92
HG001_01331	ubiE	P67062	Demethylmenaquinone methyltransferase	0,07097	2,15	0,55140	0,80
HG001_00619	yvdD	O06986	LOG family protein YvdD	0,07113	5,67	0,52230	0,82
HG001_02518	-	Q99RF5	putative oxidoreductase	0,07437	2,54	0,70360	0,92
HG001_02371	hutG	P99158	Formimidoylglutamase	0,08317	2,04	0,63040	1,13
HG001_01115	polC_1	P63982	DNA polymerase III PolC-type	0,11810	2,86	0,85860	0,96
HG001_00291	-	-	hypothetical protein	0,13910	4,33	0,71170	1,30
HG001_01646	plsC	O07584	1-acyl-sn-glycerol-3-phosphate acyltransferase	0,13910	4,33	0,98980	1,00
HG001_01485	sigA	P0A0I8	RNA polymerase sigma factor SigA	0,15750	2,30	0,97530	1,00
HG001_00854	ppnK	P65777	putative inorganic polyphosphate/ATP-NAD kinase	0,19030	2,08	0,30750	0,66
HG001_02598	copZ	Q7A3E5	Copper chaperone CopZ	0,51260	2,33	0,35120	1,61
HG001_01321	-	-	Putative neutral zinc metallopeptidase	0,51260	2,33	0,85490	1,08
HG001_02146	tdk	P65231	Thymidine kinase	0,78870	0,77	0,01676	4,00
HG001_01432	malL	P29094	Oligo-1%2C6-glucosidase	0,55480	1,14	0,10580	2,54
HG001_00927	ykoE	O34738	Putative HMP/thiamine permease protein YkoE	0,72230	0,70	0,25280	2,43
HG001_01130	-	-	Peptidase M16 inactive domain protein	0,83510	0,76	0,15750	2,00

132

133

134

135

Table S6: Differential Proteomics analysis of Δ*rpsA* and WT HG001

Proteomics Analysis: DOWN in Δ*rpsA*

S1-enriched proteins (2 MS instruments):

				TT5600+		Q-Exactive+	
accession	gene	uniprotKB	product	p.value	ΔrpsA /S1	p.value	ΔrpsA/S1
HG001_01336	rpsA_1	Q7A5J0	30S ribosomal protein S1	0,00000	S1 only	0,00000	S1 only
HG001_02674	arcA	P63554	Arginine deiminase	0,00000	S1 only	0,00004	S1 only
HG001_02245	-	A6QIG2	65 kDa membrane protein precursor Eap	0,00061	S1 only	0,00009	S1 only
HG001_00423	hslR	P0ACG8	Heat shock protein 15	0,00252	S1 only	0,04840	0,26
HG001_02673	arcB	P65602	Ornithine carbamoyltransferase%2C catabolic	0,00252	S1 only	0,02019	0,40
HG001_00175	fadN	O32178	putative 3-hydroxyacyl-CoA dehydrogenase	0,00000	0,11	0,00104	0,50
HG001_02492	pnbA	P37967	Para-nitrobenzyl esterase	0,00515	S1 only	0,14530	0,35
HG001_00177	lcfB	O07610	Long-chain-fatty-acid--CoA ligase	0,02237	S1 only	0,00153	0,43
HG001_01918	vraR	Q7A4R9	Response regulator protein VraR	0,10320	0,43	0,02070	0,43
HG001_02514	ahpD	-	Alkyl hydroperoxide reductase AhpD	0,34660	0,30	0,03668	0,40
HG001_02045	dapE	Q99SN6	putative succinyl-diaminopimelate desuccinylase	0,05977	0,33	0,06735	0,43
HG001_00016	nrnA_1	Q5SM25	Bifunctional oligoribonuclease and PAP phosphatase NrnA	0,10630	S1 only	0,14530	0,35
HG001_02159	-	-	hypothetical protein	0,19430	0,23	0,14920	0,50

S1-enriched proteins (1 MS instrument):

				TT5600+		Q-Exactive+	
accession	gene	uniprotKB	product	p.value	ΔrpsA /S1	p.value	ΔrpsA/S1
HG001_00398	speA	P21885	Arginine decarboxylase	0,01066	S1 only		
HG001_00027	yfkN_1	O34313	Trifunctional nucleotide phosphoesterase protein YfkN precursor	0,10630	S1 only		
HG001_02685	-	-	hypothetical protein	0,25340	S1 only		
HG001_01939	pcrA	Q53727	ATP-dependent DNA helicase PcrA			0,00004	S1 only
HG001_02544	ywaC	P39583	GTP pyrophosphokinase YwaC			0,00001	0,10
HG001_00277	slyA_1	-	Transcriptional regulator SlyA			0,00084	S1 only
HG001_00636	ybaK	P0AAR3	Cys-tRNA{Pro}/Cys-tRNA{Cys} deacylase YbaK			0,00179	S1 only
HG001_00140	-	-	hypothetical protein			0,00384	S1 only
HG001_01192	-	-	hypothetical protein			0,00831	S1 only
HG001_02103	kdpC	P94606	Potassium-transporting ATPase C chain			0,01824	S1 only
HG001_00949	potA	Q7A679	Spermidine/putrescine import ATP-binding protein PotA			0,01824	S1 only
HG001_02436	nasE	P42436	Assimilatory nitrite reductase [NAD{P}H] small subunit			0,01824	S1 only
HG001_01466	-	-	hypothetical protein			0,01824	S1 only
HG001_01557	lytC	Q02114	N-acetylmuramoyl-L-alanine amidase LytC precursor			0,04092	S1 only
HG001_01974	scn_3	Q2FWV6	Staphylococcal complement inhibitor precursor			0,04092	S1 only
HG001_02671	arcC2	P99069	Carbamate kinase 2			0,04092	S1 only
HG001_01723	yokF	O32001	SPBc2 prophage-derived endonuclease YokF precursor			0,04092	S1 only
HG001_02694	-	-	Flavin reductase like domain protein			0,04092	S1 only
HG001_02558	mhqR	O31672	HTH-type transcriptional regulator MhqR			0,04092	S1 only
HG001_00141	murQ	Q45582	N-acetylmuramic acid 6-phosphate etherase			0,09507	S1 only
HG001_00793	mnhG1	P60698	Na(+)/H(+) antiporter subunit G1			0,09507	S1 only
HG001_00127	-	P33160	Formate dehydrogenase			0,09507	S1 only
HG001_01670	-	-	Phosphotransferase enzyme family protein			0,09507	S1 only
HG001_02258	ecfA2	Q7A471	Energy-coupling factor transporter ATP-binding protein EcfA2			0,09507	S1 only
HG001_01642	-	P16421	Soluble hydrogenase 42 kDa subunit			0,09507	S1 only
HG001_00048	-	Q2G1Q0	putative lipoprotein precursor			0,09507	S1 only
HG001_02305	mobA	P65405	putative molybdenum cofactor guanylyltransferase			0,09507	S1 only
HG001_00262	nanE	P65517	Putative N-acetylmannosamine-6-phosphate 2-epimerase			0,09507	S1 only
HG001_00094	yfkN_2	O34313	Trifunctional nucleotide phosphoesterase protein YfkN precursor			0,09507	S1 only
HG001_00102	ywqE_1	P96717	Tyrosine-protein phosphatase YwqE			0,09507	S1 only
HG001_00403	-	Q99WB7	Initiation-control protein YabA			0,09507	S1 only
HG001_00968	-	-	hypothetical protein			0,09507	S1 only
HG001_01664	-	-	hypothetical protein			0,09507	S1 only
HG001_00126	-	-	hypothetical protein			0,09507	S1 only
HG001_01832	-	-	hypothetical protein			0,09507	S1 only

HG001_00378	nudC	-	NADH pyrophosphatase	0,09507	S1 only
HG001_02079	ilvC	P37253	Ketol-acid reductoisomerase	0,09507	S1 only
HG001_02583	ssaA2_4	Q7A423	Staphylococcal secretory antigen ssaA2 precursor	0,09507	S1 only
HG001_01614	citZ	P39120	Citrate synthase 2	0,09507	S1 only
HG001_02150	yodB	O34844	HTH-type transcriptional regulator YodB	0,09507	S1 only
HG001_01968	ytrA	O34712	HTH-type transcriptional repressor YtrA PmtR	0,09507	S1 only
HG001_01239	oppD_3	P24136	Oligopeptide transport ATP-binding protein OppD	0,09507	S1 only
HG001_02661	yxdL	P42423	ABC transporter ATP-binding protein YxdL	0,09507	S1 only
HG001_01494	ybeY	O67367	Endoribonuclease YbeY	0,09507	S1 only
HG001_00494	tagE_1	P13484	putative poly(glycerol-phosphate) alpha-glucosyltransferase	0,09507	S1 only
HG001_01944	-	-	Staphostatin A	0,23790	S1 only
HG001_00178	ydiF	Q8X5X6	Acetate CoA-transferase YdiF	0,23790	S1 only
HG001_01520	aroE	Q5HNV1	Shikimate dehydrogenase	0,23790	S1 only
HG001_01643	serA	P0A544	D-3-phosphoglycerate dehydrogenase	0,23790	S1 only
HG001_02614	-	-	Glyoxalase-like domain protein	0,23790	S1 only
HG001_01133	-	-	ACT domain protein	0,23790	S1 only
HG001_01318	cca	Q7SIB1	CCA-adding enzyme	0,23790	S1 only
HG001_01079	fapR	O34835	Transcription factor FapR	0,23790	S1 only
HG001_01964	-	-	ABC-2 family transporter protein PmtD	0,23790	S1 only
HG001_01782	liaS	O32198	Sensor histidine kinase LiaS	0,23790	S1 only
HG001_00163	-	-	Xylose isomerase-like TIM barrel	0,23790	S1 only
HG001_01153	-	-	lysophospholipase L2	0,23790	S1 only
HG001_00259	nanA	Q2G160	N-acetylneuraminate lyase	0,23790	S1 only
HG001_00299	metE	P65342	5-methyltetrahydropteroyltriglutamate--homocysteine methyltransferase	0,23790	S1 only
HG001_00282	luxA	P07740	Alkanal monooxygenase alpha chain	0,23790	S1 only
HG001_01949	nos	P0A004	Nitric oxide synthase oxygenase	0,23790	S1 only
HG001_00952	potD	P0AFK9	Spermidine/putrescine-binding periplasmic protein precursor	0,23790	S1 only
HG001_02236	lacR	P67744	Lactose phosphotransferase system repressor	0,23790	S1 only
HG001_01486	dnaG	P63964	DNA primase	0,23790	S1 only
HG001_01473	gluP	P54493	Rhomboid protease GluP	0,23790	S1 only
HG001_01023	-	P11699	Antibacterial protein 3	0,23790	S1 only
HG001_01919	vraS	Q99SZ7	Sensor protein VraS	0,23790	S1 only
HG001_02228	-	-	hypothetical protein	0,23790	S1 only
HG001_01837	-	-	hypothetical protein	0,23790	S1 only
HG001_00075	-	-	hypothetical protein	0,23790	S1 only
HG001_00223	-	-	hypothetical protein	0,23790	S1 only
HG001_00651	queC	O31675	7-cyano-7-deazaguanine synthase	0,23790	S1 only
HG001_01967	ytrB_2	O34641	ABC transporter ATP-binding protein YtrB PmtA	0,23790	S1 only
HG001_00336	-	-	PemK-like protein	0,23790	S1 only
HG001_00129	grsB	P0C064	Gramicidin S synthase 2	0,00221	0,44
HG001_02693	sraP	Q2FUW1	Serine-rich adhesin for platelets precursor	0,00251	0,39
HG001_00142	-	Q7A804	PTS system EIIBC component	0,01570	0,37
HG001_02607	oatA_2	Q7A3D6	O-acetyltransferase OatA	0,02422	0,30
HG001_01009	hly	Q2G1X0	Alpha-hemolysin precursor	0,02739	0,23
HG001_00898	sspB	Q2FZL3	Staphopain B precursor	0,03388	0,36
HG001_00463	-	-	YacP-like NYN domain protein	0,04484	0,30
HG001_02691	-	-	hypothetical protein	0,04484	0,30
HG001_00579	tagX	Q7A711	Putative glycosyltransferase TagX	0,04840	0,26
HG001_01551	rarA	P0AAZ4	Replication-associated recombination protein A	0,06735	0,43
HG001_02442	-	-	hypothetical protein	0,08449	0,30
HG001_01118	-	-	hypothetical protein	0,08449	0,30
HG001_00368	est_1	Q06174	Carboxylesterase	0,08449	0,30
HG001_02405	-	-	CDP-Glycerol:Poly(glycerophosphate) glycerophosphotransferase	0,08649	0,18
HG001_01590	engB	P64071	putative GTP-binding protein EngB	0,08649	0,18
HG001_01860	-	-	Phage major tail protein 2	0,08649	0,18
HG001_00326	tcyP	P54596	L-cystine uptake protein TcyP	0,10110	0,47
HG001_00650	queD	O31676	6-carboxy-5%2C6%2C7%2C8-tetrahydropterin synthase	0,12190	0,37
HG001_00161	ycjS_1	P77503	putative oxidoreductase YcjS	0,14530	0,35
HG001_01724	-	-	Telomeric repeat-binding factor 2	0,14530	0,35
HG001_02592	ydfJ	P96687	Membrane protein YdfJ	0,15650	0,43
HG001_00594	aes	Q8ZRA1	Acetyl esterase	0,16280	0,23

HG001_01943	sspP	Q2G2R8	Staphopain A precursor	0,19580	0,43
HG001_00542	-	-	HD domain protein	0,19580	0,43
HG001_01608	mutM	O50606	Formamidopyrimidine-DNA glycosylase	0,19580	0,43
HG001_02507	nikA	P33590	Nickel-binding periplasmic protein precursor	0,19580	0,43
HG001_00044	recD	-	RecBCD enzyme subunit RecD	0,24550	0,41
HG001_01764	ydeN	P96671	Putative hydrolase YdeN	0,24550	0,41
HG001_00179	-	-	hypothetical protein	0,24550	0,41
HG001_01488	ccpN	O34994	Transcriptional repressor CcpN	0,24550	0,41
HG001_00024	yycH	Q794W0	Two-component system YycF/YycG regulatory protein YycH	0,24550	0,41
HG001_00298	kynB	-	Kynurenine formamidase	0,30320	0,30
HG001_00412	ispE	P65178	4-diphosphocytidyl-2-C-methyl-D-erythritol kinase	0,30320	0,30
HG001_00904	yjcF	O31628	putative N-acetyltransferase YjcF	0,30320	0,30
HG001_00742	pspB	D3DFP8	Putative phosphoserine phosphatase 2	0,30320	0,30
HG001_01916	-	-	hypothetical protein	0,30320	0,30
HG001_01605	nrdR	P0A8D0	Transcriptional repressor NrdR	0,30320	0,30
HG001_00028	rlmH	P0C1V0	Ribosomal RNA large subunit methyltransferase H	0,30320	0,30
HG001_02173	czrA	O31844	HTH-type transcriptional repressor CzrA	0,30320	0,30
HG001_00656	kipA_1	Q7WY77	KipI antagonist	0,23900	0,48
HG001_00008	hutH	P64416	Histidine ammonia-lyase	0,30780	0,50
HG001_02601	crtN	Q7A3E2	Dehydrosqualene desaturase	0,30780	0,50
HG001_02581	cynR_2	P27111	HTH-type transcriptional regulator CynR	0,30780	0,50
HG001_00973	coaD	P63820	Phosphopantetheine adenylyltransferase	0,55600	0,43
HG001_00787	erpA	P45344	Iron-sulfur cluster insertion protein ErpA	0,55600	0,43
HG001_01330	hepT	P31114	Heptaprenyl diphosphate synthase component 2	0,55600	0,43
HG001_00712	cggR	O32253	Central glycolytic genes regulator	0,55600	0,43
HG001_00730	ssp	A6QF98	Extracellular matrix protein-binding protein emp precursor	0,55600	0,43
HG001_00363	yciC_1	P94400	Putative metal chaperone YciC	0,55600	0,43
HG001_02185	mtlF	P17876	Mannitol-specific phosphotransferase enzyme IIA component	0,55600	0,43
HG001_00100	cap8A_1	P72367	Capsular polysaccharide type 8 biosynthesis protein cap8A	0,55600	0,43
HG001_01309	-	-	hypothetical protein	0,55600	0,43
HG001_01302	-	-	hypothetical protein	0,55600	0,43
HG001_00037	-	-	hypothetical protein	0,55600	0,43
HG001_02300	-	-	hypothetical protein	0,55600	0,43
HG001_00819	-	-	hypothetical protein	0,55600	0,43
HG001_00511	-	-	hypothetical protein	0,55600	0,43
HG001_00029	-	-	hypothetical protein	0,55600	0,43
HG001_00247	-	-	hypothetical protein	0,55600	0,43
HG001_00492	sdrC	Q7A781	Serine-aspartate repeat-containing protein C precursor	0,55600	0,43
HG001_00285	ydaF	P96579	Putative ribosomal N-acetyltransferase YdaF	0,55600	0,43
HG001_02575	-	-	Thioredoxin	0,55600	0,43
HG001_01911	queE_2	-	7-carboxy-7-deazaguanine synthase	0,55600	0,43

S1-enriched proteins (same global trend):

				TT5600+		Q-Exactive+	
accession	gene	uniprotKB	product	p.value	ΔrpsA /S1	p.value	ΔrpsA/S1
HG001_00118	aldA	Q7A825	Putative aldehyde dehydrogenase AldA	0,00124	S1 only	0,08007	0,57
HG001_01498	-	-	hypothetical protein	0,00015	S1 only	0,75420	0,85
HG001_00501	hxlB	P42404	3-hexulose-6-phosphate isomerase	0,00002	S1 only	0,98910	1,00
HG001_00449	pdxT	Q7A7A1	Glutamine amidotransferase subunit PdxT	0,00061	S1 only	0,25210	0,69
HG001_01496	-	-	hypothetical protein	0,00061	S1 only	0,31900	0,73
HG001_01332	-	-	Heptaprenyl diphosphate synthase (HEPPP synthase) subunit 1	0,00252	S1 only	0,60700	0,77
HG001_01662	sftA	C0SP86	DNA translocase SftA	0,00252	S1 only	0,51090	0,86
HG001_00758	metQ_2	O32167	Methionine-binding lipoprotein MetQ precursor	0,00252	S1 only	0,86930	0,95
HG001_00264	lip2	P10335	Lipase 2 precursor	0,00000	0,25	0,00448	0,71
HG001_02315	modA	P45323	Molybdate-binding periplasmic protein precursor	0,00001	0,11	0,07118	0,70
HG001_00924	purD	P65896	Phosphoribosylamine--glycine ligase	0,00004	0,38	0,00286	0,61
HG001_00789	pepA_1	O86436	Cytosol aminopeptidase	0,00006	0,25	0,21480	0,76

HG001_02298	femX	Q2FVZ4	Lipid II:glycine glycyltransferase	0,00063	0,16	0,13970	0,77
HG001_00139	ptsG_1	Q7A807	PTS system glucose-specific EIICBA component	0,00148	0,26	0,63630	0,91
HG001_02330	sarR	Q7A425	HTH-type transcriptional regulator SarR	0,00149	0,35	0,33180	0,78
HG001_00582	bmrA	O06967	Multidrug resistance ABC transporter ATP-binding/permease protein BmrA	0,00186	0,18	0,29630	0,77
HG001_00274	-	-	PTS system ascorbate-specific transporter subunits IICB	0,00186	0,18	0,17150	0,53
HG001_01285	-	P67370	DegV domain-containing protein	0,00215	0,21	0,79540	0,95
HG001_02186	mtlD	P99140	Mannitol-1-phosphate 5-dehydrogenase	0,00278	0,41	0,76220	1,08
HG001_00697	uvrA	P63383	UvrABC system protein A	0,00515	S1 only	0,70990	0,92
HG001_02752	mnmE	Q8YN91	tRNA modification GTPase MnmE	0,02237	S1 only	0,68190	0,85
HG001_00774	-	-	hypothetical protein	0,01066	S1 only	0,51870	0,65
HG001_01495	ybeZ	P0A9K3	PhoH-like protein	0,02237	S1 only	0,13690	0,54
HG001_00704	aroK_1	-	Shikimate kinase	0,02237	S1 only	0,98780	1,00
HG001_01178	cls_1	P63801	Cardiolipin synthase	0,02237	S1 only	0,30820	0,61
HG001_02615	azoB	Q8KU07	NAD(P)H azoreductase	0,04792	S1 only	0,19250	0,57
HG001_01624	nrnA_2	O34600	Bifunctional oligoribonuclease and PAP phosphatase NrnA	0,04792	S1 only	0,10910	0,63
HG001_00061	sarS	Q7A872	HTH-type transcriptional regulator SarS	0,04792	S1 only	0,38600	0,75
HG001_01411	-	-	hypothetical protein	0,04792	S1 only	0,53670	0,79
HG001_01445	argR_1	P63580	Arginine repressor	0,04792	S1 only	0,42270	0,82
HG001_01673	-	-	hypothetical protein	0,04792	S1 only	0,82810	0,93
HG001_01203	-	-	hypothetical protein	0,04792	S1 only	0,84250	0,94
HG001_01278	murG	P65482	UDP-N-acetylglucosamine--N-acetylmuramyl-(pentapeptide) pyrophosphoryl-undecaprenol N-acetylglucosamine transferase	0,04792	S1 only	0,86550	0,96
HG001_01059	-	-	hypothetical protein	0,04792	S1 only	0,88170	1,05
HG001_00413	purR	P37551	Pur operon repressor	0,10630	S1 only	0,13670	0,59
HG001_01579	fgs	P15925	Folylpolyglutamate synthase	0,10630	S1 only	0,47120	0,59
HG001_02574	lipR_2	O53301	Putative acetyl-hydrolase LipR precursor	0,10630	S1 only	0,60700	0,77
HG001_02529	pgcA	Q2FVC1	Phosphoglucomutase	0,10630	S1 only	0,56460	0,81
HG001_01412	-	-	hypothetical protein	0,10630	S1 only	0,75420	0,85
HG001_01265	-	P60108	TelA-like protein	0,10630	S1 only	0,70090	0,89
HG001_02356	-	Q9X0Y1	Phosphorylated carbohydrates phosphatase	0,10630	S1 only	0,85300	0,95
HG001_01068	rsmB	P36929	Ribosomal RNA small subunit methyltransferase B	0,10630	S1 only	0,98910	1,00
HG001_01020	-	-	hypothetical protein	0,10630	S1 only	0,99140	1,00
HG001_01408	dnaQ	P03007	DNA polymerase III subunit epsilon	0,10630	S1 only	0,99330	1,00
HG001_02619	-	-	Amidohydrolase	0,10630	S1 only	0,89970	1,05
HG001_00692	prfB	Q7A6R4	Peptide chain release factor 2	0,10630	S1 only	0,80050	1,08
HG001_00886	tagE_3	P13484	putative poly(glycerol-phosphate) alpha-glucosyltransferase	0,25340	S1 only	0,16990	0,58
HG001_01523	mtnN	Q7A5B0	5'-methylthioadenosine/S-adenosylhomocysteine nucleosidase	0,25340	S1 only	0,68190	0,85
HG001_00721	rnr	P21499	Ribonuclease R	0,25340	S1 only	0,98320	1,00
HG001_01311	ponA	P39793	Penicillin-binding protein 1A/1B	0,00377	0,45	0,09972	0,77
HG001_01249	cvfB	Q2FYP3	Conserved virulence factor B	0,00680	0,46	0,02650	0,54
HG001_01088	ffh	P37105	Signal recognition particle protein	0,01330	0,19	0,38230	0,78
HG001_00486	ppaX	Q9JMQ2	Pyrophosphatase PpaX	0,02233	0,39	0,40170	0,82
HG001_02168	-	-	EVE domain protein	0,02456	0,25	0,27290	0,75
HG001_00491	azo1	Q50H63	FMN-dependent NADPH-azoreductase	0,03968	0,43	0,87110	0,97
HG001_02709	lipA_2	Q2FUU5	Lipase 1 precursor	0,04208	0,38	0,59470	0,90
HG001_01016	arcC1	Q7A627	Carbamate kinase 1	0,05934	0,15	0,67060	0,86
HG001_02098	alr1	Q5HED1	Alanine racemase 1	0,05977	0,33	0,31430	0,75
HG001_02361	-	-	hypothetical protein	0,06469	0,30	0,89320	1,04
HG001_01558	dtd	P0A026	D-tyrosyl-tRNA(Tyr) deacylase	0,07066	0,40	0,98270	1,00
HG001_00553	-	-	hypothetical protein	0,07066	0,40	0,12110	0,59
HG001_00017	rplI	P66318	50S ribosomal protein L9	0,11110	0,30	0,87110	0,97
HG001_01938	ligA	Q9AIU7	DNA ligase	0,11110	0,30	0,61750	0,92
HG001_00155	azoR	Q99X11	FMN-dependent NADH-azoreductase	0,11110	0,30	0,68110	0,91
HG001_02064	scrB	P13394	Sucrose-6-phosphate hydrolase	0,14000	0,39	0,82380	1,07
HG001_01324	-	-	tetratricopeptide repeat protein	0,19430	0,23	0,85300	0,95
HG001_01678	glpE_2	-	Thiosulfate sulfurtransferase GlpE	0,24910	0,43	0,69860	1,12
HG001_00064	yfiY	O31567	putative siderophore-binding lipoprotein YfiY precursor	0,24910	0,43	0,55510	0,86
HG001_00197	tagF	P13485	CDP-glycerol:poly(glycerophosphate) glycerophosphotransferase	0,24910	0,43	0,45320	0,75
HG001_02680	manP	O31645	PTS system mannose-specific EIIBCA component	0,29660	0,41	0,37250	0,75

145

146

147

HG001_01259	lysA	P0A5M4	Diaminopimelate decarboxylase	0,34660	0,30	0,83950	1,12
HG001_00914	purE	Q9WYS7	N5-carboxyaminoimidazole ribonucleotide mutase	0,01649	0,45	0,17530	0,73
HG001_02208	-	Q7A4A4	putative uridylyltransferase	0,04776	0,46	0,44240	0,88
HG001_01965	yxlF_3	P94374	putative ABC transporter ATP-binding protein YxlF PmtC	0,00390	0,48	0,08067	0,71
HG001_00176	acdA	P45867	Acyl-CoA dehydrogenase	0,00054	0,48	0,01163	0,63
HG001_00400	-	-	hypothetical protein	0,17600	0,46	0,81500	0,89
HG001_01434	-	-	Glyoxalase-like domain protein	0,07661	0,50	0,43370	0,85
HG001_02585	mvaA	P13702	3-hydroxy-3-methylglutaryl-coenzyme A reductase	0,21050	0,50	0,38960	0,82
HG001_01073	rpe	P74061	Ribulose-phosphate 3-epimerase	0,35440	1,86	0,55600	0,43
HG001_00818	yidA	P0A8Y5	Sugar phosphatase YidA	0,93450	0,90	0,08234	0,43
HG001_01826	perR	Q2G282	Peroxide-responsive repressor PerR	0,62460	1,30	0,08449	0,30
HG001_01491	era	P64085	GTPase Era	0,95280	1,00	0,16280	0,23

148

149

150

151

Table S7: Spectral count analysis of gel filtration fraction

LEGEND:

# spectra (BASIC Spectral Count)	= 1 spectrum
# spectra (BASIC Spectral Count)	= 2-5 spectra
# spectra (BASIC Spectral Count)	= 6-10 spectra
# spectra (BASIC Spectral Count)	= 11-30 spectra
# spectra (BASIC Spectral Count)	>= 31 spectra

Samples 36/39/42/45 min: 1µg injected
Samples 48 min: whole sample injected

(The Spectral Count values are comparable)

Total number of proteins & protein of interest (S1):

	BASIC Spectral Count									
	30S+SauS1					30S+*Sau* S1+*psm*				
Elution Time (min.)	**36**	**39**	**42**	**45**	**48**	**36**	**39**	**42**	**45**	**48**
	22	31	24	25	0	35	35	21	26	14
	BASIC Spectral Count									
Elution Time (min.)	**36**	**39**	**42**	**45**	**48**	**36**	**39**	**42**	**45**	**48**
HG001_01336|gene_rpsA_1|30S ribosomal protein S1		1	76	1475		189	62	50	1633	4
	BASIC Spectral Count									
Elution Time (min.)	**36**	**39**	**42**	**45**	**48**	**36**	**39**	**42**	**45**	**48**
HG001_02281|gene_rpsC|30S ribosomal protein S3	24	82	59	57		37	104	80	51	1
HG001_02283|gene_rpsS|30S ribosomal protein S19	17	49	90	34		33	52	97	37	
HG001_01639|gene_rpsD|30S ribosomal protein S4	14	67	43	39		28	85	48	49	1
HG001_00309|gene_rpsF|30S ribosomal protein S6	11	45	31	39		24	46	44	33	
HG001_00476|gene_rpsL|30S ribosomal protein S12	26	65	63	25		43	73	133	40	3
HG001_01510|gene_rpsT|30S ribosomal protein S20	26	75	94	28		58	74	119	38	
HG001_02270|gene_rpsE|30S ribosomal protein S5	22	54	34	17		34	64	100	28	
HG001_02263|gene_rpsM|30S ribosomal protein S13	26	91	33	14		37	104	57	22	
HG001_00477|gene_rpsG|30S ribosomal protein S7	14	41	51	19		15	57	34	31	
HG001_01107|gene_rpsB|30S ribosomal protein S2	15	64	24	30		24	77	57	36	
HG001_02262|gene_rpsK|30S ribosomal protein S11	25	64	30	23		25	66	57	15	
HG001_02273|gene_rpsH|30S ribosomal protein S8	15	49	23	15		15	44	34	18	
HG001_02288|gene_rpsJ|30S ribosomal protein S10	14	55	28	4		10	45	45	5	
HG001_00311|gene_rpsR|30S ribosomal protein S18	12	29	14	8		21	39	28	7	
HG001_02253|gene_rpsI|30S ribosomal protein S9	9	15	11	14		4	31	24	14	
HG001_02278|gene_rpsQ|30S ribosomal protein S17	5	33	42	7		23	21	52	7	
HG001_01089|gene_rpsP|30S ribosomal protein S16	3	30	5	15		7	32	20	26	2
HG001_02274|gene_rpsN1|30S ribosomal protein S14	5	5	8	1		5	2	18	3	
HG001_01196|gene_rpsN2|Alternate 30S ribosomal protein S14	1	2	2	1		1	2	1	1	
HG001_00830|gene_fabF|3-oxoacyl-[acyl-carrier-protein] synthase 2	1									2
HG001_00717|gene_eno|Enolase	1									1
HG001_00713|gene_gapA1|Glyceraldehyde-3-phosphate dehydrogenase 1	1									1
HG001_01124|gene_rpsO|30S ribosomal protein S15		16	11	18		10	26	18	13	1
HG001_02271|gene_rplR|50S ribosomal protein L18		2	1	1		2	1		2	
HG001_00976|gene_rpmF|50S ribosomal protein L32		2	1			1			1	
HG001_02284|gene_rplB|50S ribosomal protein L2		2		1		2	1		2	
HG001_01499|gene_rpsU|30S ribosomal protein S21		1	1				1			
HG001_01075|gene_rpmB|50S ribosomal protein L28		1		1		5	1			
HG001_01595|gene_rplT|50S ribosomal protein L20		1				2	1			
HG001_02269|gene_rpmD|50S ribosomal protein L30		1				1	2			
HG001_02254|gene_rplM|50S ribosomal protein L13		1				1	1			
HG001_02260|gene_rplQ|50S ribosomal protein L17		1				1				
HG001_01597|gene_infC|Translation initiation factor IF-3		1								
HG001_02287|gene_rplC|50S ribosomal protein L3				1						
HG001_02282|gene_rplV|50S ribosomal protein L22						3	3			
HG001_02280|gene_rplP|50S ribosomal protein L16						1	1			
HG001_02286|gene_rplD|50S ribosomal protein L4						1				1
HG001_01092|gene_rplS|50S ribosomal protein L19						1				
HG001_02275|gene_rplE|50S ribosomal protein L5						1				
HG001_02277|gene_rplN|50S ribosomal protein L14						1				
HG001_02285|gene_rplW|50S ribosomal protein L23							1		1	
HG001_02279|gene_rpmC|50S ribosomal protein L29							1			
HG001_00722|gene_smpB|SsrA-binding protein							1			
HG001_01572|gene_rplU|50S ribosomal protein L21							1			
HG001_02276|gene_rplX|50S ribosomal protein L24							1			
HG001_00425|gene_yugI_1|General stress protein 13									1	
HG001_00479|gene_tuf|Elongation factor Tu										12
HG001_01618|gene_pyk|Pyruvate kinase										1
HG001_00473|gene_rpoB|DNA-directed RNA polymerase subunit beta										1
HG001_01963|gene_NONE|hypothetical protein										1

References

Zuker, M. (2003). Mfold web server for nucleic acid folding and hybridization prediction. Nucleic Acids Res *31*, 3406-3415.

II. Result II: *Sau*S1 is an RNA chaperone involved in different steps of sRNA-dependent regulation and of RNA metabolism in *S. aureus*

In the previous section, I have described how *Sau*S1 affected the production of late expressed virulence factors (exotoxins and exoenzymes) and showed how it promoted the translation initiation of the highly structured α*psm1-4* mRNA. The transcriptomic and proteomics studies have also revealed other possible roles for this protein in stabilizing sRNAs or helping the correct folding of complicated RNA structures, like the riboswitches (see §I. Result I, "DISCUSSION" of the manuscript "*Staphylococcus aureus* S1 activates translation initiation of PSMα toxins and stimulates the production of several other secreted virulence factors"). This second section will focus on study of the possible extra translational functions of *Sau*S1.

II.1. *Sau*S1 helps translation initiation of structured mRNAs

In order to assess if the activity of *Sau*S1 is linked to the alleviation of translation repression mediated by cis-acting mRNA structures, besides the α*psm1-4* we tested by toe-printing one more natural *S. aureus* mRNA harbouring distinct structural features. *mgrA* mRNA carries structured 5' UTR in which the SD sequence is hidden in a double-strand region (Romilly et al., 2014; Gupta et al., 2015). We have previously shown that *E. coli* ribosomes, containing S1, are able to form initiation complexes with *mgrA* mRNAs (Khusainov et al., 2016). This efficient recognition, was linked to the presence of *Eco*S1 because S1-depleted *E. coli* ribosome, were not able to efficiently recognize *mgrA* mRNA, while mRNA binding was restored using S1-depleted 30S saturated with purified *Eco*S1 added in trans (Khusainov et al., 2016). Moreover, we had demonstrated that *Sau*30S, similarly to S1-depleted *Eco*30S, could recognize only the unstructured *spa* mRNA. As shown in **Figure 18**, *Sau*S1 enhances the formation of the initiation complex at low concentration of 30S.

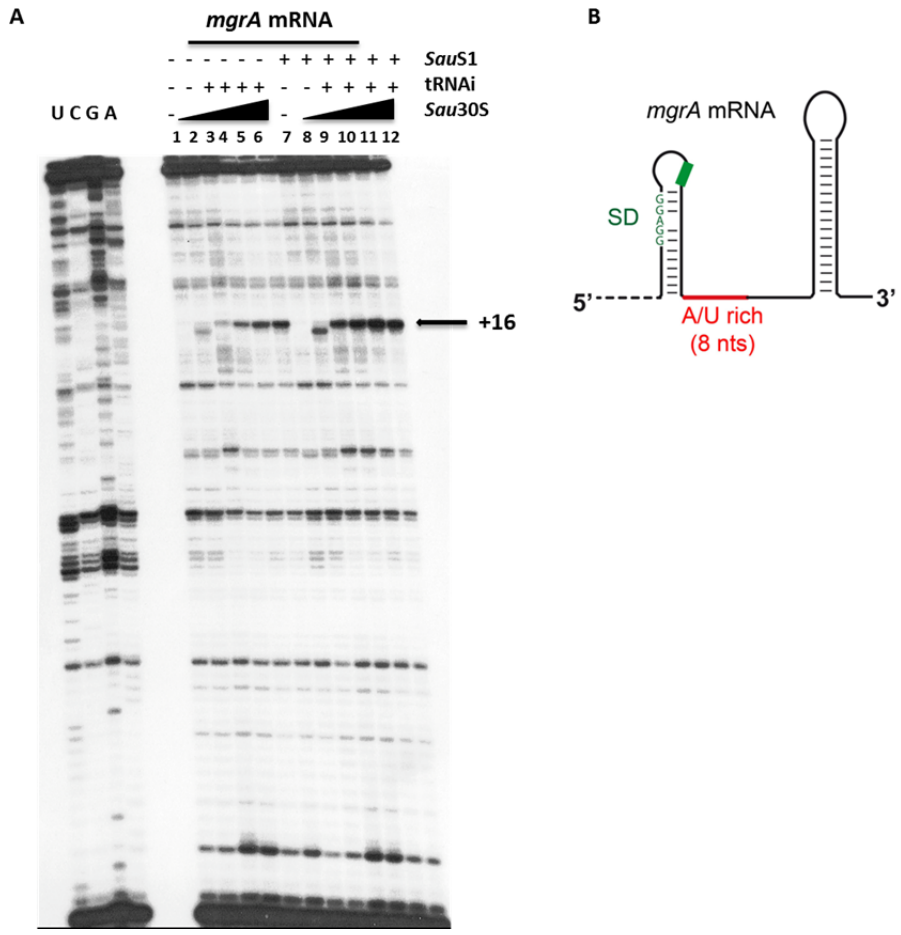

Figure 18. Toeprinting assays to monitor the effect of *Sau*S1 on the translation initiation complex formation with *mgrA* mRNA. (A) Effect of *Sau*S1 on the formation of initiation complex using *mgrA* mRNA. When present, *Sau*S1 was pre-incubated with the ribosome at a constant 1.6 molar ratio. Lane 1: incubation control of mRNA ; Lane 2: incubation control of mRNA with 30S subunits ; Lanes 3, 4, 5 and 6: formation of the initiation complex containing mRNA, increasing concentration of 30S (25, 50, 100, 200 nM) and fMet-tRNA. Lane7: incubation control of mRNA with purified *Sau*S1. Lane 8: incubation control of mRNA, 30S and *Sau*S1. Lanes 9, 10, 11 and 12: formation of initiation complex in presence of *Sau*S1 and increasing concentrations of 30S (25, 50, 100, 200 nM). Lanes U, A, G, C: sequencing ladders. The toe-printing signals at position +16 are indicated by arrows. (B) Scheme for the secondary structure of the RBS and beginning of coding region of *mgrA* mRNA.

II.2. Phenotypic characterization of *rpsA* mutants

To elucidate how *Sau*S1 is impacting the physiology of *S. aureus*, the three previously obtained mutants strains were analyzed for phenotypic alterations under different stress conditions. Two mutant strains resulted from introns insertion, one located immediately after the AUG codon (*rpsA*111::LtrB) and the second close to the stop codon (*rpsA*1029::LtrB) of the *rpsA*, while the third strain corresponded to a deletion of the gene per allelic replacement (Δ*rpsA*).

I first demonstrated that the three mutant strains grow similarly in normal laboratory conditions (e.g. rich medium at 37°C) in agreement with a previous study showing that *S. aureus rpsA* gene is not essential (Chaudhuri et al., 2009). I have then compared the growth rates of the mutant and WT (HG001) strains under various stresses. Because the expression of the virulence factors is modulated by metabolic changes and stress responses, I have analyzed whether *Sau*S1 might also be required for other adaptive processes. **Figure 19** shows growth curves in BHI (Brain Heart Infusion) at different pH, during cold and heat shocks, or in NZM minimal medium supplemented with glucose. No differences could be observed between the HG001 and the three mutants strains in BHI at 37°C (**Figures 19A and B**). Nutrient starvation conditions (NZM minimal medium supplemented with glucose) did not affect the specific growth of the WT and the mutant *rpsA*111::LtrB or *rpsA*1029::LtrB strains (**Figure 19C**) although we observed a reduced duplication time when compared with the growth in rich media.

An acid shock (pH 5) was also tested (**Figure 19D**). The main reason why this stress was selected is because in the host body, infecting microorganisms frequently face acidity e.g. in the stomach, the phagolysosomes (Jensen and Bainton, 1973) and in the oral cavity and for the presence of fermentation products from other co-colonizing anaerobic bacteria. It was also shown that mild acidic stress altered the expression of a large set of virulence factors (Weinrick et al., 2004), which most likely illustrate the ability of the bacteria to adapt to particular tissue sites of the host. The acidic stress has been applied when bacteria reached OD_{600}=1. A drastic arrest of the growth could be observed which was even more sudden for the *rpsA*111::LtrB and *rpsA*1029::LtrB strains than the WT (HG001).

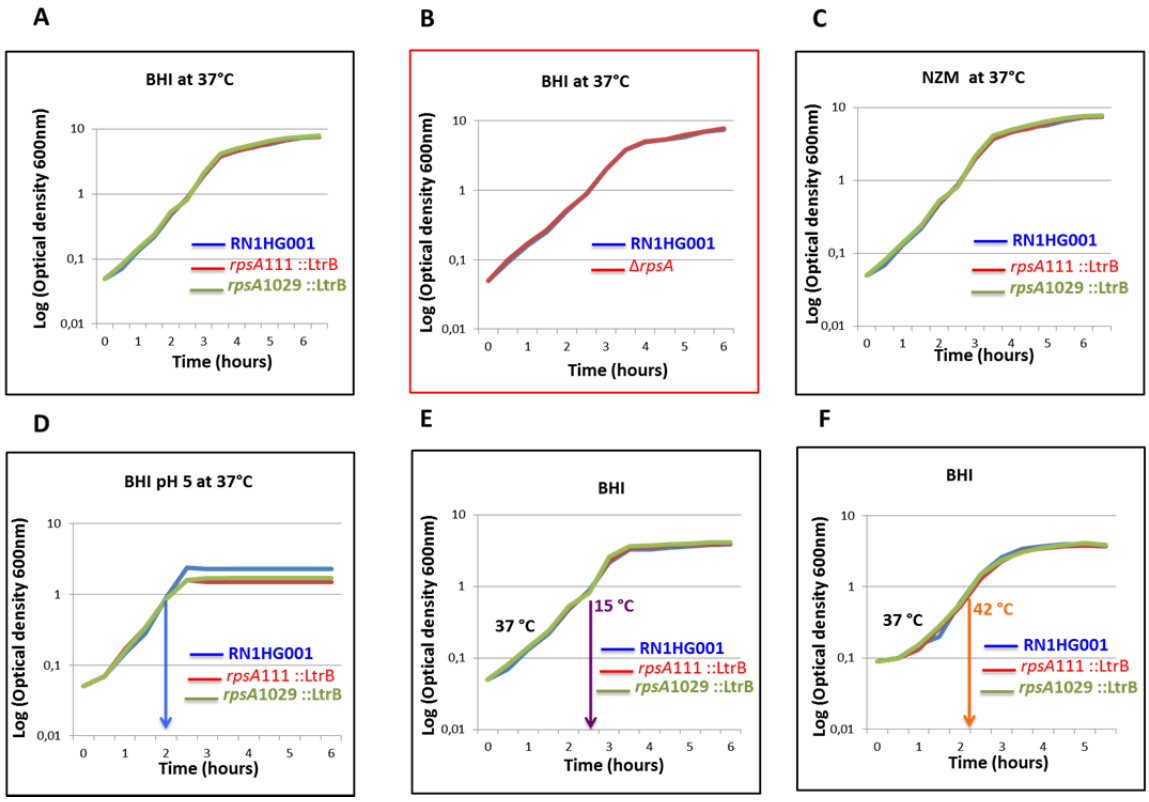

Figure 19. Bacterial growth under different stress conditions. Samples were taken each 30 min through the time course of six hours to check the optical density at OD_{600nm}. A. BHI growth at 37°C for WT (HG001) and the insertion mutants *rpsA*111 ::LtrB and *rpsA*1029 ::LtrB. B. BHI growth at 37°C for WT (HG001) and the Δ*rpsA* strain. C. Growth curves in NZM minimum media supplemented with glucose. D. Acidic stress. Growth in BHI 37°C was allowed to proceed until OD_{600nm}=1 was reached. E. The bacteria were exposed to pH 5. E. The cells were grown at 37°C in rich media and at OD_{600nm}=1 and then they were placed at 15°C. F. The bacteria were exposed to pH 5. E. The cells were grown at 37°C in rich media and at OD_{600nm}=1 and then they were placed at 42°C.

Bacterial cold shock response has been largely studied in *E. coli* and *Bacillus subtilis* (Brandi et al., 1994; Graumann and Marahiel, 1996; Graumann et al., 1996; Jones and Inouye, 1994). Exposition to cold induces the synthesis of specific set of cold-shock proteins able to help microorganisms to overcome the damaging effects of rapidly reduced temperatures on transcription and translation (Brandi et al., 1994; Giangrossi et al., 2007; Giuliodori et al., 2007; Giuliodori et al., 2004; Giuliodori et al., 2010; Gualerzi et al., 2003). These proteins are presumed to function as RNA chaperones preventing the formation of secondary structures in RNAs thereby facilitating translation at low temperature (Yamanaka et al., 1998). The common protein fold (cold shock domain CSD) of the cold shock proteins such as *E. coli* CspA is very similar to the OB-fold S1 domain. As I described above ("Introduction"), the domains of *Eco*S1 are not functionally equivalent and it has been shown that the deletion of domains 5 and 6 at the C-terminal region of *Eco*S1 (*rpsA*Δ56) does not affect the general translation, but causes a cold

sensitive phenotype ((Duval et al., 2013b). and unpublished data from the lab). The cold-sensitive phenotype could be due to an impaired ability to unfold RNA structures stabilized at low temperature. The fact that mutations could affect the chaperone activity preferentially at low temperatures is not so surprising. Indeed, *Eco*S1 does not need energy like an RNA helicase, and therefore at the permissive temperature, the thermal energy may help the protein to melt RNA secondary structures. Surprisingly, **Figure 19E** shows no difference in the behavior of the different strains subjected to cold shock. It has to be noted though that no slow down or temporary arrest of the growth was observed for any of the strains.

The bacterial heat shock response has been also extensively studied in several Gram-positive and Gram-negative bacteria (Bukau, 1993; Chuang and Blattner, 1993; Cowing et al., 1985). Upon shifts to higher temperature, the cells start to induce the expression of numerous heat-shock proteins (HSPs). Many of them are molecular chaperones including DnaK and GroEL and ATP-dependent proteases such as Lon and ClpAP that are essential to overcome protein denaturation (Barrios et al., 1994; Wild et al., 1996; Yura et al., 1993). In *P. putida*, exposure to high temperatures has been shown to downregulate *rpsA* (Ito et al., 2014). Since the unrestricted synthesis of thermolabile proteins can potentially lead the cell to danger, *P. putida* might arrest the de novo protein synthesis of non-HSPs reducing S1 level upon exposure to high temperatures. However, as evidenced in **Figure 19F,** no significant effects were produced when the WT and mutant strains were exposed to elevated (42°C) temperatures.

Although we did not monitor all the phenotypes with the three mutant strains, our data nevertheless suggested that mutations or the deletion of the gene had very similar effects, and that S1 had little effect on cell growth. These data suggest that S1 is not a ribosomal component and support the idea that *Sau*S1 is a regulatory protein.

II.3. *SauS1* and its constellation of RNAs. RIP-seq (co-immunoprecipitation and RNA-seq) analysis

As mentioned above, *Sau*S1 is able to modulate the translation of PSMα peptides by direct binding to the *αpsm1-4* operon. Other mRNAs have been also postulated to be potential target of *Sau*S1, which *in vitro* seems to modulate the translation of other

structured mRNAs (e.g. *mgrA*) while not affecting unstructured one (e.g. *spa*). Moreover, several sRNAs have been found to be downregulated in the Δ*rpsA* strain. To characterize the repertoire of RNA targets, we have performed RIP-seq analysis (co-immunoprecipitation and RNA-seq) using the *Sau*S1-3X flag-tagged strain, which allow us to detect the synthesis of *Sau*S1 during bacterial growth (Figure 1 of the manuscript). We also performed RIP-seq on the WT (HG001) strain as the negative control. The experiments where done in triplicates. Bacterial growth was performed in BHI medium for 6 h where *Sau*S1 is sufficiently abundant. After immunoprecipitation with the anti-flag agarose beads and washing to remove unspecific binders, the sample was extracted with acidic phenol and then by chloroform-isoamylic alcohol. RNA was precipitated with ethanol, treated with DNase I, extracted with phenol, precipitated and prepared for sequencing In parallel, we have performed a transcriptomic analysis from total RNA extracts prepared from the wild-type strain and the *Sau*S1 flagged strain to gain some indication on the expression levels of the mRNAs. This analysis has revealed no major changes in the corresponding transcriptomes including *rpsA* levels in the two strains (1.26 fold). The data were analyzed and visualized using Galaxy (Afgan et al., 2016) and the Integrative Genomics Viewer (IGV) browser, respectively (Thorvaldsdottir et al., 2013). A detailed protocol for the bioinformatics analysis is provided in Material and Methods. Briefly, we aligned the sequencing reads onto HG001 genome (Caldelari et al., 2017), counted per feature, and normalized. We have estimated the enrichment of putative targets by comparing the number of reads obtained from the RNA immunoprecipitated with the flag-tagged S1 and the non tagged (WT) S1 as control. **Table 3** and **Table 4** show the best hits divided into mRNAs and other classes of RNAs (sRNAs, riboswitches, tRNAs…), respectively.

RIP-seq of *Sau* S1. Co-immuno precipitated mRNAs

Virulence factors				
id	**gene**	**product**	**Enrichment**	**pvalue**
HG001_02059	agrB	Accessory gene regulator protein B	14,108	1,03E-08
HG001_02755	psm_locus	psm α operon	13,228	2,09E-08
HG001_02245	-	65 kDa membrane protein precursor Eap	12,192	9,09E-08
HG001_00728	clfA	Clumping factor A precursor	5,556	0,00011
HG001_00113	galE	UDP-glucose 4-epimerase	5,301	0,00021
HG001_00100	cap8A_1	Capsular polysaccharide type 8 biosynthesis protein cap8A	3,998	0,0012
HG001_01022	-	psm β1	3,98	0,00206
HG001_00899	sspA	Glutamyl endopeptidase precursor	3,974	0,00139
HG001_00227	esxA	Virulence factor EsxA	3,787	0,00184
HG001_00556	sarA	Transcriptional regulator SarA	3,372	0,00457
Other mRNAs				
id	**gene**	**product**	**Enrichment**	**pvalue**
HG001_01747	-	Thermophilic serine proteinase	20,53	4,20E-12
HG001_02647	hmoB	Heme-degrading monooxygenase HmoB	9,433	3,30E-07
HG001_00560	xerD_2	Tyrosine recombinase XerD	8,288	3,32E-06
HG001_01665	ytpP	Thioredoxin-like protein YtpP	8,243	1,48E-06
HG001_02406	-	putative lipoprotein precursor	7,815	1,83E-05
HG001_00733	-	cspA	7,447	2,40E-06
HG001_02161	luxS	S-ribosylhomocysteine lyase	6,734	1,38E-05
HG001_02543	zntR	HTH-type transcriptional regulator ZntR	6,58	8,53E-05
HG001_02609	isaA	putative transglycosylase IsaA precursor	6,375	1,10E-05
HG001_01549	-	CsbD-like protein	6,189	6,98E-05
HG001_02222	-	Alkaline shock protein 23	6,095	6,76E-05
HG001_02418	ydaG	General stress protein 26	5,946	0,00011
HG001_01065	-	TM2 domain protein	5,924	0,00017
HG001_00759	-	CsbD-like protein	5,663	0,00062
HG001_00087	deoC1	Deoxyribose-phosphate aldolase 1	5,502	0,00012
HG001_02655	nrdD	Anaerobic ribonucleoside-triphosphate reductase	5,237	8,47E-05
HG001_00214	degA	HTH-type transcriptional regulator DegA	5,222	0,00023
HG001_02644	fda	Fructose-bisphosphate aldolase class 1	5,124	0,00047
HG001_02628	-	Fructosamine kinase	5,111	0,00021
HG001_00131	yagU	Inner membrane protein YagU	5,066	0,00013
HG001_01336	rpsA_1	30S ribosomal protein S1	5,018	0,0005
HG001_01127	-	Ribonuclease J 2	4,93	0,00019

Table 3: List of mRNAs sequenced by RIP-seq using *Sau*S1-flag immunoprecipitation. Fold change (IP-S1flag/IP-S1) correspond to enrichment values and together with p-values were calculated for by DESeq2 using shrinkage estimation for dispersions and fold changes (Varet et al., 2016).

Interestingly, among the best enrichments obtained for mRNAs, we have found the *α psm* operon, which was previously experimentally validated (Figure 5C of the manuscript). *Sau*S1 protein was also co-purified with other mRNAs encoding virulence factors and of two main regulators of virulence (*agr*, *sarA*; **Table 3**).

RIP-seq of *Sau* S1. Co-immuno precipitated RNAs

sRNAs							
id	gene	product	Enrichment	pvalue	ΔrpsA/WT	pvalue	Binding (Kd[a])
HG001_02347	-	RsaI	70,443	6,16E-19	0,204	1,30E-31	~ 500 nM
HG001_01553	-	6S	63,163	4,87E-22	0,143	1,77E-12	n.d.
HG001_00710	-	RsaH	20,371	2,88E-09	0,832	0,59711	~ 100 nM
HG001_00584	-	RsaD	19,601	4,32E-09	0,115	1,61E-13	n.d.
HG001_00848	-	RsaE	9,727	9,48E-06	0,234	4,80E-05	> 1 µM
HG001_02057	-	RNAIII	3,885	0,00438	0,363	5,71E-09	~ 200 nM
HG001_00516	-	RsaA	3,846	0,00175	0,676	0,09411	no binding
HG001_02756	-	RsaG	2,556	0,04221	0,16	2,20E-11	no binding
New sRNAs[b]							
id	gene	product	Enrichment	pvalue	ΔrpsA/WT	pvalue	Binding (Kd[a])
HG001_03138	-	RsaOT	18,167	3,71E-09			
HG001_03067	-	SprX	6,258	0,00045			
HG001_03009	-	SprX2	6,016	0,00069			
HG001_02954	-	RsaOF	4,606	0,00119			
tRNAs							
id	gene	product	Enrichment	pvalue	ΔrpsA/WT	pvalue	Binding (Kd[a])
HG001_00443	-	tRNA-Ala(tgc)	22,261	7,49E-11	0,341	0,0021	n.d.
HG001_01823	-	tRNA-Ala(tgc)	7,036	9,03E-05	0,093	4,79E-17	n.d.
HG001_02201	-	tRNA-Ile(gat)	5,841	8,04E-05	0,05	1,35E-31	n.d.
HG001_02088	-	tRNA-Gly(tcc)	3,67	0,01249	0,12	3,00E-10	n.d.
HG001_01816	-	tRNA-Gly(gcc)	3,439	0,0506	0,523	0,04231	n.d.
HG001_01812	-	tRNA-Ala(tgc)	3,36	0,03646	0,364	0,00358	n.d.
Riboswitches							
id	gene	product	Enrichment	pvalue	ΔrpsA/WT	pvalue	Binding (Kd[a])
HG001_01602	-	T-box	5,569	7,82E-05	1,813	0,03484	n.d.
HG001_01693	-	FMN Riboswitch	5,544	7,12E-05	2,476	4,48E-09	n.d.
HG001_01462	-	Glycine Riboswitch	5,121	0,00079	0,62	0,10996	n.d.
HG001_00986	-	T-box	4,22	0,00162	0,78	0,20049	n.d.
HG001_02363	-	SAM Riboswitch	3,894	0,00756	0,71	0,03617	n.d.
HG001_01542	-	T-box	3,554	0,00509	0,728	0,28617	n.d.

Table 4: List of sRNAs, tRNAs and other *cis*-acting non coding RNAs (riboswitches) sequenced by RIP-seq using *Sau*S1-flag immunoprecipitation. Fold change (IP-S1flag/IP-S1) correspond to enrichment values and together with p-values were calculated for by DESeq2 using shrinkage estimation for dispersions and fold changes (Varet et al., 2016). For the sake of simplicity also the corresponding differences in RNA levels observed by the transcriptomic analysis (see § Result I) is reported with the corresponding p-values. [a]The last column refers to apparent Kds obtained by the gel-shift experiments (§ Result II; II.4.). [b]New sRNAs are sRNAs newly incorporated into the annotation file (Caldelari et al., 2017).

Several sRNAs have been found together with *Sau*S1 (**Table 4**). The most enriched is the sRNA RsaI (70,4 enrichment). RsaI level was also strongly decreased in the Δ*rpsA* mutant strain (0,2 **Table 4**). Interestingly, the yields of many co-IP sRNAs were also found less abundant in Δ*rpsA* mutant strain. Like RsaI, RsaD (0,11), RsaG (0,16), RsaE (0,23), RNAIII (0,36) and RsaA (0,68) might be stabilized by the binding with *Sau*S1. Such a correlation was also found for the co-IP tRNAs (**Table 4**).

These data suggested that *Sau*S1 binds to many of the co-IP RNAs, and by doing so, might activate the translation of some mRNAs and stabilize other RNAs.

II.4. *SauS1* forms stable complexes with various sRNAs but does not interact with all of them

Based on the RIP-seq data, we first analyzed whether *Sau*S1 directly binds to different sRNA candidates using gel retardation assays (**Figure 20**). In vitro 5' end-labeled RsaI, RsaH, RsaG, RsaA, RsaE, and RNAIII were incubated with increasing concentrations of purified *Sau*S1. The data show that the protein directly binds to RsaH (**Fig. 20A**, K_d 100 nM), RsaI (**Fig. 20B**, K_d 500 nM), RNAIII (**Fig. 20D**, K_d 200 nM). In contrast, no significant interaction was observed for RsaE (**Fig. 20C**, > 1 µM), RsaG (**Fig. 20E**), and RsaA (**Fig. 20F**). The apparent Kd for the different sRNAs is also included in **Table 4**.

Taken together, the gel retardation assays showed that many of the co-IP sRNAs are direct binders of SauS1. For those, which do not directly interact, their presence in the list could be explained by the formation of multi-partner complexes. *Sau*S1 could thus interact with a specific RNA or protein which in turn could establish other interaction with other RNAs.

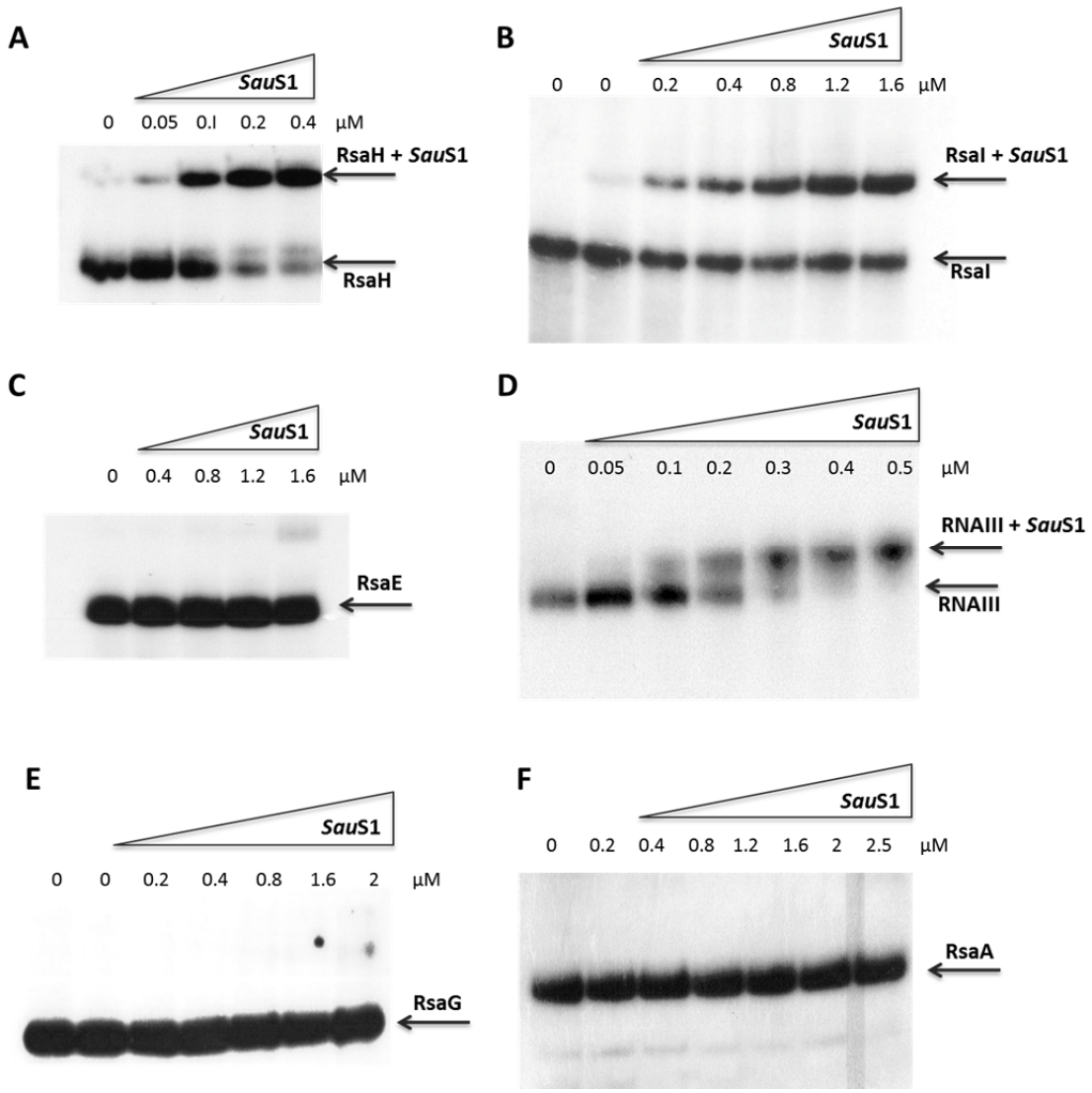

Figure 20. Gel retardation assays to monitor *Sau*S1 binding to several sRNAs. Experiments were performed on complexes formed with the 5' end-labeled RsaH (A), RsaI (B), RsaE (C), RNAIII (D), RsaG (E) and RsaA (F) in presence of increasing concentrations of *Sau*S1 as marked on the figure.

II.5. *SauS1* forms a ternary complex with RsaI and RsaG

The gel retardation analysis has shown a direct binding of *Sau*S1 to RsaI while no detectable interaction was observed with RsaG, even with high concentrations of protein (up to 3.5 µM, data do not shown). RsaG belongs to the class of sRNA, which contain a C-rich sequence motif (UCCC) as the seed sequence to interact with the SD sequence of target mRNAs (Geissmann et al., 2009a). RsaI is characterized by several conserved stretches of nucleotides including a long unpaired region rich in uridines and adenines and two G-rich tracts (**Figure 21**). MS2-affinity purification approach coupled to RNA sequencing (MAPS) (Lalaouna and Masse, 2015; Tomasini et al., 2017), used to identify

the targetomes of both RsaI and RsaG, have shown that the two sRNAs are interacting *in vivo* (Delphine Bronesky and Emma Desgranges unpublished results). The predicted interaction site would involve one of the C-rich motif of RsaG and one G-rich region of RsaI (**Figure 21**).

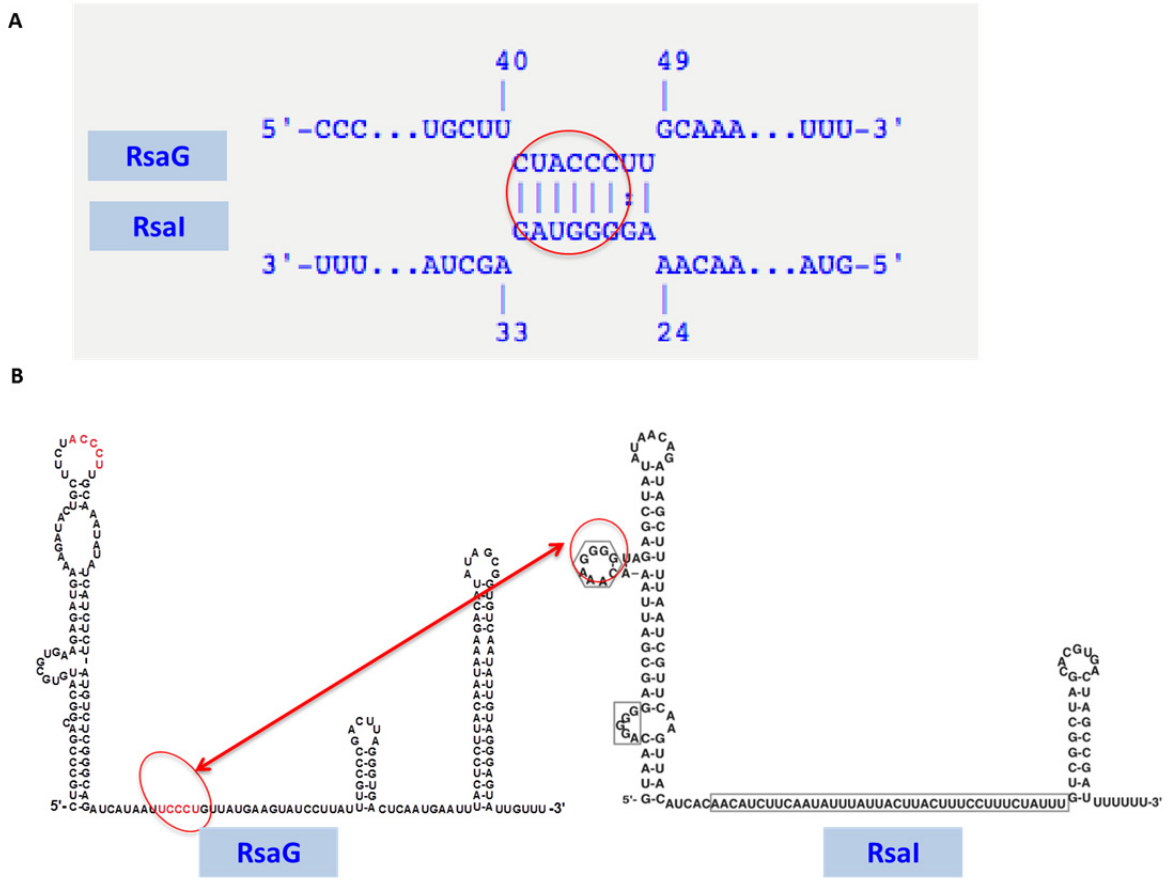

Figure 21 Predicted interaction between RsaG and RsaI. A. Predicted base-parings between C-rich motif of RsaG and G-rich tract of RsaI carried out using IntaRNA program (Mann et al., 2017). B. Secondary structures of RsaG and RsaI. The sequences involved in their interaction are highlighted by red circles and connected by an arrow. (DG= -9,5 kcal/mol).

I then checked the possibility that a ternary complex could form between *Sau*S1, RsaI and RsaG by gel-retardation assays. Increasing concentrations of cold RsaG were incubated with constant amount of 5' end-labeled RsaI in the presence and in the absence of *Sau*S1 (1 µM). The results showed that, although RsaI and RsaG are able to interact (apparent K_d= 50 nM), the addition of *Sau*S1 drastically enhances their binding affinity as shown in **Figure 22** (apparent K_d= 6,25 nM). *Sau*S1 is thus able to interact with RsaI to facilitate its binding to RsaG leading to the formation of a highly stable ternary complex both *in vitro* and *in vivo*.

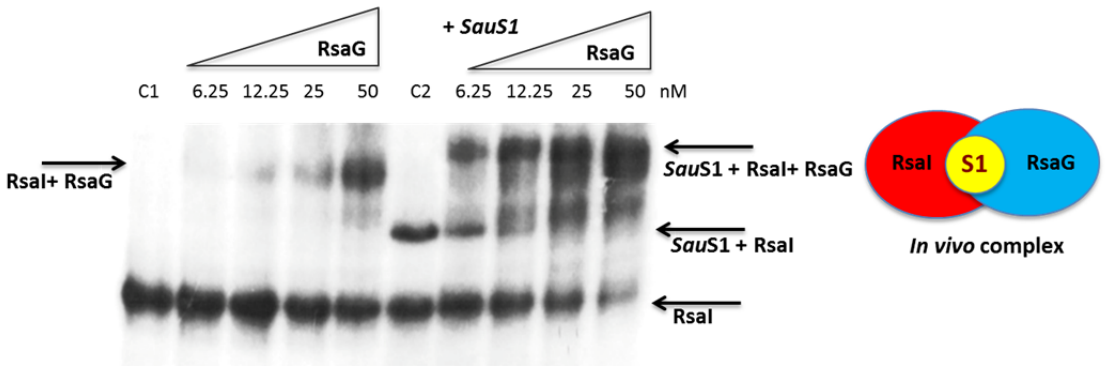

Figure 22: Gel retardation assays to follow the formation of ternary complex SauS1-RsaI-RsaG. The assay was performed on complexes formed with the 5' end-labeled RsaI, increasing concentration of cold RsaG (marked on the figure) in the presence and in the absence of *Sau*S1 (1 µM). Lanes C1 and C2 are control lanes with RsaI and RsaI-SauS1, respectively. The binary (RsaI-RsaG and RsaI-SauS1) and ternary (SauS1-RsaI-RsaG) complexes are indicated by arrows. The observed SauS1-RsaI-RsaG complex could explain the RIP-seq data.

II.6. RsaI binding site for RsaG is hindered into a pseudoknot structure

RsaI has been proposed to fold in a stable pseudoknot structure involving its highly conserved regulatory regions, the G-rich tract and the long single-stranded region (Marchais et al., 2010). This G-rich motif is supposed to bind to RsaG, and recent works have shown that the two conserved regions of RsaI are required for the recognition of target RNAs (Delphine Bronesky unpublished results). The pseudoknot structure would be thus incompatible with the regulatory functions of RsaI. This opens the following question: Is SauS1 able to help the RsaI targeting process by promoting pseudoknot remodeling?

In order to probe RsaI structure, I have performed SHAPE (Rice et al., 2014) and structure mapping using different RNases and lead (II) (Fechter et al., 2016). As an RNA folds into a defined tertiary structure, specific set of nucleotides are expected to be constrained in base-pairing interactions, while unpaired nucleotides remains exposed and flexible. SHAPE is based on the chemical modification of the ribose 2'-hydroxyl position which appears to be strongly dependent on the nucleotide flexibility (Steen et al., 2011). Hence, flexible nucleotides preferentially adopt conformations that react with a hydroxyl-selective chemical to form a 2'-O-adduct while basepaired nucleotides are unreactive. This method was particularly well appropriate to map long-range interactions such as the pseudoknot structure motif (**Figure 23**).

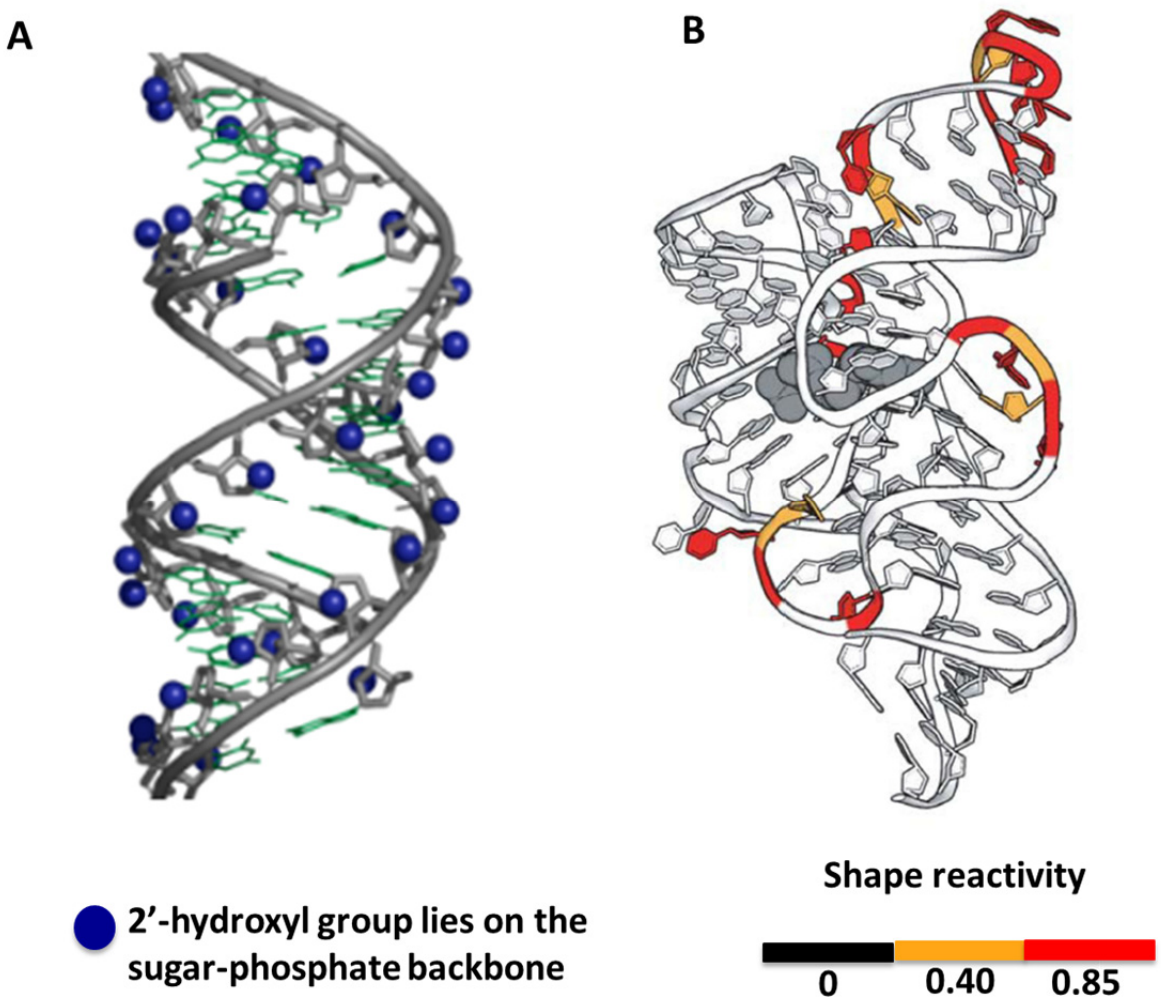

Figure 23: SHAPE reactivity. In panel A is represented a generic RNA helix where the 2'-hydroxyl groups, accessible for chemical modification, are represented as blue spheres, while the aromatic bases are in green. All the nucleotides have the same level of reactivity to chemical compound. In panel B, is shown the reactivity of nucleotides in a pseudoknot structure. The increasing reactivity of 2'-OH is indicated by different colors, from constrained and unreactive (black), to not very reactive (orange) and completely accessible nucleotides (red). The figure was adapted from (Weeks, 2015).

Double-stranded or stacked regions were tested with RNase V1, and unpaired guanine residues with RNase T1. I also used lead (II) that cleaves preferentially interhelical and loop regions, with high sensitivity for flexible regions (**Figure 24A**). Modified sites or cleaved nucleotides were detected as stops of primer extension reactions using reverse transcriptase. Our data were in agreement with the secondary structure model (**Figure 24B**) and is compatible with the presence of a pseudoknot interaction. Based on the data, a 3D structure has been built with RNAComposer (Popenda et al., 2012) (**Figure 24C**).

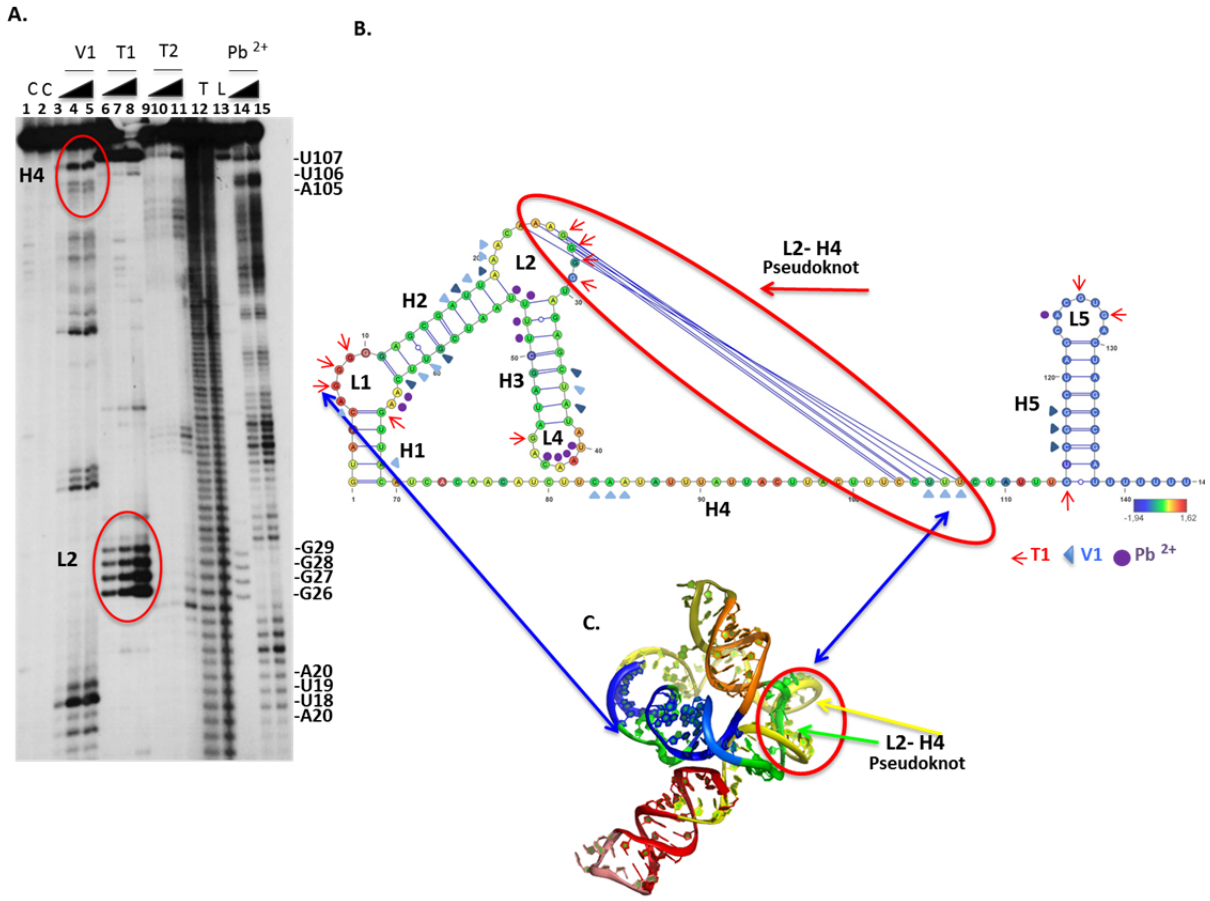

Figure 24: Results of the probing experiments. (A). Autoradiographs of enzymatic hydrolysis. Lanes 1 and 2: incubations controls. Lanes 3, 4 and 5: increasing concentration of RNase V1. The red square show the regions involved in the pseudoknot formation; Lanes 6, 7 and 8: increasing concentration of RNase T1; Lanes 9, 10 and 11, increasing concentration of RNase T2. Lanes T and L: RNase T1 in denaturing condition and formamide ladders, respectively. Lanes 15 and 16: Lead (II)-induced cleavage (B). Summary of the probing experiments reported on the secondary structural model of RsaI pseudoknot. T1 induced cuts are represented by red arrows. The reactivity of guanine residues to the V1 cuts are represented by blue triangles. The intensity of the cuts is given from weak to strong cleavages. Lead (II) induced cleavages are represented by purple circles. (C). 3D structure of RsaI pseudoknot obtained by RNAComposer. The interaction occurring between the G-rich track and the U-rich motifs, involved in the pseudoknot folding are highlighted by red circles on the structures in B and C.

II.7. Probing the interaction between RsaI and RsaG by footprinting experiments

In order to identify the sequence-specific contacts of RsaG and RsaI and to better clarify the mechanisms of action of *Sau*S1, I have performed footprinting experiments using RNases V1 and T1, and lead (II)-induced cleavages. The results, summarized in **Figure 25**, support the prediction that the G-rich tract of RsaI, which is engaged in the pseudoknot structure, interacts with RsaG. Indeed the major RsaG-induced protections were located at the G-tract motif which is not exposed to RNase T1 cuts.

We thus propose that *Sau*S1 would bind to RsaI to promote the melting of the pseudoknot and to facilitate its interaction with RsaG. I have tried to localize the

footprint of *Sau*S1 on RsaI using enzymes and lead II). However, no signature for *Sau*S1 could be detected most probably due to the dynamic nature of the RNP. This is a typical RNA chaperone behavior (Duval et al., 2017).

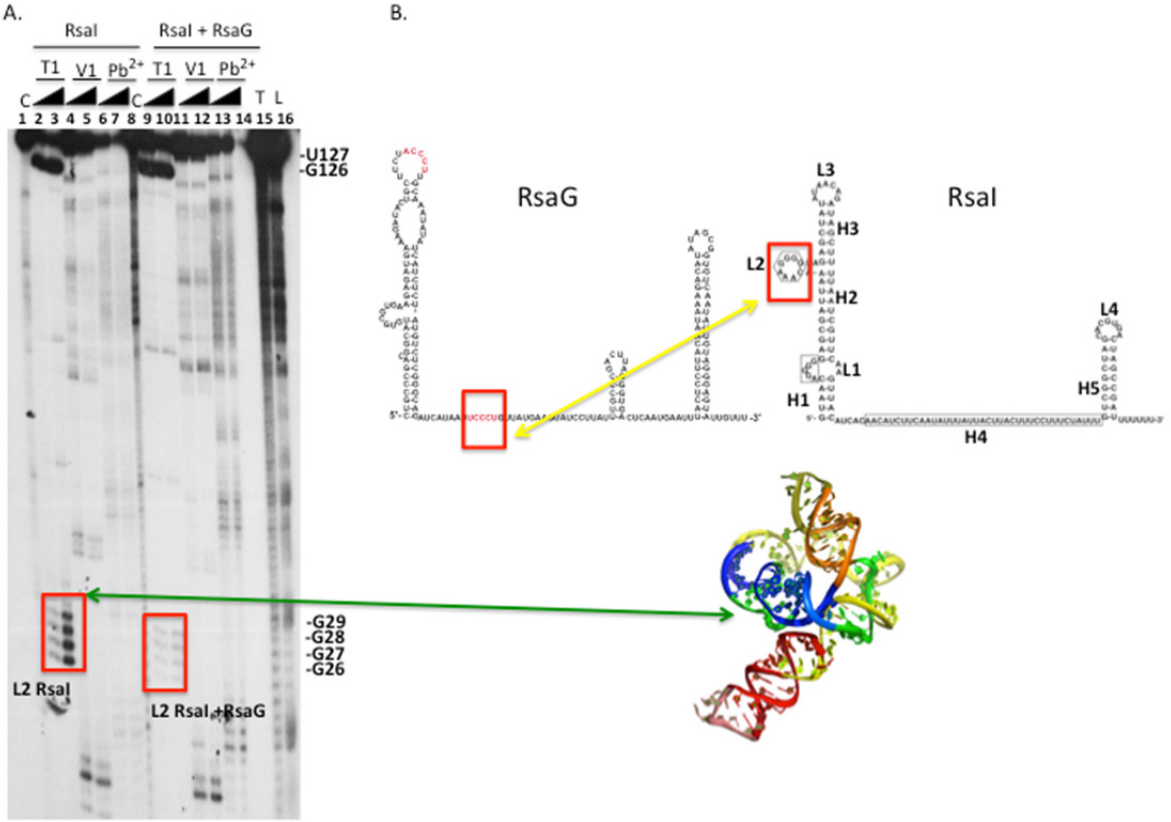

Figure 25. Footprinting assays for RsaG on RsaI. 3'-end labeled RsaI alone (first part of the autography) or in the presence of cold RsaG, was treated with RNases T1, V1 and lead (II). Lane 1: incubation control (RsaI) ; Lanes 2 and 3: RsaI with and without RNase T1, respectively ; Lanes 4 and 5: RsaI with and without RNase T1, respectively ; Lanes 6 and 7: RsaI with and without lead (II), respectively. Lane 8: incubation control (Rsai + RsaG). Lane 9 and 10: RsaI+ RsaG with and without RNase T1, respectively ; Lanes 11 and 12: RsaI + RsaG with and without RNase V1, respectively ; lanes 13 and 14: RsaI + RsaG with and without lead (II), respectively. Sequence ladder identifying position of guanines, is shown in the last line.

II.8. Characterization of RNA annealing and strand displacement activities of S1 by FRET experiments

Chaperone proteins could act in two reactions: the RNA annealing and the dissociation of RNA duplexes (Rajkowitsch and Schroeder, 2007). In order to dissect the chaperone activity of *Sau*S1, we used Fluorescence Resonance Energy Transfer (FRET) assay using the protocol proposed by Rajkowitsch and Schroeder in 2007 (Rajkowitsch and Schroeder, 2007). Briefly, for the experiment, we used two different fluorophore-labeled RNA oligonucleotides that are fully complementary. The assay was divided in two main phases (**Figure 26**). During the first step, we have followed the kinetic of annealing of

the two complementary oligonucleotides in the presence or in the absence of *Sau*S1. In the second step, we have injected an excess of a cold competitor oligonucleotide to monitor the strand displacement (**Figure 20**).

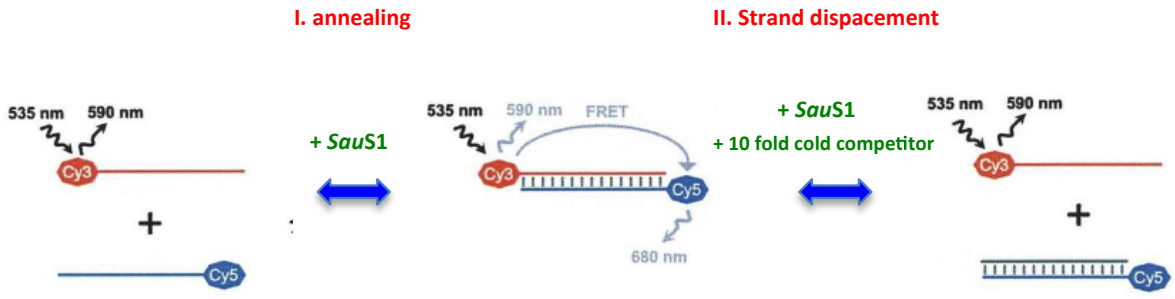

Figure 26: RNA chaperone proteins are basically active in two reactions. RNA annealing and strand displacement. The chaperone activity could be followed by FRET assay. (I.) Annealing of two fluorophore-labeled RNAs completely self-complementary gives a FRET signal that is reduced upon RNA chaperone facilitating strand displacement with a cold competitor RNA (II).

Our data shown that in contrast to *E. coli* S1, *SauS1* enhances the rate of annealing five fold (**Figure 27A**) while it is not involved in the strand displacement reaction (**Figure 27B**).

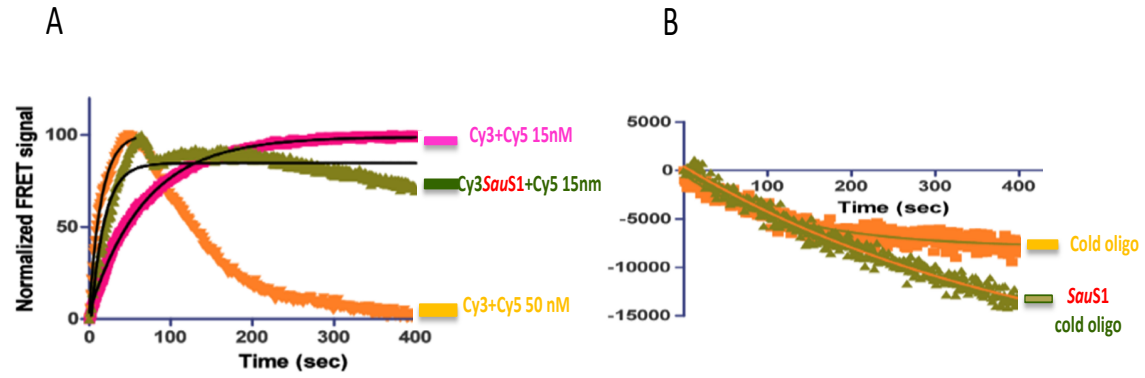

Figure 27: We used Fluorescence-based assays to monitor the chaperone activity of SauS1 in two reactions, annealing and strand displacement. In the phase I. the two flurophore-labeled oligonucleotides were mixed in a microplate reader in the absence /presence of S1. The donor (Cy3) and acceptor (Cy5) fluorescence emission, were registered each second. The FRET index was estimated and normalized at t 180 s. The annealing of two oligonucleotides, is enhanced five times by the presence of S1 (A) while no effect of S1 was monitored on the strand displacement during the phase II (B).

Discussions and Perspectives

I. *Staphylococcus aureus* S1 as translational activator. Further considerations

I.1. General discussion

In the manuscript (Results, §I) "*Staphylococcus aureus* S1 activates translation initiation of PSMα toxins and stimulates the production of several other secreted virulence factors", we have demonstrated that *Sau*S1 is not associated to the ribosome, but is required for translation initiation of *α-psm* mRNA coding for Phenol Soluble Modulines of type α. Moreover, it affects the production of many other exotoxins (α-haemolysin, δ-haemolysin and γ-haemolysins) and exoenzymes (proteases and lipases). We have proposed that, by direct binding to the mRNAs, it could remove inhibitory structures at the RBS to allow the correct 30S-mRNA interactions to take place. Our differential transcriptomics analysis has provided indications on the mRNAs which would require *Sau*S1 to be translated and protected from degradation. With the RIP-seq experiments (Results, §II.3; **Table 3** and **Table 4**), we could detect *in vivo* the whole set of mRNAs interacting with *Sau*S1. The two datasets are well correlated, providing a detailed picture of the regulatory network coordinated by *Sau*S1.

First, *α-psm* operon was found as one of the best target of *Sau*S1 (Results, §II.3; **Table 3**). In addition, the RNAIII transcript coding for another PSM peptide (*hld*) with stable structure at its RBS (Benito et al., 2000) is also downregulated in the Δ*rpsA* strain, is enriched in the RIP-seq (Results, §II.3; **Table 4**), and directly binds to *Sau*S1 (Results, **Figure 20D**). The third *psm* locus coding for two PSMβ peptides is also downregulated in Δ*rpsA* (**Table 2,** Results, §I). PSMβ1, co-immunoprecipitated with *Sau*S1 (Results, §II.3; **Table 3**) has strong and inaccessible Shine and Dalgarno sequence, suggesting possible needed of *Sau*S1 to be expressed, while the second peptides PSMβ2, results to be less structured (**Figure 28**).Although experimental validation is needed to demonstrate the *hld* and *psmβ* translation activation by *Sau*S1, it is tempting to propose that the three PSM coding genes would be coordinated both at transcriptional level by AgrA (Queck et al., 2008) and at translational level by *Sau*S1. Because their mRNAs are highly structured, there is a risk that the efficiency of translation might be different from one operon to the other.

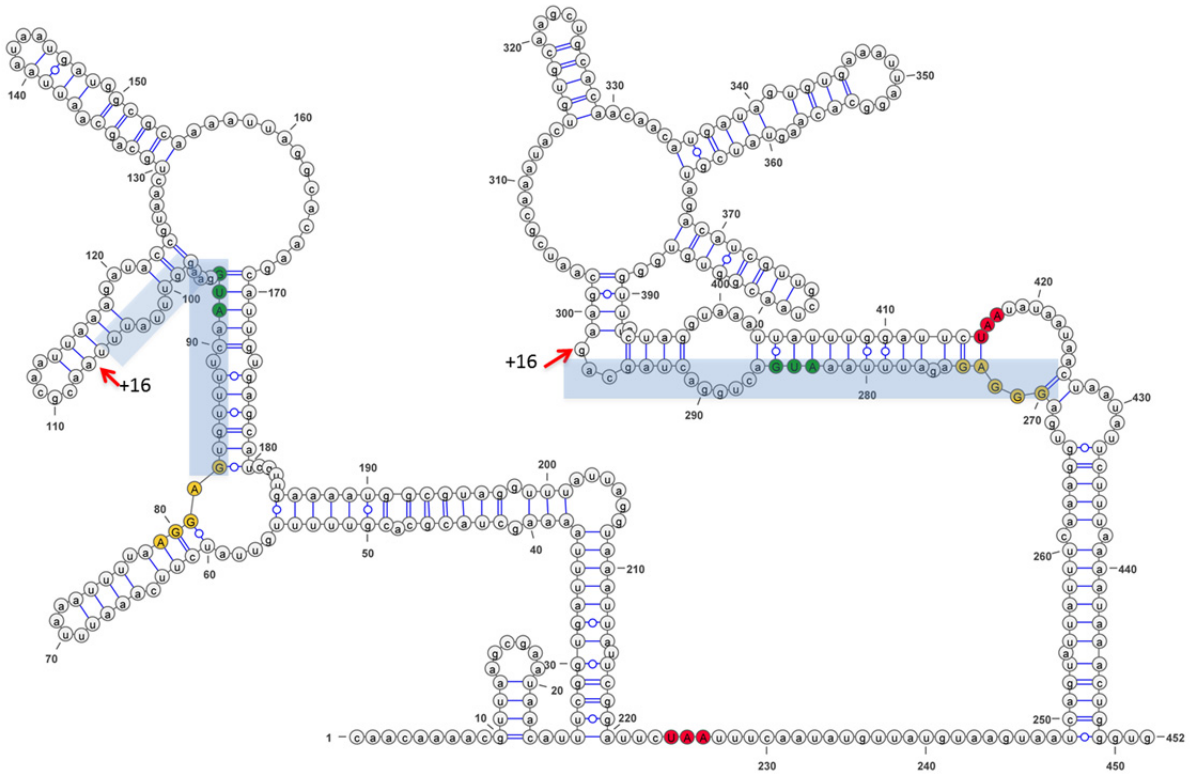

Figure 28 Secondary structure model of PSMβ operon. The PSMβ operon codes for two peptides 44 amino acids long. .PSMβ1 has strong SD sequence constrained in a stable double strand region while the SD of PSMβ2 is more accessible. Yellow and green nucleotides correspond to the SD sequences and the initiation codons, respectively. In light blue the ribosome binding sites. The position +16 is indicate by red arrows

Hence, the role of *Sau*S1 would add another layer of regulation allowing an efficient synthesis of PSM peptides at a very similar level. In favor of this hypothesis is the fact that the expression pattern of *Sau*S1 follows the expression of RNAIII and of the psm mRNAs. This fine coordination of the PSMs under both the quorum sensing control and *SauS1* might be necessary for the concerted action during acute infection, when they are produced to promote dissemination and tissue lysis. Since they contribute to biofilm detachment/dissemination (Kong et al., 2006; Periasamy et al., 2012; Tsompanidou et al., 2011), an early induction could expose *S. aureus* to the host immune system before a critical mass could have been attained. In that regard, it is worth to notice that SauS1 could also regulate the translation of the *sspABC* operon, coding endopeptidases important for immune suppression and infection dissemination (Imamura et al., 2005; Jusko et al., 2014; Ohbayashi et al., 2011). Indeed, the expression of the *sspABC* operon is strongly affected by the absence of S1 and which the RNA is among the best enriched RIP-seq targets (**Table 3)**.

The differential transcriptomics and RIP-seq experiments also revealed other virulence factors as candidates for translation activation by *Sau*S1. Among them the gene HG001_02245 coding for the Extracellular Adherence Protein (Eap) involved in adherence and internalization (Haggar et al., 2003; Palma et al., 1999). Its mRNA interacts with SauS1 (enrichment 12,2), and both the Eap protein (0,29 in the secretome) and its mRNA (0,33) levels are highly perturbed in the Δ*rpsA* strain. Also the Clumping factor *clfA*, which binds to fibrinogen to inhibit phagocytocis (Higgins et al., 2006), shares the same situation, although milder effects on the mRNA and protein levels have been detected.

Finally, two regulatory genes directly linked to virulence were found in the RIP-seq list, *agrB* and *sarA* mRNAs. AgrB is the membrane protease responsible for the release of the autoinducing peptide AIP, which is the quorum sensing signal. Its mRNA level does not change in the Δ*rpsA* strain. The significance of the possible interaction with *Sau*S1 is not clear, but since this membrane protein is detected with difficulty in *S. aureus* proteomics analyses, we cannot rule out the possibility that S1 could play a role in its translation. In that respect, the mRNA presented a short 5'UTR with a potential large hairpin motif where the SD is engaged in base-pairings. The other gene, *sarA,* is the transcription factor potentially responsible for the simultaneous expression of both *rpsA* and *psm* transcripts (see "DISCUSSION" of the manuscript). Its level is slightly increased in the Δ*rpsA* stain (1,44). The functional significance of this potential *sarA*-*Sau*S1 interaction awaits further experimental data.

I.2. Perspectives

To have a complete picture of the mRNAs, which are directly recruited by *Sau*S1 on the ribosome to be translated, ribosome profiling experiments would be an appropriate and sensitive method. Ribosome profiling approach is based on deep sequencing of ribosome-protected mRNA fragments (RPFs, usually around 30 nt). The distribution and abundance of RPF reads mapped on a given mRNA transcript reveal the locations and densities of ribosome occupation (Ingolia et al., 2009). This approach bridges the gap between global measurements of steady state mRNA and protein levels, providing a snapshot of active ribosomes in the bacteria at a specific time and under specific conditions of growth. Statistical analysis on the differential ribosome occupancy

between WT (HG001) and Δ*rpsA* would provide the extent of *Sau*S1-dependent translational control at the genome-wide scale. Furthermore, by applying different stresses encountered during the infection (*i.e.*, oxidative and NO), it would be possible to define the contribution of the *Sau*S1-mediated translational control in the regulatory circuits taking place in response to stress. Pilot experiments have been already performed (by Lucas Herrgott) to set up the conditions for optimizing cell lysis, chloramphenicol treatment to stall the elongated ribosomes on the mRNAs, nuclease digestion to recover RNA fragments protected by the ribosomes, separation of the ribosome bound mRNA fragments using sedimentation by centrifugation with a sucrose gradient, and purification of specific 25-35 nucleotides long RNA fragments before the analysis by high throughput sequencing.

Our data suggested that the *Sau*S1-mRNA complexe are dynamic explaining why I did not manage to get the footprint of *Sau*S1 on *psm* mRNA using the classical enzymatic and chemical mapping. Therefore, it would better to adapt the CLIP-seq (cross-linking immunoprecipitation and RNA-seq) approach (Jensen and Darnell, 2008) to *S. aureus*. In addition to the RIP-seq, the CLIP-seq involves a pre-treatment of the cells with UV irradiation to generate a covalent bond between RNA-protein complexes prior to the purification of RNP complexes by immunoprecipitation. RT arrest at crosslink sites during cDNA library preparation can then be used as a means of mapping the interaction sites. By combining the ribosome profiling data with the CliP-Seq, we will be able to define the interaction sites, and to gain knowledge on the regulatory mechanism at the molecular level. Our preliminary data showed that many of the mRNAs that are downregulated by *Sau*S1 carry hairpin structures with base-paired SD, and just downstream or upstream the hairpin is often present an unstructured AU rich sequence that could be appropriate for the recognition by the OB-fold domain.

Finally, to get mechanistic details on the translation activation by *Sau*S1 we could also try a more direct structural approach by analyzing ribosomal complexes using cryo-electro microscopy (cryo-EM). The gel filtration experiment (**Figure 16;** Results, §I) indicated that *Sau*S1 does not interact directly with the ribosome but together with *psm* mRNA can form a ternary complex. This complex is stable and pure (**Table S9;** Results, §I). Thus, it would be possible to get its structure by cryo-EM. In collaboration with Yaser Hashem (IBMC, Strasbourg), the laboratory contributed to the structure of the 70S

ribosome from *S. aureus* (Khusainov et al., 2017) and more ribosomal complexes are currently under investigation.

II. Involvement of *Sau*S1 in sRNAs stabilization

II.1. General discussion

*Sau*S1 was co-immunoprecipitated with numerous sRNAs (6S RNA, RsaI, RsaH, RsaE, RsaD, RNAIII, RsaA and RsaG). With the sole exception of RsaH and RsaA, their levels of expression are severely affected in the Δ*rspA* strain (**Table 4;** Results, §II.3). The observed down-regulation of these genes in the mutant strain could be due a defect of their transcription or a more rapid degradation. In Enterobacteriaceae, different classes of sRNAs are stabilized through the binding of the chaperone protein Hfq (Cui et al., 2013; Gottesman, 2004; Masse et al., 2003; Sonnleitner et al., 2006; Updegrove et al., 2016; Vogel and Luisi, 2011) and for ProQ (Smirnov et al., 2016; Smirnov et al., 2017), and more recently of another class of RNA chaperone called ProQ (Attaiech et al., 2017; Smirnov et al., 2017). It has been proposed that Hfq binding stabilizes sRNAs through a variety of mechanisms, e.g., blocking the attack of RNase E in many sRNAs (Masse et al., 2003), protect the sRNAs from a 3′-exoribonuclease attack by binding to the polyU tails of their Rho-independent terminators (Kovach et al., 2014);(Otaka et al., 2011). In contrast to this behavior, in *S. aureus* Hfq has no effect on sRNA stability (Boisset et al., 2007; Preis et al., 2009) and there is no ProQ equivalent (Attaiech et al., 2017; Olejniczak and Storz, 2017). Furthermore, in *S. aureus,* Hfq does not seem to be important for the recognition between sRNAs acting through base-pairings with target mRNAs (Zheng et al., 2016) and no major phenotypes were linked to its deletion (Bohn et al., 2007). In fact, little is known on the function of RNA-binding protein in regulation and clearly the machineries associated with RNAs have evolved differently in Gram-positive and Gram-negative bacteria. However, several ribonucleases contributed to RNA regulation such as RNase III (Boisset et al., 2007; Lasa et al., 2011; Lioliou et al., 2012), RNase J1 (Linder et al., 2014), and RNase Y (Khemici et al., 2015; Marincola et al., 2012). Besides, it was shown that the CshA DEAD-Box helicase is important to control the degradation of the *agr* operon (Oun et al., 2013) most likely through the recruitment of the degradosome (Giraud et al., 2015). Finally, SarA was unexpectedly found as an important factor that controlled mRNA stability but the binding to RNA seems to be not specific (Morrison et

al., 2012). Up to know, no major success was obtained to identify specifically RNP involving regulatory RNAs (Zhang et al., 2015).

In our study, we could demonstrate that *Sau*S1 would be responsible for a protective effect on several sRNAs. What could be the mechanism? At this regard, almost of the sRNAs strongly enriched with *Sau*S1 carry U-rich tails at their 3', which could be an appropriate binding site for S1. In these lines, RsaA, which carries a weak Rho-independent terminator (Geissmann et al., 2009a), does not bind to *Sau*S1 (**Figure 20F**). Another possibility is that SauS1 would recognize other regions on the sRNAs. Many identified sRNAs in *S. aureus*, carry C-rich regions (CRRs) predicted to interact with G-rich sequences such as SD elements in their mRNA targets. It was proposed that besides this role, the CRR could also be recognized as binding site for specific proteins, as it was demonstrated for CRR found in the 3' UTR of some mRNAs in eukaryotes (Durand et al., 2015; Makeyev and Liebhaber, 2002). The CLIP approach will be useful to map the *Sau*S1 binding site while further experiments would be necessary to clarify the stabilizing role of *Sau*S1.

II.2. Perspectives

The stability of sRNAs in the *rpsA* mutant could be determined by measuring the kinetics of their degradation after rifampicin treatment (Campbell et al., 2001). Preliminary data have been already obtained by Delphine Bronesky on the stability of RsaI, the main target of S1. The experiment was done comparing WT (HG001) with the two intron insertion mutants of *rpsA* (*rpsA*111::LtrB and *rpsA*1029::LtrB). Rifampicin was added to WT and the mutant strains grown in BHI to OD_{600}=3 (4h), when both *Sau*S1 and RsaI are present. RsaI was detected by Northern blot using total RNAs extracted after 2, 4, 8, 15, 30, 45 and 60 min (**Figure 29**). Quantification, normalization and interpolation of the data by linear regression in logarithmic scale, show an effect of *Sau*S1 on RsaI stability by factor of two, as shown in the **Figure 29**.

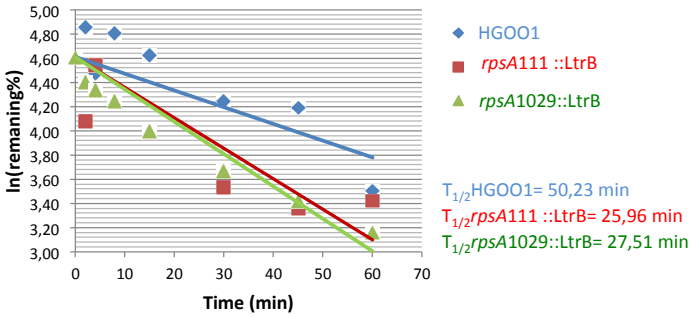

Figure 29: Stability of RsaI in different strains. After quantification of the Northern blot signals and normalization of each point to the corresponding 5S signals, the % of remaining *psm* mRNA has been plotted to calculate RsaI half-life in the three strains. $T_{1/2}$HG001 (WT) is 50.23 min, while in absence of *Sau*S1, $T_{1/2}$*rpsA*111::LtrB and $T_{1/2}$*rpsA*1029::LtrB decreased to 25.96 min and 27.51 min, respectively.

To determine the mechanism by which SauS1 recognizes sRNAs to protect them from degradation, the CLIP-seq experiment proposed above could be used to get sRNA interaction sites. Moreover, a mutagenesis analysis of those sites would be necessary to confirm their importance in *Sau*S1 recognition. At this regard, two mutants of RsaI have been obtained by Delphine Bronesky in the laboratory. RsaI regulatory regions (G-rich tract and UC-rich sequence, **Figure 24**) have been deleted separately or in combination and these RsaI variants could be used to analyze their ability to bind *Sau*S1 using gel retardation assays.

III. Involvement of *Sau*S1 in sRNA-target recognition

III.1. General discussion

Among the sRNAs isolated in complex with the protein, RsaI is the most enriched RNA. We have demonstrated that RsaI directly interacts with *Sau*S1 using gel retardation assays (**Figure 20B;** Results, §II). The works of Delphine Bronesky and Emma Desgranges in our laboratory have clarified the role of RsaI. Briefly, MS2-affinity purification approach coupled to RNA sequencing (MAPS) (Lalaouna and Masse, 2015; Tomasini et al., 2017) has allowed the characterization of its targetome. RsaG is its major sRNA target and it was demonstrated to synergically work with RsaI for the regulation of glucose metabolism. The two non-coding RNAs are expressed during the late exponential phase of bacterial growth, when *Sau*S1 is well expressed too. Both of them negatively respond to the presence of free glucose in the media (D glucose) while the expression of RsaG is enhanced by glucose 6 phosphate (G 6P). RsaI is a bifunctional

molecule able to simultaneously bind more than one target RNA throughout two different conserved regions: a G-rich tract and UC rich sequences. By footprinting experiments, I could show that the G-rich region of RsaI is responsible for the recognition of RsaG (**Figure 25;** Results, §II) while the UC rich sequence is required for the binding of many mRNA targets (D. Bronesky and E. Desgranges). Nevertheless, the predicted secondary model of RsaI (Marchais et al., 2010) and structure probing experiments (**Figure 24;** Results, §II), have evidenced that this G-rich could be constrained in a pseudoknot structure. Indeed, our preliminary probing experiments have shown that on one hand, the nucleotides of the UC rich region of RsaI are highly reactive to SHAPE, indicating a single strand conformation, but at the same time these nucleotides are also subjected to RNase V1 cuts, specific for double stranded region. On the other hand, the G rich motif is cleaved by RNase T1 (specific for unpaired G), while these nucleotides are poorly cleaved by Pb(II) induced cleavages and less reactive to SHAPE. Such mixed behavior is typical of the co-existence of multiple structures at the equilibrium and might be the signature of the presence of a pseudoknot. In fact, thermodynamic analysis has shown that an equilibrium between pseudoknot structure and alternative hairpin loop conformation existed (Philippe et al., 1990). The inaccessibility of the RsaI regulatory sequences makes necessary the action of a trans-acting factor able to unfold and remodel the secondary structure of RsaI, thus allowing target binding. RsaI and RsaG are able to interact even in the absence of *Sau*S1 (apparent K_d= 50 nM), while the addition of *Sau*S1 largely promotes the ability of RsaI to recognize RsaG (apparent K_d= 6,25 nM). Even if *Sau*S1 interacts only with RsaI, a ternary complex could be evidenced (**Figure30**).

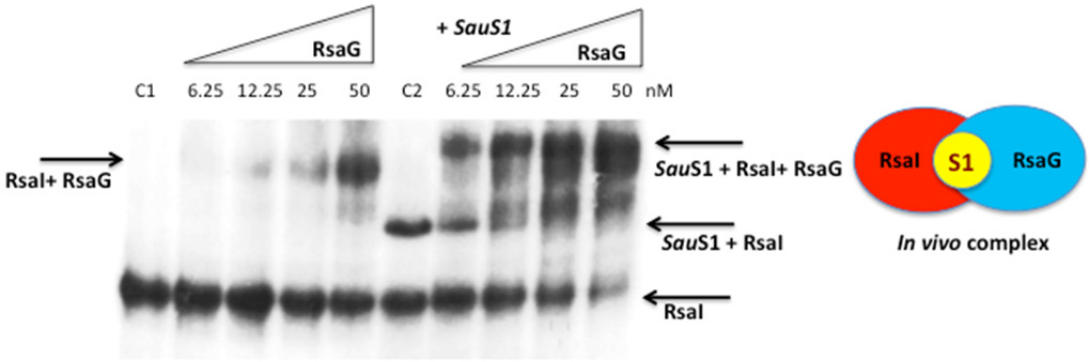

Figure 30 : Gel retardation assays to follow the formation of ternary complex *Sau*S1-RsaI-RsaG. 5' end-labeled RsaI was incubated with increasing concentration of cold RsaG in the presence and in the absence of *Sau*S1 used at 1 µM. Lanes C1 and C2 are control lanes with RsaI and RsaI-SauS1, respectively. The binary (RsaI-RsaG and RsaI-SauS1) and ternary (SauS1-RsaI-RsaG) complexes are indicated by arrows.

In Enterobacteria, the Sm protein Hfq binds to sRNAs and facilitates their base-pairing with mRNA targets. The mechanism by which it stimulates the annealing has been demonstrated by several structural works and mutagenesis analyses. Hfq from *Escherichia coli* and other Enterobacteriaceae form a compact hexamer that presents two structurally non-equivalent surfaces for RNA recognition: the proximal face, which interacts preferentially with uridine-rich sequences of sRNA and the distal face, favoring the binding of the target RNAs (Schumacher et al., 2002; Link et al., 2009; Sauer and Weichenrieder, 2011) (**Figure 31A**). In addition to the distal and proximal faces, the torus-shaped (or donut) of the Hfq hexamer bears an arginine patch sequence motif called rim that has recently been identified as a surface contributing to the annealing of both RNAs (Sauer et al., 2012; Zhang et al., 2013; (Zheng et al., 2016)). In *S. aureus*, Hfq does not accomplish this function because of the absence of this conserved rim motif of the hexamer (Panja S. *et al,* 2013(Zheng et al., 2016)). For instance, studies carried out on *S. aureus* RNAIII/*spa* mRNA model system have shown that Hfq neither form a ternary complex nor promote their annealing although it specifically binds to RNAIII and *spa* mRNA *in vitro*. Furthermore, Hfq did not affect the stability of RNAIII and *spa* mRNA *in vivo* (Eric Huntzinger et al., 2005). Therefore Hfq has probably evolved other functions in Gram-positive bacteria that are not yet determined.

Instead, in this work, we have demonstrated the ability of *Sau*S1 to promote base-pairing between short RNA molecules while the protein is not able to perform the strand displacement reaction (Figure 13). Differently from Hfq, *Sau*S1 does not interact with both RNAs (only RsaI, not RsaG) but is able to promote the formation of ternary complexes and stimulate RsaI-RsaG base pairings (**Figure 31B**). Based on the probing experiment, we proposed that this annealing activity is indirect and resulted from the remodeling of the RsaI secondary structure, i.e. melting of the pseudoknot, which would render accessible the regulatory regions of RsaI. A model is presented in **Figure 31**.

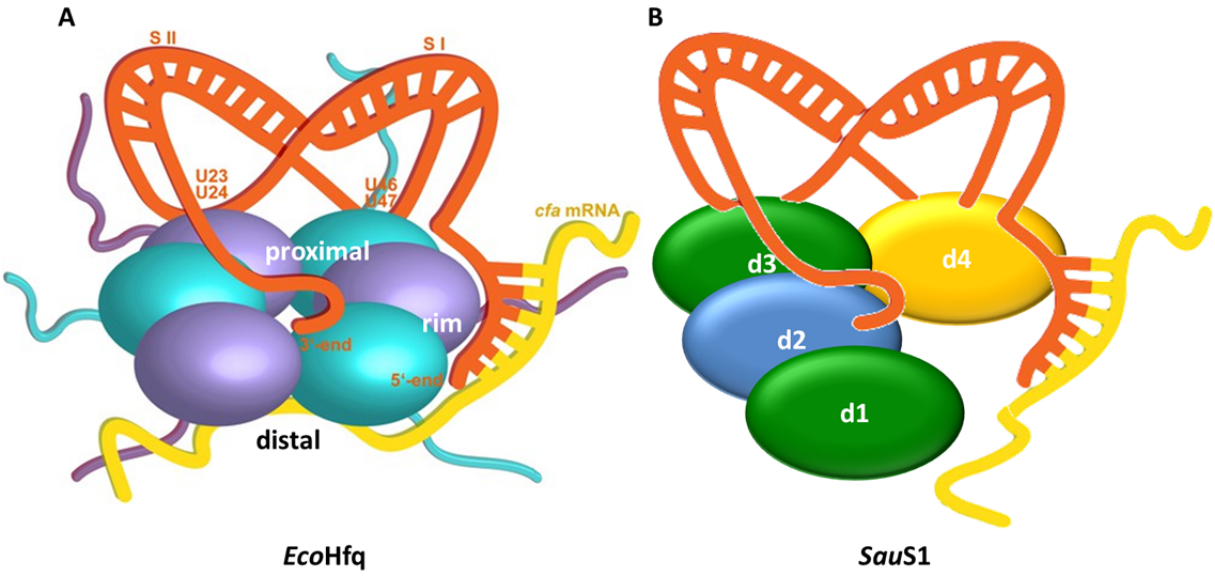

Figure 31. Hypothetical models of the sRNA/mRNA interacting with EcoHfq or *Sau*S1. Figure adapted from (Dimastrogiovanni et al., 2014). A. EcoHfq model represented by six spheres, from which the disordered C-terminal tails extend radially. sRNA (RydC pseudoknot model; orange) sits on the proximal face of Hfq, with the 3'end U-rich tail interacting with the central channel. The two double strands conferring the pseudoknot structure to RydC are indicated as S I and S II. The target mRNA (*cfa*, depicted in yellow) associates with the distal face of Hfq, and it is proposed to form a duplex with the 5' end seed region of RydC that is recognized by the circumferential rim of Hfq. B. *Sau*S1 model represented by 4 spheres for its four domains colored according to Supplementary Figure S5 of the manuscript. The sRNA (orange) binds directly to *Sau*S1 and prepare it for interaction with its target (mRNA or another sRNA as for the RsaI-RsaG case; yellow). The ternary complex thus forms via RNA-RNA base pairing
.

III.2. Perspectives

The annealing activity of *Sau*S1 could be further investigated by *in vitro* biophysical experiments. The thermodynamics of *Sau*S1-RsaI-RsaG complex formation could be obtained by ITC (Isothermal Titration Calorimetry). ITC is a quantitative technique that can determine accurately the binding affinity (Ka), the enthalpy (ΔH) and entropy (ΔS) changes, and binding stoichiometry (n) of the interaction between two or more molecules in solution. In this way, we could for example understand whether RsaI pseudoknot is melted by *Sau*S1 before RsaG binding. Another approach could be the use of the SwitchSense apparatus. In this technique, binding kinetics and conformational changes can be monitored by the real time tracking of hydrodynamic friction difference in the motion of short DNA nanolevers upon ligand binding. RsaI could be linked to the DNA levers and RsaG binding in the presence of in the absence of *Sau*S1 could be monitored. Both ITC and SwitchSense are available in our Unit.

The effect of *Sau*S1 on the kinetics of sRNA target recognition could also be monitored *in vivo*. Vanderpool and Ha laboratories have recently developed a technique to visualize

by super-resolution imaging *in vivo* fluorescently labelled sRNA (SgrS) and mRNA (*ptsG*) in *E. coli* and to determine base-pairing kinetics using mathematical modeling (Fei et al., 2015). They could quantitatively examine the effect of Hfq, showing that in the Δ*hfq* strain, the degradation rate of SgrS increased 20-fold, while the SgrS-*ptsG* mRNA association rate decreased only slightly. Similar experiments could be done to assess sRNA-target RNA couples in *S. aureus* WT or Δ*rpsA.* In collaboration with Michaël Ryckelynck (IBMC, Strasbourg), we are developing single-cell analyses on *S. aureus* RNA regulations, using microfluidics lab-on ChiP and the recently developed bright aptamer probes to visualize the sRNA (Autour et al., 2016).

IV. Involvement of *Sau*S1 in tRNA maturation

IV.I. General statement

Several tRNAs were isolated from the RIP-seq analysis. They all belong to a special class of tRNAs with chromosomally encoded CCA 3'-end. The secondary structure of the tRNAsis composed of three stem-loops (D, anticodon and T) and its 5'- and 3'-ends pair to form a fourth terminal stem, where the amino acid is attached. At the extremity of this stem a single strand region, the CCA sequence, mediates amino acid attachment occurring to the 2' or 3'-hydroxyl group of the 3' terminal A in the CCA-motif by the aminoacyl-tRNA synthetases (Meinnel *et al,* 1995; Giegé and Springer, 2016).

The presence of chromosomally encoded 3'-CCA, is not a universally conserved feature of tRNA genes. Indeed some bacteria like *E. coli*, have this sequence encoded in all tRNAs (Hartmann, 2009; Blattner, 1997), while other bacteria, such as *S. aureus*, lack the 3'-CCA in some of its tRNA genes. In these cases, the CCA-end is added post-transcriptionally like in eukaryotes by the tRNA-nucleotidyl transferase (Weiner, 2004; Xiong et al., 2006). When directly transcribed as in the *Sau*S1 interacting tRNAs, the CCA is a crucial signal required for the activation of alternative 3' maturation pathway of the tRNA primary transcript (Kirsebom and Svärd, 1994; Wegscheid and Hartmann, 2007). Indeed while the tRNA 5'-end processing is a largely conserved process catalyzed by the ubiquitous RNase P (Hartmann, 2009; Gopalan, 2007), the maturation of the 3'-end is a more complex mechanism and it varies according to the presence or not of the chromosomally encoded 3'-CCA (Hartmann et al., 2009; Marck et al., 1993). In *E. coli*, the tRNA processing is initiated by the endoribonuclease RNase E few nucleotides

downstream of the 3'-CCA sequence to generate pre-tRNAs with short or long 3' External Transcription Sequences (3'ETS) (Li and Deutcher, 2002). An AU-rich sequence in the proximity of the tRNA 3'-end (Li et al., 2005) is presumably recognized as a signal sequence during the endonucleolytic processing of the 3'-ETS. In contrast, Gram-positive bacteria lack the RNase Eand the conserved AU-rich sequence is also not present in this region. In tRNAs, where RNase E cleaves further away from the 3'-CCA sequence, exoribonucleases like RNase II and PNPase initiate 3'-end maturation producing shorter 3' trailers which are then completely matured by the action of RNase PH and RNase T (Li and Deutscher, 1995, 1996). Alternative pre-tRNA 3' end maturation processes were observed in *B. subtilis* (**Figure 32**). Indeed, the tRNAs missing the CCA end, are processed at their 3' end by a single endoribonuclease, the RNase Z. After this primary step, the CCA is added by the tRNA nucleotidyl transferase (Pellegrini et al., 2003), an enzyme also involved in the repairing of damaged 3'CCA ends in mature tRNAs. In contrast, if the 3'-CCA is encoded, the pre-tRNAs are matured by the exonucleolytic action of RNase R, PNPase and RNase PH in a process similar to *E. coli* (Pellegrini et al., 2003; Wen et al., 2005).

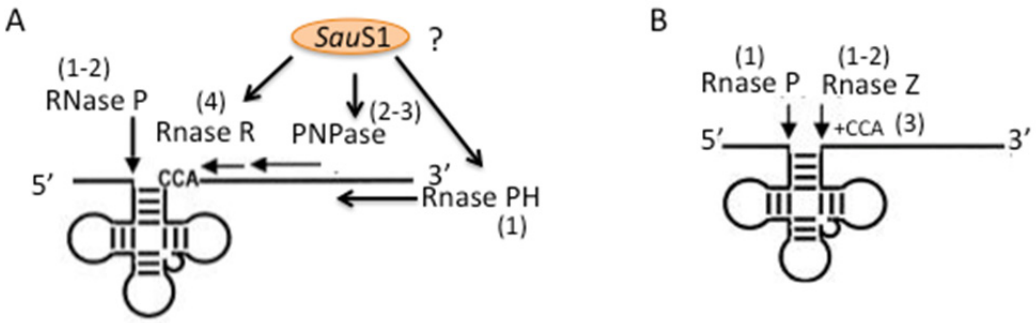

Figure 32 Processing of 3' end CCA- encoded and 3' end CCA- less tRNAs. Vertical arrows on 5' leader of tRNA precursor represents the endoribonucleolytic cleavage carried out by the RNase P (A-B)., while horizontal arrows on the 3' trailer represent the exoribonucleolytic trimming accomplished by RNase PH, PNPase RNase R (A) and RNaseZ (B). *Sau*S1 could be required for the exonucleolitic activity of one of the enzyme involved in the 3' end processing. Addition of CCA by tRNA nucleotidyl transferase is marked as "+CCA." The order of processing reactions is marked by numbers in parentheses.

By inspecting the reads distribution of the differential transcriptomic analysis at the loci of the immunoprecipitated tRNAs with the IGV browser (Thorvaldsdottir et al., 2013), an higher density could be observed at the 3'ETS in the Δ*rpsA* (**Figure 33**). We speculate a possible role of *Sau*S1 in assisting the exoribonucleolytic activity of one of the involved enzymes (RNase R, PNPase or RNase PH).

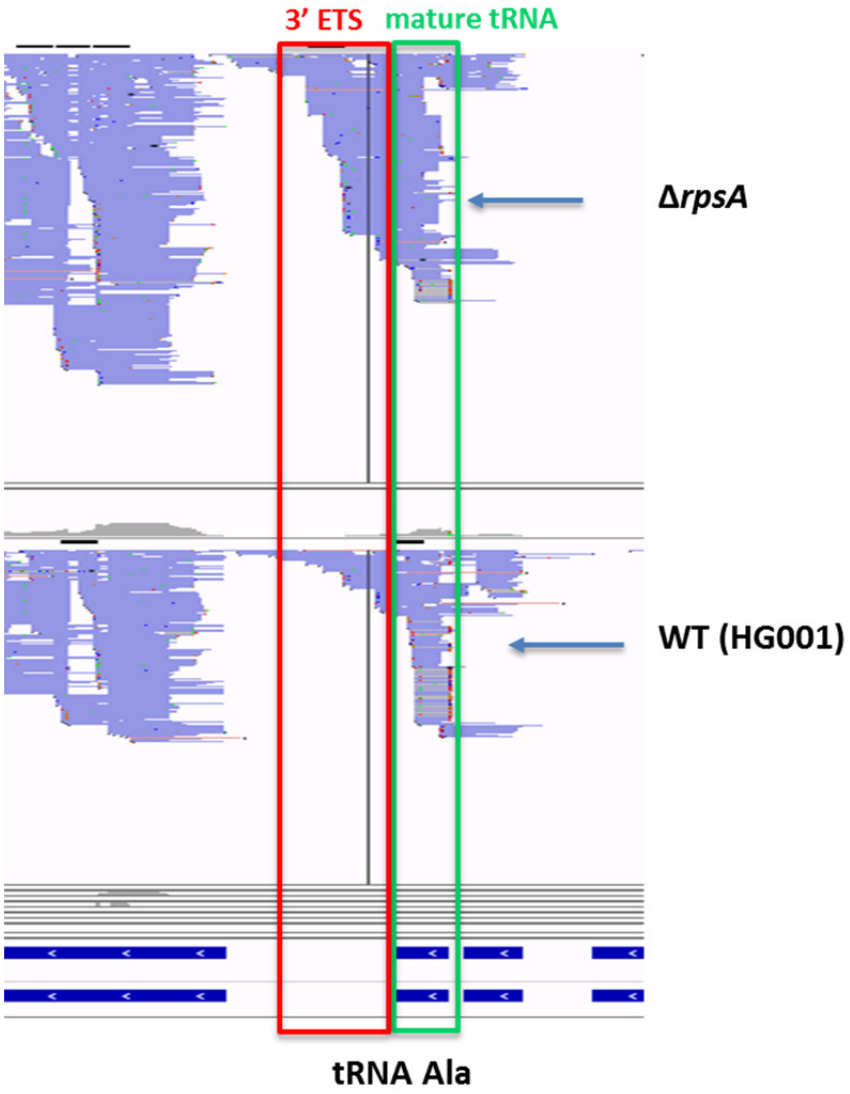

Figure 33. tRNA maturation defect in the Δ*rpsA* strain. Comparative analysis of reads accumulation between wild-type HG001 and the Δ*rpsA* strains. Here details of the HG001_00443 locus for the Ala-tRNA (tgc) that was isolated in complex with *Sau*S1. The accumulation of reads at the 3'-ETS could indicate a defect of maturation.

Moreover, defects in tRNAs processing or incorrect folding, are linked to the formation of non-functional molecules that are subjected to quality control mechanisms (Li et al., 2002) and are often rapidly degraded. It has been proposed that this process takes place at the 3'-end via the polyadenylation made by the poly (A) polymerase (PAP) followed by the trimming of the adenines by RNase R and the PNPase (Zhongwei Li et al., 2002). The presence of non-matured tRNA species in the Δ*rpsA* would imply defects in the maturation process but also an unefficient clearance of the unprocessed pre-tRNA.

To understand which nucleases might require *Sau*S1 action, we have performed an immunoprecipitation experiment under the same conditions for the RIP-seq, but looking at which protein complexes would be co-purified with *Sau*S1 by LC/MSMS. Among the most enriched proteins, we have identified several ribosomal proteins and RNases, which are known to be part of the *S. aureus* degradosome (Giraud et al., 2015; Roux et al., 2011) (**Table 5**).

Ribosome							
Name	**Gene**	**Description**	**References**	**log2FC**	**p.value**	**adjp**	**-log10(adjp)**
Small subunit							
bS16	*rpsP*	Ribosomal protein bS16	Khusainov et al., 2016	6,05	0,00005	0,00033	3,48
uS9	*rpsI*	Ribosomal protein uS9	Khusainov et al., 2016	5,77	0,00016	0,00092	3,04
uS4	*rpsD*	Ribosomal protein uS4	Khusainov et al., 2016	3,78	0,00042	0,00223	2,65
uS7	*rpsG*	Ribosomal protein uS7	Khusainov et al., 2016	3,61	0,00018	0,00098	3,01
uS17	*rpsQ*	Ribosomal protein uS17	Khusainov et al., 2016	3,57	0,00001	0,00005	4,27
uS13	*rpsM*	Ribosomal protein uS13	Khusainov et al., 2016	2,75	0,00122	0,00518	2,29
bS20	*rpsT*	Ribosomal protein bS20	Khusainov et al., 2016	2,34	0,00000	0,00000	5,48
Large subunit							
uL23	*rplW*	Ribosomal protein uL23	Khusainov et al., 2016	5,05	0,00693	0,02407	1,62
bL9	*rplL*	Ribosomal protein uL9	Khusainov et al., 2016	5,04	0,00323	0,01264	1,90
uL29	*rpmC*	Ribosomal protein uL29	Khusainov et al., 2016	4,61	0,01046	0,03454	1,46
bL12	*rplL*	Ribosomal protein uL12	Khusainov et al., 2016	4,57	0,01313	0,04175	1,38
uL6	*rplF*	Ribosomal protein uL6	Khusainov et al., 2016	1,35	0,01614	0,04905	1,31
Degradosome							
Name	**Gene**	**Description**	**References**	**log2FC**	**p.value**	**adjp**	**-log10(adjp)**
RNJ1	*rnjA*	Ribonuclease J 1	Roux et al., 2011	8,86	0,00000	0,00000	10,84
RNJ2	*rnjB*	Ribonuclease J 2	Roux et al., 2011	8,71	0,00000	0,00000	10,31
PNP	*pnp*	PNPase	Roux et al., 2011	7,80	0,00001	0,00007	4,18
RNY	*rny*	Ribonuclease Y	Roux et al., 2011	5,78	0,00142	0,00597	2,22
Tex	*Tex*	Toxin Expression, structurally similar to Eukaryotic Spt6 involved in transcription and RNA maturation		5,75	0,00143	0,00597	2,22
PNP-like	*SAOUHSC_00483*	Sequence similarity with PNPase		4,67	0,01026	0,03422	1,47
CshA	*CshA*	DEAD-box ATP-dependent RNA helicase	Giraud et al., 2015	3,67	0,06397	0,14370	0,84

Table 5. *In vivo* complexes involving *Sau*S1. SauS1 co-immunoprecipitation was performed under the same conditions as for the RIP-seq experiment (Results). The protein were extracted and analyzed by LC/MSMS. Two main cellular complexes have been found to co-purify with S1, the ribosome and the degradosome.

While RNase R and RNase PH do not seem to be associated with *Sau*S1, PNPase was found to be the most enriched together with RNases J1 and J2. It is thus possible that *Sau*S1 helps PNPase in the processing of 3'ETS of tRNAs with encoded CCA. PNPase is arrested by stem–loop structures and it is tempting to propose that the chaperone activity of *Sau*S1 would help removing them to prepare the pre-tRNA substrate for efficient maturation. RNases J1 and J2 are 5'-3' exoribonucleases (and endonucleases as well (Hausmann et al., 2017)) involved in the 5' maturation of both the 16S rRNA and the RNase P. They could also perform initial cleavages, competing with ribosomes for the stability of *S. aureus* mRNAs (Linder et al., 2014). In our transcriptomic analysis, we have removed the rRNA (RiboZero depletion; Illumina) and therefore we cannot draw any conclusion about 16S rRNA processing. Nevertheless, a slight accumulation of reads

at the 5' of the RNase P RNA could be observed in the Δ*rpsA* strain (data not shown). Is *Sau*S1 helping exoribonucleases in their maturation activities? More experiment will be necessary to clarify this possible function.

Interestingly, the multiple functions of *Sau*S1 in translation and tRNA maturation, was also demonstrated for a protein largely conserved in wide variety of eukaryotes, named protein La. As *Sau*S1, La protein is an RNA chaperone able to interact with different RNA molecules including precursor tRNAs, 5S rRNA, the signal recognition particle SRP (J.P Hendrick et al., 1981 - J Rinke, J.A Steitz, 1982 - J Rinke, J.A Steitz, 1985). The La proteins recognize their RNAs through a UUU_{OH} 3' sequence. Despite its best characterized function is to protect premature exoribonucleolitic digestion of tRNAs during their processing, La protein has been show to bind to several mRNAs affecting their translation (Christopher J Yoo1, Sandra L Wolin, 1997).). A La-related protein LARP7 is also a component of the 7SK RNP assembly and as the La protein binds to a UUU sequence motif at the 3' end of the RNA (Market et al., 2008; Uchikawa et al., 2015).

IV.2. Perspectives

To confirm the 3'ETS maturation defect, Northern blot analysis using specific probes targeting the ETSs will be performed. Alternatively, RT-PCR experiments can be envisaged. Two-dimensional (denaturing and semi-denaturing conditions) electrophoresis on polyacrylamide gels (Suyama, 1986) could also be used for the separation of mature tRNAs from unprocessed transcripts. In the long term, mutant strains at specific genes encoding exoribonucleases will be constructed and studied to define the pre-tRNA processing pathway at the 3' end, and the role of *Sau*S1 in this pathway.

V. Involvement of *Sau*S1 in *cis-acting* regulatory elements

The most widespread example of RNA regulatory elements in bacteria are riboswitches, complex folded RNA domains located in the non-coding regions of mRNAs, that control gene expression by binding specific metabolites (cofactors, vitamins, amino acids, nucleotides, Mg2+, second messenger cyclic di-GMP). Simple riboswitches are composed of two regions: an aptamer, responsible for ligand binding and an expression platform,

located in the 5' UTR of the regulated mRNA and/or operon. Upon ligand binding to the aptamer domain, a structural rearrangement is promoted on the nearby platform. Regulation mediated by riboswitches can occur at the transcriptional and/or translational levels. Translational riboswitches act throughout the formation of secondary structures, which sequester the RBS or the SD sequences of target mRNAs. This regulatory mechanism is not widespread in *S. aureus*. The only example in *S. aureus* is given by the flavin mononucleotide (FMN) riboswitch that controls the expression of *ribU* (HG001_01344 in HG001), encoding a membrane riboflavin transporter. It has been proposed that in the absence of the ligand, the platform has a conformation competent for the mRNA translation, while the binding of FMN induces the formation of a hairpin structure which sequesters the SD sequence of the mRNA thus inhibiting its translation (Geissmann et al. 2009; Marchais et al. 2009; Abu-Qatouseh et al. 2010; Beaume et al. 2010; Bohn et al. 2010; Ten Broeke-Smits et al. 2010). In general, riboswitches work by forming Rho-dependent terminators to prematurely arrest the transcription of the downstream genes (Gusarov and Nudler 1999; Yarnell and Roberts, 1999). *S. aureus* FMN riboswitch (HG001_01693) which was specifically co-immunoprecipitated with *Sau*S1, is a transcriptional riboswitch which controls the expression of genes involved in the biosynthesis and/or transport of riboflavin (vitamin B2). It has been shown that the binding of FMN to the aptamer of the *ribD* operon (*ribDEBAH* genes) induces the formation of an intrinsic transcription terminator thus blocking the synthesis of vitamin when it is not required (Pedrolli D. Biscaro, Suess B, 2015) (Serganov et al., 2009; Wickiser et al., 2005) (**Figure 34**).

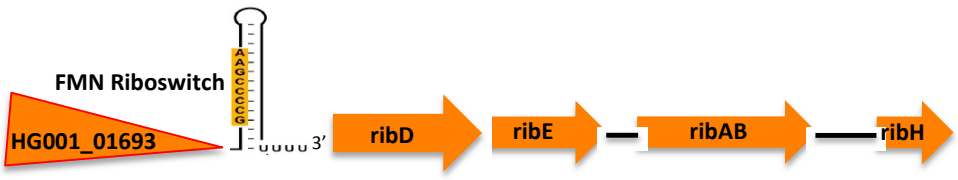

Figure 34: FMN riboswitch controlling *ribD* operon. In *S. aureus* as well as in *B. subtilis*, the riboflavin genes are organized in a large operon. The 5' UTR of the corresponding mRNA contains a riboswitch (HG001_01693) that controls the expression of the whole operon. When the levels of FMN are sufficient, it binds to the riboswitch with the formation of a terminator at the platform region. Transcription is then halted and the genes necessary for the riboflavin production and transport are repressed.

Our transcriptomic analysis of the Δ*rpsA* strain has shown an up-regulation of the FMN riboswitch (2.5) as well of the genes that are under its control (*ribD* 2.3; *ribE* 4.4; *ribBA* 2.9; *ribH* 2.6). The whole operon is thus enhanced. This indicates that in the absence of *Sau*S1, the Rho-independent terminator did not form efficiently otherwise the downstream gene of the *ribD* operon would have been repressed. It is possible that to form correctly, the terminator needs the action of *Sau*S1. By binding specifically to the riboswitch region (RIP-seq data), *Sau*S1 might acts as a helper protein to promote the switch between alternative conformers for efficient regulation.

Interestingly, other riboswitches seem to require *Sau*S1. The Glycine riboswitch (HG001_01462) interacts with *Sau*S1, its level is slightly less in the Δ*rpsA* (0.62 but with a bad p-value) while the regulated downstream operon *gcvT* is upregulated. Finally, also the T-box riboswitches for the aminoacyl tRNA synthetases ThrRS and AlaRS are enriched with *Sau*S1 as shown in the RIP-Seq, and the downstream corresponding genes are upregulated in the Δ*rpsA* mutant strain.

The CLIP-Seq approach and single-round *in vitro* transcription assays would be helpful to precisely define the role of *Sau*S1 in these processes (Choonee et al., 2007).

VI. General conclusion

Despite the fact that *Sau*S1 is not essential, we have demonstrated its crucial role in the correct coordination of different virulence factors.

First, we have shown that it acts as translational activator of PSMα peptides, even if not associated on the ribosome (**Figure 35**). *Sau*S1 could work as an RNA chaperone on its target mRNAs, removing inhibitory structures and increasing their ability to bind the ribosome and to present their AUG start codon for initiator tRNA interaction. We have also shown that the protein is involved in the production of several secreted virulence factors thus globally impacting *Staphylococcal* virulence.

In our study we have proposed the possible involvement of *Sau*S1 in RNA metabolism. Analysis of isolated S1-*in vivo* complexes has allowed the identification of several classes of RNA targets whose level of expression is affected in the Δ*rspA* strain. By binding to sRNAs, not only *Sau*S1 could protect them from rapid degradation but also we have demonstrated, at least in one case, to promote the annealing between a sRNA and its target, probably by helping the RNA to get its functional conformation.

Comparative transcriptomic analysis has been found an up-regulation of the FMN riboswitch, *in vivo* isolated with *Sau*S1, and of the genes under its control. We assume that in absence of the protein the formation of the terminator fails, thus allowing the expression of downstream genes.

Moreover we have proposed a link between *Sau*S1 and the degradosome. Indeed, in absence of the protein a defect of maturation and degradation of 3' end CCA- encoding tRNAs has been observed.

Taken together, my results highlight, a key RNA binding protein involved in gene expression regulation in *S. aureus*. Whether the action of *Sau*S1 in translation initiation as well as in regulatory mechanisms might be conserved in other Gram positive bacteria remained to be elucidated.

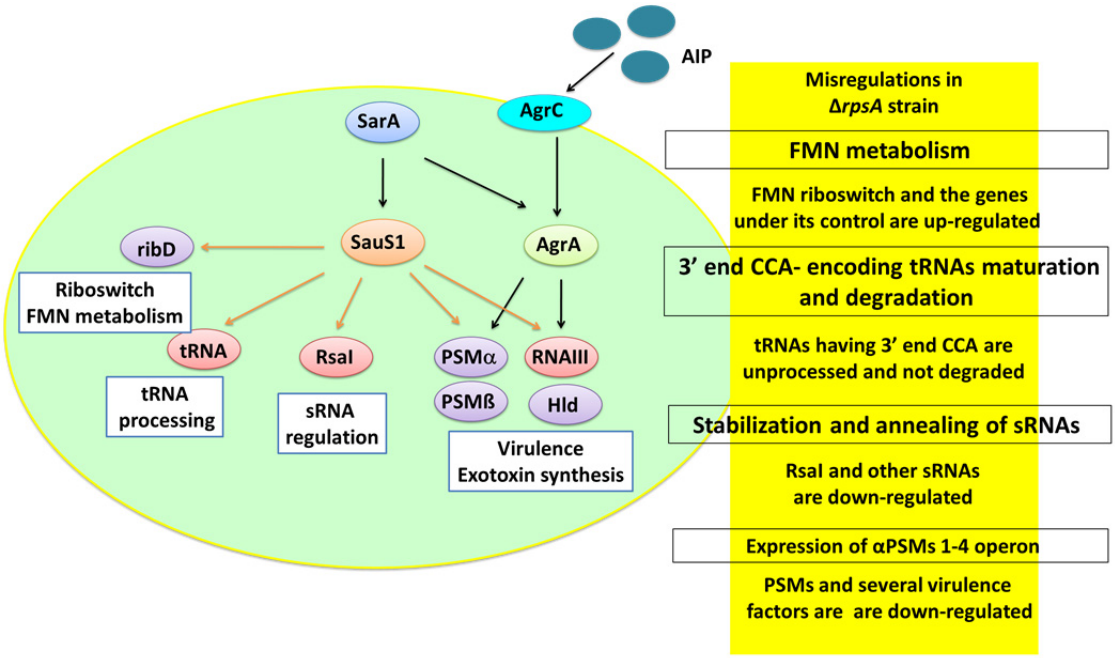

Figure 35: Summarized picture of regulatory networks coordinated by *Sau*S1: AgrC activates AgrA in response of appropriate level of secreted AIP. The three *PSM*s locus are controlled both at transcriptional level by AgrA and at translational level by *Sau*S1. SarA is responsible of the *rpsA* and *psm* transcript expression. Co-immunoprecipitation assay of a flag-tagged version of *Sau*S1 has allowed the identification of its *in viv*o targets including mRNAs, sRNAs, riboswitches and 3' end encoding CCA- tRNAs. All the identified targets are affected in the Δ*rpsA* strain. Examples of misregulation per each class of molecule are given in the yellow panel.

Materials and Methods

Media and growth of bacteria

Pre-cultures were started from glycerol stocks. *S. aureus* was grown in Brain Heart Infusion medium (Fluka, analytical) while *E. coli* in Luria-Bertani Broth Powder microbial growth medium (Sigma-Aldrich) supplemented if needed with antibiotics (100 mg/liter ampicillin and 100 mg/liter erythromycin), at 37 °C over night under constant agitation (300 rpm). The cultures were started at OD_{600}= 0,02 respecting 1:5 flask-culture volume ratio.

The tested stress conditions were applied at OD_{600}= 1 and then optical density was followed each 30 minutes until the end of bacterial growth.

Purification of SauS1

Single colony of *E. coli* M15, transformed with the pQE30 (Qiagen) plasmid carrying *Sau*S1, was grown in LB medium supplemented with 100 mg/liter ampicillin and 100 mg/liter erythromycin at 37°C under constant agitation (300 rpm) over night. The pre-culture was inoculated in 1 L of fresh LB supplemented with appropriated antibiotics and incubated at 37 °C until OD 600_{nm}=0.6, when overexpression of the protein was induced using IPTG. An aliquot of 1 ml of culture was taken before the induction (BI) as control, centrifuged (2 min at 1000g, 4°C) and resuspended in 100 µL of protein loading buffer. 1, 2 and 3 hours after induction, aliquots of 1 ml each were taken as controls after induction (AI) and treated in the same way as BI. At the end of the growth the cells were pelleted by centrifugation (15 min at 4200rpm, 4 °C), washed with 10 mM Tris-HCl pH 7.5 and then resuspended in buffer A. Before sonication (120 V, 10 sec of sonication followed by 30 sec on ice, repeated at least 15 times), 3 µl of DNAse (RNase free, Roche 10 U/ul), protease inhibitor cocktail 1X (Roche) and 35 mg lysozyme (Sigma), were added.

Sonication

Bacterial lysis was obtained for sonication (120 V, 10 sec of sonication followed by 30 sec on ice, repeated at least 15 times). In order to remove cellular debris, the sample was centrifuged at 4200 rpm for 30 min, 4 °C. The supernatant (S30) was recovered and an aliquot of 15 µl was taken for SDS-page analysis. The SDS-page gel was prepared at 12%.

First Ni-NTa column purification

The Ni-Nta agarose beads (Agarose, Qiagen) were washed using Qiagen protocol (http:///www.qiagen.com/literature/render.aspx?id=201426) and than were resuspended in 8 ml of Buffer E. The S30 was incubated with the NI-Nta beads for 1 hour at 4 °C under agitation. At the end of the incubation, the sample was loaded on Poly-prep chromatography column (Biorad). The flow-thought (FT) was recovered in a falcon tube and the column was washed with 8 ml of Buffer E. The elution of *Sau*S1 fused with 6-Hys was obtained by using increasing concentration of imidazole (10 ml of imidazole at 20 mM, 50 mM and 100 mM). An aliquot from each fraction (10 µl of FT, 30 µl of wash, 20 mM, 50 mM and 100 mM supplemented with ½ of loading proteins buffer) was loaded on 12% SDS-PAGE gel.

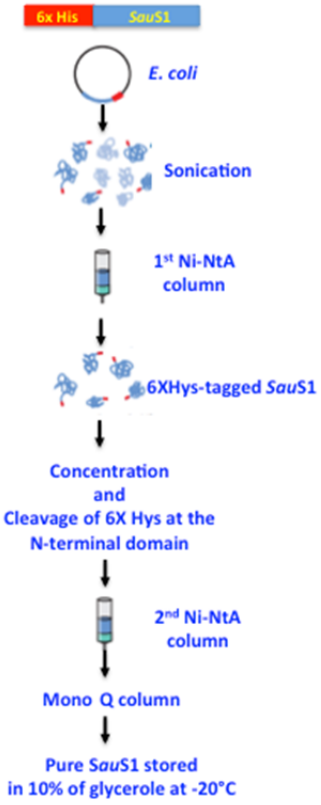

Figure 36 Schematic summary of *Sau*S1 purification

Dialysis

The fractions containing *Sau*S1, were dialyzed over night at 4 °C under agitation against

buffer Q. (Slide-A-Lyzer dialysis cassette, 3500 MWCO, 15 ml)

Protein concentration

Dialyzed protein was concentrated using M Centrifugal filter units 15 ml, 10K tubes. The centrifugation was performed for 25 minutes at 4200 rpm, 4 °C until the protein riched a final volume of 1 ml (25 mg/ml). *Sau*S1 was than enzymatically digested using 120 µl of Protean 10U Tev.

Second Ni-Nta column purification

The Ni-Nta agarose beads were washed as descrived above and then were resuspended in 8 ml of Buffer Q. The cleaved protein was incubated with the NI-Nta beads for 1 hour at 4 °C under agitation. At the end of the incubation, the sample was loaded on Poly-prep chromatography column (Biorad). The flow-thought (FT) was recovered in a falcon tube and then the column was washed with 8 ml of Buffer Q and treated with 10 ml of imidazole at 20 mM, 50 mM and 100 mM. An aliquot from each fraction (10 µl of FT, 30 µl of wash, 20 mM, 50 mM and 100 mM of imidazole, supplemented with ½ of loading proteins buffer) was loaded on 12% SDS-PAGE gel.

FPLC using anion exchange column

The fractions containing the cleaved protein (FT and wash) were centrifuged for 1 hour at 8000 rpm, 4 °C in order to pellet the cellular debris and eventually formed aggregates that could obstruct the anion exchange column (GE Healthcare). Before loading the sample, the column was washed with 5 vol of mQ water, 5 vol of buffer QB and 5 vol of buffer Q (all the buffer were filtered and degassed). Upon the injection of the sample, *Sau*S1 was eluted by gradient of HH_4Cl (from 40 mM to 1 M, buffer QB). The fraction identified on the MonoQ analysis, having an absorbance peak at 280 nm were analyzed by polyacrylamide-SDS gel 12%. The fraction containing pure protein, were poolled and dialyzed over night at 4 °C using storage buffer. As dialysis cassettes were used the Slide-A-Lyzer dialysis cassette, 3500 MWCO. The concentration of the protein was

estimated using the specific protein extinction coefficient (ε = 47565M-1cm-1, www.expasy.ch). It has to be taken into account that *Sau*S1 does not contain any Trp and this could result in more than 10% error in the computed extinction coefficient. The purified protein was finally stored at -20 °C in 10% of glycerol.

Buffer A : Tris-HCl pH 7,5 20 mM, MgCl2 2 mM, KCl 60 mM, NH4Cl 1 M, EDTA 10 mM, β mercaptoethanol 10 mM

Buffer E : Tris HCl pH 7,5 20 mM, MgCl2 2 mM, KCl 60 mM, NH4Cl 1 M, imidazole 10 mM, β mercaptoethanol 10 mM

Buffer Q : Tris-HCl pH 7,5 20 mM, MgCl2 2 mM, NH4Cl 40 mM, EDTA 1 mM, β mercaptoethanol 6 mM

Buffer QB : Tris-HCl pH 7,5 20 mM, MgCl2 2 mM, NH4Cl 1 M, EDTA 1 mM, β mercaptoethanol 6 mM

Storage buffer : Tris-HCl pH 7,5 20 mM, NH4Cl 40 mM, KCl 60 mM, TCEP 200 µM, glycerol 7 %

SDS-PAGE analysis

The SDS-PAGE gel is composed of two gels, the first of resolving and the second of running. Its concentration is depending on the size of the molecules that has to be analyzed (for *Sau*S1 10 – 12%). Before loading on the gel, the samples were diluted in 1 vol of protein loading buffer and heated at 90 °C for 3 min. The migration buffer was TGS 1X and the gel was runned at 80V until the end of the resolving part and then at 150 V until the end of the run.

Resolving gel : Tris HCl pH 6,8 80 mM, SDS 0,1%, 5% acrylamide, APS 0,1%, Temed 1/1000

Running gel : Tris HCl pH 8,8 500 mM, SDS 0,1%, 12% acrylamide, APS 0,1%, Temed 1/1000

Loading protein buffer : Tris-HCl pH 6,8 60 mM, Glycerol 25 %, SDS 2 %, β mercaptoethanol 5 % (0,7 M), bromophenol blue 0,1 %

TGS 1x : Tris 25 mM, glycine 200 mM, SDS 0,1%

Co-immunoprecipitation assays

Chromosomally flag-tagged *Sau*S1 and wild type BEJ100 strains were grown in BHI medium at 37°C, under constant agitation at late exponential phase. At the end of the growth, the cells were centrifuged for 10 min at max speed and the pellet was stored at -20 °C. Bacterial cell pellet was suspended in 2 mL of lysis buffer, transferred onto glass beads (provided by FastRNA Pro Blue Kit, Qbiogene) and processed in the FastPrep instrument (3645 s at a setting of 6.0). Samples were centrifuged at 13,000 rpm for 2 min. The supernatants were mixed with Anti-Flag M2 Affinity Gel (Sigma, A2220) and incubated at 4°C for 60 min. Then the beads were washed three times with TBS. Elution was made with 0.2 ml of 3X Flag Peptide (Sigma, F3290) prepared at the concentration recommended by the supplier. The sample was extracted with acidic phenol and then by chloroform-isoamylic alcohol. RNA was precipitated with ethanol, treated with DNase I, extracted with phenol and precipitated. The final RNA samples were dissolved in 50 ml of sterile water and lyophilized.

Deep-sequencing analysis

cDNA-seq libraries were constructed with RNA samples isolated from Co-IP experiments under late-exponential phase of growth of the Flag-tagged *Sau*S1 and wild-type BJ100. The resulting cDNA libraries were sequenced on a Roche 454 sequencer using FLX and Titanium chemistry. From the resulting cDNA reads, 5′-linker sequences and polyA-tails were clipped from the sequenced cDNA reads. Only reads of ≥18 nt were aligned to the reference genome, which was retrieved from the NCBI server (accession number of the chromosome: NC_002745.2; accession number of the plasmid: NC_003140.1), using the program segemehl. Based on the resulting mapping data, read coverage files were generated in the GR format representing the number of mapped reads per nucleotide. The GR files were visualized in combination with FASTA and GFF files of the genome using the Integrated Genome Browser (IGB) (Nicol JW *et al.,* 2009). Additionally, overlaps of mapped reads and gene annotation positions were identified and counted. The overlap between mapped read and a gene annotation had to be at least 10 nucleotides long to be taken into account. Each single overlap counting was normalized by the number of positions to which the overlapping read was mapped and the number

of annotations that overlap with the read. For instance, if reads map to multiple regions with exactly the same score (e.g. this is the case for reads that map to the different multiple copies of the rRNA genes), only a relative fraction of one read is counted instead of a count of one read. For example, if a read maps twice, each location gets a score of 0.5 reads. Moreover, if a read overlaps two annotations, each annotation gets a score of 0.5 reads.

Lysis buffer : 20 mM Tris HCl pH8 – 150 mM KCl – 1M $MgCl_2$ – 1 mM DTT.

Bandshift on polyacrylamide gel

The 5'-end labeled RNAs (50.000 cpm/line) and cold RNAs were denatured at 95 °C for 1 min, cooled on ice for 1 min and then renatured at 20 °C for 10 min in presence of 10 mM of $MgCl_2$. The protein was incubated in *Sau*S1 buffer 1X + for 15 min at 37 °C. The RNAs were incubated with increasing concentration of protein, except for the first tube used as RNA control and complex formation was performed at 37 °C for 15 min. After incubation, 1 vol of glycerol blue was added in each tube before the loading on acrylamide gel containing 1mM of $MgCl_2$ in TBE 1X. The gels were runned according to the size of the RNAs at 4°C at 300 V.

*Sau*S1 buffer 10 X + : 200 mM Tris HCl 7.5, 600 mM KCl, 400 mM NH_4Cl, 30 mM DTT, 100 mM $MgCl_2$, 0.2mg/ml BSA.

Chemical probing of S. aureus RsaI

Chemical probing with BzCN was performed as in Helfer *et al*. 2013 with the exception that Vic and Ned fluorescent labeled oligonucleotides (**Tab5**) have been used. Separation of RT fragments has been done using ABI PRISM 3I 30XI Genetic analyzer.

Enzymatic probing of RsaI

5' end-labeled RsaI (50 .000 cpm/line) was denatured in sterile water at 90°C for 1 min, cooled on ice for 2 min and briefly centrifuged. Native buffer 5X was added and the

samples are incubated at 20°C for 15 min for renaturation. 1µl of total tRNA 1 µg/µl was added to all samples. Enzymatic hydrolysis was performed by addition of 1 mL RNase as follows:

-RNase T1 10 min at 20°C

-RNase T2 10 min at 20°C

-RNase V1 5 min at 25°C

-Lead II 5 min at 20°C

0.3 M Na-acetate of pH 6.0 and cold ethanol were then added to all samples. After a vigorous mix, the samples are transferred in a dry ice-ethanol bath for 10 min. The samples are then precipitated, washed and dried and resuspended in 6 µL of urea blue.

RNase T1 ladder: labeled mRNA (25,000 cpm) is preincubated at 50°C for 5 min in 5 mL of the Buffer ΔT1 containing 1 mg total tRNA. Reaction is then performed at 50°C for 10 min in the presence of 1 mL of RNase T1 (0.5 U).

Alkaline ladder: labeled mRNA (100,000 cpm) is incubated at 90°C for 3 min in the presence of total tRNA (2 mg) in 5 mL of the Ladder Buffer.

Before loading, each sample was adjusted to contains the same amount of radioactivity (except for the ladder that should have twice more radioactivity). The samples were heated (except the RNase T1 and alkaline ladders) for 3 min at 90°C. The 12% acrylamide was prerunned at 75 W for 30 min using 1× TBE as running buffer.

The samples were finally loaded on the gel, runned in TBE 1X for 2 hours at 75W.

Native buffer 5X : Hepes Na-OH pH 7.5 100mM – Mg2+ Acetate 25 mM - KCH3COO 250 nM

Footprinting RsaI*/RsaG

5’ end-labeled RsaI (50 .000 cpm/line) and 1.25 µM of cold RsaG were denatured in sterile water at 90°C for 1 min, cooled on ice for 2 min and briefly centrifuged. Native buffer 5X was added and the samples are incubated at 20°C for 10 min for renaturation. The sample containing RsaI and the sample containing RsaG were mixed and incubated at 37 °C for 15 min. 6µl of total tRNA 1 µg/µl were added to all samples. Enzymatic hydrolysis was performed as described above.

0.3 M Na-acetate of pH 6.0 and cold ethanol were then added to all samples. After a vigorous mix, the samples are transferred in a dry ice-ethanol bath for 10 min. The samples are then precipitated, washed and dried and resuspended in 20 µL of blue formamide .

RNase T1 ladder: labeled mRNA (25,000 cpm) is preincubated at 50°C for 5 min in 5 mL of the Buffer ΔT1 containing 1 mg total tRNA. Reaction is then performed at 50°C for 10 min in the presence of 1 mL of RNase T1 (0.5 U).

Alkaline ladder: labeled mRNA (100,000 cpm) is incubated at 90°C for 3 min in the presence of total tRNA (2 mg) in 5 mL of the Ladder Buffer.

Before loading, each sample was adjusted to contains the same amount of radioactivity (except for the ladder that should have twice more radioactivity). The samples were heated (except the RNase T1 and alkaline ladders) for 3 min at 90°C. The 12% acrylamide was prerunned at 75 W for 30 min using 1× TBE as running buffer.

The samples were finally loaded on the gel, runned in TBE 1X for 2 hours at 75W.

FRET

Two fluorophore-tagged and self-complementary RNA 21mers were incubated in FRET buffer at 37°C. Annealing reaction was started by injection of 30 nM Cy3–21R+ into a cuvette containing an equal volume of 30 nM Cy3–21R– and (**Tab6**), where applicable, 6 µM (final concentration) of the *Sau*S1 protein. The reaction was allowed to proceed for 120 sec, and with Cy3 excited, donor and acceptor dye fluorescence emissions were measured once every second at 37°C. Then non labeled competitor RNA (21R–) were injected to yield a 10-fold molar excess over the labeled strands, the mixture was rapidly mixed for 2 sec, and readings were taken for another 120 sec.

Buffer FRET : 50 mM Tris HCl pH 7.5 – 3 mM $MgCl_2$ – 1 mM DTT

Northern Blot

In vitro transcription of RNA-DIG probes

The Digoxigenin (DIG)-labeled RNA antisense probes were *in vitro* transcribed starting

from PCR template of the gene of interest. (The primer, complementary to the 3' end of the strand encoding for the target gene, carries the T7 promoter at its 5'). The transcription was performed using DIG-RNA labelling mix Kit, according to the manufactor protocol (Roche 11277073910). The transcript was treated with DNase I (04716728001 10 U/µL) for 15 min at 37°C. The reaction was arrested by the addiction of 17 mM EDTA and AcNa 0.3M. The RNA-DIG were then treated with phenol/chloroforme and chloroforme/alcool isoamylique, precipitated in absolute ethanol at 20°C for 2 hours, washed, dryed and resuspended in 20 µL of mQ water. Their size and integrity were verified on 1% agarose gel in presence of guanidium thiocyanate 20 mM and ethidium bromide (5% vol/vol), runned for 30 min at 135 V. The use of DIG-labeled probes was used to follow the expression profile of *rpsA* mRNA in different bacterial strains , while DNA-labeled probes were used for the detection of the psm mRNA.

Migration, transfer, hybridization and detection

Total RNA extracted at different point of bacterial growth, was loaded on 1% agarose gel, runned at 4 °C (120 V, 3h). The RNA was then transferred on a positively charged membrane (Hybond Dutscher RPN303B) by capillarity or by vacuum absorption and cross-linked on it. The membrane was pre-hybridized for 45 min at 68°C. 1 to 5 µL of the RNA-DIG probe and the hybridation buffer, were heated for 5 min at 75°C, while the membrane hybridization was carried out at 68°C over night. The probe can be stored at -20°C, and could be reused for mounth. The membrane was washed twice for 5 min at room temperature for 5 min using wash buffer n°1 and than using the buffer n°2 for 15 min at 68°C. The membrane was than treated for 30 min with blocking buffer (Roche 11 096 176 001) diluted in 1X maleic acid buffer. 2 µL of anti-DIG antibodies (Roche 11 093 274 910) were incubated to the membrane for 30 min at room temperature. The membrane is finally washed twice using maleic/tween solution for 15 min. The addition of bioluminescent CDP-star (Roche 70427821) substrate, has allowed the detection.

Hybridization buffer : Formamide 50%, SSC 5x, NaPO4 pH 7 50 mM, blocking solution 2% (Roche 11 096 176 001 diluted in maleic acid pH 7,5 VWR 8.00380.1000), N-Lauroyl sarcosine 0,1% (Sigma L7414), SDS 7%

Wash buffer n°1 : 2x SSC, 0,1% SDS

Wash buffer n°2 : 0,2x SSC, 0,1% SDS

SSC 20 X : 3M NaCl, 300 mM Sodium Nitrate

30S ribosomal subunits purification

Purification of the 30S subunits from *S. aureus* was performed by dissociation of the 70S ribosomes. First, full 70S ribosomes were prepared as described in Khusainov et al., 2016b. The 70S ribosomes were diluted with buffer G until final concentration 6-8 mg/mL. The sample was dialyzed against 1 L of dissociation buffer for 2h. The solution was diluted in dissociation buffer until concentration 7 mg/mL, 500 µL were layered onto 0 – 30% sucrose density gradients prepared in dissociation buffer and centrifuged at 58,357 × g for 15 h using a Beckman SW28 rotor (Figure 1B). After fractionation the purity of each peak was analyzed by loading 0.03 AU_{260} of each fraction on 1% agarose gel in TAE buffer. The fractions containing mostly 30S ribosomal subunit were pooled together and dialyzed twice for 2 h against 1 L of buffer G. Sample was then concentrated using Centricon MWCO 100K until 150 – 170 AU_{260}/mL. Aliquots of 6 µL were flash frozen in liquid nitrogen and stored at -80 °C.

Buffer G: 10 mM Hepes-KOH pH 7.5, 50 mM KCl, 10 mM NH_4Cl, 10 mM $Mg(OAc)_2$

Dissociation buffer: 10 mM Hepes-KOH pH 7.5, 100 mM NH_4Cl, 1 mM $Mg(OAc)_2$, 1 mM DTT

Gel in TAE buffer: 40mM Tris, 20mM acetic acid, 1mM EDTA

Toeprinting assay

5' end Labeling of oligonucleotides

The DNA olignucleotides were labeled using γ ^{32}P ATP -370 MBq/ml – 10 mci/ml. 1 µl of oligonucleotides at 10 µM, was mixed with 1 µL of Buffer PNK 10X A (Fermentas), 1 µL of T4 PNK 10U/µL emzyme (Fermentas) and 5 µL of γ ATP. The reaction was carried out in a total volume of 10 µL at 37 °C for 1 hour. The labeled oligonucleotides were than purified on Micro Bio-spin chromatography column (Biorad) according to the manufacture protocol. The level of radioactivity was measured using Multi-purpose Scintillator counter (Beckman).

Toeprinting

The toeprintings were carried out using radiolabeled oligonucleotides.

The formation of a simplified translational initiation complex (30SIC) was done using published procedure, Fechter *et al.* 2009.

Buffer toe (-) 5x : Tris-HCl pH 7,5 100 mM, NH4Cl 300 mM, DTT 5 mM

Buffer toe(+) 5x : buffer toe (-) 5x , MgCl2 50 mM

Sequences preparation

For the preparation of sequences were used ddNTs. In aech mix there were 0,3 µM of RNA and 200.000 cpm of radioactivity. The RNA was denatured at 90 °C for 1 min, cooled for 1 min on ice and incubated in AMV 1V commercial buffer. For instance, for the tube « U », 1 mM of dTTP, dCTP, dGTP, 0,25 mM of dATP and 2 mM of ddATP were mixed in presence of 0,8 U AMV (007S-1), in a total volume of 26 µL. The RT was performed at 37 °C for 30 min.

The RNA template is than destroyed with 0,25 M of KOH and 40 µL of destroy buffer. The sample were putted for 1 min at 90°C, followed by an incubation of 15 min at 37°C. 0,4 mM of acetic acid were added in order to adjust the pH, than the sample was precipitated, centrifuged, washed, dried and resuspened in 10 µL of urea blue. Before loading on the gel, the samples were putted 3 min at 90°C.

Destroy buffer : Tris HCl 50mM pH8, SDS 0,5%, EDTA 7,5mM

Table 6 List of plasmids

Plasmid	Description
pUC18-RsaE	pUC18 expressing RsaE under T7 promoter
pUC18-RsaH	pUC18 expressing RsaH under T7 promoter
pUT7-RsaG	pUT7 expressing RsaG under T7 promoter
pCN51-RsaA	pCN51expressing RsaA under T2 promoter
pQE30Xa	6 X Hys-Tag plasmid

Table 7 List of oligonucleotides

NAME	USAGE	Sequences are 5' end to 3' end
RsaI Vic	Probing	AAA AAA ATC GGc TAG TCA CG
RsaI Ned	Probing	AAA AAA ATC GGC TAG TCA CG
S. aureus RsaI	PCR Amplification	Fw: TAA TAC GAC TCA CTA TAG TAA CAG GGG GAG CGA TTA
S. aureus RsaI	PCR Amplification	Rw: AAA AAA ATC GGC TAG TCA CG
Cy3 oligonucleotides	FRET	AUG CAC CGU AAA GC
CY5 oligonucleotides	FRET	GCU UUA CGG UGC UA
Cold competor	FRET	AUG CAC CGU AAA GC

References

Afgan, E., Baker, D., van den Beek, M., Blankenberg, D., Bouvier, D., Cech, M., Chilton, J., Clements, D., Coraor, N., Eberhard, C.*, et al.* (2016). The Galaxy platform for accessible, reproducible and collaborative biomedical analyses: 2016 update. Nucleic Acids Res *44*, W3-W10.

Allen, G.S., Zavialov, A., Gursky, R., Ehrenberg, M., and Frank, J. (2005). The cryo-EM structure of a translation initiation complex from Escherichia coli. Cell *121*, 703-712.

Anderson, K.L., Roberts, C., Disz, T., Vonstein, V., Hwang, K., Overbeek, R., Olson, P.D., Projan, S.J., and Dunman, P.M. (2006). Characterization of the Staphylococcus aureus heat shock, cold shock, stringent, and SOS responses and their effects on log-phase mRNA turnover. Journal of bacteriology *188*, 6739-6756.

Antignac, A., Sieradzki, K., and Tomasz, A. (2007). Perturbation of cell wall synthesis suppresses autolysis in Staphylococcus aureus: evidence for coregulation of cell wall synthetic and hydrolytic enzymes. Journal of bacteriology *189*, 7573-7580.

Arvidson, J., Lonnerholm, G., Tuvemo, T., Carlson, K., Lannering, B., and Lonnerholm, T. (2000). Prepubertal growth and growth hormone secretion in children after treatment for hematological malignancies, including autologous bone marrow transplantation. Pediatric hematology and oncology *17*, 285-297.

Atkins, K.L., Burman, J.D., Chamberlain, E.S., Cooper, J.E., Poutrel, B., Bagby, S., Jenkins, A.T., Feil, E.J., and van den Elsen, J.M. (2008). S. aureus IgG-binding proteins SpA and Sbi: host specificity and mechanisms of immune complex formation. Molecular immunology *45*, 1600-1611.

Attaiech, L., Glover, J.N., and Charpentier, X. (2017). RNA Chaperones Step Out of Hfq's Shadow. Trends in microbiology *25*, 247-249.

Autour, A., Westhof, E., and Ryckelynck, M. (2016). iSpinach: a fluorogenic RNA aptamer optimized for in vitro applications. Nucleic Acids Res *44*, 2491-2500.

Barrios, C., Georgopoulos, C., Lambert, P.H., and Del Giudice, G. (1994). Heat shock proteins as carrier molecules: in vivo helper effect mediated by Escherichia coli GroEL and DnaK proteins requires cross-linking with antigen. Clinical and experimental immunology *98*, 229-233.

Benito, Y., Kolb, F.A., Romby, P., Lina, G., Etienne, J., and Vandenesch, F. (2000). Probing the structure of RNAIII, the Staphylococcus aureus agr regulatory RNA, and identification of the RNA domain involved in repression of protein A expression. RNA (New York, NY) *6*, 668-679.

Bergmann, S., and Hammerschmidt, S. (2007). Fibrinolysis and host response in bacterial infections. Thrombosis and haemostasis *98*, 512-520.

Berube, B.J., and Bubeck Wardenburg, J. (2013). Staphylococcus aureus alpha-toxin: nearly a century of intrigue. Toxins *5*, 1140-1166.

Bhattacharya, S., Ploplis, V.A., and Castellino, F.J. (2012). Bacterial plasminogen receptors utilize host plasminogen system for effective invasion and dissemination. Journal of biomedicine & biotechnology *2012*, 482096.

Bischoff, M., Dunman, P., Kormanec, J., Macapagal, D., Murphy, E., Mounts, W., Berger-Bachi, B., and Projan, S. (2004). Microarray-based analysis of the Staphylococcus aureus sigmaB regulon. Journal of bacteriology *186*, 4085-4099.

Bischoff, M., Entenza, J.M., and Giachino, P. (2001). Influence of a functional sigB operon on the global regulators sar and agr in Staphylococcus aureus. Journal of bacteriology *183*, 5171-5179.

Bohn, C., Rigoulay, C., and Bouloc, P. (2007). No detectable effect of RNA-binding protein Hfq absence in Staphylococcus aureus. BMC Microbiol *7*, 10.
Boisset, S., Geissmann, T., Huntzinger, E., Fechter, P., Bendridi, N., Possedko, M., Chevalier, C., Helfer, A.C., Benito, Y., Jacquier, A.*, et al.* (2007). Staphylococcus aureus RNAIII coordinately represses the synthesis of virulence factors and the transcription regulator Rot by an antisense mechanism. Genes & development *21*, 1353-1366.
Bourgeois-Nicolaos, N., Lucet, J.C., Daubie, C., Benchaba, F., Rajguru, M., Ruimy, R., Andremont, A., and Armand-Lefevre, L. (2010). Maternal vaginal colonisation by Staphylococcus aureus and newborn acquisition at delivery. Paediatric and perinatal epidemiology *24*, 488-491.
Brandi, A., Pon, C.L., and Gualerzi, C.O. (1994). Interaction of the main cold shock protein CS7.4 (CspA) of Escherichia coli with the promoter region of hns. Biochimie *76*, 1090-1098.
Brennan, R.G., and Link, T.M. (2007). Hfq structure, function and ligand binding. Current opinion in microbiology *10*, 125-133.
Bronesky, D., Wu, Z., Marzi, S., Walter, P., Geissmann, T., Moreau, K., Vandenesch, F., Caldelari, I., and Romby, P. (2016). Staphylococcus aureus RNAIII and Its Regulon Link Quorum Sensing, Stress Responses, Metabolic Adaptation, and Regulation of Virulence Gene Expression. Annual review of microbiology *70*, 299-316.
Bukau, B. (1993). Regulation of the Escherichia coli heat-shock response. Molecular microbiology *9*, 671-680.
Burian, M., Rautenberg, M., Kohler, T., Fritz, M., Krismer, B., Unger, C., Hoffmann, W.H., Peschel, A., Wolz, C., and Goerke, C. (2010). Temporal expression of adhesion factors and activity of global regulators during establishment of Staphylococcus aureus nasal colonization. The Journal of infectious diseases *201*, 1414-1421.
Burmann, B.M., Schweimer, K., Luo, X., Wahl, M.C., Stitt, B.L., Gottesman, M.E., and Rosch, P. (2010). A NusE:NusG complex links transcription and translation. Science (New York, NY) *328*, 501-504.
Byrgazov, K., Grishkovskaya, I., Arenz, S., Coudevylle, N., Temmel, H., Wilson, D.N., Djinovic-Carugo, K., and Moll, I. (2015). Structural basis for the interaction of protein S1 with the Escherichia coli ribosome. Nucleic Acids Res *43*, 661-673.
Caldelari, I., Chane-Woon-Ming, B., Noirot, C., Moreau, K., Romby, P., Gaspin, C., and Marzi, S. (2017). Complete Genome Sequence and Annotation of the Staphylococcus aureus Strain HG001. Genome announcements *5*.
Campbell, E.A., Korzheva, N., Mustaev, A., Murakami, K., Nair, S., Goldfarb, A., and Darst, S.A. (2001). Structural mechanism for rifampicin inhibition of bacterial rna polymerase. Cell *104*, 901-912.
Campos, M., and Jacobs-Wagner, C. (2013). Cellular organization of the transfer of genetic information. Current opinion in microbiology *16*, 171-176.
Carter, A.P., Clemons, W.M., Jr., Brodersen, D.E., Morgan-Warren, R.J., Hartsch, T., Wimberly, B.T., and Ramakrishnan, V. (2001). Crystal structure of an initiation factor bound to the 30S ribosomal subunit. Science (New York, NY) *291*, 498-501.
Chambers, H.F., and Deleo, F.R. (2009). Waves of resistance: Staphylococcus aureus in the antibiotic era. Nature reviews Microbiology *7*, 629-641.
Chan, P.F., and Foster, S.J. (1998). Role of SarA in virulence determinant production and environmental signal transduction in Staphylococcus aureus. Journal of bacteriology *180*, 6232-6241.

Chapman, M.R., Robinson, L.S., Pinkner, J.S., Roth, R., Heuser, J., Hammar, M., Normark, S., and Hultgren, S.J. (2002). Role of Escherichia coli curli operons in directing amyloid fiber formation. Science (New York, NY) *295*, 851-855.

Chatterjee, S.S., Chen, L., Joo, H.S., Cheung, G.Y., Kreiswirth, B.N., and Otto, M. (2011). Distribution and regulation of the mobile genetic element-encoded phenol-soluble modulin PSM-mec in methicillin-resistant Staphylococcus aureus. PloS one *6*, e28781.

Chatterjee, S.S., Joo, H.S., Duong, A.C., Dieringer, T.D., Tan, V.Y., Song, Y., Fischer, E.R., Cheung, G.Y., Li, M., and Otto, M. (2013). Essential Staphylococcus aureus toxin export system. Nature medicine *19*, 364-367.

Chatterjee, S.S., and Otto, M. (2013). How can Staphylococcus aureus phenol-soluble modulins be targeted to inhibit infection? Future microbiology *8*, 693-696.

Chaudhuri, R.R., Allen, A.G., Owen, P.J., Shalom, G., Stone, K., Harrison, M., Burgis, T.A., Lockyer, M., Garcia-Lara, J., Foster, S.J.*, et al.* (2009). Comprehensive identification of essential Staphylococcus aureus genes using Transposon-Mediated Differential Hybridisation (TMDH). BMC genomics *10*, 291.

Chen, H., Bjerknes, M., Kumar, R., and Jay, E. (1994). Determination of the optimal aligned spacing between the Shine-Dalgarno sequence and the translation initiation codon of Escherichia coli mRNAs. Nucleic Acids Res *22*, 4953-4957.

Cheng, A.G., McAdow, M., Kim, H.K., Bae, T., Missiakas, D.M., and Schneewind, O. (2010). Contribution of coagulases towards Staphylococcus aureus disease and protective immunity. PLoS pathogens *6*, e1001036.

Chesney, P.J., Halsey, N.A., and Marcy, S.M. (1997). Treatment of bacterial infections. The New England journal of medicine *337*, 793-794.

Cheung, A.L., Bayer, A.S., Zhang, G., Gresham, H., and Xiong, Y.Q. (2004). Regulation of virulence determinants in vitro and in vivo in Staphylococcus aureus. FEMS immunology and medical microbiology *40*, 1-9.

Cheung, A.L., Eberhardt, K.J., Chung, E., Yeaman, M.R., Sullam, P.M., Ramos, M., and Bayer, A.S. (1994). Diminished virulence of a sar-/agr- mutant of Staphylococcus aureus in the rabbit model of endocarditis. The Journal of clinical investigation *94*, 1815-1822.

Cheung, A.L., Nishina, K.A., Trotonda, M.P., and Tamber, S. (2008). The SarA protein family of Staphylococcus aureus. The international journal of biochemistry & cell biology *40*, 355-361.

Cheung, A.L., Schmidt, K., Bateman, B., and Manna, A.C. (2001). SarS, a SarA homolog repressible by agr, is an activator of protein A synthesis in Staphylococcus aureus. Infection and immunity *69*, 2448-2455.

Cheung, G.Y., Joo, H.S., Chatterjee, S.S., and Otto, M. (2014). Phenol-soluble modulins--critical determinants of staphylococcal virulence. FEMS microbiology reviews *38*, 698-719.

Cheung, G.Y., Rigby, K., Wang, R., Queck, S.Y., Braughton, K.R., Whitney, A.R., Teintze, M., DeLeo, F.R., and Otto, M. (2010). Staphylococcus epidermidis strategies to avoid killing by human neutrophils. PLoS pathogens *6*, e1001133.

Chevalier, C., Boisset, S., Romilly, C., Masquida, B., Fechter, P., Geissmann, T., Vandenesch, F., and Romby, P. (2010). Staphylococcus aureus RNAIII binds to two distant regions of coa mRNA to arrest translation and promote mRNA degradation. PLoS pathogens *6*, e1000809.

Chuang, S.E., and Blattner, F.R. (1993). Characterization of twenty-six new heat shock genes of Escherichia coli. Journal of bacteriology *175*, 5242-5252.

Cogen, A.L., Yamasaki, K., Sanchez, K.M., Dorschner, R.A., Lai, Y., MacLeod, D.T., Torpey, J.W., Otto, M., Nizet, V., Kim, J.E.*, et al.* (2010). Selective antimicrobial action is provided by phenol-soluble modulins derived from Staphylococcus epidermidis, a normal resident of the skin. The Journal of investigative dermatology *130*, 192-200.

Cowing, D.W., Bardwell, J.C., Craig, E.A., Woolford, C., Hendrix, R.W., and Gross, C.A. (1985). Consensus sequence for Escherichia coli heat shock gene promoters. Proceedings of the National Academy of Sciences of the United States of America *82*, 2679-2683.

Craven, R.R., Gao, X., Allen, I.C., Gris, D., Bubeck Wardenburg, J., McElvania-Tekippe, E., Ting, J.P., and Duncan, J.A. (2009). Staphylococcus aureus alpha-hemolysin activates the NLRP3-inflammasome in human and mouse monocytic cells. PloS one *4*, e7446.

Cui, M., Wang, T., Xu, J., Ke, Y., Du, X., Yuan, X., Wang, Z., Gong, C., Zhuang, Y., Lei, S.*, et al.* (2013). Impact of Hfq on global gene expression and intracellular survival in Brucella melitensis. PloS one *8*, e71933.

Das, H.K., Goldstein, A., and Lowney, L.I. (1967). Attachment of ribosomes to nascent messenger RNA in Escherichia coli. J Mol Biol *24*, 231-245.

DeDent, A.C., McAdow, M., and Schneewind, O. (2007). Distribution of protein A on the surface of Staphylococcus aureus. Journal of bacteriology *189*, 4473-4484.

DeLeo, F.R., Otto, M., Kreiswirth, B.N., and Chambers, H.F. (2010). Community-associated meticillin-resistant Staphylococcus aureus. Lancet (London, England) *375*, 1557-1568.

Deora, R., and Misra, T.K. (1996). Characterization of the primary sigma factor of Staphylococcus aureus. J Biol Chem *271*, 21828-21834.

Deora, R., Tseng, T., and Misra, T.K. (1997). Alternative transcription factor sigmaSB of Staphylococcus aureus: characterization and role in transcription of the global regulatory locus sar. Journal of bacteriology *179*, 6355-6359.

Dimastrogiovanni, D., Frohlich, K.S., Bandyra, K.J., Bruce, H.A., Hohensee, S., Vogel, J., and Luisi, B.F. (2014). Recognition of the small regulatory RNA RydC by the bacterial Hfq protein. eLife *3*.

Dinges, M.M., Orwin, P.M., and Schlievert, P.M. (2000). Exotoxins of Staphylococcus aureus. Clinical microbiology reviews *13*, 16-34, table of contents.

Drapeau, G.R. (1978). Role of metalloprotease in activation of the precursor of staphylococcal protease. Journal of bacteriology *136*, 607-613.

Draper, D.E., Pratt, C.W., and von Hippel, P.H. (1977). Escherichia coli ribosomal protein S1 has two polynucleotide binding sites. Proceedings of the National Academy of Sciences of the United States of America *74*, 4786-4790.

Draper, D.E., and von Hippel, P.H. (1979). Measurement of macromolecular equilibrium binding constants by a sucrose gradient band sedimentation method. Application to protein-nucleic acid interactions. Biochemistry *18*, 753-760.

Dueholm, M.S., Sondergaard, M.T., Nilsson, M., Christiansen, G., Stensballe, A., Overgaard, M.T., Givskov, M., Tolker-Nielsen, T., Otzen, D.E., and Nielsen, P.H. (2013). Expression of Fap amyloids in Pseudomonas aeruginosa, P. fluorescens, and P. putida results in aggregation and increased biofilm formation. MicrobiologyOpen *2*, 365-382.

Durand, S., Tomasini, A., Braun, F., Condon, C., and Romby, P. (2015). sRNA and mRNA turnover in Gram-positive bacteria. FEMS microbiology reviews *39*, 316-330.

Duval, M., Korepanov, A., Fuchsbauer, O., Fechter, P., Haller, A., Fabbretti, A., Choulier, L., Micura, R., Klaholz, B.P., and Romby, P. (2013a). Escherichia coli ribosomal protein S1 unfolds structured mRNAs onto the ribosome for active translation initiation. PLoS biology *11*, e1001731.

Duval, M., Korepanov, A., Fuchsbauer, O., Fechter, P., Haller, A., Fabbretti, A., Choulier, L., Micura, R., Klaholz, B.P., Romby, P.*, et al.* (2013b). Escherichia coli ribosomal protein S1 unfolds structured mRNAs onto the ribosome for active translation initiation. PLoS biology *11*, e1001731.

Duval, M., Marenna, A., Chevalier, C., and Marzi, S. (2017). Site-Directed Chemical Probing to map transient RNA/protein interactions. Methods (San Diego, Calif) *117*, 48-58.

Entenza, J.M., Moreillon, P., Senn, M.M., Kormanec, J., Dunman, P.M., Berger-Bachi, B., Projan, S., and Bischoff, M. (2005). Role of sigmaB in the expression of Staphylococcus aureus cell wall adhesins ClfA and FnbA and contribution to infectivity in a rat model of experimental endocarditis. Infection and immunity *73*, 990-998.

Essmann, F., Bantel, H., Totzke, G., Engels, I.H., Sinha, B., Schulze-Osthoff, K., and Janicke, R.U. (2003). Staphylococcus aureus alpha-toxin-induced cell death: predominant necrosis despite apoptotic caspase activation. Cell death and differentiation *10*, 1260-1272.

Farwell, M.A., Roberts, M.W., and Rabinowitz, J.C. (1992). The effect of ribosomal protein S1 from Escherichia coli and Micrococcus luteus on protein synthesis in vitro by E. coli and Bacillus subtilis. Molecular microbiology *6*, 3375-3383.

Fechter, P., Chevalier, C., Yusupova, G., Yusupov, M., Romby, P., and Marzi, S. (2009). Ribosomal initiation complexes probed by toeprinting and effect of trans-acting translational regulators in bacteria. Methods in molecular biology (Clifton, NJ) *540*, 247-263.

Fechter, P., Parmentier, D., Wu, Z., Fuchsbauer, O., Romby, P., and Marzi, S. (2016). Traditional Chemical Mapping of RNA Structure In Vitro and In Vivo. Methods in molecular biology (Clifton, NJ) *1490*, 83-103.

Fei, J., Singh, D., Zhang, Q., Park, S., Balasubramanian, D., Golding, I., Vanderpool, C.K., and Ha, T. (2015). RNA biochemistry. Determination of in vivo target search kinetics of regulatory noncoding RNA. Science (New York, NY) *347*, 1371-1374.

Fitzgerald, C.J., Pranikoff, T.V., Ross, G.A., Mou, S., Givner, L.B., and Shetty, A.K. (2012). Purpura fulminans caused by community-associated methicillin-resistant Staphylococcus aureus. The American journal of emergency medicine *30*, 1013 e1011-1014.

Foster, T.J. (2005). Immune evasion by staphylococci. Nature reviews Microbiology *3*, 948-958.

Foster, T.J., Geoghegan, J.A., Ganesh, V.K., and Hook, M. (2014). Adhesion, invasion and evasion: the many functions of the surface proteins of Staphylococcus aureus. Nature reviews Microbiology *12*, 49-62.

Friedrich, R., Panizzi, P., Fuentes-Prior, P., Richter, K., Verhamme, I., Anderson, P.J., Kawabata, S., Huber, R., Bode, W., and Bock, P.E. (2003). Staphylocoagulase is a prototype for the mechanism of cofactor-induced zymogen activation. Nature *425*, 535-539.

Gao, J., and Stewart, G.C. (2004). Regulatory elements of the Staphylococcus aureus protein A (Spa) promoter. Journal of bacteriology *186*, 3738-3748.

Geiger, T., Francois, P., Liebeke, M., Fraunholz, M., Goerke, C., Krismer, B., Schrenzel, J., Lalk, M., and Wolz, C. (2012). The stringent response of Staphylococcus aureus and its impact on survival after phagocytosis through the induction of intracellular PSMs expression. PLoS pathogens *8*, e1003016.

Geiger, T., Goerke, C., Mainiero, M., Kraus, D., and Wolz, C. (2008). The virulence regulator Sae of Staphylococcus aureus: promoter activities and response to phagocytosis-related signals. Journal of bacteriology *190*, 3419-3428.

Geisinger, E., Adhikari, R.P., Jin, R., Ross, H.F., and Novick, R.P. (2006). Inhibition of rot translation by RNAIII, a key feature of agr function. Molecular microbiology *61*, 1038-1048.

Geissmann, T., Chevalier, C., Cros, M.J., Boisset, S., Fechter, P., Noirot, C., Schrenzel, J., Francois, P., Vandenesch, F., Gaspin, C.*, et al.* (2009a). A search for small noncoding RNAs in Staphylococcus aureus reveals a conserved sequence motif for regulation. Nucleic Acids Res *37*, 7239-7257.

Geissmann, T., Marzi, S., and Romby, P. (2009b). The role of mRNA structure in translational control in bacteria. RNA Biol *6*, 153-160.

Ghuysen, J.M. (1994). Molecular structures of penicillin-binding proteins and beta-lactamases. Trends in microbiology *2*, 372-380.

Giangrossi, M., Brandi, A., Giuliodori, A.M., Gualerzi, C.O., and Pon, C.L. (2007). Cold-shock-induced de novo transcription and translation of infA and role of IF1 during cold adaptation. Molecular microbiology *64*, 807-821.

Giraud, C., Hausmann, S., Lemeille, S., Prados, J., Redder, P., and Linder, P. (2015). The C-terminal region of the RNA helicase CshA is required for the interaction with the degradosome and turnover of bulk RNA in the opportunistic pathogen Staphylococcus aureus. RNA Biol *12*, 658-674.

Giraudo, A.T., Cheung, A.L., and Nagel, R. (1997). The sae locus of Staphylococcus aureus controls exoprotein synthesis at the transcriptional level. Archives of microbiology *168*, 53-58.

Giuliodori, A.M., Brandi, A., Giangrossi, M., Gualerzi, C.O., and Pon, C.L. (2007). Cold-stress-induced de novo expression of infC and role of IF3 in cold-shock translational bias. RNA (New York, NY) *13*, 1355-1365.

Giuliodori, A.M., Brandi, A., Gualerzi, C.O., and Pon, C.L. (2004). Preferential translation of cold-shock mRNAs during cold adaptation. RNA (New York, NY) *10*, 265-276.

Giuliodori, A.M., Di Pietro, F., Marzi, S., Masquida, B., Wagner, R., Romby, P., Gualerzi, C.O., and Pon, C.L. (2010). The cspA mRNA is a thermosensor that modulates translation of the cold-shock protein CspA. Molecular cell *37*, 21-33.

Goerke, C., Fluckiger, U., Steinhuber, A., Bisanzio, V., Ulrich, M., Bischoff, M., Patti, J.M., and Wolz, C. (2005). Role of Staphylococcus aureus global regulators sae and sigmaB in virulence gene expression during device-related infection. Infection and immunity *73*, 3415-3421.

Gold, L. (1988). Posttranscriptional regulatory mechanisms in Escherichia coli. Annual review of biochemistry *57*, 199-233.

Gonzalez, C.D., Ledo, C., Giai, C., Garofalo, A., and Gomez, M.I. (2015). The Sbi Protein Contributes to Staphylococcus aureus Inflammatory Response during Systemic Infection. PloS one *10*, e0131879.

Goodyear, C.S., and Silverman, G.J. (2004). Staphylococcal toxin induced preferential and prolonged in vivo deletion of innate-like B lymphocytes. Proceedings of the National Academy of Sciences of the United States of America *101*, 11392-11397.

Gordon, R.J., and Lowy, F.D. (2008). Pathogenesis of methicillin-resistant Staphylococcus aureus infection. Clinical infectious diseases : an official publication of the Infectious Diseases Society of America *46 Suppl 5*, S350-359.
Gottesman, S. (2004). The small RNA regulators of Escherichia coli: roles and mechanisms*. Annual review of microbiology *58*, 303-328.
Graumann, P., and Marahiel, M.A. (1996). Some like it cold: response of microorganisms to cold shock. Archives of microbiology *166*, 293-300.
Graumann, P., Schroder, K., Schmid, R., and Marahiel, M.A. (1996). Cold shock stress-induced proteins in Bacillus subtilis. Journal of bacteriology *178*, 4611-4619.
Grigoriadou, C., Marzi, S., Pan, D., Gualerzi, C.O., and Cooperman, B.S. (2007). The translational fidelity function of IF3 during transition from the 30 S initiation complex to the 70 S initiation complex. Journal of molecular biology *373*, 551-561.
Gualerzi, C.O., Giuliodori, A.M., and Pon, C.L. (2003). Transcriptional and post-transcriptional control of cold-shock genes. J Mol Biol *331*, 527-539.
Hacker, J., Hochhut, B., Middendorf, B., Schneider, G., Buchrieser, C., Gottschalk, G., and Dobrindt, U. (2004). Pathogenomics of mobile genetic elements of toxigenic bacteria. International journal of medical microbiology : IJMM *293*, 453-461.
Haggar, A., Hussain, M., Lonnies, H., Herrmann, M., Norrby-Teglund, A., and Flock, J.I. (2003). Extracellular adherence protein from Staphylococcus aureus enhances internalization into eukaryotic cells. Infection and immunity *71*, 2310-2317.
Haggar, A., Shannon, O., Norrby-Teglund, A., and Flock, J.I. (2005). Dual effects of extracellular adherence protein from Staphylococcus aureus on peripheral blood mononuclear cells. The Journal of infectious diseases *192*, 210-217.
Hartleib, J., Kohler, N., Dickinson, R.B., Chhatwal, G.S., Sixma, J.J., Hartford, O.M., Foster, T.J., Peters, G., Kehrel, B.E., and Herrmann, M. (2000). Protein A is the von Willebrand factor binding protein on Staphylococcus aureus. Blood *96*, 2149-2156.
Hartz, D., Binkley, J., Hollingsworth, T., and Gold, L. (1990). Domains of initiator tRNA and initiation codon crucial for initiator tRNA selection by Escherichia coli IF3. Genes & development *4*, 1790-1800.
Hausmann, S., Guimaraes, V.A., Garcin, D., Baumann, N., Linder, P., and Redder, P. (2017). Both exo- and endo-nucleolytic activities of RNase J1 from Staphylococcus aureus are manganese dependent and active on triphosphorylated 5'-ends. RNA Biol, 1-13.
Horsburgh, M.J., Aish, J.L., White, I.J., Shaw, L., Lithgow, J.K., and Foster, S.J. (2002). sigmaB modulates virulence determinant expression and stress resistance: characterization of a functional rsbU strain derived from Staphylococcus aureus 8325-4. Journal of bacteriology *184*, 5457-5467.
Hui, A., and de Boer, H.A. (1987). Specialized ribosome system: preferential translation of a single mRNA species by a subpopulation of mutated ribosomes in Escherichia coli. Proceedings of the National Academy of Sciences of the United States of America *84*, 4762-4766.
Huntzinger, E., Boisset, S., Saveanu, C., Benito, Y., Geissmann, T., Namane, A., Lina, G., Etienne, J., Ehresmann, B., Ehresmann, C.*, et al.* (2005). Staphylococcus aureus RNAIII and the endoribonuclease III coordinately regulate spa gene expression. The EMBO journal *24*, 824-835.
Imamura, T., Tanase, S., Szmyd, G., Kozik, A., Travis, J., and Potempa, J. (2005). Induction of vascular leakage through release of bradykinin and a novel kinin by cysteine proteinases from Staphylococcus aureus. The Journal of experimental medicine *201*, 1669-1676.

Ingavale, S., van Wamel, W., Luong, T.T., Lee, C.Y., and Cheung, A.L. (2005). Rat/MgrA, a regulator of autolysis, is a regulator of virulence genes in Staphylococcus aureus. Infection and immunity *73*, 1423-1431.

Ingolia, N.T., Ghaemmaghami, S., Newman, J.R., and Weissman, J.S. (2009). Genome-wide analysis in vivo of translation with nucleotide resolution using ribosome profiling. Science (New York, NY) *324*, 218-223.

Ishii, K., Adachi, T., Yasukawa, J., Suzuki, Y., Hamamoto, H., and Sekimizu, K. (2014). Induction of virulence gene expression in Staphylococcus aureus by pulmonary surfactant. Infection and immunity *82*, 1500-1510.

Ito, F., Tamiya, T., Ohtsu, I., Fujimura, M., and Fukumori, F. (2014). Genetic and phenotypic characterization of the heat shock response in Pseudomonas putida. MicrobiologyOpen *3*, 922-936.

Jacob, W.F., Santer, M., and Dahlberg, A.E. (1987). A single base change in the Shine-Dalgarno region of 16S rRNA of Escherichia coli affects translation of many proteins. Proceedings of the National Academy of Sciences of the United States of America *84*, 4757-4761.

Jensen, K.B., and Darnell, R.B. (2008). CLIP: crosslinking and immunoprecipitation of in vivo RNA targets of RNA-binding proteins. Methods in molecular biology (Clifton, NJ) *488*, 85-98.

Jensen, M.S., and Bainton, D.F. (1973). Temporal changes in pH within the phagocytic vacuole of the polymorphonuclear neutrophilic leukocyte. The Journal of cell biology *56*, 379-388.

Jin, T., Bokarewa, M., McIntyre, L., Tarkowski, A., Corey, G.R., Reller, L.B., and Fowler, V.G., Jr. (2003). Fatal outcome of bacteraemic patients caused by infection with staphylokinase-deficient Staphylococcus aureus strains. Journal of medical microbiology *52*, 919-923.

Jones, P.G., and Inouye, M. (1994). The cold-shock response--a hot topic. Molecular microbiology *11*, 811-818.

Joo, H.S., Chatterjee, S.S., Villaruz, A.E., Dickey, S.W., Tan, V.Y., Chen, Y., Sturdevant, D.E., Ricklefs, S.M., and Otto, M. (2016). Mechanism of Gene Regulation by a Staphylococcus aureus Toxin. mBio *7*.

Joo, H.S., and Otto, M. (2016). Toxin-mediated gene regulatory mechanism in Staphylococcus aureus. Microbial cell (Graz, Austria) *4*, 29-31.

Jousselin, A., Metzinger, L., and Felden, B. (2009). On the facultative requirement of the bacterial RNA chaperone, Hfq. Trends in microbiology *17*, 399-405.

Juhas, M., Reuss, D.R., Zhu, B., and Commichau, F.M. (2014). Bacillus subtilis and Escherichia coli essential genes and minimal cell factories after one decade of genome engineering. Microbiology (Reading, England) *160*, 2341-2351.

Jusko, M., Potempa, J., Kantyka, T., Bielecka, E., Miller, H.K., Kalinska, M., Dubin, G., Garred, P., Shaw, L.N., and Blom, A.M. (2014). Staphylococcal proteases aid in evasion of the human complement system. Journal of innate immunity *6*, 31-46.

Kaito, C., Saito, Y., Ikuo, M., Omae, Y., Mao, H., Nagano, G., Fujiyuki, T., Numata, S., Han, X., Obata, K.*, et al.* (2013). Mobile genetic element SCCmec-encoded psm-mec RNA suppresses translation of agrA and attenuates MRSA virulence. PLoS pathogens *9*, e1003269.

Kaito, C., Saito, Y., Nagano, G., Ikuo, M., Omae, Y., Hanada, Y., Han, X., Kuwahara-Arai, K., Hishinuma, T., Baba, T.*, et al.* (2011). Transcription and translation products of the cytolysin gene psm-mec on the mobile genetic element SCCmec regulate Staphylococcus aureus virulence. PLoS pathogens *7*, e1001267.

Kaltschmidt, E., and Wittmann, H.G. (1970). Ribosomal proteins. XII. Number of proteins in small and large ribosomal subunits of Escherichia coli as determined by two-dimensional gel electrophoresis. Proceedings of the National Academy of Sciences of the United States of America *67*, 1276-1282.

Kaneko, J., Ozawa, T., Tomita, T., and Kamio, Y. (1997). Sequential binding of Staphylococcal gamma-hemolysin to human erythrocytes and complex formation of the hemolysin on the cell surface. Bioscience, biotechnology, and biochemistry *61*, 846-851.

Karlsson, A., Saravia-Otten, P., Tegmark, K., Morfeldt, E., and Arvidson, S. (2001). Decreased amounts of cell wall-associated protein A and fibronectin-binding proteins in Staphylococcus aureus sarA mutants due to up-regulation of extracellular proteases. Infection and immunity *69*, 4742-4748.

Katunin, V.I., Semenkov, Y.P., Makhno, V.I., and Kirillov, S.V. (1980). Comparative study of the interaction of polyuridylic acid with 30S subunits and 70S ribosomes of Escherichia coli. Nucleic Acids Res *8*, 403-421.

Kennell, D., and Riezman, H. (1977). Transcription and translation initiation frequencies of the Escherichia coli lac operon. J Mol Biol *114*, 1-21.

Kerrigan, S.W., Douglas, I., Wray, A., Heath, J., Byrne, M.F., Fitzgerald, D., and Cox, D. (2002). A role for glycoprotein Ib in Streptococcus sanguis-induced platelet aggregation. Blood *100*, 509-516.

Khemici, V., Prados, J., Linder, P., and Redder, P. (2015). Decay-Initiating Endoribonucleolytic Cleavage by RNase Y Is Kept under Tight Control via Sequence Preference and Sub-cellular Localisation. PLoS genetics *11*, e1005577.

Khusainov, I., Marenna, A., Cerciat, M., Fechter, P., Hashem, Y., Marzi, S., Romby, P., Yusupova, G., and Yusupov, M. (2016). [A glimpse on Staphylococcus aureus translation machinery and its control]. Molekuliarnaia biologiia *50*, 549-557.

Khusainov, I., Vicens, Q., Bochler, A., Grosse, F., Myasnikov, A., Menetret, J.F., Chicher, J., Marzi, S., Romby, P., Yusupova, G.*, et al.* (2017). Structure of the 70S ribosome from human pathogen Staphylococcus aureus. Nucleic Acids Res *45*, 1026.

Kluytmans, J., van Belkum, A., and Verbrugh, H. (1997). Nasal carriage of Staphylococcus aureus: epidemiology, underlying mechanisms, and associated risks. Clinical microbiology reviews *10*, 505-520.

Komarova, A.V., Tchufistova, L.S., Dreyfus, M., and Boni, I.V. (2005). AU-rich sequences within 5' untranslated leaders enhance translation and stabilize mRNA in Escherichia coli. Journal of bacteriology *187*, 1344-1349.

Kong, K.F., Vuong, C., and Otto, M. (2006). Staphylococcus quorum sensing in biofilm formation and infection. International journal of medical microbiology : IJMM *296*, 133-139.

Kovach, A.R., Hoff, K.E., Canty, J.T., Orans, J., and Brennan, R.G. (2014). Recognition of U-rich RNA by Hfq from the Gram-positive pathogen Listeria monocytogenes. RNA (New York, NY) *20*, 1548-1559.

Kroh, H.K., Panizzi, P., and Bock, P.E. (2009). Von Willebrand factor-binding protein is a hysteretic conformational activator of prothrombin. Proceedings of the National Academy of Sciences of the United States of America *106*, 7786-7791.

Kwiecinski, J., Josefsson, E., Mitchell, J., Higgins, J., Magnusson, M., Foster, T., Jin, T., and Bokarewa, M. (2010). Activation of plasminogen by staphylokinase reduces the severity of Staphylococcus aureus systemic infection. The Journal of infectious diseases *202*, 1041-1049.

Laarman, A.J., Mijnheer, G., Mootz, J.M., van Rooijen, W.J., Ruyken, M., Malone, C.L., Heezius, E.C., Ward, R., Milligan, G., van Strijp, J.A.*, et al.* (2012). Staphylococcus aureus Staphopain A inhibits CXCR2-dependent neutrophil activation and chemotaxis. The EMBO journal *31*, 3607-3619.

Lalaouna, D., and Masse, E. (2015). Identification of sRNA interacting with a transcript of interest using MS2-affinity purification coupled with RNA sequencing (MAPS) technology. Genomics data *5*, 136-138.

Lasa, I., Toledo-Arana, A., Dobin, A., Villanueva, M., de los Mozos, I.R., Vergara-Irigaray, M., Segura, V., Fagegaltier, D., Penades, J.R., Valle, J.*, et al.* (2011). Genome-wide antisense transcription drives mRNA processing in bacteria. Proceedings of the National Academy of Sciences of the United States of America *108*, 20172-20177.

Lauber, M.A., Rappsilber, J., and Reilly, J.P. (2012). Dynamics of ribosomal protein S1 on a bacterial ribosome with cross-linking and mass spectrometry. Molecular & cellular proteomics : MCP *11*, 1965-1976.

Liang, X., Yu, C., Sun, J., Liu, H., Landwehr, C., Holmes, D., and Ji, Y. (2006). Inactivation of a two-component signal transduction system, SaeRS, eliminates adherence and attenuates virulence of Staphylococcus aureus. Infection and immunity *74*, 4655-4665.

Lin, Y.C., and Peterson, M.L. (2010). New insights into the prevention of staphylococcal infections and toxic shock syndrome. Expert review of clinical pharmacology *3*, 753-767.

Linder, P., Lemeille, S., and Redder, P. (2014). Transcriptome-wide analyses of 5'-ends in RNase J mutants of a gram-positive pathogen reveal a role in RNA maturation, regulation and degradation. PLoS genetics *10*, e1004207.

Lioliou, E., Sharma, C.M., Caldelari, I., Helfer, A.C., Fechter, P., Vandenesch, F., Vogel, J., and Romby, P. (2012). Global regulatory functions of the Staphylococcus aureus endoribonuclease III in gene expression. PLoS genetics *8*, e1002782.

Liu, G.Y., Essex, A., Buchanan, J.T., Datta, V., Hoffman, H.M., Bastian, J.F., Fierer, J., and Nizet, V. (2005). Staphylococcus aureus golden pigment impairs neutrophil killing and promotes virulence through its antioxidant activity. The Journal of experimental medicine *202*, 209-215.

Liu, Q., Yeo, W.S., and Bae, T. (2016). The SaeRS Two-Component System of Staphylococcus aureus. Genes *7*.

Loffler, B., Hussain, M., Grundmeier, M., Bruck, M., Holzinger, D., Varga, G., Roth, J., Kahl, B.C., Proctor, R.A., and Peters, G. (2010). Staphylococcus aureus panton-valentine leukocidin is a very potent cytotoxic factor for human neutrophils. PLoS pathogens *6*, e1000715.

Londei, P. (2005). Evolution of translational initiation: new insights from the archaea. FEMS microbiology reviews *29*, 185-200.

Lowy, F.D. (2003). Antimicrobial resistance: the example of Staphylococcus aureus. The Journal of clinical investigation *111*, 1265-1273.

Lu, T., Park, J.Y., Parnell, K., Fox, L.K., and McGuire, M.A. (2012). Characterization of fatty acid modifying enzyme activity in staphylococcal mastitis isolates and other bacteria. BMC research notes *5*, 323.

Luong, T.T., Newell, S.W., and Lee, C.Y. (2003). Mgr, a novel global regulator in Staphylococcus aureus. Journal of bacteriology *185*, 3703-3710.

Makeyev, A.V., and Liebhaber, S.A. (2002). The poly(C)-binding proteins: a multiplicity of functions and a search for mechanisms. RNA (New York, NY) *8*, 265-278.

Malachowa, N., Kohler, P.L., Schlievert, P.M., Chuang, O.N., Dunny, G.M., Kobayashi, S.D., Miedzobrodzki, J., Bohach, G.A., and Seo, K.S. (2011). Characterization of a Staphylococcus aureus surface virulence factor that promotes resistance to oxidative killing and infectious endocarditis. Infection and immunity *79*, 342-352.
Mann, M., Wright, P.R., and Backofen, R. (2017). IntaRNA 2.0: enhanced and customizable prediction of RNA-RNA interactions. Nucleic Acids Res.
Manna, A., and Cheung, A.L. (2001). Characterization of sarR, a modulator of sar expression in Staphylococcus aureus. Infection and immunity *69*, 885-896.
Manna, A.C., Bayer, M.G., and Cheung, A.L. (1998). Transcriptional analysis of different promoters in the sar locus in Staphylococcus aureus. Journal of bacteriology *180*, 3828-3836.
Manna, A.C., and Cheung, A.L. (2006). Expression of SarX, a negative regulator of agr and exoprotein synthesis, is activated by MgrA in Staphylococcus aureus. Journal of bacteriology *188*, 4288-4299.
Marchais, A., Bohn, C., Bouloc, P., and Gautheret, D. (2010). RsaOG, a new staphylococcal family of highly transcribed non-coding RNA. RNA Biol *7*, 116-119.
Marincola, G., Schafer, T., Behler, J., Bernhardt, J., Ohlsen, K., Goerke, C., and Wolz, C. (2012). RNase Y of Staphylococcus aureus and its role in the activation of virulence genes. Molecular microbiology *85*, 817-832.
Markiewski, M.M., and Lambris, J.D. (2007). The role of complement in inflammatory diseases from behind the scenes into the spotlight. The American journal of pathology *171*, 715-727.
Martin, E., Cevik, C., and Nugent, K. (2012). The role of hypervirulent Staphylococcus aureus infections in the development of deep vein thrombosis. Thrombosis research *130*, 302-308.
Marzi, S., Fechter, P., Chevalier, C., Romby, P., and Geissmann, T. (2008a). RNA switches regulate initiation of translation in bacteria. Biological chemistry *389*, 585-598.
Marzi, S., Fechter, P., Chevalier, C., Romby, P., and Geissmann, T. (2008b). RNA switches regulate initiation of translation in bacteria. Biological chemistry *389*, 585-598.
Marzi, S., Myasnikov, A.G., Serganov, A., Ehresmann, C., Romby, P., Yusupov, M., and Klaholz, B.P. (2007). Structured mRNAs regulate translation initiation by binding to the platform of the ribosome. Cell *130*, 1019-1031.
Masse, E., Escorcia, F.E., and Gottesman, S. (2003). Coupled degradation of a small regulatory RNA and its mRNA targets in Escherichia coli. Genes & development *17*, 2374-2383.
McAdow, M., DeDent, A.C., Emolo, C., Cheng, A.G., Kreiswirth, B.N., Missiakas, D.M., and Schneewind, O. (2012). Coagulases as determinants of protective immune responses against Staphylococcus aureus. Infection and immunity *80*, 3389-3398.
McAleese, F.M., Walsh, E.J., Sieprawska, M., Potempa, J., and Foster, T.J. (2001). Loss of clumping factor B fibrinogen binding activity by Staphylococcus aureus involves cessation of transcription, shedding and cleavage by metalloprotease. J Biol Chem *276*, 29969-29978.
McCormick, J.K., Yarwood, J.M., and Schlievert, P.M. (2001). Toxic shock syndrome and bacterial superantigens: an update. Annual review of microbiology *55*, 77-104.
McGavin, M.J., Zahradka, C., Rice, K., and Scott, J.E. (1997). Modification of the Staphylococcus aureus fibronectin binding phenotype by V8 protease. Infection and immunity *65*, 2621-2628.
McNamara, P.J., Milligan-Monroe, K.C., Khalili, S., and Proctor, R.A. (2000). Identification, cloning, and initial characterization of rot, a locus encoding a regulator of virulence

factor expression in Staphylococcus aureus. Journal of bacteriology *182*, 3197-3203.
Mehdi, Q., and Yudkin, M.D. (1967). Coupling of transcription to translation in the induced synthesis of beta-galactosidase. Biochim Biophys Acta *149*, 288-290.
Mertz, D., Frei, R., Jaussi, B., Tietz, A., Stebler, C., Fluckiger, U., and Widmer, A.F. (2007). Throat swabs are necessary to reliably detect carriers of Staphylococcus aureus. Clinical infectious diseases : an official publication of the Infectious Diseases Society of America *45*, 475-477.
Miller, H.K., Carroll, R.K., Burda, W.N., Krute, C.N., Davenport, J.E., and Shaw, L.N. (2012). The extracytoplasmic function sigma factor sigmaS protects against both intracellular and extracytoplasmic stresses in Staphylococcus aureus. Journal of bacteriology *194*, 4342-4354.
Milon, P., Maracci, C., Filonava, L., Gualerzi, C.O., and Rodnina, M.V. (2012). Real-time assembly landscape of bacterial 30S translation initiation complex. Nat Struct Mol Biol *19*, 609-615.
Montgomery, C.P., Boyle-Vavra, S., Adem, P.V., Lee, J.C., Husain, A.N., Clasen, J., and Daum, R.S. (2008). Comparison of virulence in community-associated methicillin-resistant Staphylococcus aureus pulsotypes USA300 and USA400 in a rat model of pneumonia. The Journal of infectious diseases *198*, 561-570.
Morfeldt, E., Taylor, D., von Gabain, A., and Arvidson, S. (1995). Activation of alpha-toxin translation in Staphylococcus aureus by the trans-encoded antisense RNA, RNAIII. The EMBO journal *14*, 4569-4577.
Morikawa, K., Takemura, A.J., Inose, Y., Tsai, M., Nguyen Thi le, T., Ohta, T., and Msadek, T. (2012). Expression of a cryptic secondary sigma factor gene unveils natural competence for DNA transformation in Staphylococcus aureus. PLoS pathogens *8*, e1003003.
Morrison, J.M., Anderson, K.L., Beenken, K.E., Smeltzer, M.S., and Dunman, P.M. (2012). The staphylococcal accessory regulator, SarA, is an RNA-binding protein that modulates the mRNA turnover properties of late-exponential and stationary phase Staphylococcus aureus cells. Frontiers in cellular and infection microbiology *2*, 26.
Myasnikov, A.G., Marzi, S., Simonetti, A., Giuliodori, A.M., Gualerzi, C.O., Yusupova, G., Yusupov, M., and Klaholz, B.P. (2005). Conformational transition of initiation factor 2 from the GTP- to GDP-bound state visualized on the ribosome. Nat Struct Mol Biol *12*, 1145-1149.
Nair, S.P., Bischoff, M., Senn, M.M., and Berger-Bachi, B. (2003). The sigma B regulon influences internalization of Staphylococcus aureus by osteoblasts. Infection and immunity *71*, 4167-4170.
Nizet, V. (2007). Understanding how leading bacterial pathogens subvert innate immunity to reveal novel therapeutic targets. The Journal of allergy and clinical immunology *120*, 13-22.
Novick, R.P., Christie, G.E., and Penades, J.R. (2010). The phage-related chromosomal islands of Gram-positive bacteria. Nature reviews Microbiology *8*, 541-551.
Novick, R.P., and Geisinger, E. (2008). Quorum sensing in staphylococci. Annual review of genetics *42*, 541-564.
Novick, R.P., and Jiang, D. (2003). The staphylococcal saeRS system coordinates environmental signals with agr quorum sensing. Microbiology (Reading, England) *149*, 2709-2717.
Novick, R.P., and Ram, G. (2016). The Floating (Pathogenicity) Island: A Genomic Dessert. Trends in genetics : TIG *32*, 114-126.

Novick, R.P., Ross, H.F., Projan, S.J., Kornblum, J., Kreiswirth, B., and Moghazeh, S. (1993). Synthesis of staphylococcal virulence factors is controlled by a regulatory RNA molecule. The EMBO journal *12*, 3967-3975.
Novick, R.P., and Subedi, A. (2007). The SaPIs: mobile pathogenicity islands of Staphylococcus. Chemical immunology and allergy *93*, 42-57.
Ogston, A. (1881). Report upon Micro-Organisms in Surgical Diseases. British medical journal *1*, 369 b362-375.
Ohbayashi, T., Irie, A., Murakami, Y., Nowak, M., Potempa, J., Nishimura, Y., Shinohara, M., and Imamura, T. (2011). Degradation of fibrinogen and collagen by staphopains, cysteine proteases released from Staphylococcus aureus. Microbiology (Reading, England) *157*, 786-792.
Olejniczak, M., and Storz, G. (2017). ProQ/FinO-domain proteins: another ubiquitous family of RNA matchmakers? Molecular microbiology *104*, 905-915.
Omotajo, D., Tate, T., Cho, H., and Choudhary, M. (2015). Distribution and diversity of ribosome binding sites in prokaryotic genomes. BMC genomics *16*, 604.
Oogai, Y., Matsuo, M., Hashimoto, M., Kato, F., Sugai, M., and Komatsuzawa, H. (2011). Expression of virulence factors by Staphylococcus aureus grown in serum. Applied and environmental microbiology *77*, 8097-8105.
Oscarsson, J., Tegmark-Wisell, K., and Arvidson, S. (2006). Coordinated and differential control of aureolysin (aur) and serine protease (sspA) transcription in Staphylococcus aureus by sarA, rot and agr (RNAIII). International journal of medical microbiology : IJMM *296*, 365-380.
Otaka, H., Ishikawa, H., Morita, T., and Aiba, H. (2011). PolyU tail of rho-independent terminator of bacterial small RNAs is essential for Hfq action. Proceedings of the National Academy of Sciences of the United States of America *108*, 13059-13064.
Otto, M. (2014). Staphylococcus aureus toxins. Current opinion in microbiology *17*, 32-37.
Oun, S., Redder, P., Didier, J.P., Francois, P., Corvaglia, A.R., Buttazzoni, E., Giraud, C., Girard, M., Schrenzel, J., and Linder, P. (2013). The CshA DEAD-box RNA helicase is important for quorum sensing control in Staphylococcus aureus. RNA Biol *10*, 157-165.
Palma, M., and Cheung, A.L. (2001). sigma(B) activity in Staphylococcus aureus is controlled by RsbU and an additional factor(s) during bacterial growth. Infection and immunity *69*, 7858-7865.
Palma, M., Haggar, A., and Flock, J.I. (1999). Adherence of Staphylococcus aureus is enhanced by an endogenous secreted protein with broad binding activity. Journal of bacteriology *181*, 2840-2845.
Panja, S., Schu, D.J., and Woodson, S.A. (2013). Conserved arginines on the rim of Hfq catalyze base pair formation and exchange. Nucleic Acids Res *41*, 7536-7546.
Parker, M.W., and Feil, S.C. (2005). Pore-forming protein toxins: from structure to function. Progress in biophysics and molecular biology *88*, 91-142.
Parrillo, J.E. (1993). Pathogenetic mechanisms of septic shock. The New England journal of medicine *328*, 1471-1477.
Periasamy, S., Joo, H.S., Duong, A.C., Bach, T.H., Tan, V.Y., Chatterjee, S.S., Cheung, G.Y., and Otto, M. (2012). How Staphylococcus aureus biofilms develop their characteristic structure. Proceedings of the National Academy of Sciences of the United States of America *109*, 1281-1286.

Pestova, T.V., Lorsch, J.R., and Hellen, C.U.T. (2007). The Mechanism of Translation Initiation in Eukaryotes,, Cold Spring Harbor edn (NY: Cold Spring Harbor Laboratory Press).
Peton, V., Breyne, K., Rault, L., Demeyere, K., Berkova, N., Meyer, E., Even, S., and Le Loir, Y. (2016). Disruption of the sigS gene attenuates the local innate immune response to Staphylococcus aureus in a mouse mastitis model. Veterinary microbiology *186*, 44-51.
Philippe, C., Portier, C., Mougel, M., Grunberg-Manago, M., Ebel, J.P., Ehresmann, B., and Ehresmann, C. (1990). Target site of Escherichia coli ribosomal protein S15 on its messenger RNA. Conformation and interaction with the protein. J Mol Biol *211*, 415-426.
Piechowicz, L., Galin'ski, J., Garbacz, K., and Haras, K. (2010). Bacteriophage analysis of staphylokinase-negative Staphylococcus aureus strains isolated from people. Journal of basic microbiology *50*, 557-561.
Piroth, L., Que, Y.A., Widmer, E., Panchaud, A., Piu, S., Entenza, J.M., and Moreillon, P. (2008). The fibrinogen- and fibronectin-binding domains of Staphylococcus aureus fibronectin-binding protein A synergistically promote endothelial invasion and experimental endocarditis. Infection and immunity *76*, 3824-3831.
Popenda, M., Szachniuk, M., Antczak, M., Purzycka, K.J., Lukasiak, P., Bartol, N., Blazewicz, J., and Adamiak, R.W. (2012). Automated 3D structure composition for large RNAs. Nucleic Acids Res *40*, e112.
Potempa, J., Dubin, A., Korzus, G., and Travis, J. (1988). Degradation of elastin by a cysteine proteinase from Staphylococcus aureus. J Biol Chem *263*, 2664-2667.
Preis, H., Eckart, R.A., Gudipati, R.K., Heidrich, N., and Brantl, S. (2009). CodY activates transcription of a small RNA in Bacillus subtilis. Journal of bacteriology *191*, 5446-5457.
Prokesova, L., Potuznikova, B., Potempa, J., Zikan, J., Radl, J., Hachova, L., Baran, K., Porwit-Bobr, Z., and John, C. (1992). Cleavage of human immunoglobulins by serine proteinase from Staphylococcus aureus. Immunology letters *31*, 259-265.
Proshkin, S., Rahmouni, A.R., Mironov, A., and Nudler, E. (2010). Cooperation between translating ribosomes and RNA polymerase in transcription elongation. Science (New York, NY) *328*, 504-508.
Qin, L., McCausland, J.W., Cheung, G.Y., and Otto, M. (2016). PSM-Mec-A Virulence Determinant that Connects Transcriptional Regulation, Virulence, and Antibiotic Resistance in Staphylococci. Frontiers in microbiology *7*, 1293.
Que, Y.A., Haefliger, J.A., Piroth, L., Francois, P., Widmer, E., Entenza, J.M., Sinha, B., Herrmann, M., Francioli, P., Vaudaux, P.*, et al.* (2005). Fibrinogen and fibronectin binding cooperate for valve infection and invasion in Staphylococcus aureus experimental endocarditis. The Journal of experimental medicine *201*, 1627-1635.
Queck, S.Y., Jameson-Lee, M., Villaruz, A.E., Bach, T.H., Khan, B.A., Sturdevant, D.E., Ricklefs, S.M., Li, M., and Otto, M. (2008). RNAIII-independent target gene control by the agr quorum-sensing system: insight into the evolution of virulence regulation in Staphylococcus aureus. Molecular cell *32*, 150-158.
Rachid, S., Cho, S., Ohlsen, K., Hacker, J., and Ziebuhr, W. (2000). Induction of Staphylococcus epidermidis biofilm formation by environmental factors: the possible involvement of the alternative transcription factor sigB. Advances in experimental medicine and biology *485*, 159-166.
Rajkowitsch, L., and Schroeder, R. (2007). Dissecting RNA chaperone activity. RNA (New York, NY) *13*, 2053-2060.

Reed, S.B., Wesson, C.A., Liou, L.E., Trumble, W.R., Schlievert, P.M., Bohach, G.A., and Bayles, K.W. (2001). Molecular characterization of a novel Staphylococcus aureus serine protease operon. Infection and immunity *69*, 1521-1527.
Reingold, A.L., Hargrett, N.T., Dan, B.B., Shands, K.N., Strickland, B.Y., and Broome, C.V. (1982). Nonmenstrual toxic shock syndrome: a review of 130 cases. Annals of internal medicine *96*, 871-874.
Rice, G.M., Busan, S., Karabiber, F., Favorov, O.V., and Weeks, K.M. (2014). SHAPE analysis of small RNAs and riboswitches. Methods in enzymology *549*, 165-187.
Romby, P., and Springer, M. (2007). Translational control in prokaryotes. In Translational control in biology and medicine, M.B. Mathews, Sonenberg, N., and Hershey, J. W. B., ed. (Cold Spring Harbour: Cold Spring Harbour Laboratory Press), pp. 803-827.
Romero, D., Aguilar, C., Losick, R., and Kolter, R. (2010). Amyloid fibers provide structural integrity to Bacillus subtilis biofilms. Proceedings of the National Academy of Sciences of the United States of America *107*, 2230-2234.
Rooijakkers, S.H., van Kessel, K.P., and van Strijp, J.A. (2005). Staphylococcal innate immune evasion. Trends in microbiology *13*, 596-601.
Rosenbach, F.J. (1884). Mikro-Organismen bei den. In Wund-Infections-Krankheiten des Menschen, J.F. Bergman, ed. (Wiesbaden, Germany), pp. 1–122.
Roux, C.M., DeMuth, J.P., and Dunman, P.M. (2011). Characterization of components of the Staphylococcus aureus mRNA degradosome holoenzyme-like complex. Journal of bacteriology *193*, 5520-5526.
Ruiz de los Mozos, I., Vergara-Irigaray, M., Segura, V., Villanueva, M., Bitarte, N., Saramago, M., Domingues, S., Arraiano, C.M., Fechter, P., Romby, P.*, et al.* (2013). Base pairing interaction between 5'- and 3'-UTRs controls icaR mRNA translation in Staphylococcus aureus. PLoS genetics *9*, e1004001.
Said-Salim, B., Dunman, P.M., McAleese, F.M., Macapagal, D., Murphy, E., McNamara, P.J., Arvidson, S., Foster, T.J., Projan, S.J., and Kreiswirth, B.N. (2003). Global regulation of Staphylococcus aureus genes by Rot. Journal of bacteriology *185*, 610-619.
Salah, P., Bisaglia, M., Aliprandi, P., Uzan, M., Sizun, C., and Bontems, F. (2009). Probing the relationship between Gram-negative and Gram-positive S1 proteins by sequence analysis. Nucleic Acids Res *37*, 5578-5588.
Salis, H.M., Mirsky, E.A., and Voigt, C.A. (2009). Automated design of synthetic ribosome binding sites to control protein expression. Nature biotechnology *27*, 946-950.
Sanderson-Smith, M.L., De Oliveira, D.M., Ranson, M., and McArthur, J.D. (2012). Bacterial plasminogen receptors: mediators of a multifaceted relationship. Journal of biomedicine & biotechnology *2012*, 272148.
Schuwirth, B.S., Borovinskaya, M.A., Hau, C.W., Zhang, W., Vila-Sanjurjo, A., Holton, J.M., and Cate, J.H. (2005). Structures of the bacterial ribosome at 3.5 A resolution. Science (New York, NY) *310*, 827-834.
Schwartz, K., Syed, A.K., Stephenson, R.E., Rickard, A.H., and Boles, B.R. (2012). Functional amyloids composed of phenol soluble modulins stabilize Staphylococcus aureus biofilms. PLoS pathogens *8*, e1002744.
Seemann, T. (2014). Prokka: rapid prokaryotic genome annotation. Bioinformatics (Oxford, England) *30*, 2068-2069.
Serganov, A., Huang, L., and Patel, D.J. (2009). Coenzyme recognition and gene regulation by a flavin mononucleotide riboswitch. Nature *458*, 233-237.

Shaw, L., Golonka, E., Potempa, J., and Foster, S.J. (2004). The role and regulation of the extracellular proteases of Staphylococcus aureus. Microbiology (Reading, England) *150*, 217-228.
Shin, D.H., and Moldave, K. (1966). Effect of ribosomes on the biosynthesis of ribonucleic acid in vitro. J Mol Biol *21*, 231-245.
Shine, J., and Dalgarno, L. (1974). The 3'-terminal sequence of Escherichia coli 16S ribosomal RNA: complementarity to nonsense triplets and ribosome binding sites. Proc Natl Acad Sci U S A *71*, 1342-1346.
Sibbald, M.J., Ziebandt, A.K., Engelmann, S., Hecker, M., de Jong, A., Harmsen, H.J., Raangs, G.C., Stokroos, I., Arends, J.P., Dubois, J.Y.*, et al.* (2006). Mapping the pathways to staphylococcal pathogenesis by comparative secretomics. Microbiology and molecular biology reviews : MMBR *70*, 755-788.
Simonetti, A., Marzi, S., Fabbretti, A., Hazemann, I., Jenner, L., Urzhumtsev, A., Gualerzi, C.O., and Klaholz, B.P. (2013). Structure of the protein core of translation initiation factor 2 in apo, GTP-bound and GDP-bound forms. Acta crystallographica Section D, Biological crystallography *69*, 925-933.
Simonetti, A., Marzi, S., Myasnikov, A.G., Fabbretti, A., Yusupov, M., Gualerzi, C.O., and Klaholz, B.P. (2008). Structure of the 30S translation initiation complex. Nature *455*, 416-420.
Smirnov, A., Forstner, K.U., Holmqvist, E., Otto, A., Gunster, R., Becher, D., Reinhardt, R., and Vogel, J. (2016). Grad-seq guides the discovery of ProQ as a major small RNA-binding protein. Proceedings of the National Academy of Sciences of the United States of America *113*, 11591-11596.
Smirnov, A., Wang, C., Drewry, L.L., and Vogel, J. (2017). Molecular mechanism of mRNA repression in trans by a ProQ-dependent small RNA. The EMBO journal *36*, 1029-1045.
Smith, E.J., Corrigan, R.M., van der Sluis, T., Grundling, A., Speziale, P., Geoghegan, J.A., and Foster, T.J. (2012). The immune evasion protein Sbi of Staphylococcus aureus occurs both extracellularly and anchored to the cell envelope by binding lipoteichoic acid. Molecular microbiology *83*, 789-804.
Smith, E.J., Visai, L., Kerrigan, S.W., Speziale, P., and Foster, T.J. (2011). The Sbi protein is a multifunctional immune evasion factor of Staphylococcus aureus. Infection and immunity *79*, 3801-3809.
Sonnleitner, E., Schuster, M., Sorger-Domenigg, T., Greenberg, E.P., and Blasi, U. (2006). Hfq-dependent alterations of the transcriptome profile and effects on quorum sensing in Pseudomonas aeruginosa. Molecular microbiology *59*, 1542-1558.
Steen, K.A., Siegfried, N.A., and Weeks, K.M. (2011). Selective 2'-hydroxyl acylation analyzed by protection from exoribonuclease (RNase-detected SHAPE) for direct analysis of covalent adducts and of nucleotide flexibility in RNA. Nature protocols *6*, 1683-1694.
Stent, G.S. (1964). THE OPERON: ON ITS THIRD ANNIVERSARY. MODULATION OF TRANSFER RNA SPECIES CAN PROVIDE A WORKABLE MODEL OF AN OPERATOR-LESS OPERON. Science (New York, NY) *144*, 816-820.
Storz, G., Vogel, J., and Wassarman, K.M. (2011). Regulation by small RNAs in bacteria: expanding frontiers. Molecular cell *43*, 880-891.
Sun, X., Zhulin, I., and Wartell, R.M. (2002). Predicted structure and phyletic distribution of the RNA-binding protein Hfq. Nucleic Acids Res *30*, 3662-3671.

Surewaard, B.G., Nijland, R., Spaan, A.N., Kruijtzer, J.A., de Haas, C.J., and van Strijp, J.A. (2012). Inactivation of staphylococcal phenol soluble modulins by serum lipoprotein particles. PLoS pathogens *8*, e1002606.
Suyama, Y. (1986). Two dimensional polyacrylamide gel electrophoresis analysis of Tetrahymena mitochondrial tRNA. Current genetics *10*, 411-420.
Tamber, S., and Cheung, A.L. (2009). SarZ promotes the expression of virulence factors and represses biofilm formation by modulating SarA and agr in Staphylococcus aureus. Infection and immunity *77*, 419-428.
Tao, L., Wu, X., and Sun, B. (2010). Alternative sigma factor sigmaH modulates prophage integration and excision in Staphylococcus aureus. PLoS pathogens *6*, e1000888.
Tayeb-Fligelman, E., and Landau, M. (2017). X-Ray Structural Study of Amyloid-Like Fibrils of Tau Peptides Bound to Small-Molecule Ligands. Methods in molecular biology (Clifton, NJ) *1523*, 89-100.
Thammavongsa, V., Kim, H.K., Missiakas, D., and Schneewind, O. (2015). Staphylococcal manipulation of host immune responses. Nature reviews Microbiology *13*, 529-543.
Thorvaldsdottir, H., Robinson, J.T., and Mesirov, J.P. (2013). Integrative Genomics Viewer (IGV): high-performance genomics data visualization and exploration. Briefings in bioinformatics *14*, 178-192.
Toapanta, F.R., and Ross, T.M. (2006). Complement-mediated activation of the adaptive immune responses: role of C3d in linking the innate and adaptive immunity. Immunologic research *36*, 197-210.
Tomasini, A., Moreau, K., Chicher, J., Geissmann, T., Vandenesch, F., Romby, P., Marzi, S., and Caldelari, I. (2017). The RNA targetome of Staphylococcus aureus non-coding RNA RsaA: impact on cell surface properties and defense mechanisms. Nucleic Acids Res.
Tsompanidou, E., Sibbald, M.J., Chlebowicz, M.A., Dreisbach, A., Back, J.W., van Dijl, J.M., Buist, G., and Denham, E.L. (2011). Requirement of the agr locus for colony spreading of Staphylococcus aureus. Journal of bacteriology *193*, 1267-1272.
Tsui, H.C., Leung, H.C., and Winkler, M.E. (1994). Characterization of broadly pleiotropic phenotypes caused by an hfq insertion mutation in Escherichia coli K-12. Molecular microbiology *13*, 35-49.
Updegrove, T.B., Zhang, A., and Storz, G. (2016). Hfq: the flexible RNA matchmaker. Current opinion in microbiology *30*, 133-138.
Valentin-Hansen, P., Eriksen, M., and Udesen, C. (2004). The bacterial Sm-like protein Hfq: a key player in RNA transactions. Molecular microbiology *51*, 1525-1533.
van Wamel, W.J., Rooijakkers, S.H., Ruyken, M., van Kessel, K.P., and van Strijp, J.A. (2006). The innate immune modulators staphylococcal complement inhibitor and chemotaxis inhibitory protein of Staphylococcus aureus are located on beta-hemolysin-converting bacteriophages. Journal of bacteriology *188*, 1310-1315.
Varet, H., Brillet-Gueguen, L., Coppee, J.Y., and Dillies, M.A. (2016). SARTools: A DESeq2- and EdgeR-Based R Pipeline for Comprehensive Differential Analysis of RNA-Seq Data. PloS one *11*, e0157022.
Vellanoweth, R.L., and Rabinowitz, J.C. (1992). The influence of ribosome-binding-site elements on translational efficiency in Bacillus subtilis and Escherichia coli in vivo. Molecular microbiology *6*, 1105-1114.
Vimberg, V., Tats, A., Remm, M., and Tenson, T. (2007). Translation initiation region sequence preferences in Escherichia coli. BMC molecular biology *8*, 100.

Vogel, J., and Luisi, B.F. (2011). Hfq and its constellation of RNA. Nature reviews Microbiology *9*, 578-589.
Wagner, E.G., and Romby, P. (2015). Small RNAs in bacteria and archaea: who they are, what they do, and how they do it. Advances in genetics *90*, 133-208.
Wang, R., Braughton, K.R., Kretschmer, D., Bach, T.H., Queck, S.Y., Li, M., Kennedy, A.D., Dorward, D.W., Klebanoff, S.J., Peschel, A.*, et al.* (2007). Identification of novel cytolytic peptides as key virulence determinants for community-associated MRSA. Nature medicine *13*, 1510-1514.
Weeks, K.M. (2015). Review toward all RNA structures, concisely. Biopolymers *103*, 438-448.
Weinrick, B., Dunman, P.M., McAleese, F., Murphy, E., Projan, S.J., Fang, Y., and Novick, R.P. (2004). Effect of mild acid on gene expression in Staphylococcus aureus. Journal of bacteriology *186*, 8407-8423.
Wertheim, H.F., Melles, D.C., Vos, M.C., van Leeuwen, W., van Belkum, A., Verbrugh, H.A., and Nouwen, J.L. (2005). The role of nasal carriage in Staphylococcus aureus infections. The Lancet Infectious diseases *5*, 751-762.
Wickiser, J.K., Winkler, W.C., Breaker, R.R., and Crothers, D.M. (2005). The speed of RNA transcription and metabolite binding kinetics operate an FMN riboswitch. Molecular cell *18*, 49-60.
Wild, J., Rossmeissl, P., Walter, W.A., and Gross, C.A. (1996). Involvement of the DnaK-DnaJ-GrpE chaperone team in protein secretion in Escherichia coli. Journal of bacteriology *178*, 3608-3613.
Wyatt, M.A., Wang, W., Roux, C.M., Beasley, F.C., Heinrichs, D.E., Dunman, P.M., and Magarvey, N.A. (2010). Staphylococcus aureus nonribosomal peptide secondary metabolites regulate virulence. Science (New York, NY) *329*, 294-296.
Xu, S.X., and McCormick, J.K. (2012). Staphylococcal superantigens in colonization and disease. Frontiers in cellular and infection microbiology *2*, 52.
Yamanaka, K., Fang, L., and Inouye, M. (1998). The CspA family in Escherichia coli: multiple gene duplication for stress adaptation. Molecular microbiology *27*, 247-255.
Yotis, W.W. (1963). ABSORPTION OF THE ANTIBACTERIAL SERUM FACTOR BY STAPHYLOCOCCI. Journal of bacteriology *85*, 911-917.
Yura, T., Nagai, H., and Mori, H. (1993). Regulation of the heat-shock response in bacteria. Annual review of microbiology *47*, 321-350.
Yusupov, M.M., Yusupova, G.Z., Baucom, A., Lieberman, K., Earnest, T.N., Cate, J.H., and Noller, H.F. (2001). Crystal structure of the ribosome at 5.5 A resolution. Science (New York, NY) *292*, 883-896.
Yusupova, G., Jenner, L., Rees, B., Moras, D., and Yusupov, M. (2006). Structural basis for messenger RNA movement on the ribosome. Nature *444*, 391-394.
Zecconi, A., and Scali, F. (2013). Staphylococcus aureus virulence factors in evasion from innate immune defenses in human and animal diseases. Immunology letters *150*, 12-22.
Zhang, X., Zhu, Q., Tian, T., Zhao, C., Zang, J., Xue, T., and Sun, B. (2015). Identification of RNAIII-binding proteins in Staphylococcus aureus using tethered RNAs and streptavidin aptamers based pull-down assay. BMC Microbiol *15*, 102.
Zheng, A., Panja, S., and Woodson, S.A. (2016). Arginine Patch Predicts the RNA Annealing Activity of Hfq from Gram-Negative and Gram-Positive Bacteria. J Mol Biol *428*, 2259-2264.

Zielinska, A.K., Beenken, K.E., Joo, H.S., Mrak, L.N., Griffin, L.M., Luong, T.T., Lee, C.Y., Otto, M., Shaw, L.N., and Smeltzer, M.S. (2011). Defining the strain-dependent impact of the Staphylococcal accessory regulator (sarA) on the alpha-toxin phenotype of Staphylococcus aureus. Journal of bacteriology *193*, 2948-2958.

Alessandra MARENNA

Staphylococcus aureus protein S1, an RNA chaperone involved in translation initiation and sRNA regulation

Résumé

Bien que l'initiation de la traduction soit un processus conservé entre les bactéries, nous avons montré que le mécanisme par lequel les ARNm structurés sont reconnus et adaptés sur le ribosome diffère chez *Staphylococcus aureus*, un micro-organisme avec un bas taux de G+C et chez *Escherichia coli*. Une particularité du ribosome de *S. aureus* est l'absence de la protéine ribosomale S1, qui non seulement est plus courte que celle de *E. coli* mais qui possède également une organisation distincte des domaines. Mes expériences suggèrent que la protéine S1 (*Sau*S1) favorise spécifiquement l'initiation de la traduction de l'opéron α-*psm* 1-4 en liant son ARNm hautement structuré. En outre, il influence aussi l'expression et la production de facteurs de virulence comme les exotoxines (α-haemolysine, δ-hémolysine et γ-hémolysine) et les exoenzymes (protéases et lipases). En plus de son rôle dans la traduction, *Sau*S1 pourrait être impliquée dans d'autres processus cellulaires tels que le métabolisme de l'ARN et la régulation par des ARN non-codants (ARNnc). Elle forme des complexes *in vivo* avec plusieurs ARNnc dont la stabilité serait affectée dans la souche délétée du gène *rpsA* codant S1. *Sau*S1 a donc une activité chaperonne favorisant la cinétique d'appariement entre deux molécules d'ARN et au moins dans un cas, elle stimule la reconnaissance entre un ARNnc et son ARN cible.

Ainsi, *Sau*S1 appartient à une nouvelle classe de chaperons d'ARN qui jouent un rôle clé dans la régulation du virulon de *S. aureus*.

Mots-clés:

S. aureus S1, traduction, ARNnc, régulation du virulon

Résumé en anglais

Even if translation initiation is a conserved process among bacteria, we have recently shown that low G+C content Gram-positive, such as *Staphylococcus aureus*, differ from *E. coli* on the mechanism by which structured mRNAs are recognized and adapted on the ribosome. One peculiarity of the *S. aureus* ribosome is the absence of ribosomal protein S1, which is shorter than *E. coli* S1 and has different domains organization. My work could demonstrate that *S. aureus* S1 (*Sau*S1) specifically promotes translation initiation of the α-*psm* 1-4 operon by binding its highly structured mRNA. Moreover, it influences the expression and production of other exotoxins (α-haemolysin, δ-haemolysin and γ-haemolysins) and exoenzymes (proteases and lipases). Besides its role in translation, *Sau*S1 could be implicated in other cellular processes such as RNA maturation/degradation and sRNA-mediated regulation. It forms in vivo complexes with several sRNAs whose level is affected in a strain deleted of *rpsA* gene, coding for S1. Preliminary results show that *Sau*S1 has a chaperone activity promoting the kinetic of annealing of two model RNA molecules and at least in one case, we could demonstrate that it stimulates the recognition between a sRNA and its target RNA.

Taken together, *Sau*S1 belongs to a new class of RNA chaperones that play key roles in the regulation of *S. aureus* virulon.

Key words:

S. aureus S1, translation, sRNA, regulation of *S. aureus* virulon